1994

Laboratory studies on the anaerobic sequencing batch reactor

Shihwu Sung
Iowa State University

Order Number 9518447

Laboratory studies on the anaerobic sequencing batch reactor

Sung, Shihwu, Ph.D.

Iowa State University, 1994

U·M·I
300 N. Zeeb Rd.
Ann Arbor, MI 48106

Laboratory studies on the anaerobic sequencing batch reactor

by

Shihwu Sung

A Dissertation Submitted to the

Graduate Faculty in Partial Fulfillment of the

Requirements for the Degree of

DOCTOR OF PHILOSOPHY

Department: Civil and Construction Engineering
Major: Civil Engineering (Environmental Engineering)

Approved:

Signature was redacted for privacy.

In Charge of Major Work

Signature was redacted for privacy.

For the Major Department

Signature was redacted for privacy.

For the Graduate College

Members of the Committee:

Signature was redacted for privacy.

Signature was redacted for privacy.

Signature was redacted for privacy.

Signature was redacted for privacy.

Iowa State University
Ames, Iowa

1994

TABLE OF CONTENTS

LIST OF TABLES

LIST OF FIGURES

LIST OF ABBREVIATIONS

AIA	Automatic Image Analyzer
ALK	Alkalinity
ASBR	Anaerobic Sequencing Batch Reactor
BOD_5	5-day Biochemical Oxygen Demand
COD	Chemical Oxygen Demand
CSR	Continuously Stirred Reactor
ERI	Engineering Research Institute
F/M	Food to Microorganisms Ratio
GC	Gas Chromatograph
hrs	Hours
HRT	Hydraulic Retention Time
in	Inch
k	Specific Substrate Utilization Rate
k_1	First-Order Kinetic Constant
K_S	Half Saturation Constant
mgd	Million Gallons per Day
mg/L	Milligram per Liter
ml	Milliliter
min	Minute
MLSS	Mixed Liquor Suspended Solids

MLVSS	Mixed Liquor Volatile Suspended Solids
mm	Millimeter
NFDM	Non-Fat Dry Milk
PLC	Programmable Logic Control
rpm	Revolutions per minute
SBR	Sequencing Batch Reactor
SCOD	Soluble Chemical Oxygen Demand
SRT	Solids Retention Time
STP	Standard Pressure (1 atm) and Temperature (25°C)
TCOD	Total Chemical Oxygen Demand
TKN	Total Kjeldahl Nitrogen
TSS	Total Suspended Solids
TVA	Total Volatile Acids
UASB	Upflow Anaerobic Sludge Blanket
VSS	Volatile Suspended Solids

I. INTRODUCTION

The first high-rate anaerobic reactor process was developed as a result of studies by Fullen (1953), Schroepfer et al. (1955), Steffen (1958), and Schroepfer and Ziemke (1959). The process was analogous to the aerobic activated sludge process and was called the "anaerobic contact process." Several other high rate anaerobic processes have been developed and are being applied throughout the world. These include the anaerobic filter, the upflow anaerobic sludge blanket (UASB), and the fluidized-bed process. Speece (1983) listed and described these processes.

The success of high rate anaerobic treatment processes is primarily dictated by biomass retention in the reactor. Several methods have been used for the maintenance of a high solids retention time (SRT): External clarifier and vacuum degasification in the anaerobic contact process, natural or synthetic media in the anaerobic filter and fluidized-bed reactor, internal settler/gas separator in the UASB, and usage of coagulants in the suspended growth process.

In the 1960s, Dague conducted laboratory studies on methods of increasing the microbial population in anaerobic reactors involving batch feeding, internal solids separation, and supernatant wasting. The process was called "anaerobic activated sludge" (1966). The anaerobic activated sludge process was capable of achieving long SRTs with relatively short hydraulic retention times (HRTs) as a result of bioflocculation and efficient solids separation within the reactor.

A new anaerobic biological process is under development at Iowa State University.

The process is being called the "anaerobic sequencing batch reactor" (ASBR) (U.S. Patent No. 5,185,079). The ASBR offers attractive fundamental advantages over continuous-flow, suspended-growth anaerobic processes. The system allows biomass separation and liquid clarification to occur within the reactor, and no external clarifier is required. As a result of batch feeding, it is possible to achieve a low substrate level just prior to the settling phase and a quiescent settling condition during the settling phase. This leads to good bioflocculation and efficient solids separation, thus leading to long solids retention times (SRT) and efficient conversion of organic substrates to methane and carbon dioxide. Unlike the anaerobic filter and fluidized-bed reactor, the ASBR does not require media for biomass separation and retention.

The operating principles for the ASBR are simple. The reactor sequences through four steps: settle, decant, feed, and react. The ASBR can be sequenced as frequently as possible within the limitations of providing the necessary settling, decanting, feeding, and reaction time. The frequency of sequencing and the volume of feed processed with each sequence determines the hydraulic loading (detention time) and the strength of the waste establishes the organic loading. The concentration of mixed liquor suspended solids (MLSS) in the reactor is an important variable affecting the settling velocity of the biomass and also the achievement of a clear supernatant for discharge as effluent.

Since the ASBR relies on internal solids separation and supernatant clarification, it was hypothesized that reactor geometry (depth-to-diameter ratio) would be an important parameter affecting solids retention and reactor performance. It has also been observed

that the mixing pattern and mixing intensity are important parameters affecting anaerobic biomass flocculation and granulation. Further, since the ASBR process operates in a non-steady state, mathematical models developed for continuous-flow biological processes are not applicable to the ASBR. Thus, the purpose of the research was to evaluate the effects of reactor geometry and mixing on the performance and operating characteristics of the ASBR process and to develop a design model for the process.

Scope and Objectives of Study

In this study, four ASBRs with the same operating volume but different heights and diameters were designed and operated using a non-fat dry milk (NFDM) synthetic substrate as feed. The experimental ASBRs were operated at HRTs of 48 hour, 24 hour, and 12 hour over a range of chemical oxygen demand (COD) loadings to evaluate whether differences in reactor configuration could result in different treatment performance. The ASBR performance data were measured under pseudo-steady state conditions at various HRTs and organic loadings. The performance parameters included biogas production, methane production, COD, volatile acids, biomass concentrations, biomass zone settling velocity, and biosolids particle sizes.

Specific objectives of the study were:

1. To demonstrate the fundamental advantages of the new high rate ASBR process.
2. To investigate ASBR performance at various HRTs over a range of COD loadings.
3. To investigate the effects of reactor geometry on system performance including:
    a. Effect on biomass retention,

b. Effect on biomass settling characteristics,

c. Effect on progression of biomass granulation.

4. To compare performance differences between intermittent mixing and continuous mixing.

5. To develop an ASBR system design model and overall design concepts.

II. LITERATURE REVIEW

Fundamentals of Anaerobic Digestion

Anaerobic digestion is a series of biological reactions in which complex organic wastes are stabilized to methane and carbon dioxide in an oxygen-free environment. The methanogenic anaerobic system has been considered to be a two-stage process (Henze et al., 1983; McCarty, 1964a). In the first stage, the complex organics such as carbohydrates, proteins, and fats are hydrolyzed, fermented, and biologically converted to simple organic materials, mainly organic acids. The conversions are carried out by a group of facultative and anaerobic bacteria called "acid formers." During the second stage, the organic acids are utilized by a special group of bacteria named "methanogens" into the final products of carbon dioxide and methane. Anaerobic digestion has been also described as a multistep process of series and parallel reactions. Figure 2.1 shows the substrate conversion flow of each distinct reaction among the various groups of bacteria. First, complex polymeric materials are hydrolyzed by extracellular enzymes to soluble products. Secondly, these relatively simple, soluble compounds are fermented or anaerobically oxidized to short-chain fatty acids, alcohols, carbon dioxide, and hydrogen. The short-chain fatty acids (intermediary products) are converted to acetate, hydrogen, and carbon dioxide. Lastly, methanogenesis occurs through carbon dioxide reduction by hydrogen and from the fermentation of acetate.

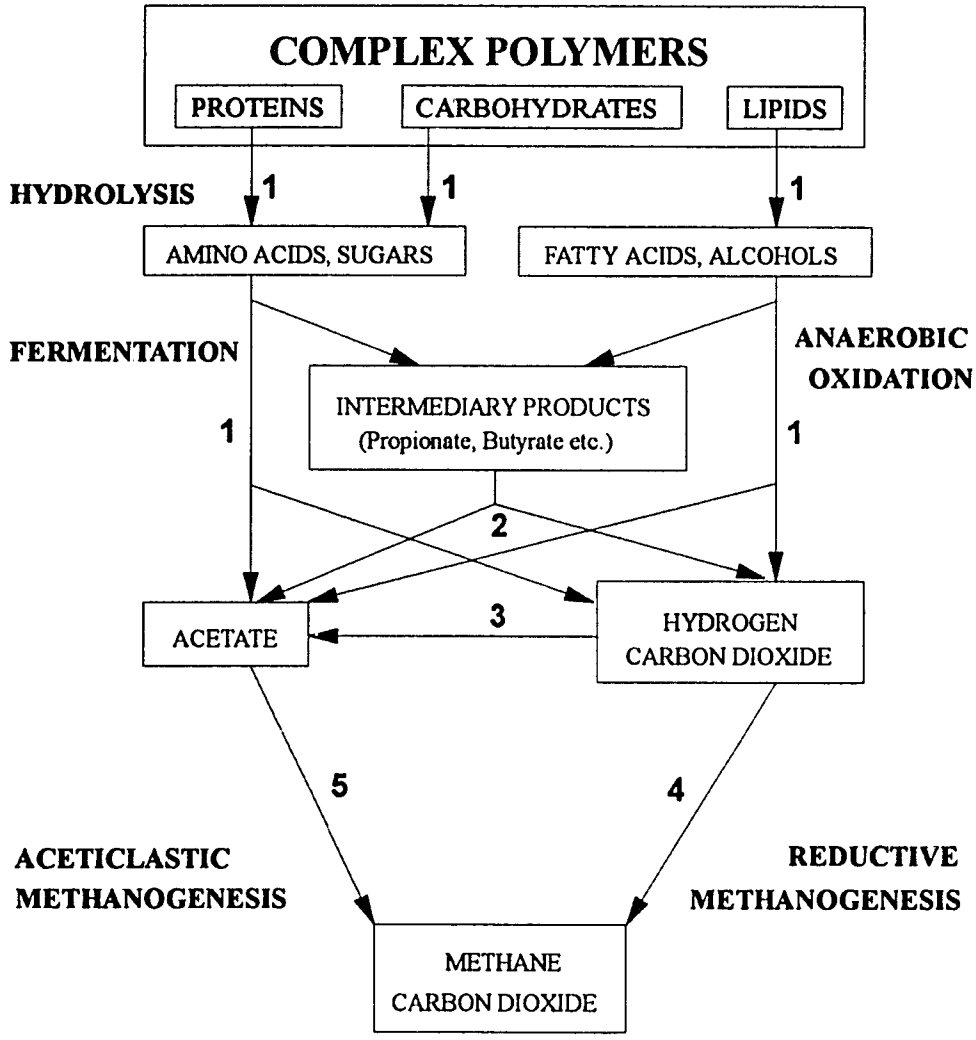

BACTERIAL GROUPS:

1. **HYDROLYTIC/FERMENTATIVE BACTERIA**
2. **HYDROGEN-PRODUCING ACETOGENIC BACTERIA**
3. **HYDROGEN-CONSUMING ACETOGENIC BACTERIA**
4. **CARBON DIOXIDE-REDUCING METHANOGENS**
5. **ACETICLASTIC METHANOGENS**

Figure 2.1 Reaction scheme of the anaerobic digestion (Zender, 1984; Parkin, 1986)

Anaerobic Bacteria

Anaerobic degradation involves a consortium of bacteria with the end-products from one group of bacteria used as the substrates for another group of bacteria. Zender (1984) and Parkin (1986) have classified these bacteria into five distinctive groups based on their trophic levels: group 1) fermentative bacteria, group 2) hydrogen-producing, acetogenic bacteria, group 3) hydrogen-consuming, acetogenic bacteria, group 4) carbon dioxide-reducing methanogens, and group 5) aceticlastic methanogens.

Hydrolytic/fermentative bacteria The hydrolysis of carbohydrates, proteins, and lipids is a complex process involving many different kinds of microorganisms. In general, carbohydrates are hydrolyzed to sugars which are fermented to volatile acids, CO_2, and H_2. For example, cellulose, the most abundant carbohydrate on earth, can be fermented by a number of anaerobic cellulolytic bacteria. *Ruminococci* are the most numerous of the bacteria isolated from bovine rumen (Colberg, 1988). Other species of anaerobic cellulose degrading bacteria include *Butyrivibrio fibrisolvens*, *Bacteroides succinogenes,* and *Eubacterium cellulosolens* (Fan et al., 1987). Fermentative bacteria are also referred to as acidogens because of their common end products of volatile acids.

Proteins are hydrolyzed to volatile acids, CO_2, H_2, NH_4^+, and S^{2-} by fermentative bacteria such as *Clostridium* species (McInerney, 1988). Lipids are hydrolyzed by fermentative bacteria into fatty acids and galactose, and glycerol moieties are fermented to similar products without NH_4^+ or S^{2-} production (McInerney, 1988).

Hydrogen-producing, acetogenic bacteria Acetate-forming organisms have conveniently been addressed as acetogens. In general terms, two different types of acetogenic bacteria can be distinguished: 1) hydrogen-producing acetogens which carry out the oxidation of the substrate and a reduction of protons to form molecular hydrogen and acetate as end products (acetogenic dehydrogenation), and 2) hydrogen-consuming acetogens which use hydrogen and carbon dioxide to form acetate (acetogenic hydrogenation).

Acetogenic dehydrogenation occurs in two major groups of bacteria: the fermentative bacteria, which can use various electron acceptors and produce hydrogen and acetate, butyrate, propionate, and long-chain fatty acids (previously discussed); and the obligate proton-reducing acetogens, which can utilize only protons as electron acceptors and produce hydrogen and acetate as major end products.

Acetogenic dehydrogenation bacteria are the critical link between acidogenesis and methanogenesis in anaerobic ecosystems. Acetogenesis provides the two main substrates, acetate and hydrogen-carbon dioxide, for the terminal step in the methanogenic conversion of organic material. Interspecies hydrogen transfer with methanogens as hydrogen consumers makes acetogenic dehydrogenations possible for both fermentative and obligate proton-reducing bacteria.

The oxidation of the substrates used by fermentative bacteria yields a substantial amount of energy. This amount of energy is maximal if hydrogen can be formed as electron acceptor, but increased hydrogen concentrations inhibit the formation of hydrogen.

At elevated concentrations of hydrogen, these oxidations become endothermic. Acetogenic conversion of butyrate, propionate, ethanol, and higher volatile acids to acetate will not be thermodynamically feasible at substrate concentration of 10^{-6} M when the hydrogen partial pressure is higher than 10^{-5} atm for propionate, 10^{-6} atm for butyrate, and 10^{-3} atm for ethanol (McInemey and Bryant, 1980). This can be easily understood from Table 2.1 which shows that propionate oxidation is least favored considering the most positive ΔG^0. Under anaerobic digestion ecosystem, propionate oxidation can become an exothermic reaction with an extremely low hydrogen partial pressure.

Table 2.1. Gibb's free energies of hydrogen-producing acetogentic reactions (Dolfing, 1988; Stams and Zehnder, 1990)

Acetogenic Conversion Reaction	ΔG^0 (KJ/reaction) Standard Conditions
$CH_3CH_2COO^- + 3H_2O \rightleftharpoons CH_3COO^- + HCO_3^- + H^+ + 3H_2$	+76.1
$CH_3CH_2CH_2COO^- + 2H_2O \rightleftharpoons 2CH_3COO^- + H^+ + 2H_2$	+48.1
$CH_3CH_2OH + H_2O \rightleftharpoons CH_3COO^- + H^+ + 2H_2$	+9.6

Bacteria capable of butyrate oxidation to acetate include *Syntrophomonas wolfei*, *Syntrophomonas sapovorans*, and *Clostridium bryantii* (Stams and Zehnder, 1990). Common propionate oxidizing bacteria found in anaerobic digester include *Syntrophobacter wolinii* and *Desulfobulbus propionicus* (Houwen et al., 1990).

Hydrogen-consuming, acetogenic bacteria This group of bacteria (also called homoacetogens) can utilize carbon dioxide as the electron acceptor to produce acetate as the sole product. Acetogenic hydrogenation can process via the reduction of carbon dioxide (one-carbon) to acetate or via multi-carbon acetate-yield hydrogenation (Dolfing, 1988). Many of the hydrogen-consuming acetogens include *Acetobacterium wieringae*, *Acetobacterium woodii*, *Clostridium aceticum*, and *Clostridium thermoaceticum* isolated to date possesses the capacity to ferment sugar to acetic acid and to grow on H_2-CO_2 with concomitant acetate production (Dolfing, 1988). The simultaneous utilization of organic and inorganic substrates for energy conversation by the acetogens may be important under condition of energy limitation. Methanogens gain more energy per mole of hydrogen converted than acetogens, so the mixotrophy of the homoacetogenic acetogens is probably the factor that secure the presence of acetogens in various ecosystem (Dolfing, 1988).

Methanogens Methanogens have been recognized as a distinctive group of microorganism due to their unique physiology in producing methane. Based on the 16S ribosomal RNA sequence homology, methanogens were separated from procaryote to form a new kingdom of Archaebacteria (Daniels, 1984; Jones, 1987). Taxonomically, methanogenic bacteria, which are all obligate anaerobic, consist of three orders, the methanobacteriales, the methanococcales, and the methanomicrobiales, subdivided into six families (Vogel et al., 1988). Table 2.2 lists the known methanogens along with their morphology and substrate requirement.

Methnogenic bacteria are limited to simple growth substrates, acetate, hydrogen-

Table 2.2. Classification and properties of methanogens (Vogels, 1988)

Genus		Morphology	Substrate	Number of species
		ORDER I. METHANOBACTERIALES		
Family I.	**Methanobacteriaceae**			
Genus I.	*Methanobacterium*	Rods, long rods to filaments	H_2/CO_2, formate	10
Genus II.	*Methanobrevibacter*	Short rods, short chains	H_2/CO_2, formate	3
Family II.	**Methanothermaceae**			
Genus I.	*Methanothermus*	Short rods	H_2/CO_2	1
		ORDER II. METHANOCOCCALES		
Family I.	**Methanococcaceae**			
Genus I.	*Methanococcus*	Cocci, irregular cocci	H_2/CO_2, formate	9
		ORDER III. METHANOMICROBIALES		
Family I.	**Methanomicrobiaceae**			
Genus I.	*Methanomicrobium*	Short rods	H_2/CO_2, formate	2
Genus II.	*Methanogenium*	Irregular cocci	H_2/CO_2, formate	9
Genus III.	*Methanospirillum*	Regular curved rods to long spiral filament	H_2/CO_2, formate	1
Family II.	**Methanosarcinaceae**			
Genus I.	*Methanosarcina*	Irregular cocci, forming cysts or aggregates	H_2/CO_2, methanol, methylamines, acetate	5
Genus II.	*Methanococcoides*	Irregular cocci	Methanol, methylamines	1
Family III.	**Methanoplanaceae**			
Genus I.	*Methanoplanus*	Plate-shaped	H_2/CO_2, formate	2
Family not assigned				
Genus	*Methanothrix*	Rods to filaments	Acetate	3
Genus	*Methanosaeta*	Rods to filaments	Acetate	1

Table 2.2. (Continued)

Genus	Morphology	Substrate	Number of species
Order and family not assigned			
Genus *Methanolobus*	Irregular cocci	Methanol, methylamines	1
Genus *Halomethanococcus*	Irregular cocci	Methanol, methylamines	1 1
Genus *Methanosphaera*	Spherical	Methanol	1

carbon dioxide, formate, methanol and methylamines, and do not gain a rich living. Table 2.3 shows a comparison of the free energies of hydrolysis of ATP (-32 KJ/mol) and those of methane formation from the substrates hydrogen and carbon dioxide (-139 KJ/mol of CH_4), formate (-127 KJ/mol), methanol (103 KJ/mol), methylamines (-102 KJ/mol), and acetate (-28 KJ/mol). Growth on carbon monoxide (CO) is possible but slight, despite the high free energy of CO (Daniels et al., 1977). This leads to the conclusion that only small amounts of energy are available to methanogens for new biomass synthesis.

Of the reactions listed in Table 2.3, hydrogen/carbon dioxide and formate are utilized by the most of methanogenic bacteria. However, it has been estimated that approximately 70% of the methane formed in nature is via acetate cleavage to methane and carbon dioxide. This is despite the fact that the free energy associated with acetate cleavage is extremely low. Additionally, only three genera of methanogens, *Methanosarcina*, *Methanothix*, and *Methanosaeta*, are capable of utilizing acetate to

Table 2.3. Energy yield in methanogenic reactions (Daniels, 1984; Oremland, 1988)

Reaction	ΔG° (KJ/mol) Standard Conditions
1. $4H_2 + CO_2 \rightarrow CH_4 + 2H_2O$	-139
2. $4HCOO^- + 2H^+ \rightarrow CH_4 + CO_2 + 2HCO_3^-$	-127
3. $4CH_3OH \rightarrow 3CH_4 + CO_2 + 2H_2O$	-103
4. $4CH_3NH_2 + 2H_2O + 4H^+ \rightarrow 3CH_4 + CO_2 + NH_4^+$	-102
5. $CH_3COO^- + H_2O \rightarrow CH_4 + HCO_3^-$	-28
6. $4CO + 2H_2O \rightarrow CH_4 + 3CO_2$	-186

produce methane and carbon dioxide (Jones et al., 1987; Vogels, 1988; Zeikus, 1977).

Methanogens require a very reduced environment with a redox potential less than -330 mV. In most cases, an environment with long detention times is necessary for sufficient growth, especially for methanogens of non-thermophiles. Dague (1970) reported that the required solid retention time (SRT) for stable anaerobic treatment at 35 °C is approximately 10 days. Because of increased metabolic rates at higher temperatures, the minimum SRT for thermophilic anaerobic treatment can be as low as 2 to 3 days.

Methanogens are entirely dependent upon the metabolic activities of other anaerobes for providing their growth substrates. In the real world, syntrophic or competitive relationships among methanogens and other groups of bacteria may actually exist to form a very dynamic system.

The hydrogen-consumption methanogens scavenge the H_2 produced by the other groups of bacteria and lower the hydrogen partial pressure in the anaerobic ecosystem.

Under this low hydrogen partial pressure environment, the butyrate and propionate oxidation reactions carried out by acetogens become thermodynamically feasible, since the free energy of these reactions are positive (not spontaneous reactions) at standard condition.

The relationship between sulfate-reducing bacteria and methanogens is a typical subtrate competition example. Sulfate-reducing bacteria obtain energy for growth from the oxidation a limited number of organic substrates and molecular H_2. Most of the sulfate-reducing bacteria grow on hydrogen or acetate as electron donor and sulfate or thiosulfate as terminal acceptors (Widdel, 1988). In the absent of sulfate, some sulfate-reducing bacteria actually produce substrates (acetate and H_2) for methnogens. However, in the presence of sulfate, the sulfate-reducing bacteria generally outcompete the methanogens for acetate and H_2.

Anaerobic Biosolids

Anaerobic Sludge Sedimentation

Sludge sedimentation is the separation of suspended biological flocs or particles from water by gravitational settling. In suspended growth anaerobic system, microorganisms have the characteristics of flocculating under proper conditions. This allows sedimentation to produce a clarified effluent or concentrated solids which can be more easily handled or disposed. In high-rate anaerobic system, sludge sedimentation is one of the key elements in retaining high levels of biological mass which ensure efficient performance.

The sedimentation is described into four settling types: discrete settling, flocculent

settling, zone settling, and compression settling. These types of settling phenomena are described in Table 2.4. During any sedimentation operation, it is possible to have more than one type of settling occurring at any given time. For a low biosolids concentration, for instance, both discrete settling and floccuent settling can occur in the settling phase. In systems that contain high concentrations of suspended solids, both zone settling and compression settling usually occur in the settling phase. As a result, the contacting particles tend to settle as a "blanket," maintaining the same relative position with respect to each other.

Anaerobic Granulation Process

Microbial attachment to a living or non-living surface is a very fundamental biological process which is inherent in certain microorganisms in nature. In anaerobic processes, it often leads to the further development of a biofilm or granule. The process is very complicated because of the involvement of many kinds of microorganisms and various environmental factors. Microbial adhesion and aggregation is generally believed to be the result of a number of interactions between the microorganisms and the surface to which they attach, whether that surface be an inert solid, an organic particle, or another microorganism. Three factors governing the anaerobic bacterial aggregation can be described as follow (Hulshoff Pol, 1989):

1. Environmental factors such as pH, temperature, ionic strength, composition and concentration of the organic substrate (Grotenhuis, et al. 1991).
2. The characteristic of substratum (support particle), including its porosity, charge of

Table 2.4. Types of settling and description (Metcalf and Eddy, Inc., 1991)

Type of settling	Description
Discrete (Class I)	Refer to sedimentation of particles in a suspension of low solids concentration. Particles settle as individual entities, and there is no significant interaction with neighboring particles.
Flocculent (Class II)	Refers to a rather dilute suspension of particles that coalesce, or flocculate, during the sedimentation operation. By coalescing, the particles increase in mass and settle at a faster rate.
Zone (Class III)	Refers to suspensions of intermediate concentration, in which inter-particle forces are sufficient to hinder the settling of neighboring particles. The particles tend to remain in fixed positions with respect to each other, and the mass of particles settles as a unit. A solids-liquid interface develops at the top of the settling mass.
Compression (Class IV)	Refer to settling in which the particles are of such concentration that a structure is formed, and further settling can occur only by compression of the structure. Compression takes place from the weight of the particles, which are constantly being added to the structure by sedimentation from the supernatant liquid.

surface, density of particles, specific surface area, and surface tension.

3. The properties of microorganisms such as surface characteristics including hydrophobic, ionic, dipolar, and hydrogen bond interactions, bacterial physiology (e.g. the production of extracellular polymers), and the bacterial morphology.

Granular biomass is visually and physically different from the usual flocculent biomass, such as would be obtained from a typical anaerobic digester at a municipal wastewater treatment plant. Dubourguier et al. (1988) defined granular biomass as a

mixture of biomass and other material which have a well-defined structure and boundary to the unaided eye. Granules are visible as separate entities in mixed liquor during both mixing and settling phases. Granules settle as discrete particles, similar to the settling characteristics of sand and pebbles, which settle much faster than flocculent biomass.

The majority of the literature concerning granulation in anaerobic systems to date has been focused on the upflow anaerobic sludge blanket reactor (UASB) and fluidized-bed reactor, each of which will be described latter. Granular biomass has been studied with respect to its microbiology, chemistry, and activity.

Hulshoff Pol (1987) described the "selection pressure" in the UASB system as the determining factor in the granulation process. The selection pressure was regarded as a combination of the effects of the hydraulic loading rate and the biogas loading rate.

Species of *Methanothrix* and *Methanosarcina* have been implicated by many researchers as being the most abundant methanogens present in granules treating a wide variety of wastewaters. *Methanothrix* especially is a key structure element in all granules observed, suggesting that it plays an important role in granulation (Fang, 1994; MacLeod, 1990).

From the discussion of the interaction of the various anaerobic bacterial groups presented earlier, it is apparent that the formation of compacted granule, which contains members from all five groups of bacteria, would be beneficial to each group in that efficient transfer of intermediate products could result. In fact, the thermodynamics of the entire anaerobic degradation process are improved by granule formation. Although this

transfer also occurs in flocculent biomass systems, the distance that each intermediate product must travel is minimized in a system in which the bacteria are fixed in a position close to other bacteria (Pauss et al., 1990; Schink and Thauer, 1988).

McCarty and Smith (1986) reported that reactors fostered biofilms (granular sludge) produced lower hydrogen (H_2) partial pressures and more rapid H_2 utilization than did reactors with dispersed sludge. This results in enhanced propionate degradation for systems in which granular sludge predominates over flocculent sludge.

Thiele et al. (1988), comparing freely suspended biomass with granular biomass, stated that in syntrophic ethanol conversion granules were the site of more than 75% of the microbial activity. The methanogenic formate turnover rate within the granule (0.28/min) was almost twice as fast as the turnover rate outside the granule (0.15/min). This indicates that higher microbial activity results when anaerobic microorganisms reside within a short distance of each other, as is the case with granular sludge.

Acetate thresholds in acetoclastic methanogens The acetate threshold is defined as the concentration of acetate below which acetate consumption stops. Table 2.5 summarizes the acetate threshold values of major acetoclastic methanogens. Westermann et al. (1989) proposed that acetate thresholds in acetoclastic methanogens are responsible for the predominance of *Methanothrix* species over *Methanosarcina* species at low acetate concentrations. The acetate threshold phenomenon has important implications for the minimum effluent oxygen demand that can be obtained by anaerobic processes since volatile acids are the primary organic substrates in the effluent and approximately 70% of

these total volatile acids are normally attributed to acetate. Depending on the predominance of acetoclastic methanogens (*Methanothrix* species or *Methanosarcina* species), different acetate-COD concentrations can remain in the effluent (Pavlostathis and Giraldo-Gomez, 1991). Based on the values reported in Table 2.5, granular sludge has the lowest acetate threshold value of 0.25 mg/L. This lowest threshold value coincides with the common findings of 1) the predominance of *Methanothrix species* in most anaerobic granules, and 2) lower volatile acid concentrations in the effluent of granular sludge systems than of non-granular sludge systems.

Besides the organic biological composition of granules, inert material often comprise a significant portion of the granule. Inert materials include sulfides, carbonates, potassium, sodium, heavy metals, and several other compounds (Dolfing et al., 1985;

Table 2.5. Summary of acetate threshold values for various acetoclastic methanogens (Pavlostathis and Giraldo-Gomez, 1991)

Methanogens	Temperature °C	Threshold mg/L	Reference
Granular Sludge	37	0.25	Jetten et al., 1990
Methanothrix sp.	37	4.1	Westermann et al., 1989
Methanothrix sp.	58	0.72-1.26	Min and Zinder, 1989
Methanothrix soehnegenii	37	0.42	Jetten et al., 1990
Methanosarcina sp.	58	60-90	Min and Zinder, 1989
Methanosarcina barkeri	37	14.6	Jetten et al., 1990
Methanosarcina barkeri	37	70.8	Westermann et al., 1989
Methanosarcina barkeri	37	15.6-130	Fukuzaki, 1990
Methanosarcina mazei	37	23.8	Westermann et al., 1989

Ross, 1984). Calcium carbonate has been observed at high concentrations within the granular matrix. It has been suggested that precipitated inert particles may act as nuclei to which bacteria attach and begin to grow as a granule (Mahoney et al., 1986). Table 2.6 presents the general composition of typical granules. The chemical composition of various granular systems has been shown to vary significantly. These variations are normally attributed to the substrate, including the inorganic compounds contained in the substrate, as well as the bacteria present within the granule. The nitrogen content value of 11 percent agrees with the nitrogen value of empirical cell formulation $C_{60}H_{87}O_{23}N_{12}P$. Granular biomass normally contains significant extracellular polysaccharides, proteins, and lipids. This extracellular biopolymers may only consist of 1 to 4 percent of the dry weight of the granule, but it has been suggested that it play a role in stabilizing and strengthening the granule structure (Ross, 1984).

Table 2.6. General chemical composition of various granular sludges (Dolfing et al., 1985; Ross, 1984)

Components	% of dry weight
Ash	10 - 23
Nitrogen content	11
Protein	35 - 60
Carbohydrate	
Total	6 - 7
Extracellular polymers	1 - 4
Organic content	90
TOC	41-47

Anaerobic Biosorption

Biosorption may be simply defined as the uptake or accumulation of chemicals and particulates from the solution by microbial materials (Tsezos and Bell, 1989). The mechanisms responsible for this accumulation are complex and involves adsorption or absorption into various components of the microbial cell.

In the last two decades, the biosorption process has been wildly used by different researchers for the removal of heavy metal ions and hazardous organic pollutants, namely Co, Ni, Cu, Ag, and chlorinated hydrocarbons from wastewater, by both live and dead biomass (Hunt, 1986; Portier, 1986). Biopolymers which may be extracellular polysaccharides, pigments, or other materials in the cell wall structure are responsible for metabolism independent binding or biosorption of metal and radionuclide species. The binding of metal ions to biopolymers is by means of two major mechanisms, the first of these being simple ion-exchange and the second through the formation of complexes which may be chelates (Hunt, 1986).

Ullrich and Smith (1951) developed the first biosorption process for sewage and wastewater treatment. In their 15 gpm pilot plant, activated sludge was brought in contact with raw sewage and mixed for 15 to 30 min. The activated sludge adsorbed and absorbed the BOD and suspended solids of the raw sewage in a range of 90 to 95 %. The main advantages of the process were the elimination of the need for primary clarification, and the requirement of less aeration tank capacity. This process was used successfully in the full-scale and remodeled wastewater treatment plant in Austin, Texas (Ullrich and Smith,

1957; Sawyer, 1960).

Mortenson obtained a patent in 1953 for an anaerobic sludge biosorption process for treating raw sewage. In the process, anaerobic sludge was recycled from a digester and contacted with raw swage in a biosorption unit for a short retention time. Then the mixture was allowed to settle in a settling tank. The clear supernatant liquid was withdrawn from the top as effluent, and the concentrated sludge with the adsorbate attached and suspended solids was delivered from the bottom the settling tank to the digester for further degradation. The main advantage of this process was that the biosorption unit did not have to be heated. This process was suitable for the treatment of relatively cool wastes with low concentrations of suspended solids.

Schroepfer and Ziemke (1959) applied Mortenson's process (Mortenson, 1953) to the treatment of synthetic milk waste and domestic sewage. The results showed that the initial uptake or sorption of organic matter by anaerobic sludge was quite rapid and reached equilibrium in less than 30 min of contact time. The process is capable of removing about 80% of the BOD applied to it at a BOD loading of 2 g/L/day for the synthetic milk waste. For domestic sewage, BOD removal remained constant at 70 to 75% across a range of BOD loads from 0.8 g/L/day to 2.3 g/L/day.

Kinetics of Anaerobic Digestion

The anaerobic processes are not more unstable than aerobic process. One of the reasons why anaerobic processes do not have their deserving reputation, is that engineering design practice for the processes through the years have been operating with poor process

control. Kinetics of anaerobic treatment provides a valuable tool in anaerobic process control.

Process kinetics have been used for the mathematical description of both aerobic and anaerobic biological treatment process. In designing a biological treatment process, the engineer is generally interested in the substrate removal rate and the biomass production rate. These rates of change are important because they directly affect the size of the reactor required for a specific degree of treatment. Therefore, biological process kinetics are initiated on two fundamental relationships: biomass growth rate and substrate utilization rate.

Biomass Growth Rate

Some of the prerequisites for growth of biomass in an anaerobic bacterial culture are 1) an energy source, 2) a carbon source, 3) an external electron acceptor, and 4) a suitable physicochemical environment. When all the requirements for growth are met, then the rate of microbial growth can be expressed by the Equation 2.1.

$$\frac{dX}{dt} = \mu \cdot X \qquad (2.1)$$

where X = biomass concentration (ML^{-3}),
t = time (T), and
μ = specific growth rate (T^{-1}).

Monod (1949) described the relationship between the residual concentration of the growth-limiting substrate and the specific growth rate of biomass by Equation 2.2.

$$\mu = \mu_m \cdot \frac{S}{Ks + S} \tag{2.2}$$

where μ = specific growth rate (T-1),
μ_m = maximum specific growth rate (T-1),
S = residual growth-limiting substrate concentration (ML^{-3}), and
K_s = saturation constant numerically equal to the substrate constant at which $\mu = \mu_m/2$ (ML^{-3}).

Growth Yield and Substrate Utilization Rate

Growth yield Y is defined mathematically as

$$\frac{dX}{dS} = Y \tag{2.3}$$

where dX is the incremental increase in biomass which results from the utilization of the incremental amount of substrate, dS. Monod (1949) observed that as long as there was no change in the composition of the biomass and environmental conditions remained constant, the growth yield remained constant. Thus, designating the initial biomass and substrate concentrations as X_0 and S_0, respectively, and letting X and S represent the corresponding concentrations during growth, the relationship between growth and substrate utilization can be expressed as follow.

$$\frac{(X - X_0)}{(S_0 - S)} = Y \tag{2.4}$$

Equation 2.5 shows that the substrate utilization rate (dS/dt) is proportional to the concentration of biomass (X). The proportionality constant (q) in the equation is termed

the specific substrate utilization rate and has the dimension of time^{-1}.

$$\frac{dS}{dt} = q \cdot X \tag{2.5}$$

The relationship between specific substrate utilization rate, specific growth rate, and growth yield can be derived from Equations 2.1, 2.2 and 2.3.

$$\frac{(dS/dt)}{X} = q = \frac{(dX/dt) / X}{dX / dS} = \frac{\mu}{Y} \tag{2.6}$$

Equation 2.6 can be used to estimate the substrate demand at various growth rates.

Kinetic Relationships Applied in Process Design

The Monod equation expressed in terms of the rate of substrate utilization to the concentration of biomass in the reactor and to the concentration of substrate surrounding the biomass is:

$$\frac{dS}{dt} = \frac{k \cdot X \cdot S}{K_s + S} \tag{2.7}$$

where k = maximum specific substrate utilization rate, g COD/g VSS-day.

For the limiting case, when S is much greater than K_s, K_s can be neglected in the sum term given in the denominator of Equation 2.7. In this condition, Equation 2.7 reduces to an expression that is zero-order with respect to substrate concentration:

$$(dS/dt) = k \cdot X \qquad (2.8)$$

For another limiting case, when S is much smaller than K_s, S can be neglected in the sum term given in the denominator. In this situation, Equation 2.7 reduces to an expression that is first-order with respect to substrate concentration:

$$(dS/dt) = K \cdot X \cdot S \qquad (2.9)$$

where $K = k/K_s$ = first-order substrate utilization rate constant ($L^3M^{-1}T^{-1}$).

Endogenous decay, commonly defined as cell death and lysis, leads to a decrease in biomass. Equation 2.10 describes the relationship between the rate of substrate utilization and the net growth rate of biomass. To account for the effect of the endogenous decay, a biomass decay rate constant (k_d) is used for the modification of the growth rate.

$$\frac{dX}{dt} = Y \cdot \frac{dS}{dt} - k_d \cdot X \qquad (2.10)$$

where k_d = specific endogenous decay coefficient (T^{-1}).

Rate-Limiting Step

The rate-limiting step approach has been used for describing the overall kinetics of the anaerobic treatment process. When a process involves a sequence of reactions, one reaction is usually slower than the other reactions. The slowest reaction in the sequence is called the rate-limiting step. Under this situation, the rate of final product formation depends on the rates of all the steps preceding the slowest step, but not the rates of any of

the subsequent, more rapid steps. As previously described, the anaerobic degradation of complex substrates is a multistep reaction. Lawrence (1971) defined the rate-limiting step in anaerobic digestion processes as that step which caused process to fail under imposed conditions of kinetic stress. The kinetic stress of anaerobic treatment processes most commonly refers to a continuously reducing of solids retention time until it is lower than the minimum time requirement and results in washout of the microorganisms. This description indicates that process failure is attributed to the washout of methanogens. Thus, methanogenesis is the rate-limiting step due to its slowest growth kinetics of the anaerobic bacteria groups. However, one must recognize that steps preceding the rate-limiting step can influence the overall rate. It is specially true when methane fermentation is applied to particulate organic substrates. The rate of hydrolysis of particulate substrate determines the maximum substrate concentration possible for methanogens, which in turn determines their maximum possible specific growth rate. The anaerobic degradation of raw cellulosic materials such as wheat straw, cornstalks, and wood are severely limited in the hydrolysis step by the lignin sheath surrounding the cellulose (Fan et al., 1987).

In an effort to model anaerobic digestion kinetics, some of the steps outlined in Figure 2.1 need to be considered in the overall mathematical description. Speece (1983) stated that the rate-limiting step in the overall process is related to the nature of the substrate, process configuration, temperature, and organic loading rate. Based on an extensive literature review, Pavlostathis and Giraldo-Gomez (1991) concluded that steps needed to be considered in overall kinetic formulations were dictated by the type of waste

being digested (e.q., soluble vs. particulate; or its chemical composition).

A large number of anaerobic process studies using complex substrates have derived values of kinetic parameters without reference to the individual reactions discussed in Figure 2.1. A summary of kinetic data from these studies is presented in Table 2.7.

Although the rate-limiting step approach leads to relatively simple mathematical descriptions of the anaerobic process, examining the kinetics of each major substep of the anaerobic process is required for a better understanding of the process. The hydrolysis step is usually assumed to follow first-order kinetics (Eastman and Ferguson, 1981). With the exception of the hydrolysis step, all other subprocesses of anaerobic treatment have been successfully modeled by Monod kinetics (Pavlostathis and Giraldo-Gomez, 1991). A summary of reported values for the kinetic constants of each subprocess is given in Table 2.8.

High Rate Anaerobic Process

Anaerobic Contact Process

The first "high rate" anaerobic process (Figure 2.2) was developed by Fullen in 1953. The solid retention time was maintained much longer than the hydraulic retention time by recycling the settling solids in a clarification basin back to the digester. The process consisted of mixing the incoming raw waste with an activated sludge at a temperature of 92 to 94°F. A degasification facility was introduced before the clarification basin to effect the removal of gases in the effluent solids. This process, which was later called the anaerobic contact process, removed the BOD_5 of the packing house wastewater

Table 2.7. Overall kinetic constants, anaerobic processes (Henze and Harremoës, 1983; Pearson, 1966)

Type of waste	Maximum specific rate	Yield coefficient	Substrate utilization rate	Decay rate constant"	"Half Velocity	Temperature	Solubility index
	μ_{max} 1/day	Y mg VSS/mg CODmg	k COD/(mg VSS•d)	k_d 1/day	K_s mg COD/L	°C	%
Hexose		0.04-0.20					100
Hexose (Theoretical)		0.17					-
Synthetic			1.0			38	100
Glucose	0.16	0.21		0.03	2000		100
Glucose, peptone	0.27	0.19		0.02	3000		100
Palm oil		0.14	0.9	0.04	4000		
Sauerkraut		0.05-0.07	0.6-1.0			30	97
Bean blanching unsoured		0.15	0.5-0.7			30	90
Dairy		<0.18	0.4-0.5			30	> 75
Long-chain sat. fatty acids			0.8-1.0		100-400	37	100
Long-chain unsat. fatty acids			4-5		1800-3200	37	100
Sucrose		0.08-0.23				35	100
Alcoholic			0.5			30	100
Synthetic stillage		0.046-0.076				30	100
Piggery waste			1.1-1.4			35	50
Whey permeate		0.06-0.07		0.01		35	89
Various industry wastes		0.024-0.083				35	85-100
Dextrose, peptone beef extract	0.07-0.19	0.11-0.18		0.025-0.10	2760-6700	35	
Glucose and starch		0.46		0.088		35	

Table 2.8. Summary of values of kinetic constants for various substrates utilized in anaerobic treatment processes (Pavlostathis and Giraldo-Gomez, 1991)

Type of waste	Process	Maximum specific rate	Yield coefficient	Substrate utilization rate	Decay rate constant"	"Half Velocity
		μ_{max} 1/day	Y mg VSS/mg COD	k mg COD/(mg VSS•d)	k_d 1/day	K_s mg COD/L
Carbohydrate	Acidogenesis	7.2-3.0	0.14-0.17	1.33-70.6	6.1	22.5-630
Long-chain fatty acids	Anaerobic oxidation	0.085-0.55	0.04-0.11	0.77-6.67	0.01-0.015	105-3180
Short-chain fatty acids	Anaerobic oxidation	0.13-1.20	0.025-0.047	6.2-17.1	0.01-0.027	12-500
Acetate	Aceticlastic methanogenesis	0.08-0.7	0.01-0.054	2.6-11.6	0.004-0.037	11-421
Hydrogen/carbon dioxide	Methanogenesis	0.05-4.07	0.017-0.045	1.92-90	0.088	4.8×10^{-5}-0.60

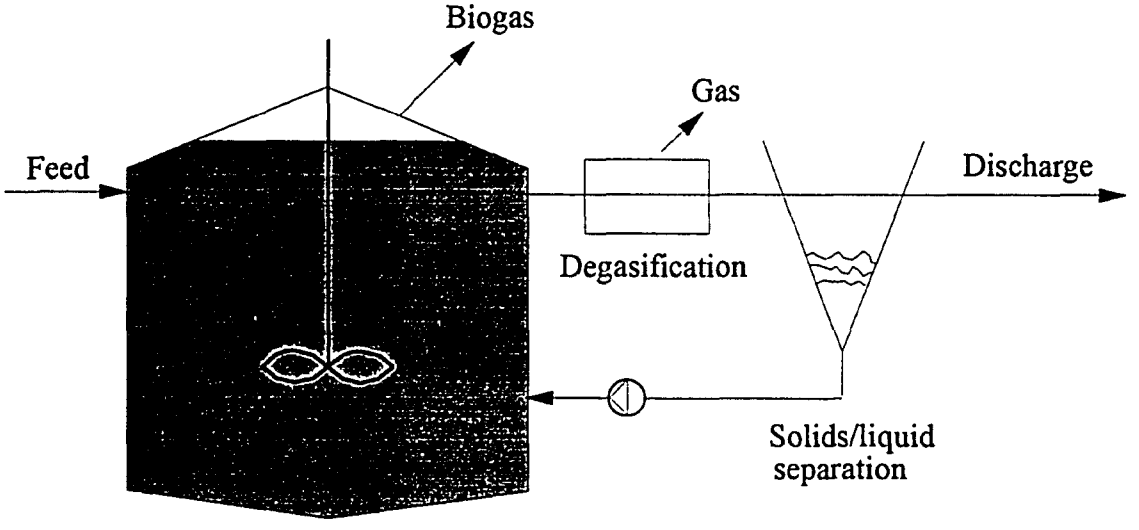

Figure 2.2. Anaerobic contact process

by 95% with a hydraulic retention time of 24 hours or less.

In 1955, Schroepfer et al. reported on a comprehensive study of the anaerobic contact process as applied to packinghouse wastes. The results indicated that this process was capable of accomplishing removals in BOD_5 of 95% and in suspended solids of 90% at loading more than 0.2 lb $BOD_5/ft^3/day$. This was attributed to the greater mixed liquor suspended solids (MLSS) concentrations that could be maintained in the anaerobic contact process. The MLSS could be up to 15,000 mg/L as compared to 3,000 to 4,000 mg/L in aerobic systems. Table 2.9 shows that this process is able to treat a variety of wastewaters, including packinghouse waste, creamery and milk products, cider and pectin, yeast, distillery, bean blanching waste, and simulated sewage sludge.

Table 2.9. Operating conditions and performance of various wastewaters using the anaerobic contact process

Wastes	Loading Rate		Temp.	Detention Time,day		Removal, %				Ref.
	kg BOD/m^3/day	kg COD/m^3/day	°C	SRT	HRT	BOD	COD	TSS	TVS	
Packinghouse wastes	2.1-3.5	---	30-35	---	0.42-0.54	90-95	---	58.6-94.0	63.8-78.6	1
Packinghouse waste	1.4	3.0	35	---	2.5	93	84	75	---	2
Creamery and Milk Products	1.6	2.5	35	50-60	1.9	96.6	---	---	---	3
Cider and Pectin	1.1	1.2	30	150	0.96	97	93.4	---	---	3
Yeast	2.3	4.3	35	---	3.5	99	---	---	---	
Distillery	2.0	3.3	37	200	15	98.5	96.2	---	---	3
Bean Blanching waste	---	7	35	---	3	---	80	---	---	4
Simulated Sewage Sludge	10	---	35	---	5.5	---	78	---	---	4

References:

1) Schroepfer et al., 1955

2) Stebor et al., 1987

3) Anderson, 1980b

4) van den Berg et al., 1980

Anaerobic Filter

The anaerobic filter (Figure 2.3) was introduced by Coulter et al. (1957) and Young and McCarty (1969). The packing material provided contact surface for biofilm development. Several physical parameters, such as diffusional resistance of substrate into biofilm and types of media used as attachment, have been investigated to assess the overall performance of the anaerobic filter process.

Diffusional resistance of substrate into biofilm is a major concern with the overall performance in the anaerobic biofilter process. Harremoës (1978) evaluated the significance of diffusional resistance. The final result is illustrated in Figure 2.4 which shows that the diffusional resistance does not become significant until the

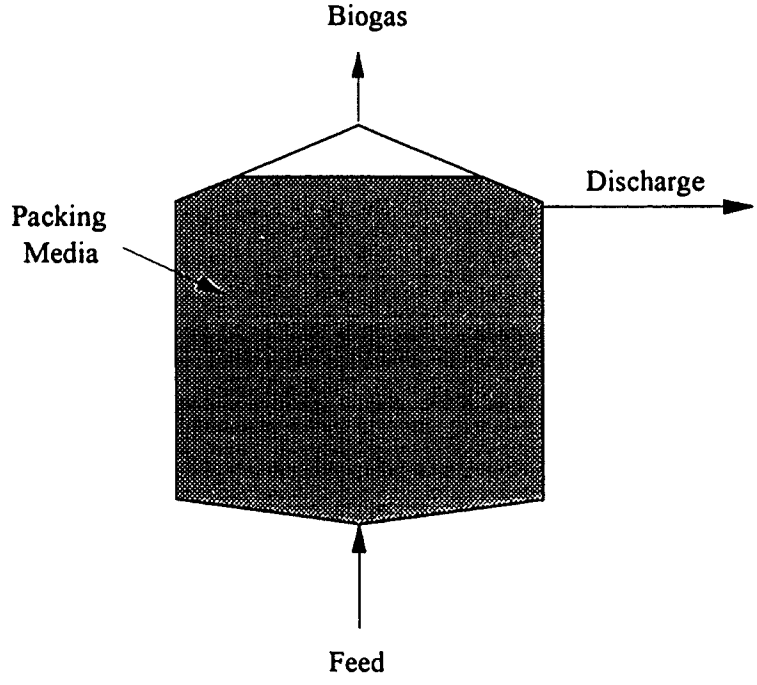

Figure 2.3. Upflow anaerobic filter process

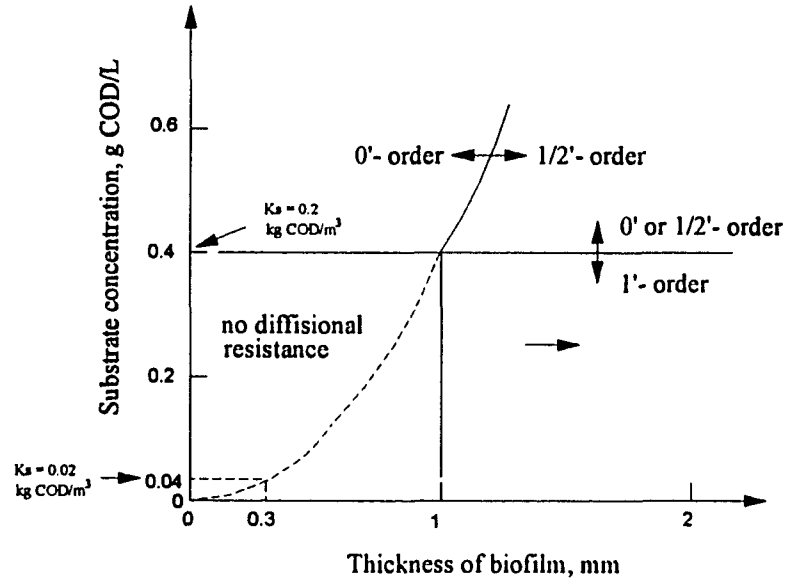

Figure 2.4. Diffusional resistance in an anaerobic biofilm

biofilm thickness reaches values above approximately 1 mm for K_s = 0.2 g COD/L and approximately 0.3 mm for K_s = 0.4 g COD/L. For a bulk concentration of 0.4 g COD/L, the transition occurs for a film thickness to 1 mm.

Specific area of attached media had been thought to be important in the anaerobic biofilter process. The surface area present in the various fixed film reactors depends not only on the type of the reactor media but also on the mode of operation and the wastewater under treatment. The effect of the inert support material on biofilm development have been studied by Murry and van den Berg (1981) and Salkinoja et al. (1982). The conclusion is that a porous inert media enhances biofilm development considerably as compared to a more smooth media. Investigations by van den Berg and Lentz (1980a) and Young and Dahab (1982) have demonstrated that in biofilter reactors, a substantial part of the biomass is present

in non-attached form, even pelletization/granulation is observed. Young and Dahab (1982) have demonstrated that the efficiency of biofilter reactors has no correlation to specific surface area. The above mentioned investigations suggest that biofilm surface area might not be important in biofilter reactors and the biofilm may be regarded as very nonhomogeneous.

For tolerance of shock loading, Frostell (1981) has demonstrated that the biofilter reactor is more capable of handling hydraulic shock loadings and has lower effluent solids than the UASB. However, the use of packing media in the biofilter may increase initial costs and create plugging problems, if not properly designed and operated. Table 2.10 shows that treatment efficiency for most of the wastes is greater than 80%. Basically, the biofilter is a good candidate for the treatment of low solids or highly soluble substrate.

Plugging of the media over time is the biggest concern with the anaerobic filter. Plugging of media results in channeling of the influent through the filter and decreases organic removal efficiencies. A modification to the anaerobic filter is made by removing the lower portion (one-third to a half) of the packing media. The new reactor, termed the hybrid anaerobic filter, or the upflow blanket filter, reduces the chances of plugging by having a suspended growth system in the bottom of the filter. The media at the top of the filter is still able to maintain high biomass concentrations within the filter. Additionally, filter construction costs are reduced because of the lower amount of the filter media required.

Guiot and van der Berg (1985) studied a hybrid filter which consisted of an open volume in the bottom two-thirds of the reactor and the top third containing plastic rings as the support media. A soluble sugar waste was used in this study. The COD removal efficiencies were above 90% for the organic loads up to 25 g COD/L/day at the HRTs as low as 3 hours.

Table 2.10. Operating conditions and performance of various wastewaters using the anaerobic filter process

Wastes	COD g/L	Loading Rate kg COD/m³/day	Porosity	Temp. °C	HRT day	Removal COD,%	Ref.
Food Processing	8.5	2.2	0.68	35	6.9	92	5
Vegetable Tanning	16.0	2.4	0.42	22-33	6.0	90-96	1
	16.0	3.6	0.42	22-33	4.0	90-93	1
	16.0	4.4	0.42	22-33	3.0	90-93	1
	16.0	16.0	0.42	22-33	1.0	84-89	1
Pharmaceutical	16.0	8.0	0.44	35	2.0	87	4
Pharmaceutical	2.0	1.5	0.43	35	36	83	4
Dairy	1.0	2.3	0.96	35	0.3	91	2
	3.2	0.8	0.96	35	3.6	97	2
Dairy	3.8	1.1	0.91	23	1.0	76	6
	3.8	1.2	0.91	23	3.0	87	6
Landfill Leachate	27.0	3.3	0.94	25	8.0	89	3

References:

1) Aeroa, and Chattopadhya, 1980.

2) Backman et al., 1986.

3) DeWalle and Chian, 1976.

4) Jennett and Dennis, 1975.

5) Plummer et al., 1969.

6) Rittman et al., 1982.

Upflow Anaerobic Sludge Blanket

One of the most widely-used of the so-called second generation anaerobic reactors is the upflow anaerobic sludge blanket reactor (UASB) which was developed by Lettinga et al. in the Netherlands in 1971. A schematic of the UASB is shown in Figure 2.5. The UASB is a continuous anaerobic filter, except that the UASB does not contain attachment media. Wastewater enters the UASB at the bottom and exits at the top. UASB reactors can be successfully applied for the anaerobic treatment of wastewater if well-settling sludges with high methanogenic activity are developed

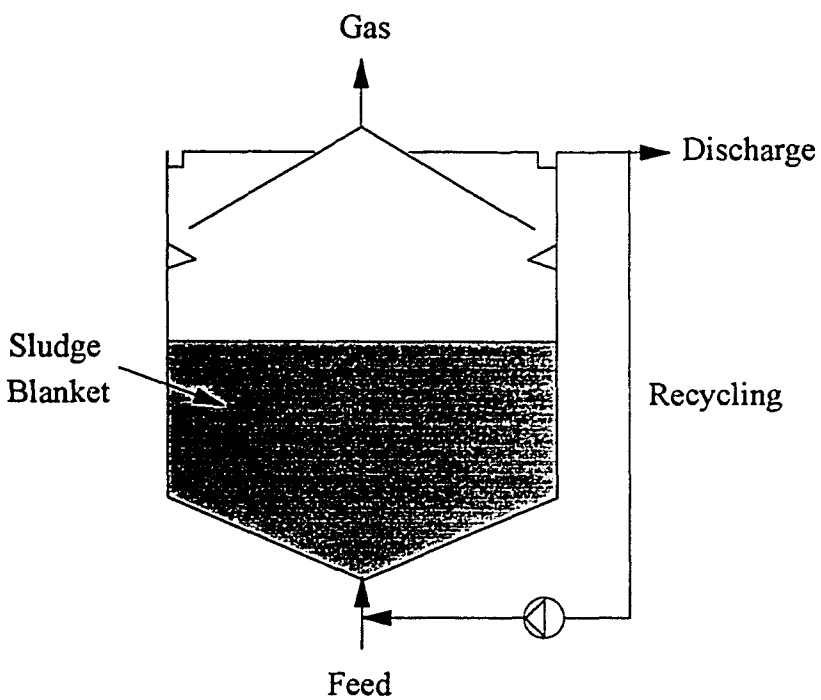

Figure 2.5. Upflow anaerobic sludge blanket

(Lettinga et al., 1980). The formation of granular anaerobic sludge in UASB reactors improves the operational efficiencies of this high rate wastewater treatment process. Not only is a high organic loading rate possible but stability to shocks induced by temperature, loading, and inhibitors is increased (Lettinga et al., 1985).

Due to its good settling velocity (0.012 m/sec.) and high specific activity (4 kg COD removed/kg VSS/day) (Hulshoff Pol et al., 1982), granulated sludge fulfills the essential requirement of any high rate system by retaining a high concentration of active biomass in the reactor. Typical values for the biomass concentrations that can be achieved with granulated sludge range from 40 to 150 g/L (Lettinga et al., 1980). Despite the operational advantages of well-formed granules, the precise mechanisms are not completely understood.

In order to achieve the highest possible sludge hold-up under operational conditions, it is necessary to equip the UASB reactor with a gas/solids separator (Figure 2.6). The sophisticated gas/solids separator is even required for the treatment of very dilute wastewaters (Lettinga and Hulshoff pol, 1991). Proper feed-inlet points and liquid recycle are also required for even distribution of substrate and releasing trapped gas within the granules (Lettinga and Hulshoff pol, 1991). For high-strength wastewaters it is recommended that effluent recycle should be applied in order to dilute the influent COD level to lower than 15 g/L. Treatment of mainly soluble wastewaters has been sufficiently demonstrated, both at full scale and at pilot-plant scale (Lettinga et al., 1979, 1980, 1983, 1984, 1986). Treatment efficiency for a variety of wastewater is summarized in Table 2.11.

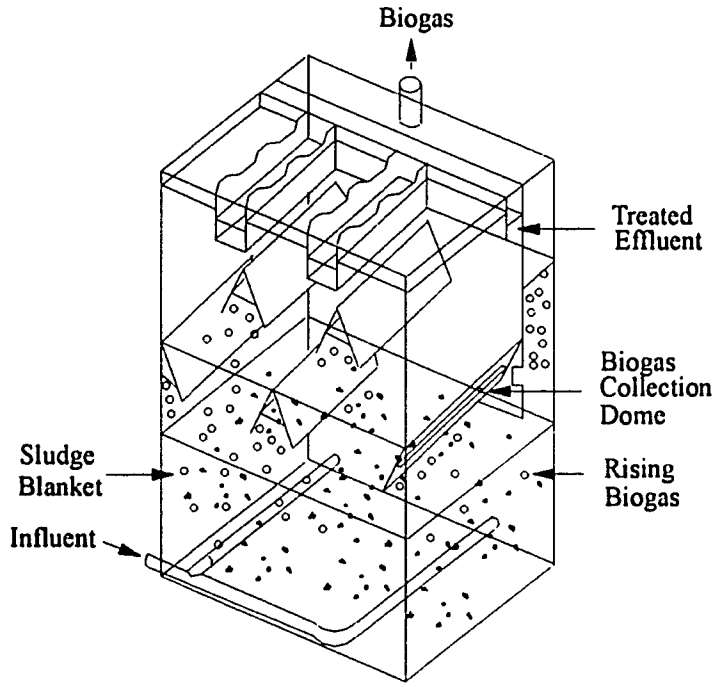

Figure 2.6 Gas solid separator system in the UASB reactor

Fluidized Bed

The fluidized bed (Figure 2.7) developed by Jeris (1982) incorporates an upflow reactor partly filled with sand. The upflow velocity is sufficient to fluidize the sand to fill about 75% of the reactor. A very large surface is provided by the sand and uniform biofilm develops on the sand grains. The internal sand grain markedly increases the net density and settling velocity of the attached biofilm and ensures efficient cell retention within the reactor.

Bacteria attach to the matrix, which may consist of sand, granular activated carbon, glass beads, or a number of other materials. The biofilm covered media is fluidized by a high vertical velocity, demanding a very high degree of recycle. The single particles do not have a

Table 2.11. Operating conditions and performance of various wastewaters using the upflow anaerobic sludge blanket

Wastes	COD g/L	Loading Rate kg COD/m^3/day	Temp. °C	HRT day	Removal, % Soluble	Removal, % Total	Ref.
Potato Processing	3.5-7.1	25-45	35	0.26	84	93	2
Domestic Sewage	0.32-0.95	0.6-2.0	15-20	0.5	---	30-80	2
Calf-Fattening	9.5	4	30	2.4	93	90	2
	9.5	2	25	4.8	90	85	2
Slaughterhouse	2.2	3.0	30	1.4	75	65	3
	2.2	2.5	20	1.1	78	55	3
Sucrose	1.5-3.6	3.2-28.7	35	0.23-0.52	71-98	---	4
Acetate	1.6-3.8	2.5-29.1	35	0.22-0.54	87-97	---	4
Icecream Waste	1.5-3.5	3.0-29.4	35	0.24-0.57	---	78-94	4
Brewery Wastewater	1.0-1.5	4.5-7.0	30	0.2	---	75-80	1
Maize Starch Wastewater	10	10-25	30	0.7	---	90-95	1
Papermill Wastewater	1	4.4	28	0.2	---	72	1

References:

1) Hulshoff pol Pol and Lettinga, 1986

2) Lettinga and Vinken, 1980

3) Samch, de Secuw, and Lettinga, 1984

4) Yang and Anderson, 1993

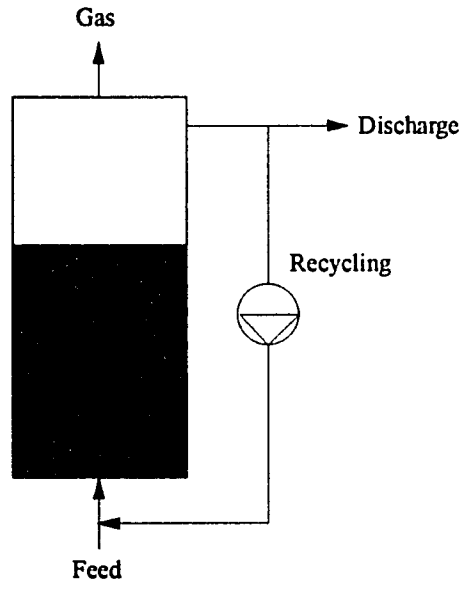

Figure 2.7. Fluidized bed process

fixed position in the bed, but are gently moved around. Therefore, the system is able to overcome the problem of clogging that sometimes occurs in the upflow anaerobic filter, and readily allows passage of refractory particulates that could plug a packed bed.

Operating conditions and treatment performance of various wastewaters using fluidized bed anaerobic processes are shown in Table 2.12. A study conducted by Fox et al. (1990) compared the performance of the fluidized bed reactor with respect to types of media. Results from this study, as shown in Table 2.12, indicate that removal efficiencies for all media were consistently greater than 90%. However, granular activated carbon (GAC) accumulated biomass at a faster rate during start-up than the other media studied, and , therefore, required less time to reach maximum efficiency based on COD removal.

Table 2.12. Operating conditions and performance of various wastewaters using the anaerobic fluidized bed process

Wastes	Media mm	Loading Rate kg BOD/m^3/day	Loading Rate kg COD/m^3/day	Temp. °C	HRT day	Removal, % BOD	Removal, % COD	Ref.
Pulp and Paper wastewater	Resin	0.5	1.1	35	1	67	21	1
		0.8	1.3	35	1	73	46	1
Acetate	GAC		2.8	35	2.3	---	98	3
Acetate	Sand(0.7)	---	10	35	0.5	---	90-97	2
	GAC(0.7)	---	10	35	0.5	---	90-98	2
	Anthracite(0.7)	---	10	35	0.5	---	99	2
	Sand(0.35)	---	10	35	0.5	---	99	2

References:

1) Hakulinen and Salkinoja-Salonen, 1982

2) Fox, Suiden, and Brandy, 1990

3) Wang, Suiden, and Rittman, 1985

Two-phase Anaerobic Process

The two-phase anaerobic process was developed by Ghosh and Poland in 1971. The flow scheme is shown in Figure 2.8. Two anaerobic units of continuously stirred tank reactors were operated in series. The basic idea of two-phase anaerobic digestion is to provide optimal environmental conditions for two different groups of syntrophic bacteria (acidogens and methanogens). The process can be accomplished by maintaining acidogens and methanogens in the first and second reactor, respectively. The principal function of the first reactor is the hydrolysis of complex substrates or particulates into soluble products or small particulates. The end products of acidogenic fermentation (acetate, methanol, and carbon dioxide) are converted into methane gas in the second reactor.

Two-phase anaerobic digestion can avoid system failure due to the severe pH drop since acidogens can function well at low pH (less than 6.0) and keep the same metabolic activity at

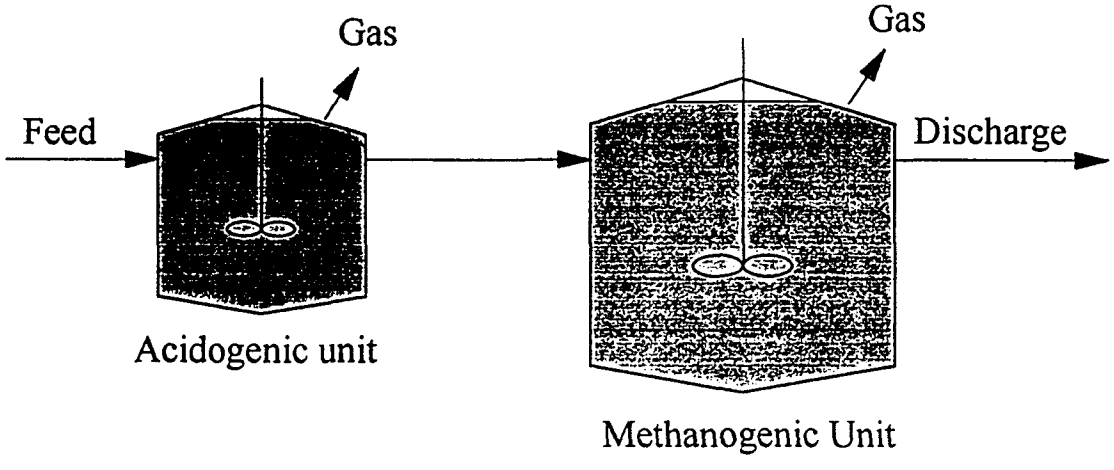

Figure 2.8. Two-phase anaerobic process

the total volatile acid (TVA) concentrations less than 6,000 mg/L (Chyi and Dague, 1994). The potential benefits of two-phase separation in comparison with the conventional one-phase process can be summarized as follows (Cohen et al., 1979).

1) Optimization: The possibility of maintaining optimal environmental condition for each group of organisms and concomitantly increasing the rate of substrate turnover which may allow a reduction in total reactor volume.

2) Increased stability: By means of appropriate control of the loading rate on the methane reactor, mutual adaptation between acid and methane formers can be regulated, and the cessation of methane production by lowered pH or the accumulation of VFAs can be prevented.

3) Sludge disposal: Disposal of relatively fast growing acid forming sludge can occur without loss of methane producing bacteria.

Ghosh reported the performance of single-phase and two-phase digestion on the treatment of primary sludge at 35°C in 1986. In this study, the HRTs (SRTs) and loading rates were controlled at 7 days and 7 kg VS/m^3/day, respectively. At steady-state performance, 34 and 47% more of methane production rate (m^3 CH_4/m^3/day) and VS reduction, respectively, appeared in the two-phase system. Treatment of a high oil content of wastewater using two-phase anaerobic digestion had also shown better methane production than using single-stage anaerobic digestion (Hanaki et at., 1990; Komatsu and Hanaki, 1991). Table 2.13, summary of operating conditions and performance for the treatment of various wastewaters using two-phase anaerobic process, shows that this process is a good candidate for the treatment of high-solids content wastes.

Table 2.13. Operating conditions and performance of various wastewaters using the two-phase anaerobic process

Reactor Combination			Loading Rate	Loading Rate	Temp.	HRT, day		Removal, %		
FP[a]	SP[b]	Wastes	kg COD/m^3/day	kg VS/m^3/day	°C	FP	SP	TCOD	VS	Ref.
UASB	UASB	Distillery	17.2	---	37	0.83	0.58	---	80	5
UASB	Filter	Baby milk	4-7.2	---	20	0.17-0.51	0.5	---	89	6
CSTR	Filter	Cafeteria wastewater	0.4-0.8	---	20	1.25	1	---	80	1
CSTR	CSTR	Glucose	3.2	---	35	0.08-0.33	6	---	95	4
Leachate bed	Filter	Wheat Straw	---	2.6-15	20	1-6	1	---	25-40	3
CSTR	CSTR	Swine Waste	0.63-0.55	---	--	3-6	16	78-85	---	2

[a] First phase.
[b] Second phase.

References:

1) Hanaki, Matsuo, Kumazak, 1990.

2) Jern, 1986.

3) Llabres-Luengo, and Mata-Alvarez, 1988.

4) Roy and Jones, 1985.

5) Shin et al., 1992.

6) Komatsu and Hanaki, 1991.

III. FUNDAMENTAL PRINCIPLES OF ASBR PROCESS

Operating Principles

The operating principles for the ASBR are simple. The ASBR is fed during a discrete period of time and then operated as a batch reactor. After a desired reaction time, the mixed liquor is allowed to settle and the clarified supernatant is decanted from the reactor. The decant is the treated effluent. As illustrated in Figure 3.1, the reactor sequences through four steps in a complete cycle: feed, react, settle, and decant.

The feed step involves the addition of substrate to the reactor. The feed volume is normally equal to the volume decanted during the previous decant step (the effluent). With mixing during feeding, the substrate concentration increases rapidly and metabolic rates increase to their highest values. Mixing can be implemented by a motor driven impeller, a hydraulic circulation pump, or a biogas recirculation pump with a bubble diffuser. The feed volume is determined on the basis of a number of factors, including the desired HRT, organic loading, and expected settling characteristics of the biomass.

The react step is most important in the conversion of organic substrates to biogas. To provide intimate contact between substrate and microorganisms, mixing is required in the react step. Mixing intensity and duration are preferably operated at minimums so that substrate removal and biomass bioflocculation or granulation are not adversely affected. The time required for the react step depends on several parameters, including substrate characteristics, required effluent quality, biomass concentration, and waste temperature.

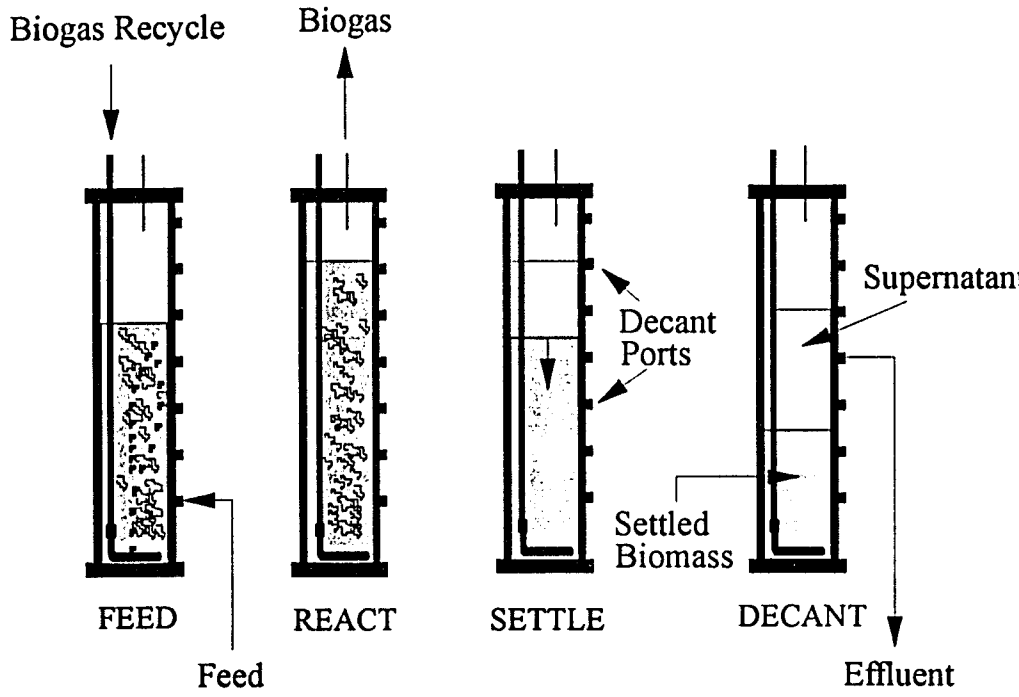

Figure 3.1. Operating steps for ASBR

As will be demonstrated later, these parameters can be incorporated into a model that enables the prediction of react time.

During the settle step, mixing is shut off to enable an ideal quiescent settling condition that allows biomass to flocculate and settle. The reactor itself acts as the clarifier. The time required for clarification varies, depending on biomass settleability, but typically ranges from 10 to 30 minutes. From an operational standpoint, it is essential that the sludge blanket be below a predetermined decanting elevation and that the blanket not rise due to the accumulation of biogas within the settled biomass. As will be discussed later, the concentration and particle sizes of mixed liquor suspended solids (MLSS) in the

reactor are important variables affecting the settling velocity of the biomass and the ability to achieve a clear supernatant for discharge as effluent. An important related variable is the specific process loading rate (food to microorganism ratio, F/M).

The decant step takes place after sufficient solids separation has occurred. The decanting mechanism can be a pot fixed at a predetermined level with the flow regulated by a valve or a pump, or the decant may be an adjustable or floating weir just beneath the liquid surface. The time required for the decant step is governed by the total volume to be decanted during each cycle and the decanting rate. Once the decant step is completed, the reactor is ready to be fed another batch of substrate.

Process Description

The ASBR is a non-steady-state, high rate anaerobic treatment system. By definition of non-steady-state, the system substrate conversion rate and biogas production rate vary during the cycle. The substrate concentration and liquor volume in the reactor increase during the feed step from the lowest level at the beginning to the highest level at the end. The feed step can be simulated as a non-steady state, continuously-stirred reactor with the volume varying with time. In the next step, react step, the liquor volume remains constant and substrate concentration decreases as a function of the react time. The react step in the ASBR is a true batch reactor in which the substrate concentration can be simulated by the batch reactor model.

The unique nature of the ASBR system offers different characteristics as compared to the conventional continuous flow system. Mixed liquor solids are not washed out by

hydraulic surges since mixed liquor can be held in the reactor as long as necessary. No short circuiting occurs in the reactor and no solids or liquid recycle is required. An external clarifier is not involved, since biomass separation occurs internally. The time-oriented nature of the ASBR provides the freedom of changing the operating conditions by simply resetting the feed or decant volume, or resetting the sequence time. This flexibility is not possible in a spacial-oriented continuous flow system.

Anaerobic Bioflocculation and Granulation

Dague and co-authors McKinney and Pfeffer (1966) reported that anaerobic biomass was observed to flocculate in a manner not unlike aerobic activated sludge and that food to microorganism (F/M) ratio was an important parameter affecting anaerobic bioflocculation. At low F/M ratios, the biomass flocculated well and settled rapidly, providing a reactor effluent low in suspended solids. Although not recognized at the time (1966), Dague now reports that what was called "bioflocculation" in the 1966 paper was actually "granulation" in today's (1994) understanding of this term (personal communication from R. R. Dague, the writer's major professor).

An important question is, "How does one maintain a low F/M ratio in order to achieve efficient flocculation and solids separation and still process wastes at a high rate?" A low F/M ratio can be achieved in one or a combination of two ways: 1) lower the food concentration (F) and/or 2) increase the mass of microorganisms (M). There is a limit to the microorganism density that can be achieved in a reactor through solids separation and recycling. The other variable is food concentration (F).

In a continuously-fed, completely-mixed reactor operating at steady-state, the food concentration surrounding the microorganisms is constant. In contrast, in a batch-fed reactor the food concentration is high immediately after feeding and declines until the reactor is fed again, as illustrated in Figure 3.2. The food concentration just prior to feeding is lower in the batch-fed system than at any time in a continuously-fed system. Thus a batch system is capable of achieving more efficient biomass flocculation and solids separation than is possible in a continuously-fed system.

The phenomenon just described is one of the key characteristics of the ASBR process. At any given mixed liquor suspended solids concentration in the reactor, the substrate concentration is high immediately after the feed step is completed. This provides a high driving force for metabolic activity and high overall rates of waste conversion to methane, in accordance with Modod kinetics. Near the end of the react step, the substrate concentration is at its lowest level, resulting in a low gas production rate and providing ideal conditions for biomass flocculation and separation during settle step.

An important feature of the ASBR is the gradual conversion of the flocculent biomass into a well settling and highly active granular biomass. The granulation process can be noticed as the anaerobic microorganisms tend to adhere to one another, as well as to inorganic and/or organic support particles to form firm, dense granules. The ASBR tends to promote the granulation process by imposing a selection pressure during the decant step. The decanting process tends to wash out the poorly settling flocs and dispersed organisms

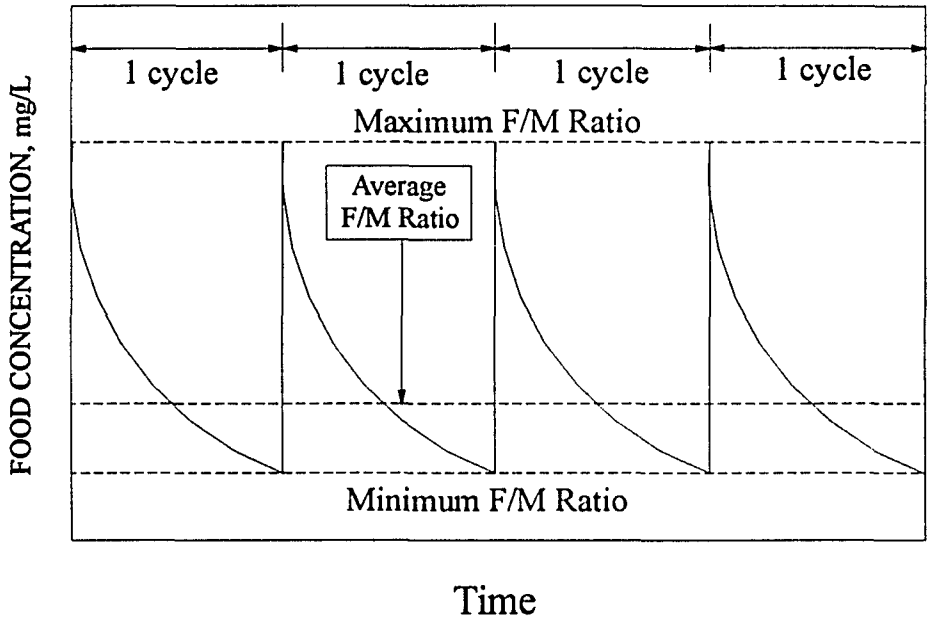

Figure 3.2. Illustration of the effect of batch feeding on food concentration

and selects for the heavier, more rapidly settling aggregates. Thus, over time, granular biomass becomes dominant and leads to a rapidly settling biomass and a highly stable reactor system.

Mixing

Some of the earliest studies on anaerobic digestion assessed the effects of mixing on the kinetics of the process (Streeter, 1937 and 1938). The early work generally concluded that mixing was important and should be continuous and at a sufficient intensity to ensure uniform conditions (temperature, pH, substrate concentration, etc.) throughout the reactor. However, more recently, Dague et al. (1966,1970) conducted fundamental studies on

solids retention in suspended growth anaerobic processes and reported that overly intense mixing could shear the fragile anaerobic bioflocs and result in poor solids separation. It was also reported that mixing need not be continuous, contrary to earlier research. In fact, the research indicated that intermittent mixing (two minutes per hour) actually improved biomass solids separation and overall performance of the reactors, based on COD removal efficiency.

Temperature Compensation

Papers by Dague et al. in 1966 and 1970 reported that equal COD removals could be achieved by an anaerobic activated sludge process operating at temperatures of either 25°C or 35°C. In the reactors that made use of internal solids separation and supernatant wasting, the process compensated for reduced temperatures by increasing the biomass concentration in the reactor. The increase in biomass concentration results from the reduced endogenous decay rates that occur as temperature is lowered.

In the 1970 paper, Dague et al. stated:

"The increase in microbial population at the lower temperature results in a rate of waste removal equal to the rate at the higher temperature. Of course, the organisms must be held in the system efficiently at both temperatures... and the solids retention time must be greater than critical at both temperatures."

The ASBR is highly efficient in holding microorganisms in the reactor as a result of bioflocculation/granulation and low rates of internal gassing during the settling cycle. This enables the system to adjust to significant temperature swings.

IV. EXPERIMENTAL STUDY

The experimental studies were conducted between April, 1991 and March, 1992 in the Environmental Engineering Laboratory located in the Town Engineering Building at Iowa State University, Ames, Iowa. The experimental set-up including four, 12-liter Anaerobic Sequencing Batch Reactors (ASBRs). A synthetic waste of animal-grade, non-fat, dry milk (NFDM) solution was fed to the reactors. The entire set-up was housed in a constant temperature room which was kept at 35 ± 0.5°C for the duration of the experiments.

ASBR Design, Mechanics, and Equipment

A complete ASBR system consists of several components which can be divided into two groups. Group 1 consists of the main reactor body and its operating components: a feed pump, a decant pump, a biogas recirculation pump, a ring diffuser, and a foam separation bottle. Group 2 includes all of the biogas collection components: a gas bag, a check valve, a biogas observation bottle, a sulfide scrubber, a biogas sampler, and a Wet-Test Gas Meter[1]. Each component will be described later in this section. The complete system, using only one of the reactors as an example, is shown in Figure 4.1.

Four reactors, designated A, B, C, and D, with the same active volume of 12 liters, but different depth-to-diameter ratios (Table 4.1) were operated under various conditions of COD load, HRT, and MLSS.

---

[1] Precision Scientific Inc., Cat. No. 63115, Chicago, Illinois 60647.

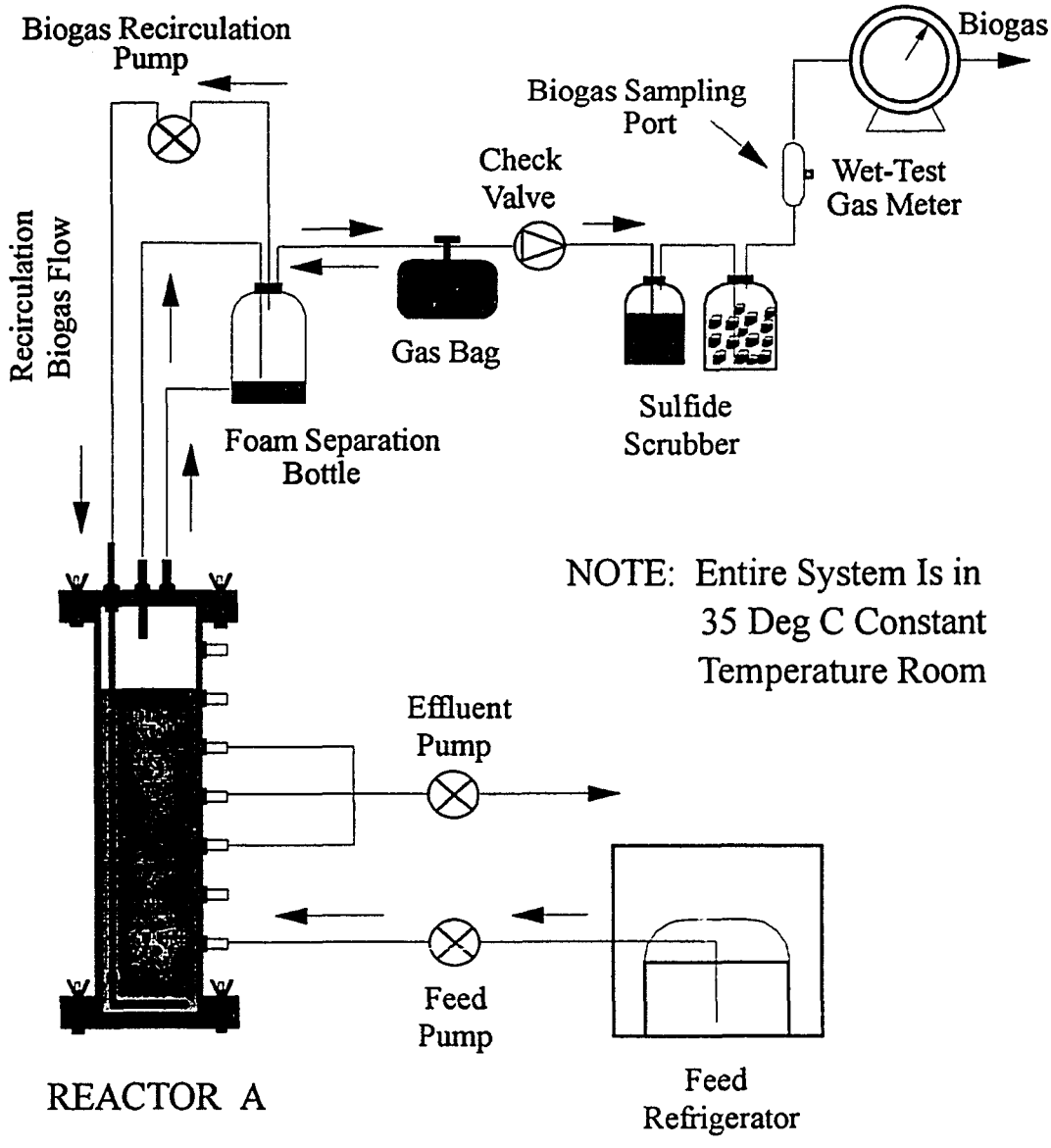

Figure 4.1. Experimental set-up of ASBR

Table 4.1. Physical dimensions of the ASBRs

Reactor	Diameter inch (cm)		Depth[a](active) inch (cm)		Depth/Diameter ratio
A	5.5	(14.0)	30.8	(78.3)	5.60
B	8.0	(20.3)	14.6	(37.0)	1.83
C	10.0	(25.4)	9.3	(23.7)	0.93
D	11.5	(29.2)	7.1	(17.9)	0.61

[a] Liquid depth at volume of 12 liters in the reactor

Main Reactor Body

The main body of each reactor was made of Plexiglas and had the same active volume of 12 liters (0.42 cu ft). A schematic diagram of reactor A is shown in Figure 4.2. Reactor A had the highest depth-to-diameter ratio of 5.6, and had a height of 36 inches (91.4 cm) and an inside diameter of 5.5 inches (14.0 cm). A top lid, 9 inches in diameter, was attached by 12-3/8 inch x 1/2 inch hex-head bolts to a flange that was glued to the reactor. The flanges were sealed by a 0.125 inch O-ring which fits into a groove in the reactor flange. A bottom lid was similarly attached and sealed to the bottom of the reactor. Nine evenly spaced ports designed for feeding, wasting, and sampling, were located on the front side of the reactor. The ports were also made of Plexiglas tubing and had a 0.5 inch (1.3 cm) inside diameter. The ports were glued into holes in the side of the reactor and were reinforced by 1 in x 1 in x 0.25 in Plexiglas plates. A 1/2 inch glass manometer tube, located on the side of each reactor, was interconnected with these side ports to aid in accurately detecting the liquid level inside the reactor. Three other ports were built in the

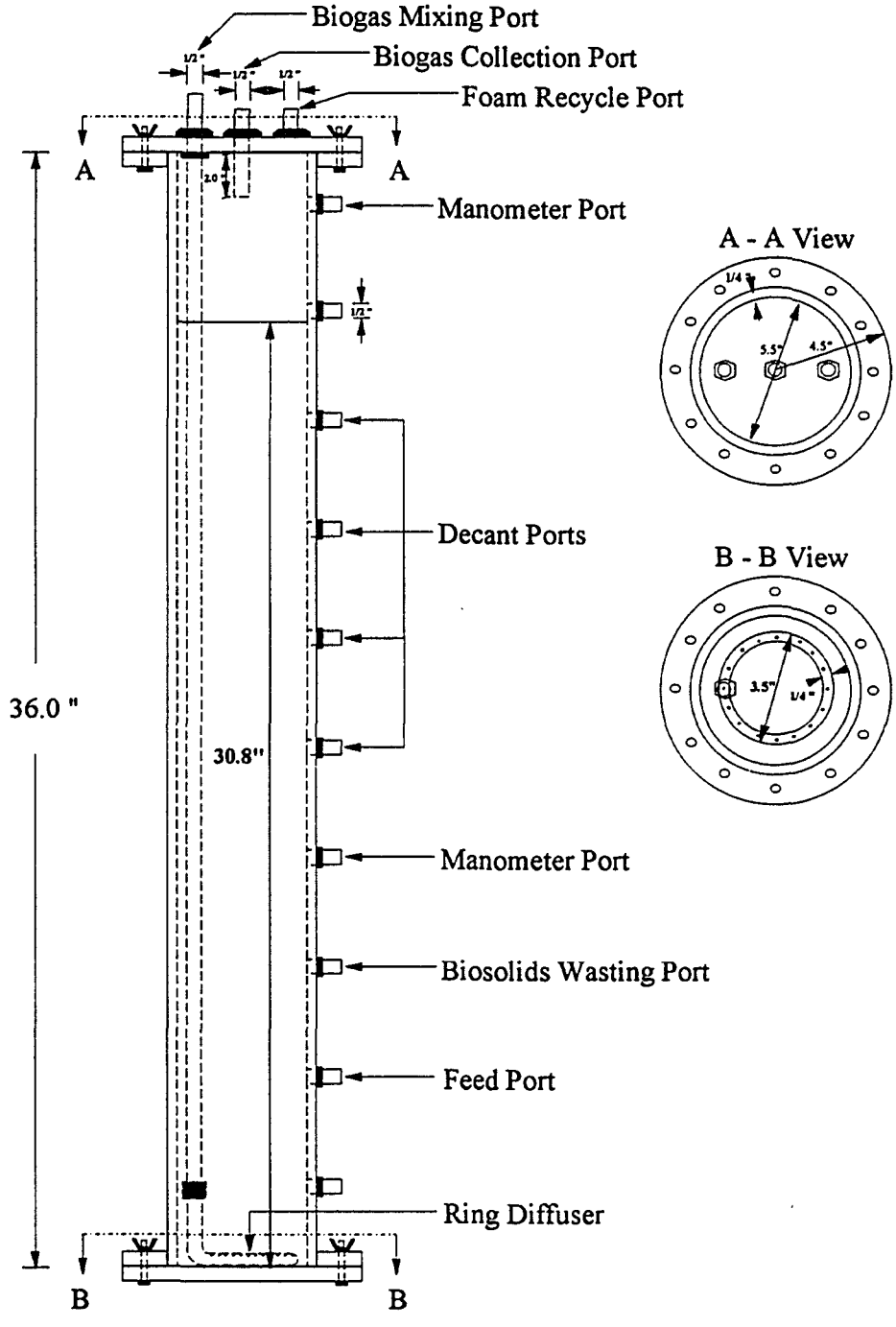

Figure 4.2. Schematic diagram of Reactor A

top lid for the purposes of biogas recirculation, biogas collection, and foam recycle, respectively.

Reactors B, C, and D were designed by the author and fabricated at the ERI Machine Shop at Iowa State University. A few changes in design were made in these three reactors, compared to Reactor A. 1) All the ports were made of stainless steel pipes which were coupled at the side or top of the reactor by a swage-lock fitting. The swage-lock fitting was threaded into the side wall or top lid of the reactor and sealed with Teflon tape. 2) The top or bottom lid of these three reactors was attached by 12-3/16 inch x 1 1/2 inch wing-nut bolts to the reactor flange. 3) A copper tube made ring diffuser was equipped on the bottom of these four reactor (including reactor A) serving as a biogas recirculation mixing device.

The port locations and functions of these four reactors are summarized in Table 4.2. The schematic diagrams of reactors A, B, C, and D are shown in Figures 4.2, 4.3, 4.4, and 4.5, respectively. More than one decant ports were provided in each reactor. The decant port was selected based on the operating HRT of the system. As the HRT was decreased, a lower port was used for decanting due to the larger volume of liquid that was required to be decanted each cycle.

Feed Pump and Decant Pump

A refrigerator, located just outside the 35°C constant temperature room in which the reactors were operated, stores the milk feed. Four, 20-liter rectangular plastic containers were used for feed storage inside the refrigerator. In order to prevent the milk substrate

Table 4.2. Summary of reactor ports and their functions

Reactor	No. of Ports in the Wall	No. of Ports in the Lid	Spacing/Volume[a] inch / Liter	Function	Refer to
A		1		Biogas mixing line	Figure 4.2
A		1		Biogas collection line	
A		1		Foam recycle line	
A	9		4.0/1.56	Feeding, wasting, decanting, sampling, and manometer	
B		1		Biogas mixing line	Figure 4.3
B		1		Biogas collection line	
B		1		Foam recycle line	
B	9		2.0/1.65	Feeding, wasting, decanting, sampling, and manometer	
C		1		Biogas mixing line	Figure 4.4
C		1		Biogas collection line	
C		1		Foam recycle line	
C	8		1.5/1.93	Feeding, wasting, decanting, sampling, and manometer	
D		1		Biogas mixing line	Figure 4.5
D		1		Biogas collection line	
D		1		Foam recycle line	
D		5[b]	1.0/1.70[b]	Feeding, decanting, and manometer	
D	1			manometer	
D	1			Sampling	

[a] Decanting volume difference between two adjacent ports.
[b] Five vertical tubes with the active lengths (only the length inside the reactor) of 3, 4, 5, 6, and 7 inches, respectively; two adjacent length tubes has decanting volume difference of 1.70 liters.

from spoiling, as it was pumped across the floor of the constant temperature room, the feed tubing was encased in an insulated cold water jacket. Cold water was pumped by a peristaltic pump[2], with a size 18 pump head[3], out of the freezer portion of the refrigerator, through the cold water jacket and back into the freezer where it was re-cooled. Four feed

[2] Masterflex peristaltic pump (50 to 600 rpm), Cat. No. L-07553-50, Cole-Parmer Company, Chicago, Illinois.
[3] Materflex pump head (size 18), Cat. No. L-07018-21, Cole-Parmer Company, Chicago, Illinois, 60648.

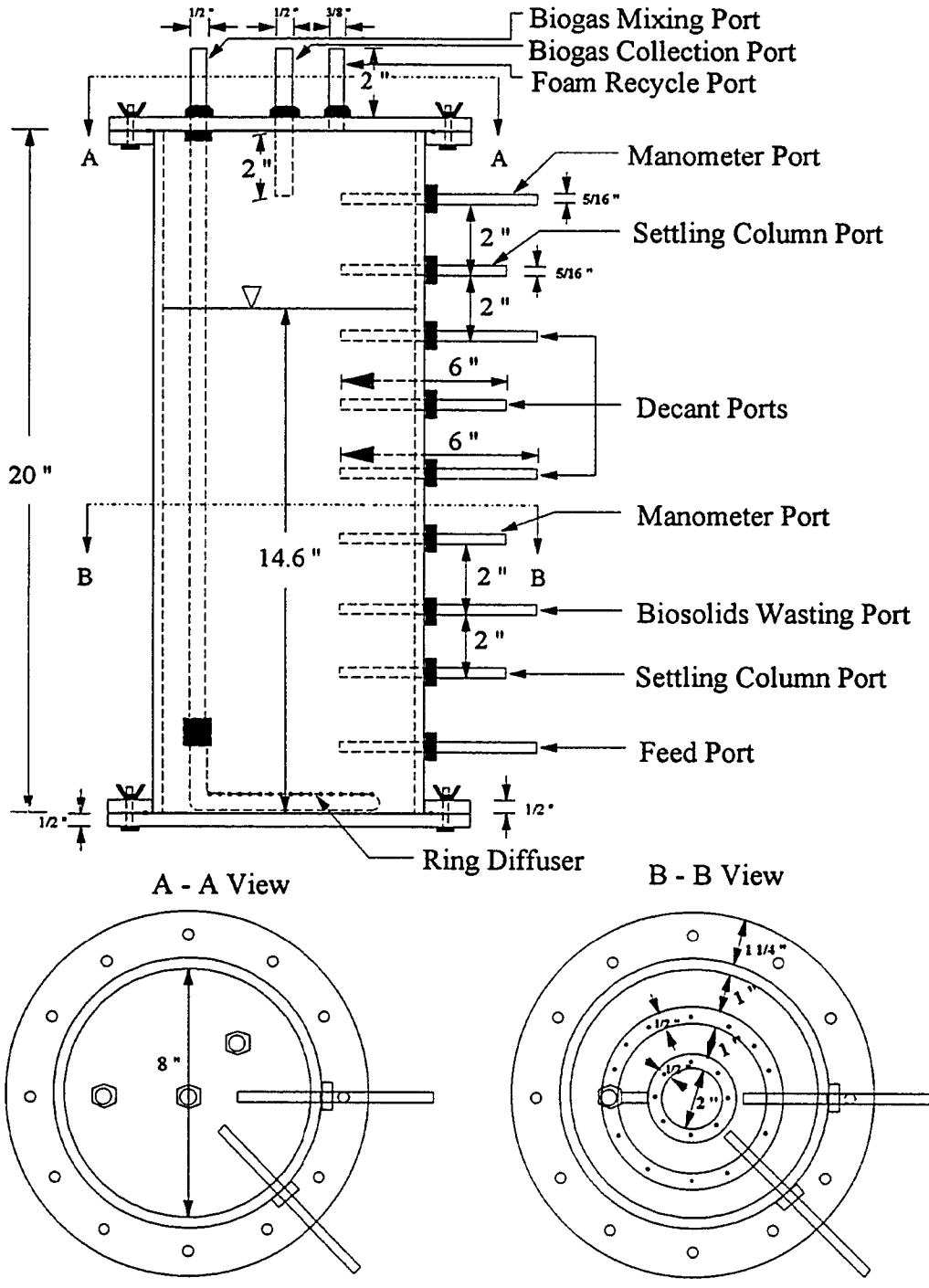

Figure 4.3. Schematic diagram of Reactor B

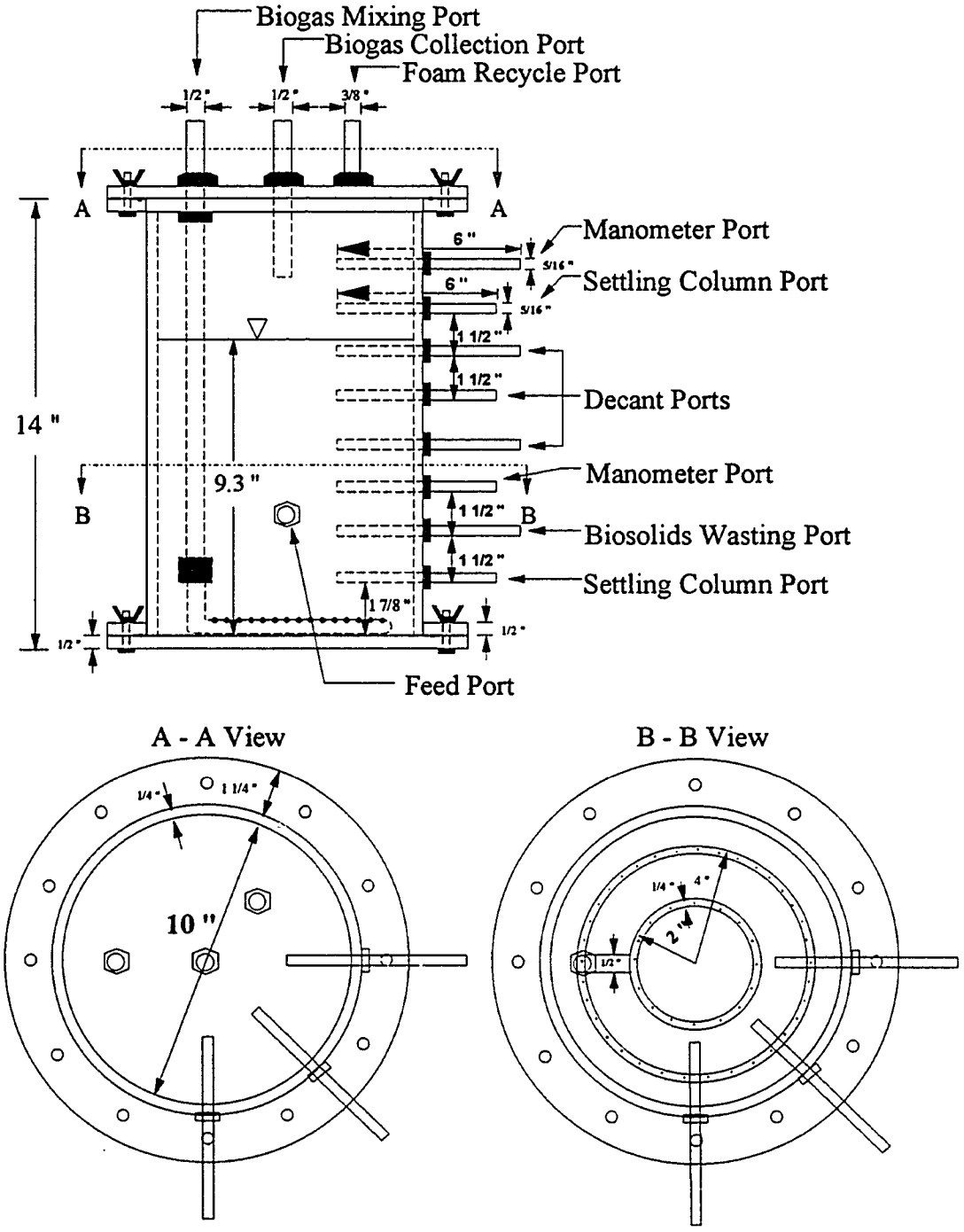

Figure 4.4. Schematic diagram of Reactor C

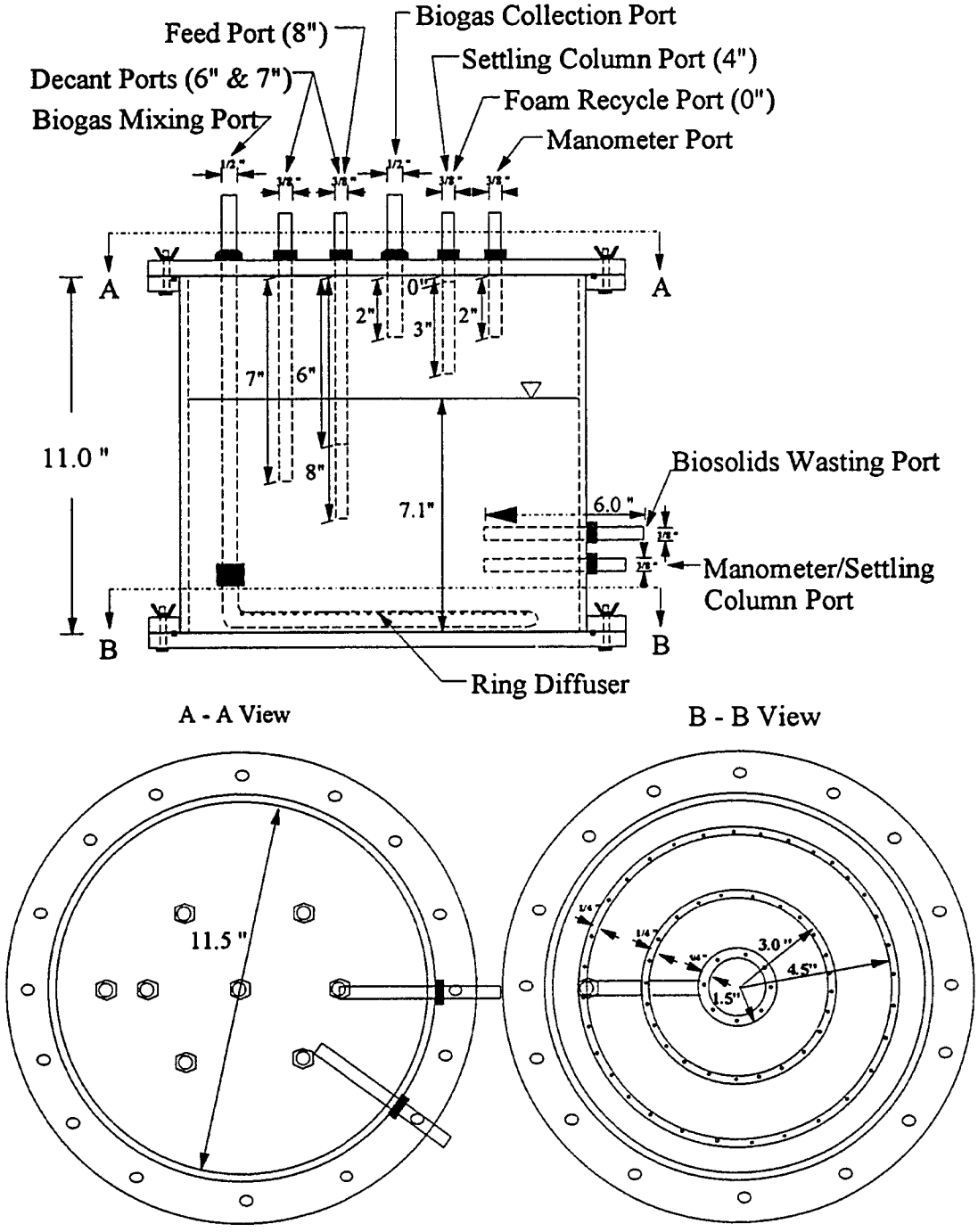

Figure 4.5. Schematic diagram of Reactor D

pumps located beside the refrigerator transported the milk feed from the containers in the refrigerator to the reactors in the constant temperature room through the cold water jacket. The feed pumps were precise ten-turn potentiometer, peristaltic pumps[4], fitted with a size 17 pump head[5]. The flow rate of the feeding pump was calibrated once a week to maintain a constant feed volume.

The decant pump removed the supernatant from one of the ports on the side or top of the reactor to a 20-liter rectangular plastic effluent container. Which decanting port was connected depends on the predetermined effluent volume to be decanted. The volume difference between two adjacent ports for each reactor is shown in Table 4.2. The decanting peristaltic pump[6] had a single turn potentiometer and utilized a size 18 pump head.

Three microprocessor-based timer/controller[7] were used to turn the pump on and off at predetermined intervals. Each timer had four circuit outlets and could control the operation of four pumps. One timer was used to control the feed pumps of the four reactors and the other two times were used to operate the decant pumps and the biogas mixing pumps.

---

4 Masterflex peristaltic pump (6 to 600 rpm), Cat. No. L-07520-25, Cole-Parmer Company, Chicago, Illinois 60648.

5 Materflex pump head (size 17), Cat. No. L-07017-21, Cole-Parmer Company, Chicago, Illinois, 60648.

6 Masterflex peristaltic pump (1 to 100 rpm), Cat. No. L-07553-30, Cole-Parmer Company, Chicago, Illinois 60648.

7 Chrontrol Model CD-4, Cat. No. L-08614-00, Cole Parmer Company, Chicago, Illinois 60648.

Ring Diffuser, Biogas Recirculation Pump, and Foam Separation Bottle

The main component used to mix the reactor contents was the copper tubular ring bubble diffuser which rested on the bottom lid of the reactor. The schematic diagrams of the diffuser in each reactor are also shown in Figure 4.2, 4.3, 4.4, and 4.5. On the top of the diffuser tube, a series of orifices with 1/32 inch openings and spacings varying from 1 to 2 inches were placed and create bubbles which agitated the reactor contents as they rose to the surface. The diffuser was fed by a 1/2 inch stainless steel pipe, which was fixed to the top of the reactor by a swage-lock fitting. The biogas recirculation pumps[8] of reactors A and B were fitted with a size 18 pump head, and those for the reactors C and D were fitted with two pump heads of size 18 and size 17. Each recirculation pump was connected to the stainless steel pipe by tygon tubing. The recirculation pump drew biogas from a foam separation bottle[9], which drew biogas from the biogas collection port at the top of the reactor. The 4-liter foam separation bottle was used to hold the foam until it condensed to a liquid state. Once the foam collapsed, the liquid flowed back into foam recycle port at the top of the reactor. The foam separation bottle was needed to prevent any solids that might be carried in the foam from plugging the orifice of the ring diffuser.

---

[8] Masterflex peristaltic pump (6-600 rpm), Cat. No. L-07553-20, Cole-Parmer Instrument Company, Chicago, Illinois 60648.

[9] Aspirator bottle (outlet/tubing), Cat. No. 02-972F, Fisher Scientific Company.

Biogas Collection System

The biogas collection system included six components: a gas bag, a check valve, a biogas observation bottle, a H_2S scrubber, a gas sampler, and a Wet-Test Gas Meter.

Gas Bag A gas bag was necessary for the batch reactor with a closed-loop gas handling system. The main function of the gas bag was to provide for the displacement of biogas during the decant period. As the reactor was decanted, biogas was pulled from the gas bag and the bag deflated to maintain a constant pressure in the gas collection system. Thus, the working volume of the gas bag must be at least as great as the largest volume that was decanted from the reactor at any one time. Each ASBR system in this experiment was equipped with a 20-liter polyvinyl plastic gas bag in the biogas collection system (connected right after the foam separation bottle).

Check valve and observation bottle A polyethylene check valve[10] followed the gas bag in the biogas collection system for each reactor set-up. Thus, biogas could flow from the gas bag and through the check valve but not in the reverse direction.

The observation bottle consisted of a 0.95 liter (32 oz) wide month glass bottle partially filled with water and sealed with a rubber stopper. Two, 3/8-inch glass tubes were inserted into the stopper. One of them was connected to tubing from the check valve

---

[10] Nalgen check valve, Cat. No. 15-339-2, Fisher Scientific Company.

and submerged into the water in the bottle. The other tube just penetrated the stopper and was connected to tubing leading to the biogas scrubber.

Hydrogen sulfide scrubber When protein or sulfate containing substrate is anaerobically degraded, hydrogen sulfide (H_2S) is formed in the gas phase. Hydrogen sulfide is extremely toxic to human beings and also corrosive to metal objects.

The device used for removing H_2S gas in the experiment was the H_2S scrubber. The scrubber consisted of a 0.95 liter (32 oz) wide-month glass bottle. The bottle was filled with pieces of sponge soaked in ferric oxide. Two, 3/8-inch glass tubes were inserted into a rubber stopper. The influent tube extended nearly to the bottom of the scrubber while the exit tube just penetrated the stopper.

Removal of H_2S from the gas phase is chemisorption by ferric oxide:

$$Fe_2O_3 \cdot 3H_2O + 3\,H_2S \rightleftharpoons Fe_2S_3 + 6\,H_2O \qquad (4.1)$$

After the ferric oxide, a red colored substance, fully reacts with hydrogen sulfide in the scrubber, a black colored product of ferric sulfide is produced. When sufficiently black, the scrubber needs to be taken out of the service and regenerated by introducing excess air through the bottle in order to restore its proper function. The ferric oxide regeneration reaction can be described by the equation below.

$$Fe_2S_3 + 3/2\,O_2 + 3\,H_2O \rightleftharpoons Fe_2O_3 \cdot 3H_2O + 3\,S \qquad (4.2)$$

The sulfur is a nontoxic end product of the regeneration reaction. It comes from the highly toxic H_2S and finally deposits on the surface of the sponge. The regeneration was carried out by blowing the air through the scrubber for 3 to 4 hours. The regeneration schedule of

the scrubber was approximately 60 days.

Gas sampler and Wet-Test Gas Meter A 50 ml gas sampler[11] was fitted with a septum to facilitate biogas sampling. The Wet-Test Gas Meter positioned after the gas sampler was used to measure biogas production. The device was a rotating drum-type gas meter and was calibrated in the factory to an accuracy within $\pm 0.5\%$ and a least count of 0.01 liter. The biogas exiting the meter was drawn through a laboratory exhaust fan.

Intercomponents Connection

Tygon tubing was used to connect the various components of the system. The 5/8 inch x 1/16 inch tubing was fitted around ports and the glass manometer tube, 3/8 inch x 1/16 inch tubing was fitted to the glass tubing on the biogas observation bottle and gas scrubber, and 3/16 inch x 1/16 inch tubing was fitted to the gas sampler. To close off the tygon tubing fitted on the side and top ports of the reactor, the tubing was clamped with Hoffman screw clamps[12]. Tygon tubing was also used for pump head tubing. The 5/16 inch x 1/16 inch, 1/4 inch x 1/16, and 1/8 inch x 1/16 inch sized tubing fitted the size 18, 17, and 16 pump head, respectively. Interchangeable polyethylene connectors[13] were used to connect the different sized tubing and pump head tubing.

---

[11] Manufactured by the Iowa State University Glass Blowing Shop, Ames, Iowa 50011.

[12] Cat. No. 05-875-A, Fisher Scientific Company.

[13] Cat. Nos. 15-315A, 15-315B, and 15-315C, Fisher Scientific Company.

Substrate and Nutrients

The organic feed stream was provided by non-fat dry milk (NFDM)[14]. Dry milk was used because it is easily diluted with tap water to produce the desired feed strength and it can be stored in bulk for long periods of time. Additionally, it contains some essential nutrients. The NFDM had a COD of 1.04 g COD/g NFDM. The properties of the NFDM are shown in Table 4.3. To insure that the systems were not inhibited due to trace mineral deficiencies, the NFDM was supplemented with the minerals of the types and amounts shown in Table 4.4.

Table 4.3. Properties of the non-fat dry milk (NFDM).

Parameter	Value
Chemical Oxygen Demand, g/g NFDM	1.04
Five-day Biochemical Oxygen Demand, g/g NFDM	0.49
Total Kjeldahl Nitrogen, %	5.4
Total Phosphate, as PO_4, %	2.2
Lactose, %[a]	51.0
Protein, %[a]	>36.0
Fat, %[a]	<1.0
Ash, %[a]	8.2
Trace Minerals[a]:	
Iron, ppm of NFDM	4.6
Nickel, ppm of NFDM	1.0
Cobalt, ppm of NFDM	0.8
Molybdenum, ppm of NFDM	3.0
Zinc, ppm of NFDM	15.0

[a] Source of data is Swiss Valley Farms, Inc., Davenport, Iowa.

[14] Purchased from J. M. Swank Company, West Liberty, Iowa 52776.

Table 4.4. Recipe for trace mineral stock solution.

Chemical Compound	Concentration	Criteria[a]
$FeCl_2 \cdot 4H_2O$	35.60 g/L	Fe = 200 ppm
$ZnCl_2$	2.08 g/L	Zn = 20 ppm
$NiCl_2 \cdot 6H_2O$	4.05 g/L	Ni = 20 ppm
$CoCl_2 \cdot 6H_2O$	4.04 g/L	Co = 20 ppm
$MnCl_2 \cdot 4H_2O$	3.61 g/L	Mn = 20 ppm

[a] The numbers shown are the ratios of the element to the quantity of NFDM on a dry weight basis. For example, Fe = 200 ppm means that 200 parts of iron were added per million parts of NFDM.

Alkalinity was added to the substrate in the form of sodium bicarbonate ($NaHCO_3$). The quantity of alkalinity was established on the basis of the alkalinity to COD ratio (Alk/COD) that would maintain the pH of the reactors within the 6.9 to 7.2 range. The specific Alk/COD ratios and the resulting alkalinity, as $CaCO_3$, for the various COD loadings and HRTs investigated are shown in Table 4.5.

The substrate was prepared in batches of 13 liters for the HRT runs of 48 and 24 hours, and in the batches of 17 liters for the HRT runs of 12 hours. Proper amounts of

Table 4.5. Alkalinity addition recipe at the various COD loads and HRTs investigated.

COD Load	Hydraulic Retention Time, hours					
	48		24		12	
g/L/day	Alk/COD	Alkalinity	Alk/COD	Alkalinity	Alk/COD	Alkalinity
2	0.11	458	0.16	350	0.46	458
4	0.10	801	0.15	613	0.40	801
6	0.07	916	0.12	700	0.30	916
8	0.07	1145	0.11	875	0.28	1145
10					0.27	1374
12					0.23	1374

NFDM, sodium bicarbonate, and minerals were mixed with water in a blender. The substrate mixture was then transferred into the 20 liter plastic container and tap water was added to a total volume of 13 liters or 17 liters. The plastic container was then agitated to completely mix the contents. Each reactor system had its own substrate container that was stored in the refrigerator at 5°C while the substrate was pumped to the reactors.

ASBR Operating Procedures

Leakage Check

A gas leak check was a necessary procedure to be carried out once the equipment was assembled and prior to seeding the reactors. A leak detection device was fabricated and used by the author. A schematic diagram of the leak detector is shown in Figure 4.6. The testing procedures involved three steps. In the first step, the section to be checked in the ASBR system was selected and both the section ends closed with clamps. The second step involved raising the hydraulic pressure by adding water in the Plexiglas column and maintaining a hydraulic pressure of at least 3 feet (90.5 cm) in the section checked. Then the water level in the Plexiglas column watched for 10 minutes. If the water level remained the same after 10 minutes, it implied a leak proof condition for the section tested. Contrarily, a drop in water level revealed a leak in the section tested. The location of the leak could be detected by narrowing the number of components in the test section and repeating the checking procedures until the leak was found. Small leak was fixed with silicone caulking. Once all the leaks were detected and fixed, the reactors were ready to be seeded.

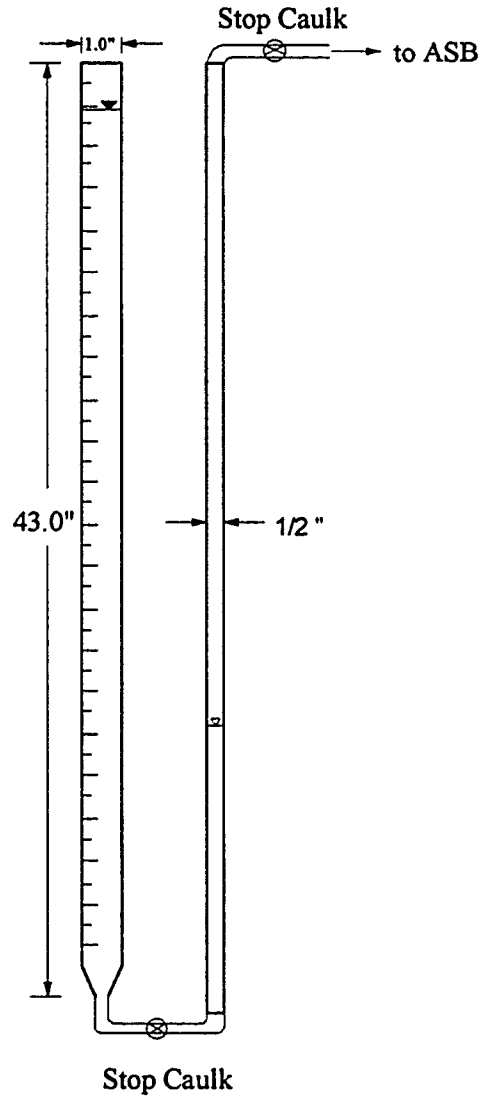

Figure 4.6. Schematic diagram of the leak detection manometer

Mixing Intensity Adjustment

In order to precisely study the reactor configuration effects in the ASBR system, the same mixing intensity was maintained in all four reactors. Mixing intensity can be measured in terms of velocity gradient. A gentle mixing pattern was created by biogas recirculation. A reasonable velocity gradient of 100 1/sec was maintained in the four reactors throughout the entire study.

The biogas mixing intensity has been estimated using the isothermal energy dissipation theory (USEPA, 1979). Assuming biogas bubbles produced at pressure P_2 (orifices on the diffuser top) and allowing for an isothermal expansion to pressure P_1 (liquid surface in the reactor), the energy dissipation rate (E) and the mean velocity gradient (G) resulting from the expansion are:

$$E = P_1 \cdot Q_g \cdot \ln(P_1 / P_2) \tag{4.3}$$

$$G = (E / (V \cdot \mu))^{1/2} \tag{4.4}$$

Where, E = energy dissipation rate (power), kW;

G = mean velocity gradient, 1/sec;

P_1 = pressure at biogas production point, kN/m^2;

P_2 = pressure at biogas expansion, kN/m^2;

Q_g = biogas flow rate at P_1, m^3/s;

V = liquid volume of the reactor, m^3;

μ = Newton's viscosity of the liquid, $kN\text{-}sec/m^2$.

The velocity gradient in each reactor can be calculated using Equations 4.3 and 4.4. An average barometer reading of 740 mm Hg in the city of Ames and the reactor volume of 1.2×10^{-2} m^3 were used in the velocity gradient calculations. The Newton's viscosity value of the mixed liquor was assumed constant at 0.726 kN-sec/m^2, which is the viscosity of water at 35°C. The pressure at the reactor head space (P_2) can be measured by a manometer and the pressure at orifices of the diffuser is equal to the sum of P_2 and the hydraulic pressure of the liquid above. In the ASBR system, the biogas is recirculated by a ten-scale potentiometer, peristaltic pump. The biogas flow rate can be adjusted by turning the scale button between the numbers 0 through 10 on the pump control box. The velocity gradient is a function of the mixing biogas flow rate and the reactor active depth. For a particular reactor, velocity gradient is a sole function of the mixing biogas flow rate, since the active depth remains constant. In order to measure the biogas flow rate in the diffuser, a Wet-Test Gas Meter was connected in biogas recirculation line between the recirculation pump and the diffuser. The summary of the biogas flow measurement data and calculations of velocity gradients for Reactor A, B, C and D are presented in Section A of the Appendix. The plots of the velocity gradient versus the biogas flow rate and the associated potentiometric scale on the recirculation pump for each ASBR are shown in Figure 4.7, 4.8, 4.9, and 4.10, respectively. The recirculation pump operating potentiometric scales at the velocity gradient of 100 1/sec are indicated in the figures. For example, a 3.5 scale is indicated in Figure 4.7 for the recirculation pump in Reactor A.

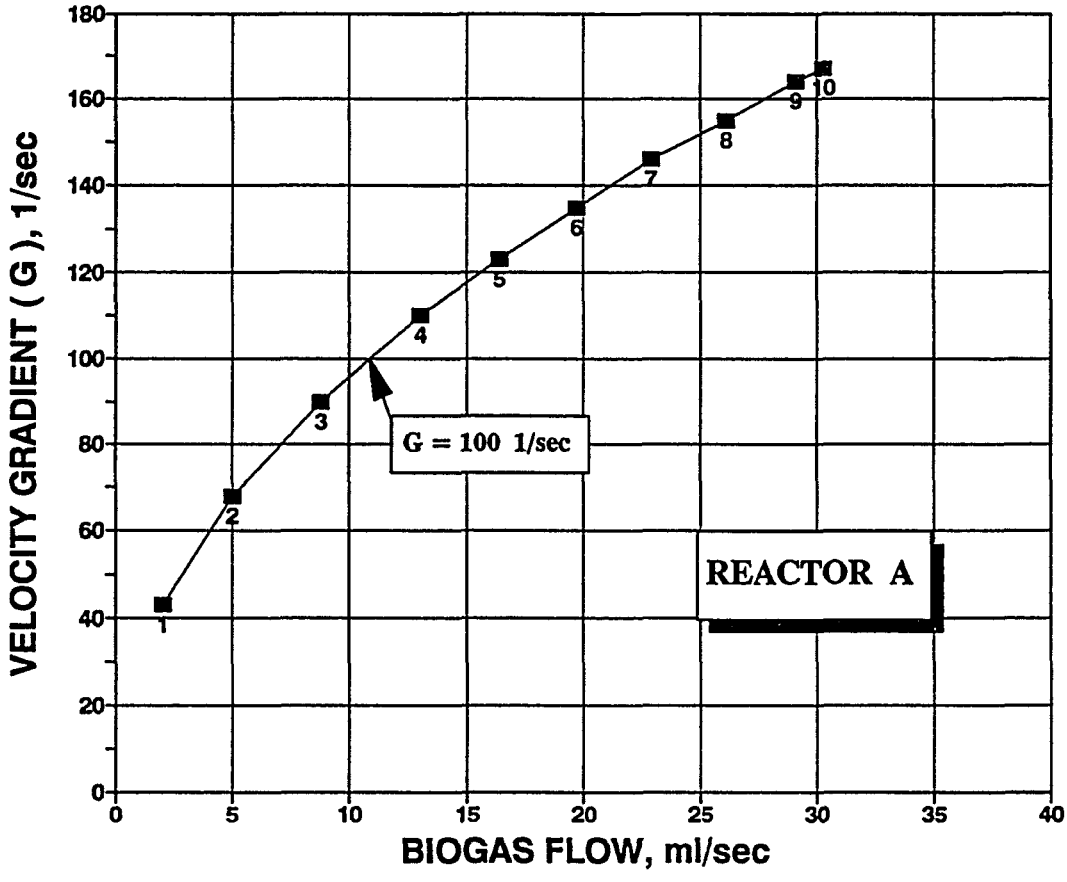

Figure 4.7. Velocity gradient calibration curve for biogas recirculation pump of Reactor A

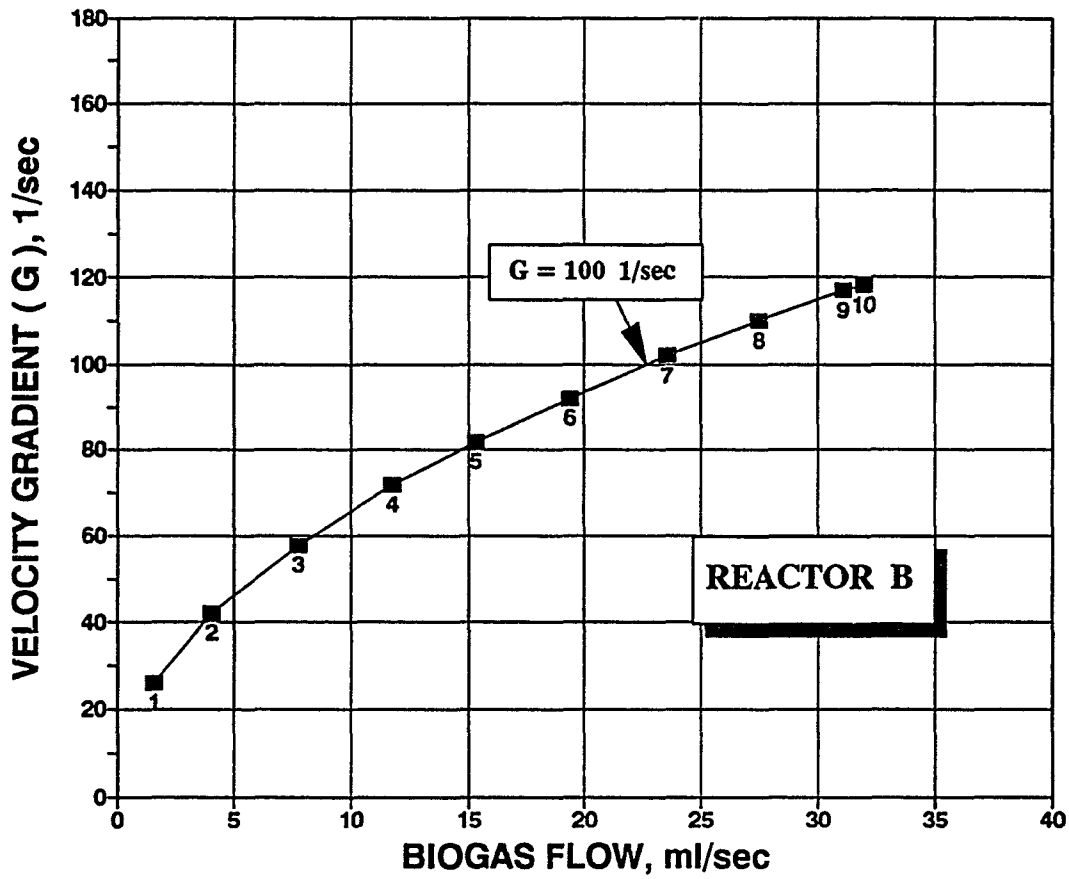

Figure 4.8. Velocity gradient calibration curve for biogas recirculation pump of Reactor B

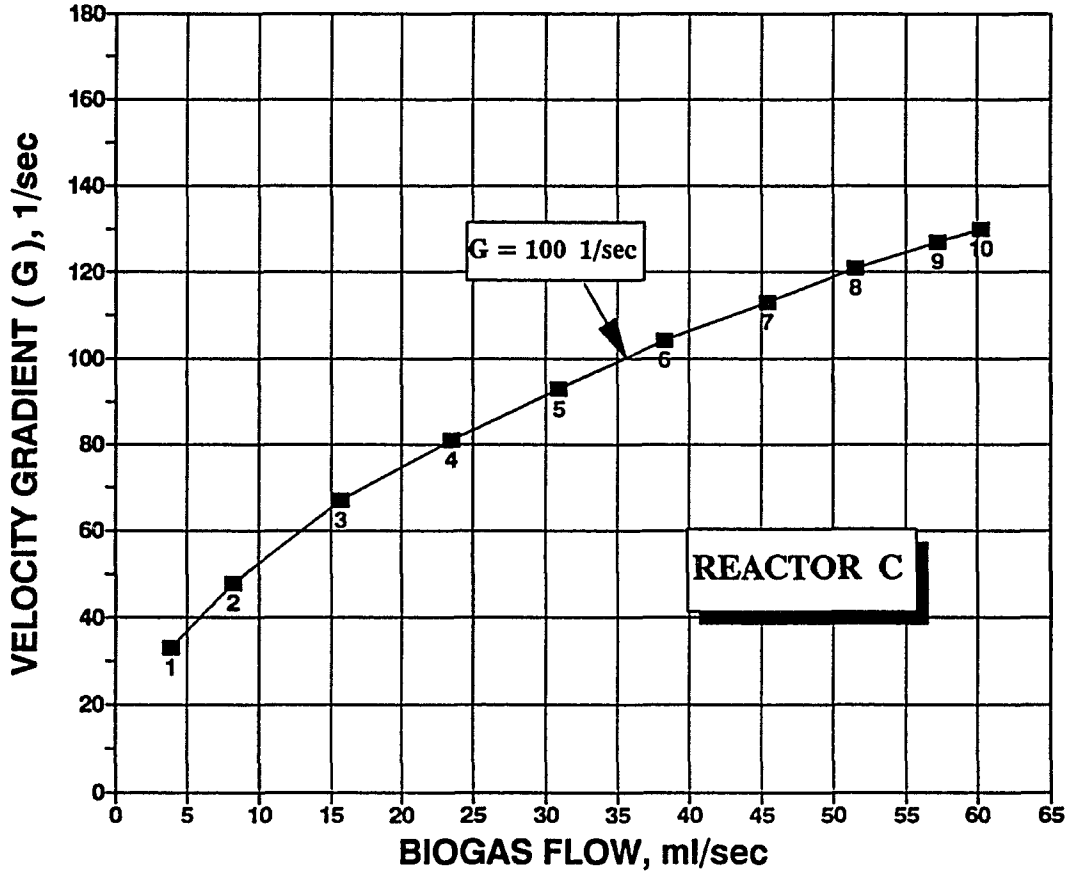

Figure 4.9. Velocity gradient calibration curve for biogas recirculation pump of Reactor C

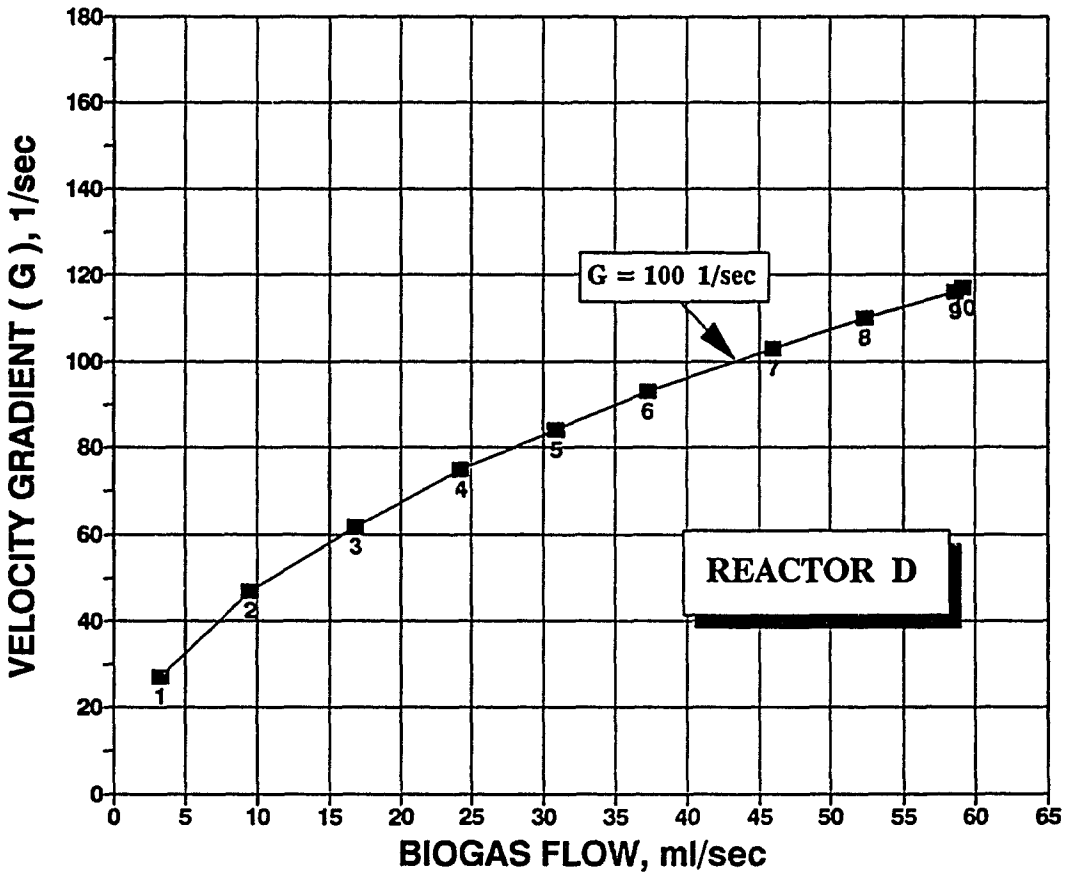

Figure 4.10. Velocity gradient calibration curve for biogas recirculation pump of Reactor D

Start-up and Acclimation

Ten gallons of primary anaerobic digester sludge were obtained from Water Pollution Control Plant of Ames, Iowa on April 15, 1991. The digester sludge was blended with 2-liter biomass transferred from an ASBR which had been previously used by Habben (1991) for the degradation of NFDM. The sludge from both sources was first screened through a sieve (U.S. Standard Sieve No. 20) with an opening of 0.841 mm and then through another sieve (U.S. Standard Sieve No. 45) with an opening of 0.354 mm. The screened sludge with a total suspended solid concentration of 25,500 mg/L was then seeded into each reactor. Each reactor received about 4 liters of the seed and 8 liters of warm tap water to make a total 12 liters active volume.

Once the reactor was seeded, the system was flushed for 10 minutes with nitrogen gas to remove oxygen from the gaseous areas in the system (reactor head space, tubing, foam separation bottle, etc.). The reactor contents were mixed during the last 5 minutes of the flushing procedure to enhance the removal of dissolved oxygen in the liquid phase. Initial substrate was fed 24 hours after seeding into the reactor at a COD loading of 2.0 g/L/day. The reactor was mixed for 5 minutes once per hour for a cycle length of 6 hours. After a four week acclimation period, the substrate feed sequence was started at the desired loading and the rest of the operational sequence was implemented.

Experimental Operation

The experimental ASBRs were operated at HRTs of 48 hour, 24 hour, and 12 hour over a range of COD loadings, as shown in Table 4.6 for the four reactors. The upper

loading rates were determined based on reactor performance. The maximum load possible, up to biosolids washout, was the load limit for each HRT during the experiments.

Two different cycle lengths of 6 hours and 4 hours were used in this study. The 6 hour-cycle (15 min of feed time, 5 hour of react time, 10-30 min of settle time, 15 min decant time, and 0-20 min idle time) was operated at HRTs of 48 hour and 24 hour. The 4 hour-cycle (15 min of feed time, 3 hour and 15 min of react time, 10 min of settle time, 15 min decant time, and 5 min idle time) was operated at an HRT of 12 hour. Intermittent mixing was used throughout the COD removal performance study and consisted of 5 min of mixing every hour. The rest of the sequence information is shown in Table 4.7.

Table 4.6. Hydraulic retention times and COD loadings investigated.

HRT, hours	COD Loadings for the HRTs Shown, g/L/day			
	Reactors			
	A	B	C	D
48	2,4,6,8	2,4,6,8	2,4,6,8	2,4,6,8
24	2,4,6,8	2,4,6,8	2,4,6,8	2,4,6,8
12	2,4,6,8	2,4,6,8	2,4,6,8,10,12	2,4,6,8,10,12

Pseudo steady-state conditions at each specific loading were assumed to be achieved if the daily average methane production rate varied within $\pm 3\%$ for at least three consecutive days and the reactor biosolids were not in a washout condition. Steady-state samples were taken at various locations in each ASBR system with regard to the following

procedures:

(1) Gas meter readings were recorded and biogas was sampled for immediate gas content analysis using Gas Chromatography.

(2) Influent feed volume was measured and influent was sampled for COD analysis.

(3) Effluent was collected in a 20 liter container and a well mixed sample was obtained from the container for the solids, COD, alkalinity, and volatile acids analyses.

(4) Mixed liquor was sampled from the sampling port for solids analyses.

Table 4.7. Operating sequence information of the ASBRs

Sequence Characteristic	HRT, hour		
	48	24	12
Number of sequences per day	4	4	6
Length of sequence, hours	6	6	4
Substrate processed per day, liters	6	12	24
Volume decanted per sequence, liters	1.5	3	4
Length of feed period, minutes	15	15	15
Schedule[a]	0:00-0:15	0:00-0:15	0:00-0:15
Length of react period, hours	5	5	3.25
Schedule[a]	0:15-5:15	0:15-5:15	0:15-3:30
Length of settle period, minutes	30	15-25	10
Schedule[a]	5:15-5:45	5:15-5:40	3:30-3:40
Length of decant period, minutes	15	15	15
Schedule[a]	5:45-6:00	5:40-5:55	5:25-5:40
Intermittent mixing schedule[a]	0:10-0:15 1:10-1:15 2:10-2:15 3:10-3:15 4:10-4:15 5:10-5:15	0:10-0:15 1:10-1:15 2:10-2:15 3:10-3:15 4:10-4:15 5:10-5:15	0:35-0:40 1:35-1:40 2:35-2:40 3:35-3:40

[a] Assume the sequence starting from feed phase at 0:00 (hour:min).

Steady-state performance data were then analyzed to evaluate the stability of the ASBR system and reactor configuration effects under various operational conditions.

Other Studies

Mixing pattern study The ASBR performance throughout the sequence was compared between intermittent mixing and continuous mixing. Three different intermittent mixing patterns and a continuous mixing pattern (1. 5 min/hour, 2. 2.5 min/30 min, 3. 100 sec/20 min, 4. continuous mixing) were investigated in both reactors A and B. Biogas production and COD remaining throughout the sequence were monitored. This was accomplished by measuring the biogas production at several periods during the sequence, and by taking samples every 20 to 30 minutes throughout the sequence and performing COD analyses on them. Biogas characteristics were determined by GC analysis to determine the methane production during the sequence. This mixing study was conducted on four consecutive days in order to minimize the difference in biomass characteristics. The biomass concentration in the reactor investigated was maintained at the same level during these four days. All other operating parameters, cycle length, COD loading and HRT, were unchanged during the course of the mixing study except for the difference in mixing. The operating conditions are listed in Table 4.8 for the reactors A and B.

Study of biosolids characteristic In ASBR systems that contain high concentrations of suspended solids, both zone settling and compression settling can occur in the settling phase. The zone settling velocity of the ASBR sludge is an important parameter that

Table 4.8. Summary of the operating parameters on the mixing pattern study

PARAMETERS	Day 1	Day 2	Day 3	Day 4
Mixing Pattern	2.5 min/30 min	5 min/hour	100 sec/20 min	continuous
Cycle Length, hours	6	6	6	6
COD Loading, g/L/day	6	6	6	6
HRT, hours	24	24	24	24
MLVSS of Reactor A, g/L	12.7	12.7	12.7	12.7
MLVSS of Reactor B, g/L	14.0	14.0	14.0	14.0

establishes the liquid clarification rate and the time required for settling. Solids separation characteristics are constantly monitored by performing settling column tests and biomass particle size analyses. In each reactor, the zone settling velocity was measured at various concentrations of mixed liquor suspended solids. Biomass particle-size distribution curves were determined as frequently as once per month in order to characterize the progression of the anaerobic sludge granulation process. The effects of reactor configuration on granulation were also hypothesized based on the difference in the sludge settling velocity and the particle sizes in the four reactors.

Methods of Analysis

The reactor performance parameters were monitored on a routine basis throughout the study. The parameters included pH, barometric pressure, alkalinity, COD, biogas production, methane content, solids, total volatile acids, sludge settling velocity, and biosolids particle sizes. The analytical methods used, and sampling frequencies are

summarized in Table 4.9.

Biogas Analysis

The biogas production for each reactor was measured daily by Wet-test gas meter in the 35°C temperature room. The daily barometric pressure was measured with a barometer. The daily biogas production was converted to standard temperature and pressure (STP) conditions, i.e., 273°K and 760 mm Hg., in order to compare the biogas data for different runs at the standard conditions. The following equation was used to convert an average biogas production rate of day 1 and day 2 to STP:

$$GAS_{STP} = \frac{r_2 - r_1}{t_2 - t_1} \times \frac{P_1 + P_2}{2 \times 760} \times \frac{273}{273 + 35} \qquad (4.5)$$

where,

GAS_{STP} = Biogas production at STP, L at STP/day,

r_1 = Biogas reading on day 1, liter

r_2 = Biogas reading on day 2, liter

t_1 = The time of taking reading on day 1,

t_2 = The time of taking reading on day 2,

P_1 = Barometric pressure on day 1, mm Hg,

P_2 = Barometric pressure on day 2, mm Hg,

Because the experiment was set-up in a 35°C constant temperature room, the temperature was corrected to 273°K by multiplying a factor of 273/(273+35).

Table 4.9. Summary of analytical methods and sampling frequencies

Parameter	Methods	Sample	Frequency
Biogas			
Gas production	Wet-Test Meter	Biogas	Daily
Methane content	Gas Chromatography	Biogas	Weekly & S.S.[a]
Atmosphere pressure	Barometer		Daily
Biomass			
Solids	Standard Methods[b] 209C & 209D	Effluent & mixed liquor	Weekly & S.S.
Settling velocity	Settling column	Mixed liquor	Every 2-7 days
Particle sizes	AIA[c]	Mixed liquor	Monthly
Liquid			
pH	pH meter	Effluent	Daily
Alkalinity	Standard Methods 403	Effluent	S.S.
Total volatile acids	Standard Methods 504B	Effluent	S.S.
TCOD & SCOD	Standard Methods 508B	Influent & effluent	S.S.

[a] Pseudo steady-state.
[b] Standard Methods for the Examination of Water and Wastewater, 16th edition, American Public Health Association, Washington, DC (1985).
[c] Automatic Image Analysis system.

In terms of methane content, biogas was analyzed using a gas chromatograph (GC) equipped with a thermal conductivity detector. The specifications of the gas chromatograph are shown in Table 4.10. The GC column used for the analyses detected relative proportions of nitrogen, carbon dioxide, and methane. The typical gas standard[15] used for the GC calibration contained 5% nitrogen, 25% carbon dioxide, and 70% methane.

Table 4.10. GC operating parameters

Item	Specification
Model	Gow-Mac 69-350
Column	
Packing	Chromosorb P
Packing size	80/100 mesh
Temperature	65°C
Carrier gas	Helium
Flowrate	60 ml/min
Detector	
Thermal conductivity	
Temperature	150°C
Injection block temperature	100°C
Sample size	0.9 ml
Data acquisition	Maxima Software

[15] Union Carbide Industrial Gases, Inc., East Chicago, Indiana.

Biogas samples were taken from gas sampling port in the gas collection line after the H_2S scrubber and ahead of the gas meter using a gas-lock syringe[16] and were analyzed immediately. A 0.9 ml sample size was consistently used in the GC analysis. The main purpose of the GC analyses was to determine methane production for each reactor. Methane production is the most important measurement of anaerobic degradation rate and also is the basis for establishing reactor pseudo-equilibrium state.

Solids Analysis

Suspended solids concentrations were determined for both total and volatile fractions. Each sample was run in duplicate and a sample size of 10 to 50 ml was used, depending on the solids concentration. Solids analyses were performed at each pseudo-steady-state datum point, and, quite often, was jointly performed with each zone settling velocity test. For the solids analysis, a piece of 9.0 cm Fisher brand G6 glass fiber filter paper[17] was used. Disposable aluminum planchets were used to hold the filter paper.

Settling Velocity

In systems that contain high concentration of suspended solids, both zone settling and compression settling usually occur in the settling phase. Because of the high concentration of particles in the ASBR, the liquid tends to move up through the interstices of the contacting particles. As a result, the contacting particles tend to settle as a zone or

---

[16] Gastight Series 1000, Model No. 1001-TTL, Hamilton Company, Reno, Nevada.
[17] Cat. No. 09-804-90A, Fisher Scientific Company.

"blanket," maintaining the same relative position with respect to each other. In most cases, an identifiable interface develops between the more or less clear upper region and the zone settling region. Settling column tests are required to determine the settling characteristics of the sludge. The position of the interface as time elapses plotted in the settling column tests. The settling velocity at which the interface subsides is then equal to the slope of the curve at that point in time. The zone settling velocity is a function of the concentration of solids and their characteristics.

Settling column tests can be conducted inside the reactor if the reactor provides enough vertical depth in order to have sufficient observation time for the zone settling phenomenon. An active liquid depth of 30.8 inches in Reactor A is a proper environment for the settling column test. Therefore, the settling column test for the sludge in Reactor A was solely conducted inside the reactor itself. For Reactor B, C, and D, the settling column tests were conducted in an external settling column. The settling column made of Plexiglas was designed by the author and built at the ERI Machine Shop. A schematic diagram of the settling column is shown in Figure 4.11. The settling column is 48 inches tall and has an inside diameter of 3 inches. Three ports, with 1/2 inch internal diameter, are provided in the column. One port in the side wall functioned as a sampling port. The other two ports are located in the center of the top cover and the bottom plate, respectively.

Six hours prior to the settling test, the top port of the settling column was connected by a 1/2 inch Tygon tubing to the top side port of the reactor which provided biogas

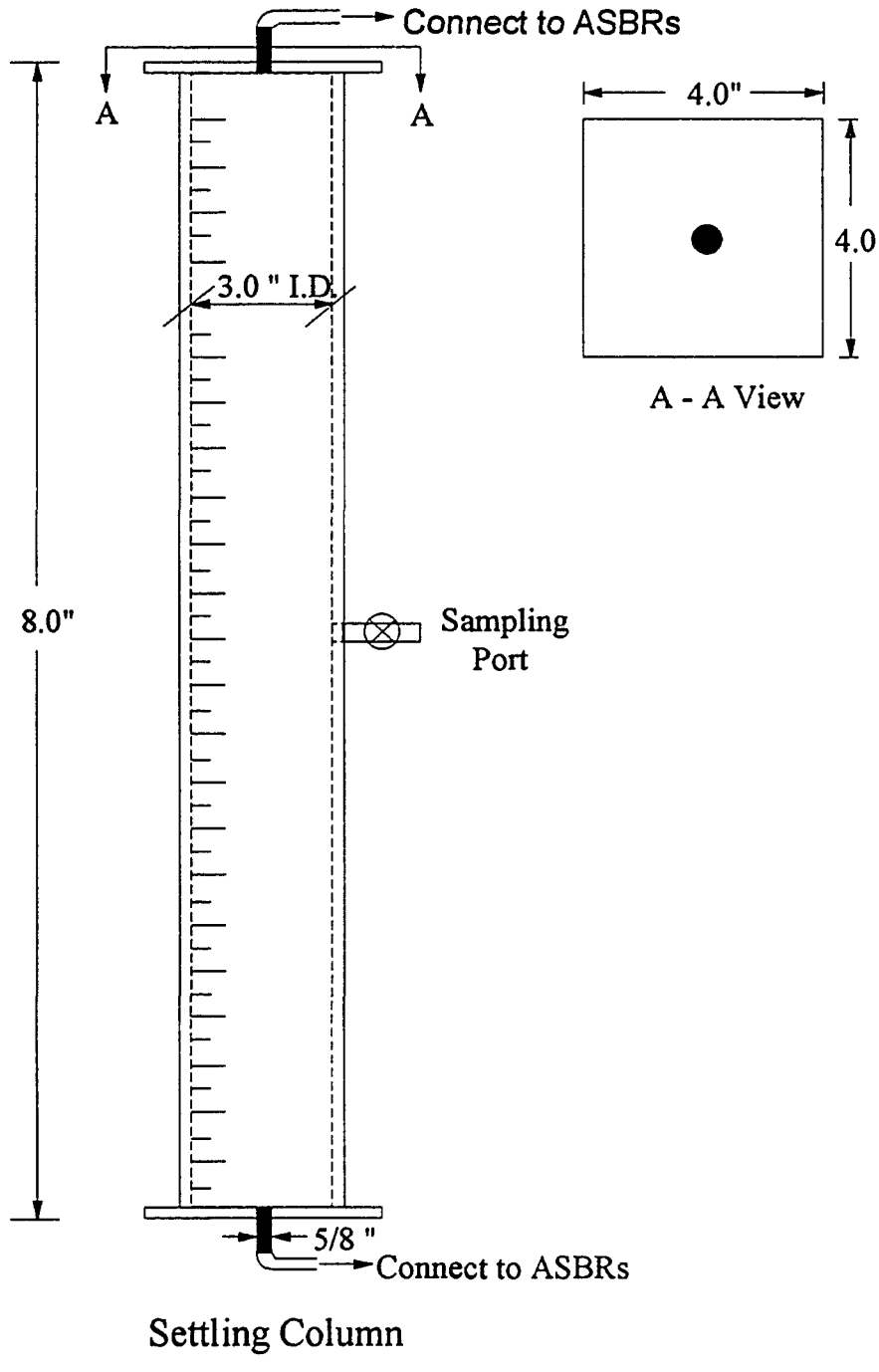

Figure 4.11. Schematic diagram of the settling column

passage between the settling column and the reactor head space. The bottom port of the settling column was connected by a tygon tubing to one of the mixed liquor sampling ports. These connections allowed the transfer of the mixed liquor from the reactor to the settling column prior to the settling test and also allowed for the transfer of the mixed liquor back to the reactor after the test. The mixed liquor was gently transferred by gravity through the tubing during the reactor mixing phase. Biogas composition in the top space of the settling column was the same as the composition in the head space of the reactor when the settling test was conducted, thus voiding settling disturbance caused by degasification that might occur with different gas partial pressure. This closely simulates the settling conditions in the reactor itself.

Particle Size Analysis

Sludge particle size distributions were determined using automatic image analysis (AIA), coupled to an Olympus BH-2S upright, transmitted light microscope. The particle image to be analyzed by AIA is obtained through a TV/video camera mounted on a microscope and input to the system as a digitized image. The digitized image can be mathematically manipulated to enhance desired feature appearance by using the system editorial functions such as small feature enhancement, erosion, dilation, and so on. Once the particle image is extracted from the surrounding background, it can be sent to the system computation unit for the final report. The report includes particle counts, cover area density, particle orientation (degrees), particle area distribution plot, particle width and length distribution plots, and so on.

Image processing used in this study consisted of five steps: magnification calibration, setting gray levels for analysis, image acquisition, editing displayed image, and frame analysis. The first step of image processing is to calibrate the magnification of the optical system (microscope-AIA combination) using a 0.5 mm ruler and record the magnification into the computation program. The optical system can provide magnification ranging from 10 to 60x. A pertinent magnification of the optical system can be selected by the operator depending on the particle sizes of the sample. Generally, for particle sizes ranging from 0.1 to 3 mm, a magnification range of 10 to 20x is adequate.

The second step is to set gray levels for analysis. The AIA identifies and measures the objects based on the contrast between the object and the background, which is represented by the level of gray in the field of view. There are 256 levels of gray, from black at level zero, to white at level 256, to be used according to the characteristics of particle. This option allows the operator to set upper and lower thresholds for gray level. When a particle image is thresholded properly, the AIA can correctly identify, count, and size the particle. In the study of anaerobic sludge particles, the gray levels are easy to set because the particle is quite dark and distinct compared to the surrounding background. The set level for anaerobic sludge used in this study was low level 0 and high level 50. After setting the threshold gray level, the image acquisition step is entered. The image acquisition is to acquire an optical image from the video camera. The AIA directs the video signal to the monitor. Adjustment of the light contrast and focus are needed in this stage in order to gain the most clear image possible. The image can then be frozen for

processing.

Image editing operation is the fourth step performed for the displayed image on the screen. For editing the image, first the small feature enhancement is processed. This operation amplifies the gray level at locations of rapid change, where the edges of small features are detected and presented on the screen. Next, erode and dilation options are sequentially performed to lead to a more accurate feature count during analysis. The processed image frame is finally sent to AIA computation unit for analysis, and then the results are stored to disk as well as printed on a printer.

A sample cell of Plexiglas and glass was made by the author and used for holding the sludge sample under the microscope. A schematic of the sample cell is shown in Figure 4.12. When preparing the sample, dilution of the sludge sample was necessary to obtain a sample with a single particle layer in the sample cell and to minimize the contact among particles. The sample cell was covered with a microscope cover glass[18] of size 45 x 50 mm and a thickness of 0.15 mm.

pH

pH values were measured using a standard glass membrane-type pH probe[19] coupled with an Altex pH meter[20]. The pH meter was calibrated every day with two standard buffers of 4.00 and 7.00[21].

---

[18] Cat No. 12-544F, Fisher Scientific Company.
[19] Cat. No. H778, Markson Corporation.
[20] Model 4500, Altex Corporation.
[21] Cat. Nos. SB101-500, and SB107-500, Fisher Scientific Company.

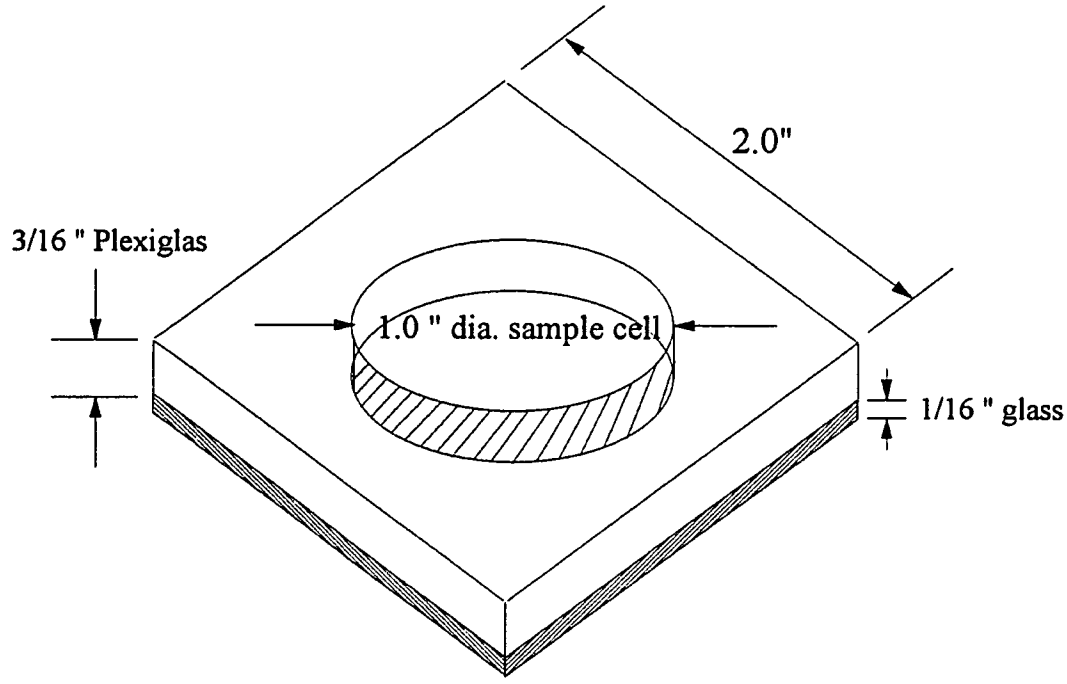

Figure 4.12. Schematic of the AIA sampling cell

Approximately 30 ml of the sample were collected from the effluent during the decanting period of a cycle and the pH was measured immediately to prevent the errors caused by carbon dioxide released from the liquid.

Alkalinity, Total Volatile Acids, and COD

For each COD loading/HRT datum point, a set of analyses, including solids, alkalinity, volatile acids, and COD, was performed on the effluent. The procedure for each analysis is described in Standard Methods (1985).

Volatile acids are water soluble and can be separated by distillation and condensation

methods. Since some volatile acids have higher boiling points than water, a 70% recovery rate of the total volatile acids was estimated, as outlined in Standard Methods.

The chemical oxygen demand test was one of the main parameters used to determine reactor performance and efficiency during this research. Samples were taken for COD analysis during the effluent decanting period in a cycle. The effluent sample was collected shortly after the effluent decanting cycle had begun. Approximately 30 seconds of the decanting cycle were allowed to elapse prior to sampling to allow any accumulated solids in the reactor ports to be evacuated.

The total COD was performed on the well-mixed sample as collected. The soluble COD was determined on the filtrate of the samples which passed through a 24 mm Fisher brand GF/C glass filter paper[22] with a pore size of 1.2 μm. A 30 ml disposable plastic syringe coupled with a syringe-type filter holder[23] was used to aid in filtering the samples. For each sample, the total and soluble COD were run in duplicate. For this experiment, pseudo-equilibrium is defined when the methane production from a reactor does not vary by more than three percent from day to day and reactor solids are not in a washout condition. At least three COD runs were performed after the reactor reached pseudo-equilibrium.

---

[22] Cat. No. 09-874-32, Fisher Scientific Company.
[23] Cat. No. 09-730-225, Fisher Scientific Company.

V. RESULTS AND DISCUSSION

Start-up Operation

Four ASBRs were seeded with a initial MLSS of 8,500 mg/L on April 18, 1991. The ASBRs were initially loaded at 1 g COD/L/day. The organic loading was then increased to 2 g COD/L/day on the third day of the start-up period. The acclimation period after seeding involved the weeding out of the poor settling suspended solids as well as the dissolved solids. A solids/supernatant interface would form after the first day of operation, but the supernatant was dark due to high amounts of dissolved solids. pH adjustment with sodium bicarbonate was carried out twice per day during the first two weeks of the start-up period. The amount of sodium bicarbonate addition was determined by titrating a sample from the reactor with 0.1N sodium bicarbonate solution to a pH of 7.0. After three weeks of operation, the pH in the reactor became stable within an optimal range between 6.8 and 7.2. Sodium bicarbonate was then routinely added into the feed solution on the basis of the alkalinity to COD ratio (See Experimental Study chapter for $NaHCO_3$ dosage).

On the eighth day of start-up, MLSS concentrations in Reactors A and B decreased to 5,540 mg/L and 7,790 mg/L, respectively. Decreasing MLSS concentration indicated excessive biosolids washout from these reactors. Additional seed was introduced into Reactors A and B on April 26, 1991, to bring the MLSS concentrations to 11,000 mg/L, which was close to MLSS concentrations in Reactors C and D at that time.

The acclimation in the start-up phase should involve 1) adapting the fermentative and

acetogenic bacteria to the new NFDM substrate, and 2) establishing a new population balance between methanogens and other bacterial groups at the operating conditions. After one month of the start-up period, stable performance of the reactor pH and biogas production indicated that the ASBRs were well acclimated and ready for steady-state studies.

Phase 1 Study at 48 Hour HRT

The ASBRs were designed to operate at HRTs of 48 hour, 24 hour, and 12 hour over the highest COD loading range that the ASBR was anticipated to successfully operate. The ASBR were operated at the HRT of 48 hour in this phase of the experimental study. Reactor performance was analyzed at pseudo-steady-state conditions, and at least three sets of performance data were collected for each organic load. Pseudo-steady-state was defined as the state when reactor daily methane production rate varied within $\pm 3\%$ at least three consecutive days and reactor biosolids were not in a washout condition (a condition with decreasing biosolids concentration over time). The biosolids profile and daily methane production information for each ASBR during the entire performance study period between April 18, 1991, and December 23, 1991, are shown in the Appendix, Section A.

Studying the maximum organic loading rate which the reactors could sustain was not the objective of this research. Risk of losing valuable biomass when pushing up organic loading was not warranted for the overall objective of this research.

All four ASBRs reached pseudo steady-state after three weeks into the start-up period. ASBRs were operated for two subsequent weeks for monitoring the MLSS

concentrations before the first set of performance data were analyzed on May 22, 1991 (day 35).

ASBR Responses to Organic Loading Increase

Organic loading was increased by 2 g COD/L/day to the next predetermined level (See Table 4.6) after enough pseudo steady-state performance data were collected. A phenomenon of the ASBR responding to a shock load during organic load increase might be noticed, manifested in the changes of the reactor operating parameters which could be described as: 1) a sudden increase in effluent solids concentration, 2) a pH drop, 3) a decrease in methane content of biogas, and 4) an increase in effluent total volatile acids concentration.

Table 5.1 presents an example of the ASBR responding to an organic load increase from 4 g COD/L/day to 6 g COD/L/day in Reactor A. MLSS, alkalinity addition, methane content, methane production, and effluent total volatile acids concentration are summarized over a 5-day period. June 19, 1991 (day 63) was the last operating day before the organic loading was increased to 6 g COD/L/day.

The increase of effluent biosolids was caused by higher internal gassing disturbance during the ASBR decant period. Internal gassing intensity depended on the biogas production rate, which was governed by the substrate concentration in the reactor. In the transition stage of the organic load increase, higher substrate concentration during the settle and decant periods resulted from higher remaining substrate concentration and temporary

Table 5.1. Transition conditions of increasing organic loading from 4 to 6 g COD/L/day in Reactor A

Date	MLSS mg/L	pH[a]	Alkalinity Added[b] mg/l as $CaCO_3$	CH_4 Content %	CH_4 Production L/day @ STP	Effluent TVA mg/L Acetate
June 19	20,750	7.0		67.5	16.0	23
20	15,930	6.4	545	58.5 - 63.1	20.7	339
21	14,370	6.5	397	56.2	22.5	86
22	14,230	6.7		60.9	24.6	57
23	15,890	6.9		61.6	24.7	23

[a] pH before alkalinity addition.
[b] alkalinity not including the amount supplemented to the feed solution.

increase of volatile acids concentrations in the reactor. This reactor would either re-establish its solids balance conditions by further weeding out of poor settling suspended solids and soon recover the temporary biosolids washout situation, or potentially lead to a disastrous solids washout situation. In Phase 1 of the study, reactors A and B were loaded up to 10 g COD/L/day for 2 days. Severe biosolids washout occurred. The experiment at the 10 g COD/L/day loading was terminated due to the impending failure of Reactors A and B. Also, the washout loss of the valuable biosolids retained throughout this phase of the study were not warranted for the research objectives.

The pH drop was the result of a higher volatile acids concentration due to an unbalanced population of methane formers during the transition stage of the loading change. The decrease in methane content of the biogas was the outcome of shifting chemical equilibrium of carbon dioxide-bicarbonate system, which is also related to the pH drop (McCarty, 1964b). A precautionary procedure in pH control of the reactor was taken whenever operating conditions were changed. The changes included lowering the HRT

and increasing the organic loading. The procedure required a constant monitoring of pH. If pH in the reactor liquid was lower than 6.7, sodium bicarbonate solution was added into the reactor to neutralize the liquor. The undesirable condition of depressed pH could be attributed to an insufficient population of methane formers and normally would correct itself within two to four days. This indicates that the methane former population could catch up within two to four days after a change in organic loading amounting to a 2 g COD/L/day increase, if the reactor pH were corrected. The ASBRs which had high MLVSS or low food to microorganism ratio (F/M) appeared to be better able to handle organic shock loads. F/M ratio is equivalent to COD loading rate divided by microorganism concentration, which is represented by MLVSS and has units of g COD/g MLVSS-day. Reactors C and D retained higher MLVSS concentrations than Reactors A and B throughout Phase 1 of the research and had no additional alkalinity requirement during the transition stage of organic loading increase. The alkalinity supplement in the feed solution seemed to be sufficient to buffer Reactors C and D. Reactors A and B demanded more attention during the start-up period of Phase 1 of the research.

Phase 1 Biosolids Study

The biosolids concentration could increase over time if the amount of new biomass yielded is higher than the amount of the biomass washed out during the decant step. The biosolids concentration could also decrease, if significant amount of biosolids are washed out in the effluent. Figure 5.1 shows biosolids concentration profiles of the ASBRs in the start-up and Phase 1 operations. During the start-up phase, the solids concentrations

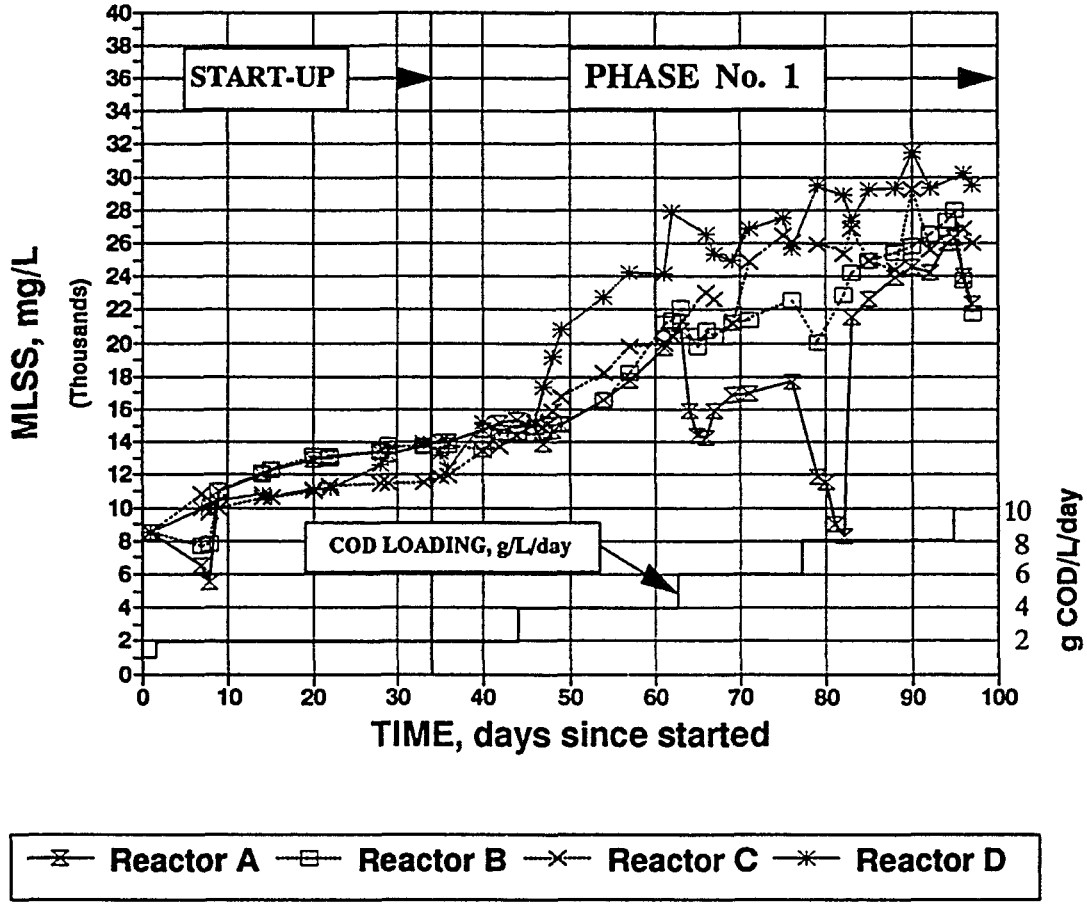

Figure 5.1. MLSS concentration profile in the start-up and Phase 1 period

gradually increased from 8,500 mg/L to approximately 14,000 mg/L for Reactors A and B and to approximately 12,000 mg/L for Reactors C and D. The biosolids concentrations of the four reactors were close to each other at the beginning of Phase 1, and then moved up at different accumulation rates, once the organic loading increased to above 4 g/L/day. Reactor D retained the highest biomass concentration of 30,000 mg/L at the end of Phase 1. Foaming occurred in Reactor A during the transition period of the organic load increase to 8 g COD/L/day. The foaming resulted in a massive biosolids loss and led the reactor to failure conditions. The effluent solids were separated and returned to Reactor A on the sixth day of the 8 g COD/L/day run.

Both zone settling and compression settling occurred at the high sludge concentrations in the reactors. An identifiable interface developed between the clear upper region and the zone settling region. Zone settling velocity was an important parameter in determining the settling characteristics and was measured by the settling column test. The rate of settling is a function of the concentration of solids and biomass settling characteristics. The results of the column tests performed between May 20, 1991 (day 33) and July 3 (day 77), 1991, at different solids concentrations are shown in Figure 5.2. The plots show poor correlations between settling rate and the concentration of solids for all cases from the four reactors. However, the settling velocities of Reactor A are relatively higher than those for Reactors B, C, and D. The poor correlation is caused by the continuously changing biosolids characteristics over the time and the effects of reactor geometry on solids settleability. The ASBR tended to select biomass with better settleability. Reactor A, with the tall, slender

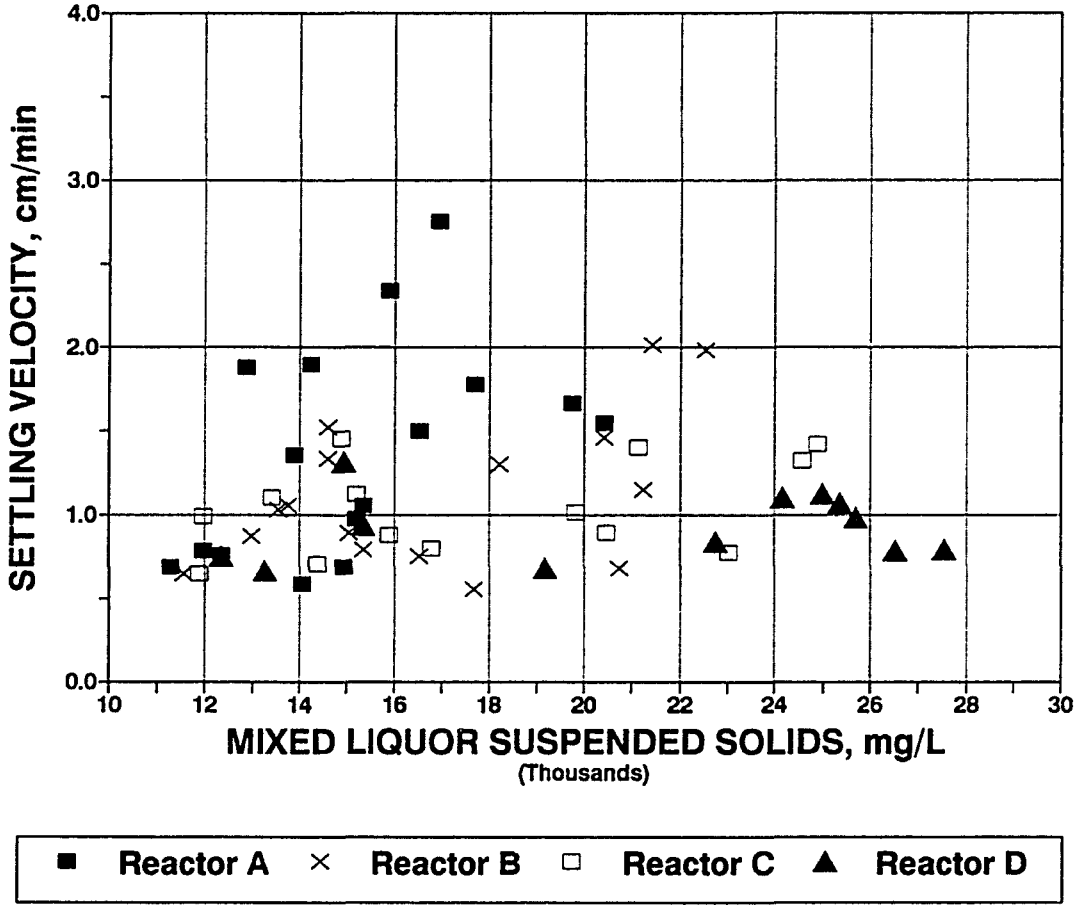

Figure 5.2. Zone settling velocity of reactor solids at various MLSS concentrations between day 33 and day 77

shape retained the biomass with higher settling velocity. In this phase of the study, biomass concentration showed a general increasing trend for the four reactors. The higher concentrations of biomass normally corresponded to the latter phase of the study which underwent a longer period of biomass selection. The phenomenon of solids characteristics as a function of the time and reactor geometry will be addressed in the following sections.

Biosolids Settling Within a 6-hour Cycle

Biosolids settleability could be affected by the substrate concentration surrounding the microorganisms or expressing as a parameter of F/M ratio. An experiment was conducted on June 17, 1991 (day 61) to measure hourly zone settling rates in Reactor A at the organic loading of 4 g/L/day, an MLSS concentration of 19,750 mg/L and an F/M ratio of 0.23. Six zone settling rates were measured in a 6-hour cycle. Each of the measurements started at the end of each 5 min/hour mixing period. The same study was repeated on July 21, 1991 (day 95) at the same organic loading of 4 g COD/L/day, but with a different MLSS concentration of 26,280 mg/L, and an F/M ratio of 0.18 g/g-day.

The data are plotted in Figures 5.3 and 5.4 and reported in Appendix, Section B. Interface disruption points are marked in Figures 5.3 and 5.4 to indicate the time when the solids/liquor interface was first disrupted by rising biogas (biogas gassing) generated in the settled biosolids matrix. The experimental observation of this study shows the biogas gassing turmoil continued and often intensified after the first disruption. The disruption caused discrete biosolids particles or flocs to escape from the sludge blanket. The escaped

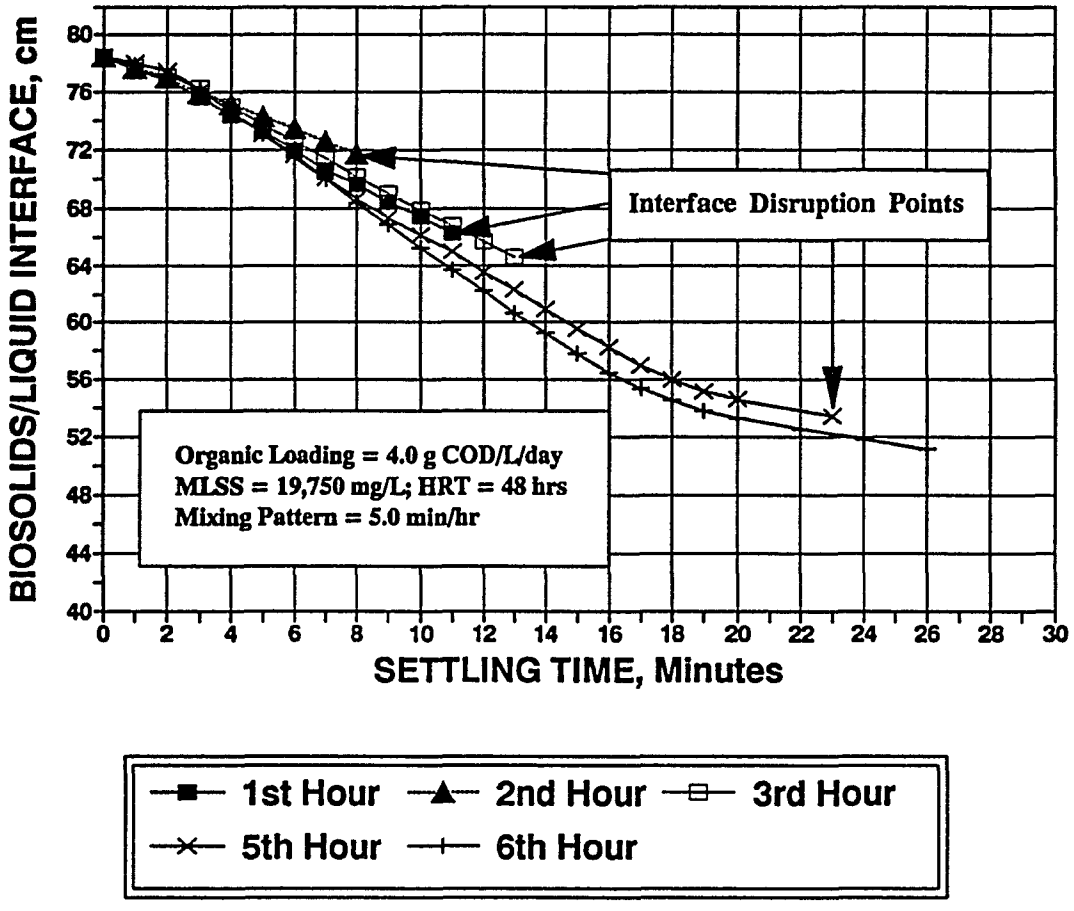

Figure 5.3. Biosolids settling within a 6-hour cycle in Reactor A on day 61

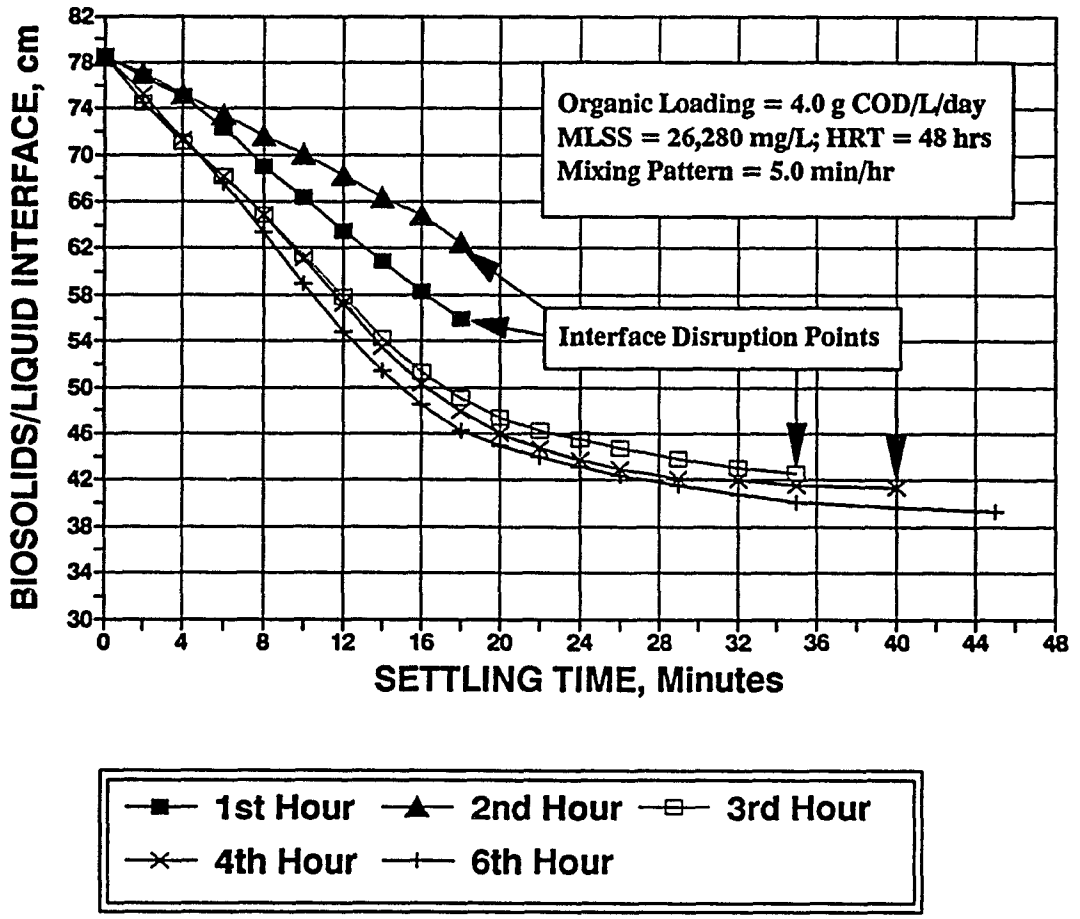

Figure 5.4. Biosolids settling within a 6-hour cycle in Reactor A on day 95

particles would settle back to the sludge blanket or be washed out with the effluent if the incidence happened during the decant step. The interface holding against the biogas gassing time was the function of biosolids characteristics and biogas production rate. Heavier biosolids might hold the interface longer. In the 6-hour experiment within the same cycle, biosolids characteristics were not a variable. Therefore, biogas production rate became a focal point of this study. Biogas production rate is a function of the microorganism metabolic rate, which is also a function of substrate concentration surrounding the biosolids.

Figure 5.5 shows a typical 6-hour cycle biogas production rate curve at the same operating conditions as the 6-hour settling experiment. The curve with a "saw tooth" pattern of biogas production is the result of intermittent mixing. Biogas tends to release from the liquor at a higher rate during mixing periods. Each biogas production peak in the curve corresponds to a 5 min/hour mixing period. The substrate reaches the highest concentration at the end of feed period at 0.25 hour. However, the highest biogas production rate is in the second hour of the cycle. A lag period is necessary in order to carry out the metabolic conversion from substrate to biogas.

The interface holding lengths shown in Figures 5.3 and 5.4 follow the trend of the biogas production rates. The trend indicates that the higher the biogas production rate, the shorter the interface holding period. Zone settling velocities determined from the experiment are presented in Table 5.2. Two sets of velocity data show a similar pattern

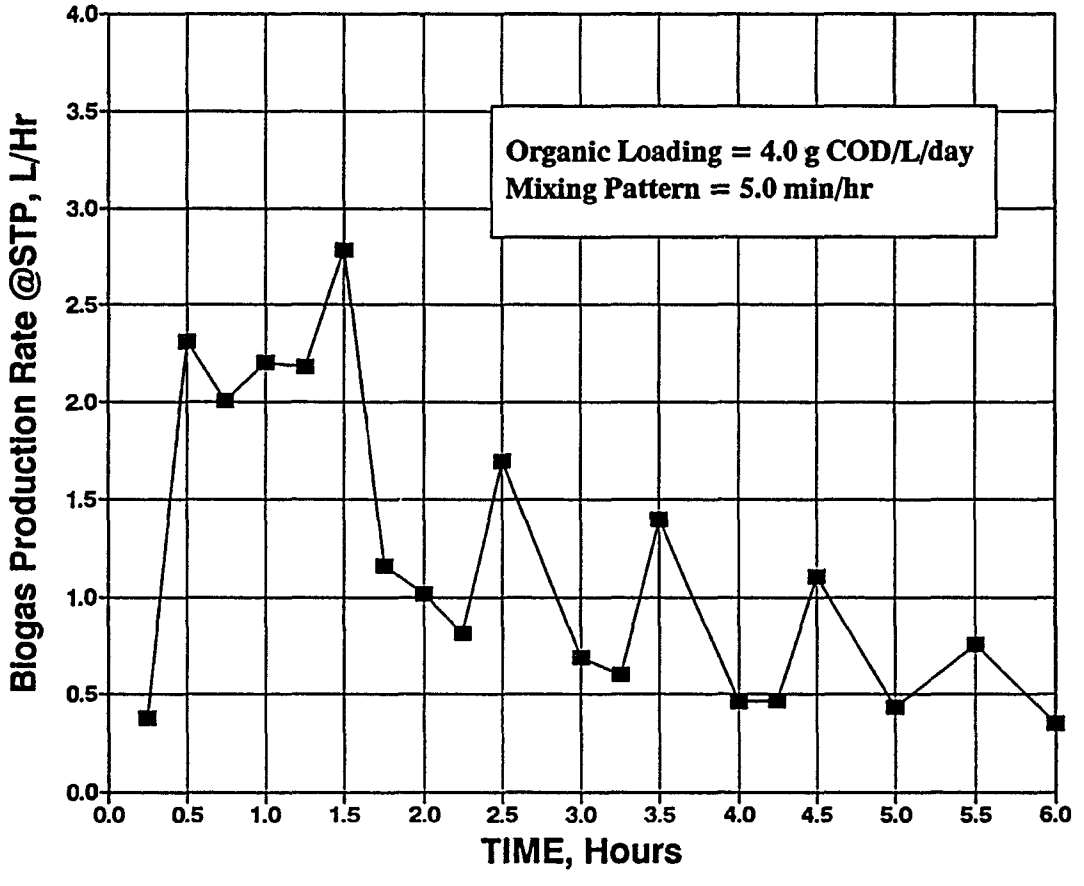

Figure 5.5. Biogas production rate curve in a typical 6-hour cycle

Table 5.2. Summary of zone settling velocities in two 6-hour settling tests

Date	Zone Settling Velocity, cm/min					
	1st Hour	2nd Hour	3rd Hour	4th Hour	5th Hour	6th Hour
June 17	1.17	0.88	1.20	1.33	1.45	1.54
July 21	1.45	0.91	1.73	1.82	1.95	2.10

with the lowest value in the second hour and increasing velocities after that. The zone settling velocity results also follow the trend of the biogas production rates. This trend shows that the lower the biogas production rate, the faster the biosolids' settling velocity.

The following concepts can be learned from this experiment.

1. The biosolids/liquor interface holding time can be affected by the biogas production rate.
2. The zone settling velocity can be hindered by the biogas production rate.
3. Comparing the data of interface holding time in two sets of settling tests, the set with a lower F/M ratio suggests a longer interface holding time. A longer interface holding time means a longer period of time available for effluent decanting without interference from biogas gassing.
4. The decant timing could be an important operating factor when the ASBR has a flocculent-type of biomass or is operated at a high F/M ratio.

Phase 1 Performance

Performance data for the reactors at an HRT of 48 hour and the various COD loads investigated are shown in Table 5.3. The data indicate that removal of the NFDM substrate was excellent over the range of COD loads from 2 to 8 g COD/L/day. The COD removal rates, both total and soluble, were above the 90% range. Average methane production data were well correlated (within a $\pm 10\%$) with theoretical values, calculated on the basis of 0.35 liter of methane (STP) for each gram of COD removed. The effluent suspended solids and COD concentrations increased as the organic loadings increased. However, the effluent total volatile acids stayed low and relatively stable within a 40 mg/L range. The food to microorganism ratios investigated were in the range of 0.16 - 0.39 g/g-day.

Phase 2 Study at 24 Hour HRT

Phase 2 of the study was initiated on July 24, 1991 (day 98) and ended on October 24, 1991 (day 190) with the HRT of 24 hours. The organic loadings of 2, 4, 6, and 8 g COD/L/day were investigated in this phase of the study.

Biosolids Selection Pressure

The ASBR tends to wash out the poorly settling flocs and dispersed organisms and selects for the heavier, more rapidly settling aggregates. As a result, granular biomass becomes dominant and leads to a rapid solids settling. The results of the ASBR granulation process will be discussed in the next phase of the research. The ASBR

Table 5.3. Performance of the ASBR at a 48-hour HRT and various COD loadings

Reactor	MLSS	MLVSS	F/M	Effluent Characteristics					COD Removal		CH_4 Prod.*
				TCOD	SCOD	TSS	VSS	TVA*	Total	Soluble	@STP
	mg/L	mg/L	g/g-day	mg/L	mg/L	mg/l	mg/L	mg/L as Acetate	%	%	L/day
				COD Loading = 2.0 g/L/day							
A	14,040 - 15,180	11,200 - 12,420	0.18 - 0.16	202 - 246	40 - 69	164 - 190	140 - 164	10	94.1	98.7	7.8
B	13,590 - 14,580	11,230 - 12,620	0.18 - 0.16	187 - 231	50 - 62	139 - 183	119 - 157	22	94.8	98.7	7.6
C	11,860 - 13,680	9,810 - 11,550	0.20 - 0.17	184 - 218	38 - 65	129 - 154	102 - 131	17	95.1	98.6	7.3
D	12,340 - 14,710	10,460 - 11,920	0.19 - 0.17	207 - 266	46 - 74	160 - 192	132 - 167	14	94.6	98.5	7.3
				COD Loading = 4.0 g/L/day							
A	15,050 - 20,420	12,250 - 17,850	0.33 - 0.22	273 - 355	43 - 59	240 - 286	207 - 248	22	96.3	99.4	15.9
B	15,140 - 21,410	12,070 - 18,440	0.33 - 0.22	293 - 352	50 - 74	238 - 289	211 - 252	17	96.3	99.1	16.0
C	16,780 - 20,470	14,130 - 17,600	0.28 - 0.23	306 - 361	52 - 82	234 - 301	201 - 263	26	95.9	99.0	15.3
D	20,810 - 27,890	18,380 - 24,010	0.22 - 0.17	303 - 366	57 - 114	271 - 292	236 - 259	29	96.0	98.9	15.1
				COD Loading = 6.0 g/L/day							
A	16,880 - 17,670	14,460 - 15,320	0.41 - 0.39	429 - 627	61 - 96	364 - 516	324 - 445	24	95.2	99.2	25.2
B	21,240 - 22,540	18,230 - 19,580	0.33 - 0.31	344 - 477	68 - 100	279 - 405	243 - 359	21	96.5	99.4	24.2
C	21,140 - 26,040	18,380 - 22,700	0.33 - 0.26	371 - 597	89 - 99	307 - 487	273 - 431	30	95.7	99.3	23.8
D	24,980 - 26,900	21,640 - 23,490	0.28 - 0.26	386 - 461	88 - 111	295 - 347	247 - 295	30	96.7	99.2	23.5
				COD Loading = 8.0 g/L/day							
A	23,930 - 24,580	20,570 - 21,120	0.39 - 0.38	625 - 975	86 - 143	572 - 998	498 - 882	27	89.4	99.1	29.7
B	25,420 - 26,510	21,670 - 23,200	0.37 - 0.34	494 - 873	55 - 137	496 - 884	430 - 776	28	91.4	99.4	31.3
C	24,425 - 29,210	21,340 - 25,790	0.37 - 0.31	507 - 749	110 - 141	452 - 725	391 - 633	35	91.9	99.1	29.7
D	29,290 - 31,480	25,280 - 27,630	0.32 - 0.29	511 - 783	97 - 135	430 - 673	378 - 582	38	92.0	99.2	29.3

* Average of all performance analysis data.

biosolids selection pressure, a governing factor in the biosolids selection process, is introduced in this section.

The biosolids selection pressure imposed through the decanting process can be quantitatively factored into three parameters which are: 1) decant volume, 2) static hydraulic pressure change in the decant step, and 3) operating F/M ratio.

The ASBR decants a predetermined volume of supernatant after a biosolids settling step. The decant volume in each operating cycle is determined by the HRT and the cycle length. Higher selection pressure is imposed upon the reactor with more decant volume, simply because larger decant volumes carry out more of the poorly settling biosolids.

Static hydraulic pressure is decreasing during the decant period due to the decant process lowering the liquor surface in the reactor. The larger the hydraulic pressure drop during the decant step, the higher the biosolids selection pressure imposed. The reason for this can be explained by the correlation between the biogas internal gassing effect and the difference in hydraulic pressure. A biogas bubble is initially formed at a microscopic scale on the surface of biomass. The microscopic bubbles coalesce to form bigger bubbles as the result of continuous metabolic activities. The bubble will rise to the surface when the buoyancy of the bubble is strong enough to overcome the cohesive force between the biomass surface and the bubble or once the dead weight of the settled biosolids matrix above the bubble is counterbalanced. The buoyancy of the bubble depends on the bubble size, a function of the hydraulic pressure. The larger the hydraulic pressure drop, the bigger the bubble expansion and the greater the increase in bubble buoyancy; the larger the

hydraulic pressure drop, the wider range of the bubble size is affected. As the biogas bubble rises from the biomass surface, bubble expansion energy is released. The biogas expansion energy causes an agitation in the area of the bubble travelling that is called the internal gassing effect. Internal gassing during the decant step results in a biomass selection process. Therefore, the magnitude of hydraulic pressure drop during the decant step affects the intensity of internal gassing or the degree of the biomass selection pressure.

Operating F/M ratio is one of the factors affecting biosolids selection pressure. Biogas produced during the settle and decant steps is the driving force for biosolids/liquor interface disruption and internal gassing effect. The settle and decant steps should always be operated within the limits of the interface holding period to prevent excess biosolids loss and to obtain a better quality of effluent. The interface holding time is a function of the biosolids settleability and operating F/M ratio. The biogas production rate is higher during the settle and decant periods with the ASBR operated at a higher F/M ratio, in accordance with Monod kinetics.

If reactors are operated at the same cycle length, the decant volumes are inversely proportional to the reactor HRT. In Phase 2 of the research, the HRT was one half of the HRT in Phase 1. Thus, the decant volume was doubled from 1.5 to 3 liters per cycle. The degree of biosolids selection pressure was also doubled in Phase 2.

The hydraulic pressure drop during the decant step in Phase 2 operations was twice as much as the pressure drop in Phase 1 operations. For instance, in Reactor A, the decant depth was 3.9 inches in Phase 1 and 7.7 inches in Phase 2. Biosolids selection pressure

was magnified because the amount of the hydraulic pressure drop increased.

The biosolids selection pressure could be elevated by increasing the F/M ratio in one or a combination of two ways: 1) raise the organic loading (F) and/or 2) lower the mass of microorganisms (M).

Phase 2 Biosolids Study

Figure 5.6 shows the biomass concentration profiles of the ASBRs in this phase of the study. MLSS concentrations in the four ASBRs were above 22,000 mg/L at the beginning of this Phase and the ASBRs were operated at the F/M ratio below 0.1 g/g-day. The effluent was quite dark under these operating conditions. Biosolids wasting was first conducted on August 3, 1991 (day 108) to lower the MLSS concentrations of Reactors B, C and D to approximately 20,000 mg/L which was the MLSS concentration of Reactor A at that time. The biosolids wasting was performed by connecting a pump to the biosolids wasting port located on the side of each reactor and pumping out the settled biosolids from each reactor during the decant period. Biosolids wasting was conducted in Reactor D on August 29 (day 134) to lower the MLSS concentration to 17,000 mg/L. This second wasting action was triggered by an accidental biosolids wasting in Reactor B and C which was caused by a timer malfunction.

In Phase 2, a noticeable difference in effluent suspended solids concentrations during the transition stage of increasing organic loading was observed between Reactor A and Reactors B, C, and D. More suspended solids were washed out with effluent in Reactor A

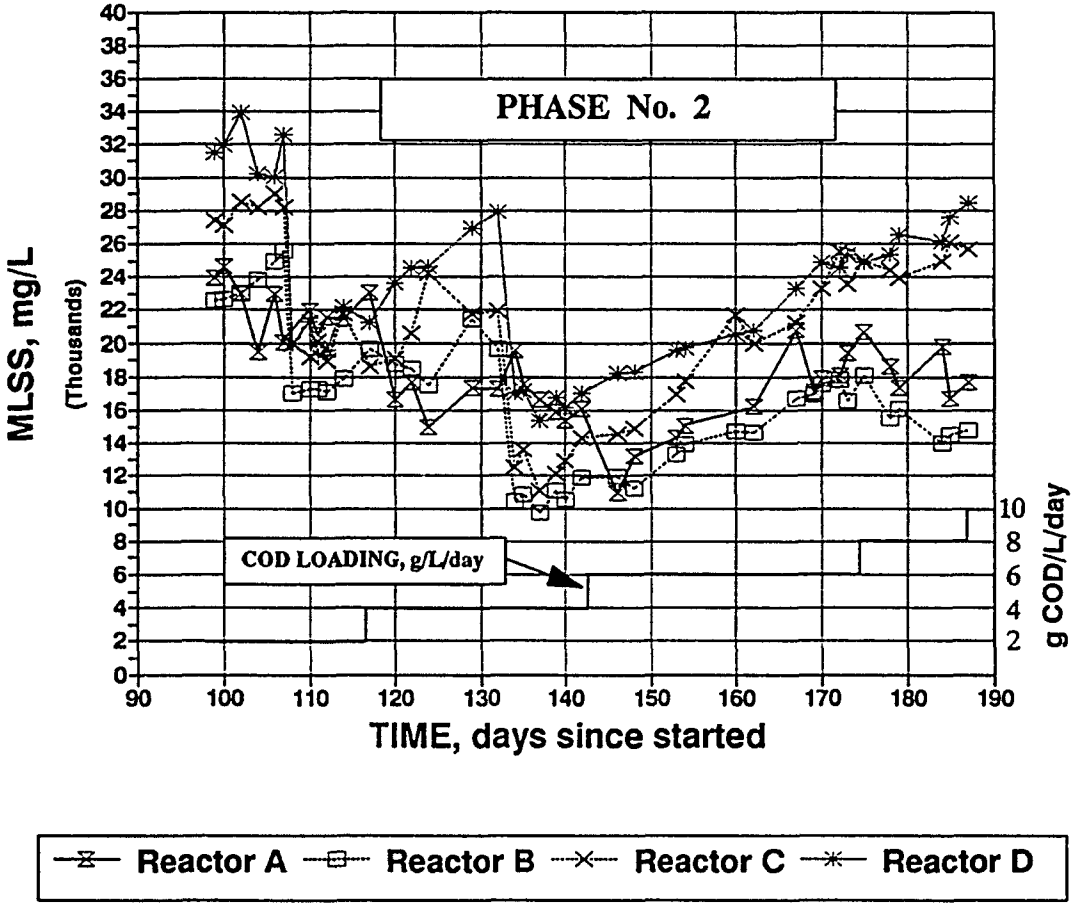

Figure 5.6. MLSS concentration profile in Phase 2 period

due to the increase of biosolids selection pressure.

As a result of the biosolids selection process, the biosolids gradually converted from flocculent biomass into more rapidly settling granular aggregates. Under this circumstance, a single clear solids/supernatant interface during the settling test no longer existed. Instead of one clear interface moving downward from the liquor surface, two interfaces, one on the surface and the other on the bottom, were formed at the beginning of the settling tests. The top interface moved downward with or without a clear interface, depending on the concentration of flocculent biosolids. The other interface built up with heaviest granules from the bottom of the reactor. Once the two interfaces appeared in the biosolids settling, the settling test was no longer a valid tool in describing the biosolids characteristics in the ASBRs. Biosolids particles settled as individual entities (discrete particles) and there was no significant interaction with neighboring particles. The settling tests were last performed on August 31, 1991, which was the 136th day of operation. The biosolids were then measured by the Automatic Image Analyzer (AIA) for the particle size distribution information.

Reactor Geometry Effects

The characteristics of the biomass (flocculent vs granular) were influenced significantly by reactor geometry. Different reactor shapes imposed different levels of selection pressure on the biomass. Reactor A, the reactor with the highest depth-to-diameter of 5.60, was most effective in biosolids selection for granules. Reactors B, C, and D, with a range of depth to diameter ratios between 1.83 and 0.61, imposed a lower

selection pressure for granules. These phenomena can be explained by the following: 1) Reactor A imposed the highest selection pressure because the highest decant depth (hydraulic pressure drop) was encountered in Reactor A during the decanting process. Table 5.4 shows the decant depths of each reactor in 3 phases of experimental study. 2) Reactor A imposed the highest selection pressure because the highest internal gassing energy could be released during the settle and decant steps in Reactor A. Reactor A had the highest liquid depth providing the greatest bubble expansion when biogas rose to the surface. 3) Reactor A imposed the highest selection pressure because the longest settling distance was required in Reactor A to achieve clarification of a predetermined decant volume.

Table 5.4. Decant depths for each ASBR at various experimental phases

Experiment Phase	Decant Volume Liters	Decant Depth, inches			
		Reactor A	Reactor B	Reactor C	Reactor D
1	1.5	3.9	1.8	1.2	0.9
2	3.0	7.7	3.6	2.3	1.8
3	4.0	10.3	4.9	3.1	2.4

The settling velocity data collected from each ASBR between July 5, 1991 (day 79) and August 31, 1991 (day 136) are shown in Figure 5.7. In this stage of collecting data, biomass concentration showed a general decreasing trend for the four reactors and zone settling was still the predominant process in solids separation. The lower concentrations of

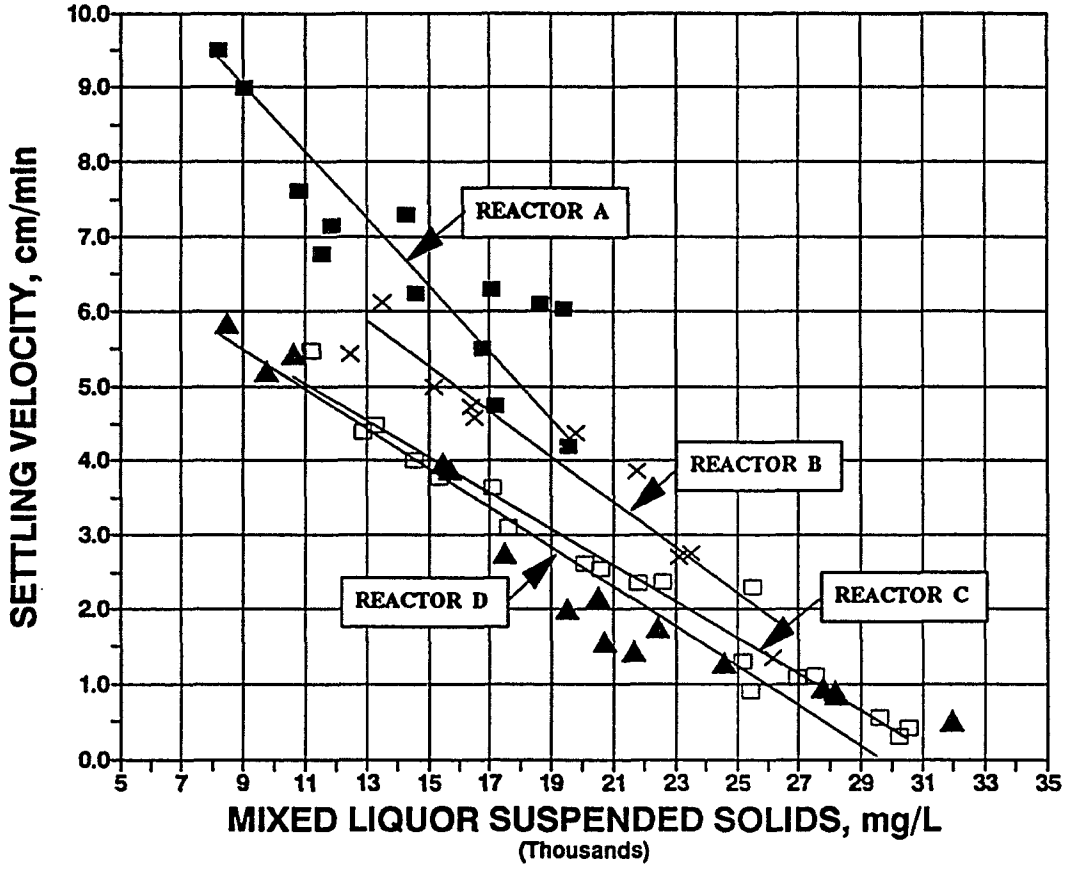

Figure 5.7. Zone settling velocity of reactor solids ar various MLSS concentrations between days 79 and 136

MLSS normally corresponded to the latter phase of the study after a long period of biomass selection. Figure 5.7 shows a general trend toward higher settling velocities associating with lower MLSS. The zone settling velocities are significantly higher for Reactor A and B (slender shape) than for Reactor C and D (stout shape). Under the same operating conditions, Reactor C and D, which have low depth to diameter ratios, retained more solids than the reactors with high depth-to-diameter ratios.

Phase 2 Performance

Performance data for the reactors at an HRT of 24 hours and the various COD loads investigated are shown in Table 5.5. The data indicate that the removal of the NFDM substrate was excellent over the range of COD loads from 2 to 8 g COD/L/day. The total and soluble removal rates were above 85 and 95%, respectively. Average methane production data were well correlated within $\pm 5\%$ with theoretical values, calculated on the basis of 0.35 liter of methane (STP) production for each gram of COD removed. The effluent suspended solids and COD concentrations increased as the organic loadings increased. However, the effluent total volatile acids values stayed low and relatively stable within a 60 mg/L range. The food to microorganism ratios investigated were in the range of 0.08 - 0.66 g/g-day, which was wider than the range in Phase 1.

Phase 3 Study at 12 Hour HRT

Phase 3 was initiated on October 22, 1991 (day 188) with the HRT set at 12 hours. Organic loadings of 2, 4, 6, and 8 g COD/L/day were investigated in all four

Table 5.5. Performance of the ASBR at a 24-hour HRT and various COD loadings

Reactor	MLSS	MLVSS	F/M	Effluent Characteristics					COD Removal		CH4 Prod.*
				TCOD	SCOD	TSS	VSS	TVA*	Total	Soluble	@STP
	mg/L	mg/L	g/g-day	mg/L	mg/L	mg/l	mg/L	mg/L as Acetate	%	%	L/day
				COD Loading = 2.0 g/L/day							
A	21,450 - 24,650	17,920 - 21,080	0.11 - 0.09	195 - 265	44 - 61	151 - 209	135 - 186	13	88.0	97.3	7.9
B	17,130 - 22,640	15,010 - 19,930	0.13 - 0.10	142 - 294	40 - 58	109 - 207	92 - 184	15	86.5	97.4	8.1
C	18,630 - 27,140	16,570 - 24,030	0.12 - 0.08	137 - 260	39 - 62	78 - 182	69 - 162	18	88.9	97.6	7.5
D	19,555 - 22,210	17,150 - 19,440	0.19 - 0.17	215 - 304	53 - 61	148 - 236	130 - 209	21	85.4	97.1	7.8
				COD Loading = 4.0 g/L/day							
A	14,930 - 16,090	13,410 - 13,890	0.30 - 0.29	185 - 497	47 - 76	135 - 324	119 - 289	33	89.9	98.6	15.5
B	10,530 - 17,500	9,375 - 14,790	0.42 - 0.27	232 - 355	65 - 118	153 - 225	131 - 193	51	92.5	97.7	15.6
C	12,880 - 24,260	11,500 - 21,280	0.35 - 0.19	274 - 489	70 - 92	181 - 345	164 - 303	42	90.3	97.7	14.8
D	16,140 - 24,670	14,310 - 22,180	0.28 - 0.18	352 - 660	88 - 162	219 - 448	192 - 393	46	86.3	96.8	14.7
				COD Loading = 6.0 g/L/day							
A	16,260 - 20,750	14,280 - 18,680	0.42 - 0.32	320 - 439	78 - 112	254 - 310	223 - 274	19	93.4	98.6	23.9
B	14,610 - 18,090	13,205 - 16,260	0.45 - 0.37	394 - 570	104 - 150	261 - 379	235 - 335	49	91.7	97.6	23.4
C	19,960 - 24,970	17,950 - 21,580	0.33 - 0.28	223 - 496	81 - 114	171 - 329	151 - 299	32	93.6	98.5	23.1
D	20,760 - 25,380	18,815 - 22,170	0.32 - 0.27	353 - 408	97 - 146	240 - 281	210 - 246	37	93.8	97.7	22.6
				COD Loading = 8.0 g/L/day							
A	16,740 - 19,810	14,930 - 18,280	0.54 - 0.44	409 - 497	91 - 135	287 - 329	256 - 293	27	94.5	98.6	29.7
B	13,970 - 14,790	12,125 - 12,900	0.66 - 0.62	451 - 499	118 - 160	250 - 306	223 - 274	45	94.0	98.5	27.3
C	25,000 - 26,070	22,440 - 23,190	0.36 - 0.35	367 - 630	89 - 127	276 - 460	235 - 408	35	94.1	98.3	28.5
D	26,190 - 28,440	23,640 - 24,170	0.34 - 0.33	481 - 673	122 - 172	346 - 474	313 - 426	38	92.9	98.1	29.4

* Average of all performance analysis data.

ASBRs and higher organic loadings of 10 and 12 g COD/L/day were investigated in Reactors C and D. Reactors A and B were subjected to severe biosolids washout as the result of foam formation on the top portion of the reactors, when the COD loading increased beyond the 8 g/L/day. The causes of foaming in the ASBR were not fully understood. Van Niekerk et al. (1987) suggested that anaerobic digestion foaming is associated with high alkalinity, high ammonia, and high volatile fatty acid level.

The last pseudo-steady-state performance data were collected on December 23, 1991 (day 250). The COD loading of all four ASBRs was then reduced to 6 g/L/day after completion of the phase 3 performance study. The ASBRs were operated for another 80 days in order to complete the biosolids granulation study.

Phase 3 Biosolids Study

The biomass concentration profiles of the reactors in Phase 3 are shown in Figure 5.8. The biomass concentrations in Reactors C and D, ranging between 22,000 and 34,000 mg/L, were significantly higher than the biomass concentrations in Reactors A and B, ranging between 6,000 and 14,500 mg/L. More biomass was retained in Reactors C and D because a lower level of the biosolids washout pressure was imposed in these stout shape reactors.

In Phase 3 of the experimental study, the HRT was lowered to 12 hours and decant volume was increased to 4 liters per cycle. The biosolids selection pressure was the highest of the three phases. The decanting process gradually washed out the smaller,

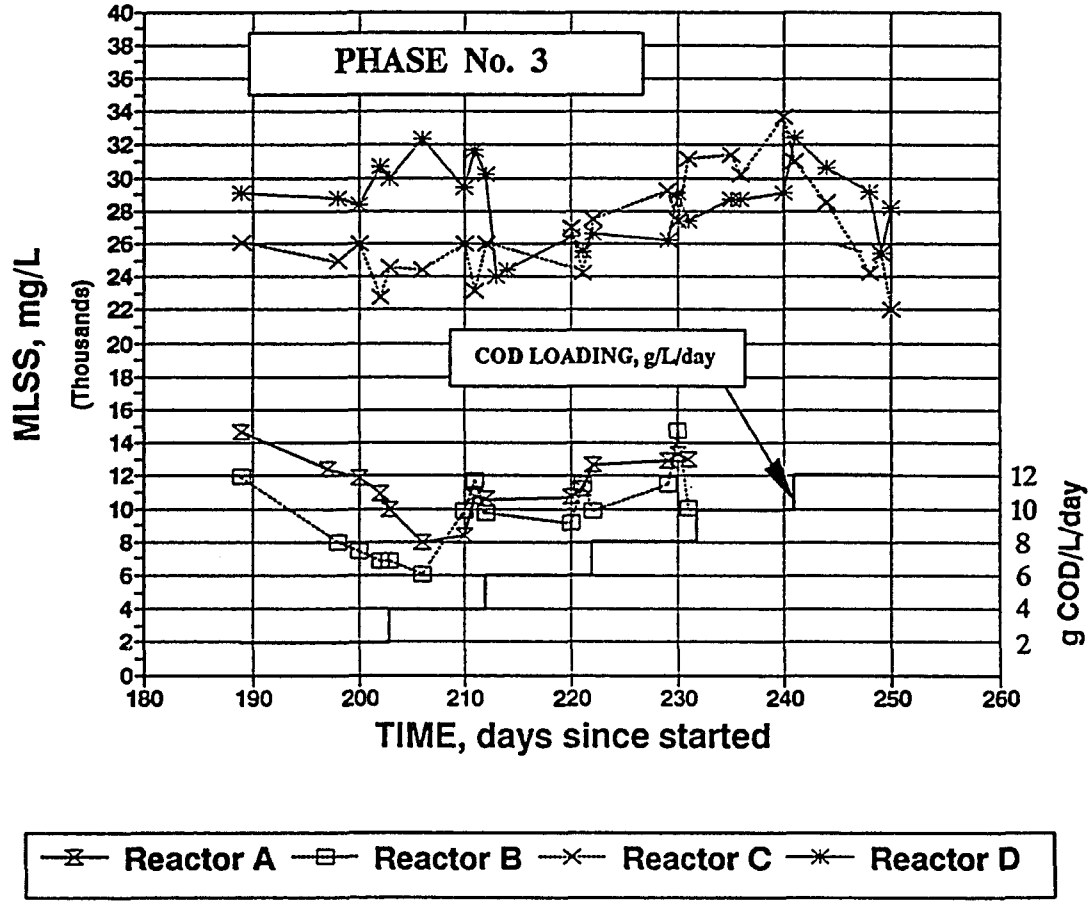

Figure 5.8. MLSS concentration profile in phase 3 period

lighter dispersed particles. Consequently granular biomass became dominant and led to a rapidly settling, discrete particle settling (Type I) biomass and the settling time required for solids clarification could be reduced to less than 10 minutes.

The ASBR became a very stable system when the granular biomass was formed. The internal gassing appeared less effective in agitating the heavier granular biomass because a higher energy was required for mixing the bigger and heavier particles. For the same reason, the ASBRs with granular biomass were less sensitive changes in hydraulic pressure during the decant steps and less sensitive to biosolids/liquor disruption.

Since the ASBR relies on internal solids separation for retention of biomass, efficient solids clarification and/or granulation of the biomass is essential to achieving high rates of conversion of COD to methane. In the course of this research, maintaining a stable biomass concentration in the reactor proved to be the key element of success. The granulation process reinforces biosolids retention and leads to a highly stable reactor system.

Once the granular biomass predominated in the reactor, the predetermined mixing intensity of 100 1/sec could no longer sustain a complete-mix system. The biosolids were stratified into layers during the mixing periods like an expanded solids blanket with the heaviest particles at the bottom and the lightest particles near the surface. This phenomenon made for a difficult situation in sampling the MLSS.

Phase 3 Performance

The performance data at the organic loading of 2 g COD/L/day and HRT of 12 hour were not reported. Biosolids washout conditions persisted in Reactors A and B due to a low net yield of biomass and high decant volume during the operating period at 2 g COD/L/day. The Reactors might regain their pseudo-steady-state conditions after a period of time. However, to prevent further loss of valuable biomass, the system was continued on to the next COD load of 4 g COD/L/day.

Performance data for the reactors at HRT of 12 hours and the various COD loads investigated are shown in Table 5.6. The data show the removal of NFDM substrate over the range of COD loads from 4 to 12 g COD/L/day. Removals were particularly good at COD loadings from 4 to 10 g/L/day but dropped slightly at the higher COD load of 12 g/L/day. Average methane production data were well correlated (within $\pm 5\%$) with theoretical values calculated from COD removal. The effluent suspended solids and COD concentrations increased as the organic loadings increased. The food to microorganism ratios investigated were in the range of 0.14 - 0.90 g/g-day. A wider range of F/M ratios reported in this phase might suggest that the ASBR with the granular biomass could be successfully operated at a higher F/M ratio due to the enhancing settleability and biological activity of the granular biomass.

In this phase of the study, the effluent total volatile acids concentrations were lower than 60 mg/L over the range of COD loads from 4 to 10 g COD/L/day and increased to 98 mg/L at COD load of 12 g COD /L/day.

Table 5.6. Performance of the ASBR at a 12-hour HRT and various COD loadings

Reactor	MLSS	MLVSS	F/M	Effluent Characteristics					COD Removal		CH_4 Prod.*
				TCOD	SCOD	TSS	VSS	TVA*	Total	Soluble	@STP
	mg/L	mg/L	g/g-day	mg/L	mg/L	mg/l	mg/L	mg/L as Acetate	%	%	L/day
				COD Loading = 4.0 g/L/day							
A	8,360 - 10,780	7,120 - 9,440	0.56 - 0.42	235 - 471	63 - 91	154 - 370	138 - 325	25	81.0	96.1	15.3
B	6,075 - 11,710	5,435 - 10,400	0.74 - 0.38	247 - 667	40 - 92	189 - 523	163 - 460	30	77.7	96.4	15.7
C	23,160 - 26,020	20,080 - 22,880	0.20 - 0.17	362 - 669	50 - 101	259 - 545	234 - 478	21	78.2	95.9	15.5
D	29,440 - 31,720	26,735 - 28,450	0.15 - 0.14	306 - 535	67 - 83	220 - 416	171 - 359	23	82.5	96.2	15.5
				COD Loading = 6.0 g/L/day							
A	10,740 - 12,620	9,400 - 10,370	0.64 - 0.58	349 - 554	121 - 156	208 - 413	185 - 361	35	85.1	95.1	22.8
B	9,190 - 11,480	8,190 - 9,950	0.73 - 0.60	374 - 440	101 - 152	211 - 297	183 - 258	49	86.7	95.4	23.0
C	24,270 - 27,510	20,790 - 23,840	0.29 - 0.25	505 - 623	120 - 159	344 - 461	310 - 407	35	82.6	95.5	22.8
D	25,500 - 26,655	22,370 - 24,225	0.27 - 0.25	480 - 656	124 - 177	269 - 512	233 - 452	34	82.3	94.8	22.6
				COD Loading = 8.0 g/L/day							
A	12,890 - 13,290	10,600 - 11,350	0.75 - 0.70	402 - 634	98 - 194	334 - 476	288 - 417	37	86.4	96.1	30.7
B	10,010 - 14,730	8,800 - 12,830	0.90 - 0.62	484 - 686	127 - 195	349 - 515	304 - 464	41	83.5	95.8	29.9
C	27,460 - 31,190	24,270 - 26,940	0.33 - 0.30	488 - 631	175 - 222	347 - 448	306 - 395	42	87.7	96.2	29.6
D	26,230 - 29,050	23,410 - 26,510	0.34 - 0.30	528 - 656	147 - 215	355 - 443	317 - 392	54	86.8	96.5	28.7
				COD Loading = 10.0 g/L/day							
A	-	-	-	-	-	-	-	-	-	-	-
B	-	-	-	-	-	-	-	-	-	-	-
C	30,190 - 33,665	25,940 - 30,100	0.38 - 0.33	612 - 748	196 - 278	416 - 594	373 - 507	49	86.4	95.1	35.3
D	28,670 - 32,460	25,180 - 28,810	0.40 - 0.35	598 - 669	173 - 281	408 - 589	359 - 521	54	88.1	95.3	36.8
				COD Loading = 12.0 g/L/day							
A	-	-	-	-	-	-	-	-	-	-	-
B	-	-	-	-	-	-	-	-	-	-	-
C	22,040 - 25,450	18,910 - 22,500	0.63 - 0.53	959 - 1,142	358 - 447	666 - 914	585 - 803	85	82.2	92.8	39.9
D	25,410 - 28,250	22,930 - 25,930	0.52 - 0.46	1,207-1,674	319 - 585	848 - 1,149	740 - 1,018	98	74.8	91.3	38.9

* Average of all performance analysis data.

The volatile acids are the intermediate products of the complex anaerobic degradation reactions. The intermediate products can accumulate in the anaerobic system if the population of the three different bacteria groups (fermentative, acetogenic, and menthanogenic bacteria) are not well balanced or if an inhibitory environment is present in the system. The effluent volatile acids concentrations were lower than 100 mg/L throughout the performance studies. The fact of low volatile acids concentrations indicated that the ASBR system was operated in a well balanced environment and at optimal operating conditions. The volatile acids (organic acids with a carbon-chain number between 2 and 5) contents in the effluent were analyzed by gas chromatography. Table 5.7 shows typical volatile acid compositions in the effluent of the ASBRs. The data presented in the table were collected on December 2, 1991, at the COD load of 8 g COD/L/day. Acetic and propionic acids were the primary acids in the effluent.

Table 5.7. Typical volatile acid species in the effluent of the ASBRs

Volatile Acids	Reactor A	Reactor B	Reactor C	Reactor D
	Concentration, mg/L as Acetic			
Acetic	17.3 (70%)	21.7 (69%)	10.7 (51%)	11.1 (46%)
Propionic	5.1 (21%)	6.7 (21%)	5.8 (28%)	6.1 (25%)
Butyric	0.9 (4%)	1.5 (5%)	0.6 (3%)	1.6 (7%)
Iso Butyric	0.2 (1%)	0.3 (1%)	1.2 (6%)	1.0 (4%)
Methyl Butyric	0.8 (3%)	1.1 (3%)	2.1 (10%)	3.1 (13%)
Valeric	0.3 (1%)	0.2 (1%)	0.5 (2%)	1.1 (5%)
TOTAL	24.6 (100%)	31.5 (100%)	20.9 (100%)	24.0 (100%)

Operating Conditions: 1) Organic loading = 8 g COD/L/day.
2) HRT = 12 hours.

The maximum organic loading rate without excessive loss of biomass was 12 g/L/day at HRT of 12 hours. This does not necessarily suggest that the system would not handle higher organic loadings. Throughout each of the phases of this study, a continuous improvement in the ASBRs biosolids separation and retention ability ensured the system with a better stability and higher organic or hydraulic loads. On the other hand, the primary limitation of the ASBR process, with respect to the high loading rates, was shown to be the biomass retaining ability or the biosolids washout condition during the decant step. Therefore, the development of granular biomass was considered to be one of the primary advantages of the ASBR process. Granulation increase system stability in terms of the effectiveness of solids separation and retention.

The last performance data were collected on December 23, 1991 (day 250). Reactors A and B were then used in the study of intermittent mixing between December 17 and 20, 1991.

Habben (1991) conducted initial studies on the ASBR using the same reactor (Reactor A) and the same substrate (NFDM). The initial study was carried out in a continuously-mixed system. The ASBR system was operated over a range of COD loads from 0.5 to 4.7 g/L/day at HRTs of 2.17 days, 1.08 days, and 0.54 days. Granular biomass was not developed after eleven months of operation.

In this experimental study, four ASBRs were operated at the mixing patterns of five minutes mixing per hour and a velocity gradient of 100 per second through of the ASBR performance study. Excellent COD removals in the ASBRs indicated that intermittent

mixing did not restrain the biological conversion, but possibly enhanced the formation of granular biomass as compared to the continuously-mixed unit. A combination of the intermittent mixing (5min/hour) and the mixing caused by the internal gassing proved to be sufficient in biological conversion of NFDM substrate in the ASBR. Excess mixing intensity or duration could physically shear the biomass flocs or particles and inhibit the granulation process. The granular biomass with highly effective solids separation and retention characteristics enabled the ASBR to be operated at higher organic loads as compared with the ASBR operated without granular biomass in the previous research by Habben (1991).

Granulation Study in ASBR

In the early stages of the study, zone settling was the predominant process in solids separation. After about five months of operation, a noticeable difference in the solids separation pattern occurred in the reactor due to the gradual conversion of the flocculent biomass to granular biomass. The granulation process can be cultivated by many factors, as mentioned in the Literature Review section. In this research, the study of the granulation process in the ASBR was focused on the biosolids selection pressure effects caused by the difference in reactor geometry, the system hydraulic retention time (HRT), and the operating food to microorganisms ratio (F/M). Different reactor geometries or operating HRTs impose different levels of selection pressure on the biomass. The decant volume governed by the HRT affects the amount of biosolids washout, the consequence of selection pressure. The higher the F/M ratio, the more the internal gassing and the greater

the selection pressure. A detailed discussion of biosolids selection pressure was addressed in previous sections under the subheadings of Biosolids Selection Pressure and Reactor Geometry Effects.

The biosolids particle size distribution information for each ASBR was measured by the Automatic Image Analyzer (AIA). The first AIA measurement was performed on the 187th day of the experimental study when the granular biosolids were well developed in the reactors. The seed particle sizes were also recorded as a base line for measuring the progression of the granulation process. AIA data and calculations of cumulative particle weight percentages are reported in Section D of the Appendix. Mean particle size (d50) is defined as the particle size which divides the distribution such that 50% of the biosolids by weight is finer and 50% is coarser than this size. Mean particle size is easily read from the 50% line on a particle size distribution curve and is an indicator of overall particle sizes.

The ASBR biosolids particle size distribution curves on days 187, 223, 260, and 310 are shown in Figures 5.9, 5.10, 5.11, and 5.12, respectively. The results show that the differing rates of granulation were clearly related to reactor geometry. The tall, slender reactor (Reactor A) selected much larger biosolids particle sizes than the other three reactors in all four times. The biosolids particle sizes in Reactors C and D (stout shape) are quite similar to each other and are the lowest in all four cases. Reactor A, the reactor with the highest depth-to-diameter ratio, was most effective in optimizing granulation, as can be seen by the differences in the mean particle sizes illustrated in Figure 5.9, 5.10, 5.11, and 5.12. These larger granules also correspond to higher settling velocities. The

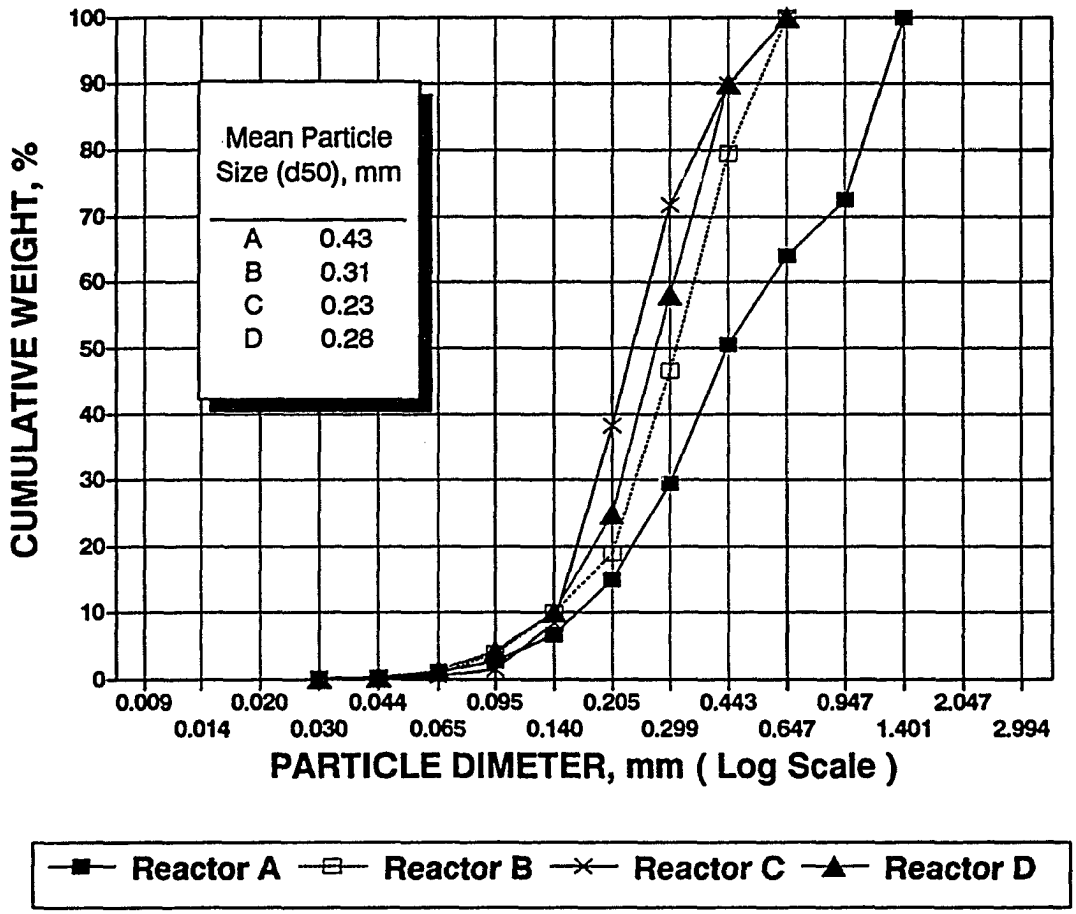

Figure 5.9. Biosolids particle size distribution curves in the various reactors on day 187

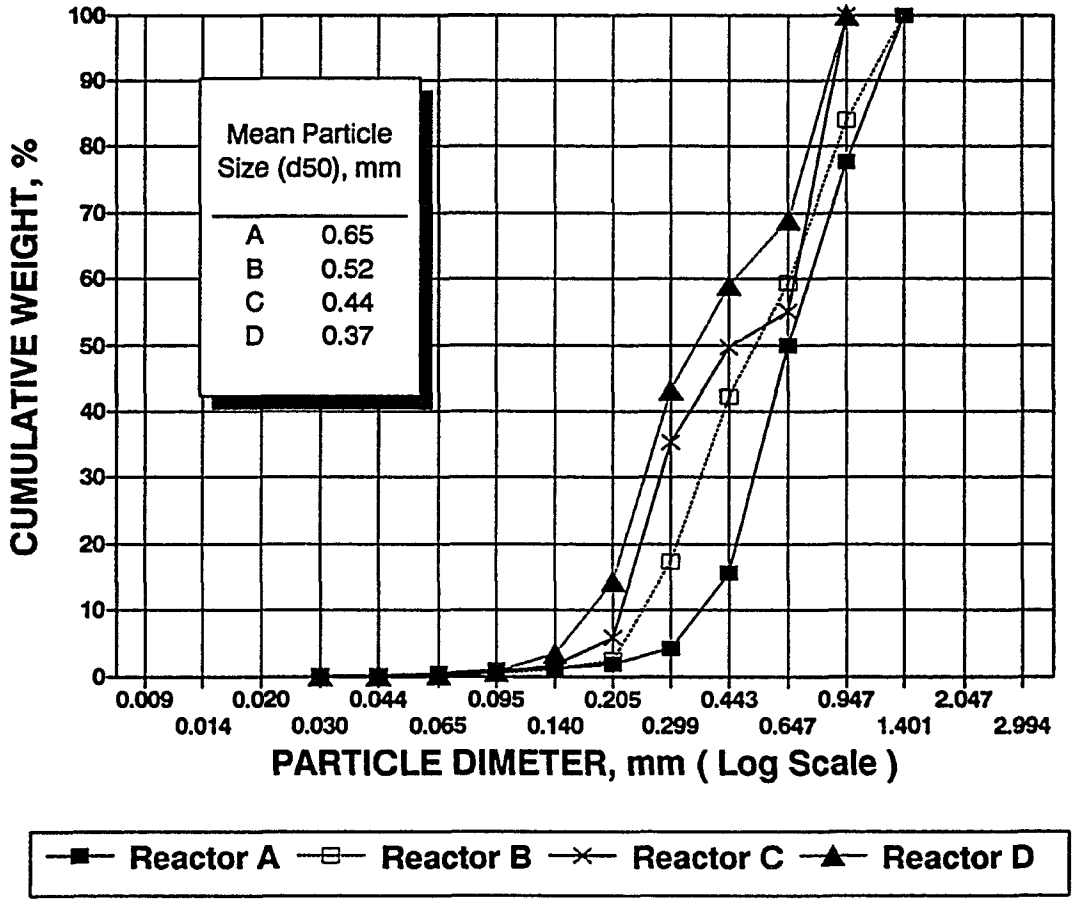

Figure 5.10. Biosolids particle size distribution curves in the various reactors on day 223

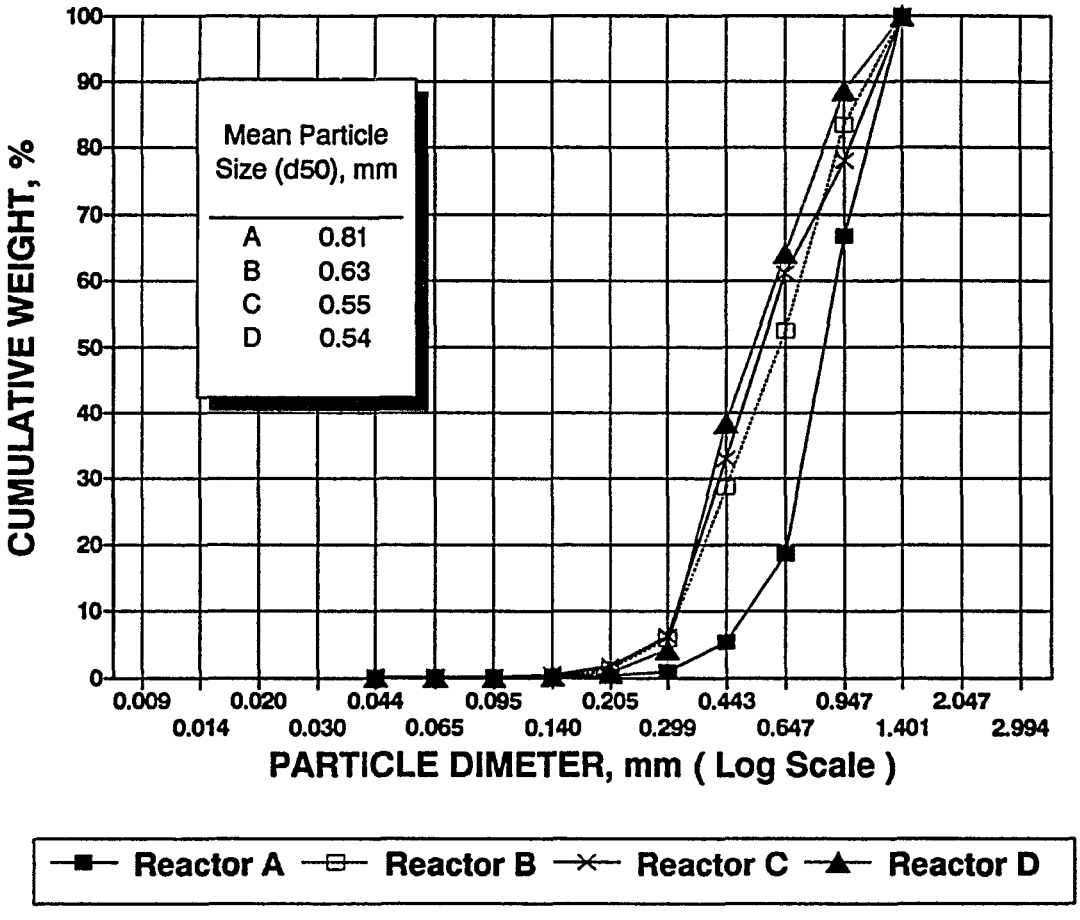

Figure 5.11. Biosolids particle size distribution curves in the various reactors on day 260

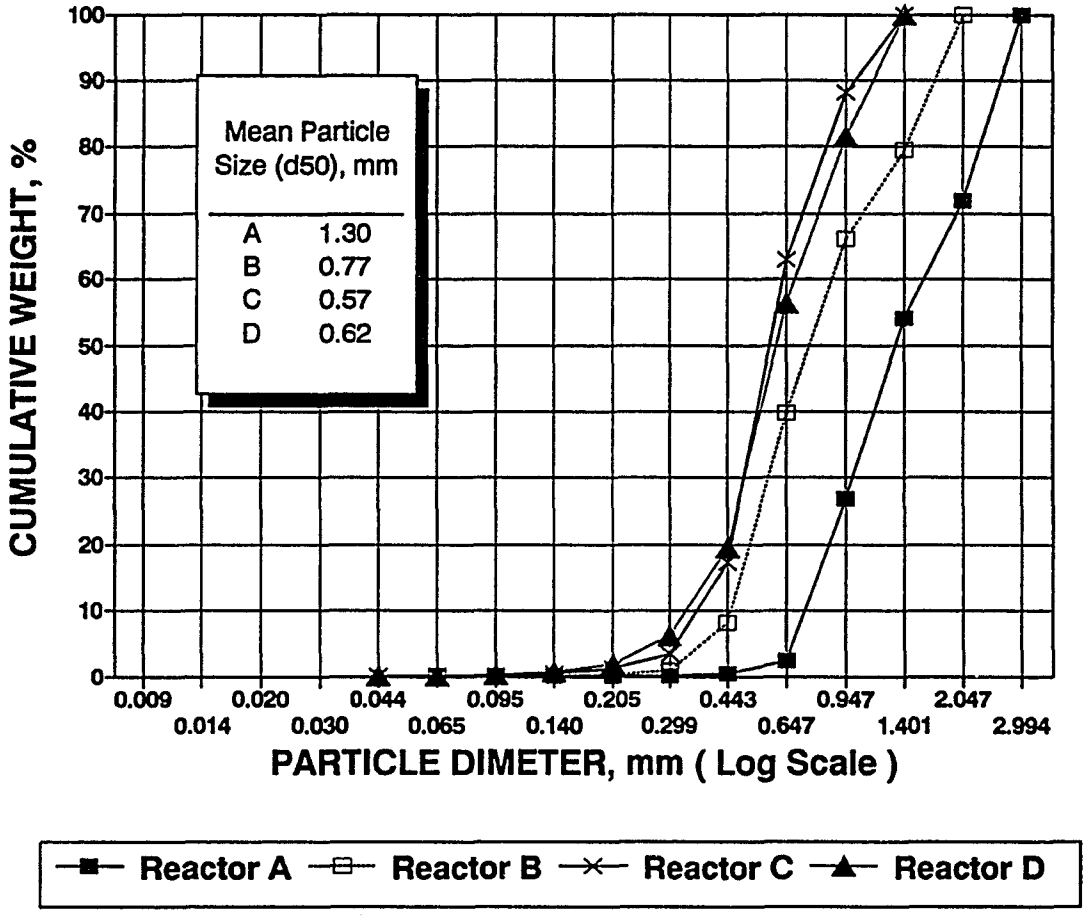

Figure 5.12. Biosolids particle size distribution curves in the various reactors on day 310

granular biosolids in Reactors A and B had mean settling velocities (determined at the 50% cumulative weight) of 72 m/hour and 59 m/hour, respectively.

Figures 5.13, 5.14, 5.15, and 5.16 show the changes in particle size distribution from the first day of operation to day 310 in Reactor A, B, C, and D, respectively. The progression of the granulation is indicated by the increasing particle sizes. The particle sizes increased at an exponential rate as the hydraulic pressure on the system was increased by reducing HRTs from 48 hour to 24 hour and then to 12 hour. Mean particle sizes increased from day 1 of 0.16 mm to day 310 of 1.30 mm, 0.77 mm, 0.57 mm, and 0.62 mm for Reactors A, B, C, and D, respectively.

The granule morphology was characterized using scanning electron microscopy (SEM). Scanning electron microscopy was used to view the surface of the granules at two different magnifications, 200 and 4,000x. The photograph in Figure 5.17 at 200x magnification shows the granule surface with a porous structure. The porous structure allows the substrate to diffuse into the inner part of the granule and creates a tremendous micro-organisms/substrate contact area for bioconversion to take place. The photographs in Figure 5.18 show the surface of the granule at 4,000x is covered with bacteria of many morphologies. The predominant morphologies are large and small rods and rods in chains. Single coccus, cocci in clumps, and irregular spaghetti shaped chains can also be found in large numbers. It is apparent that most of the granule structure is bacterial in nature. Close examination of the microbial system connected with granular particles reveals a symbiotic association between the microbial consortia.

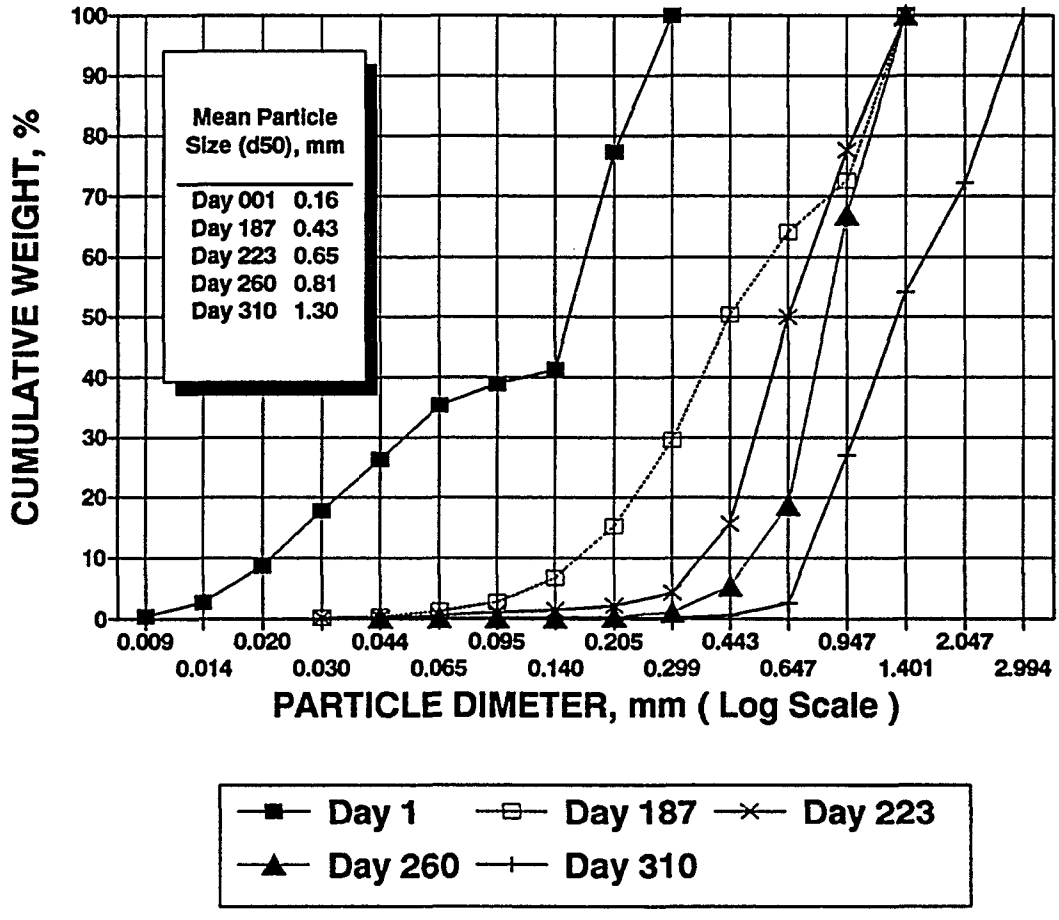

Figure 5.13. Particle size distribution in Reactor A

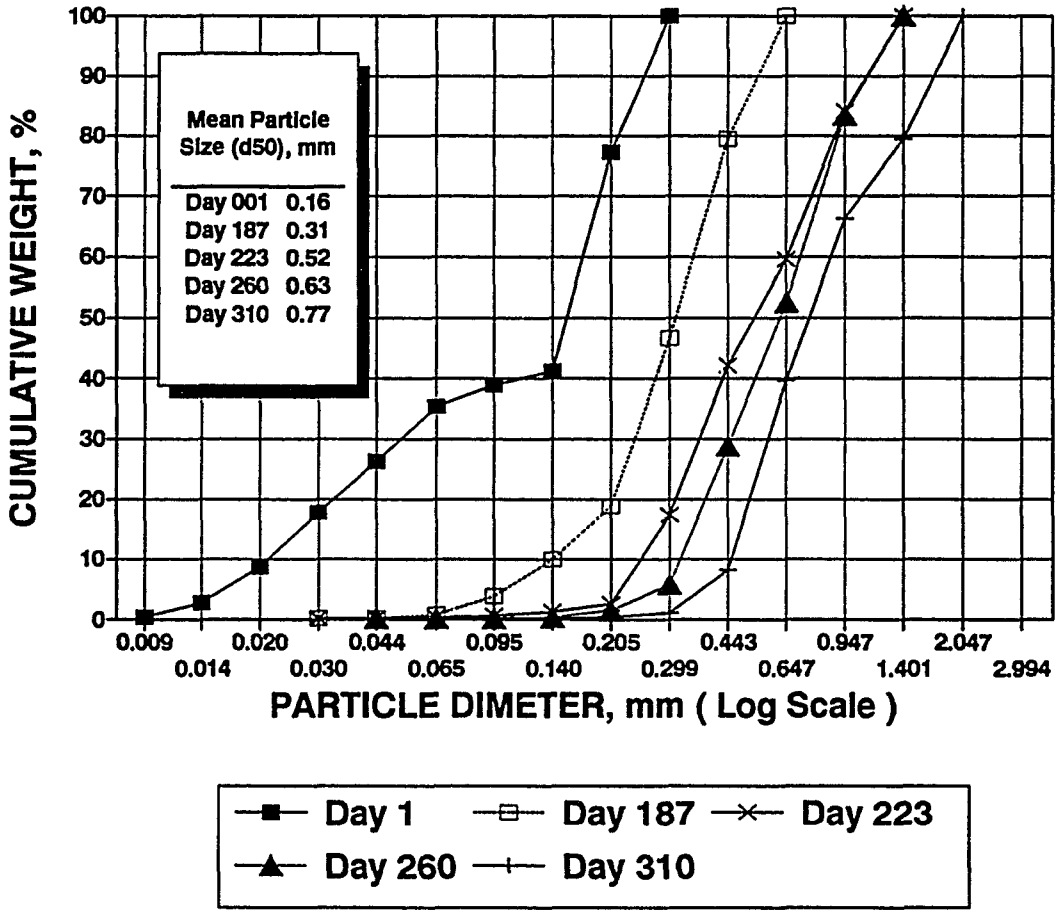

Figure 5.14. Particle size distribution in Reactor B

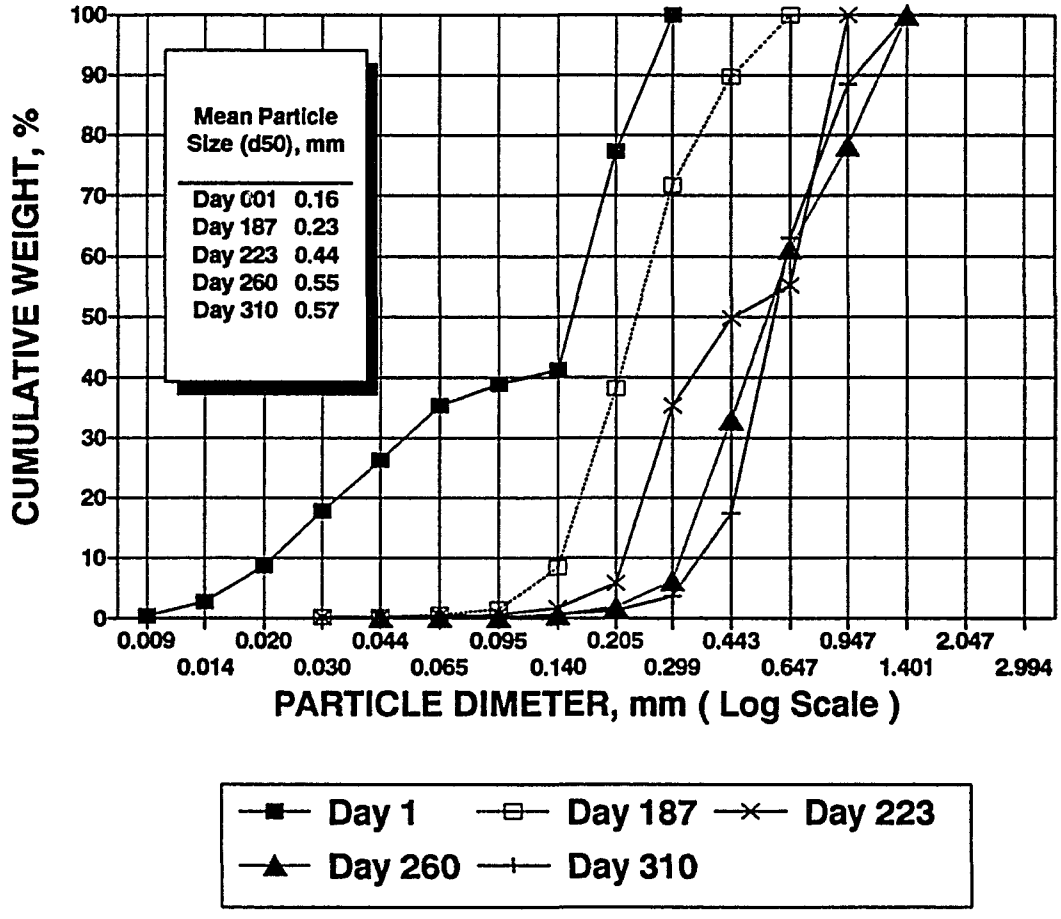

Figure 5.15. Particle size distribution in Reactor C

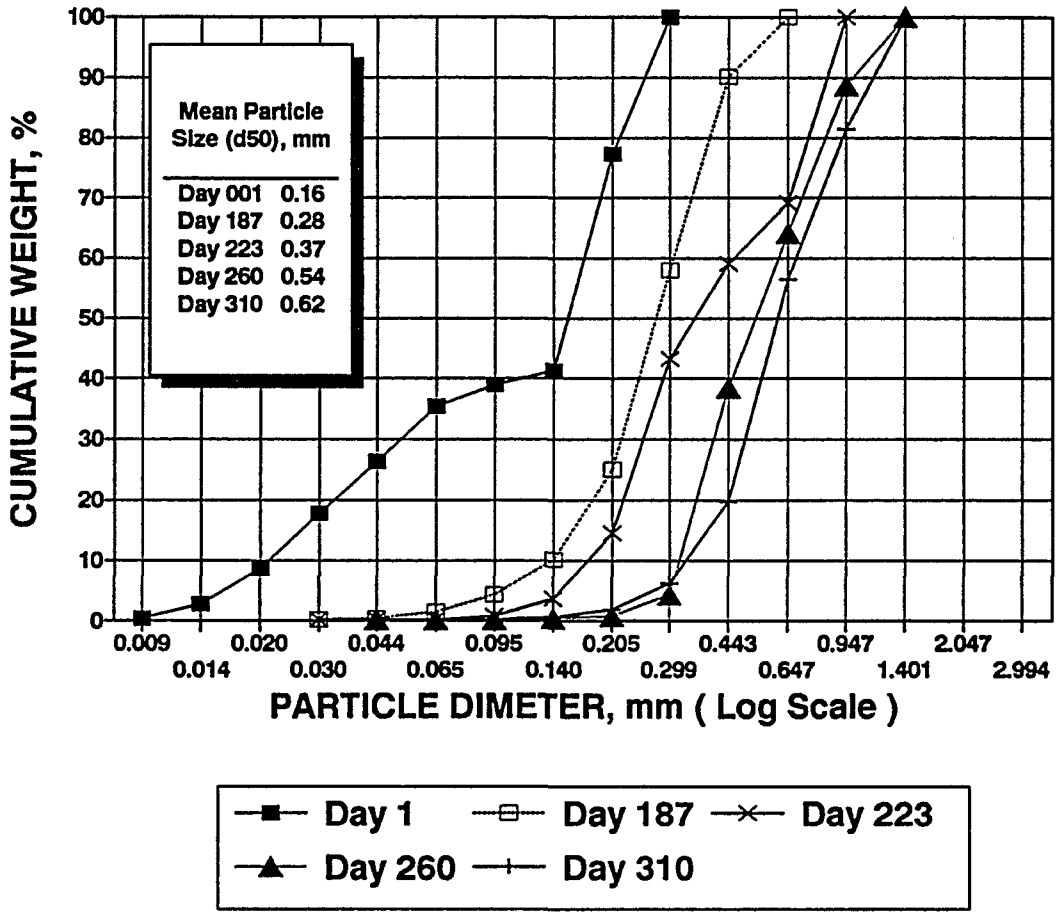

Figure 5.16. Particle size distribution in Reactor D

Figure 5.17. Scanning electron microscope view (200X) of a typical ASBR granule (bar = 0.1mm)

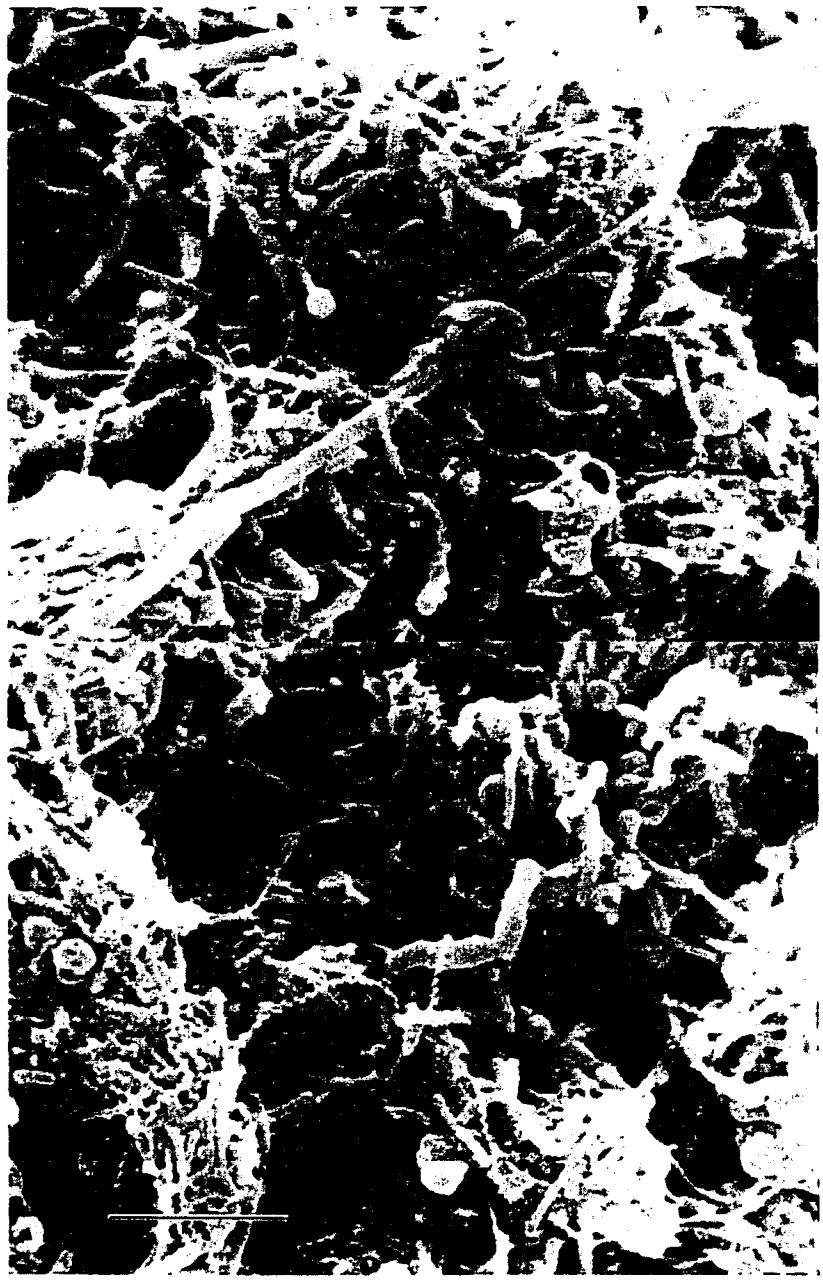

Figure 5.18. Scanning electron microscope view (4,000X) of a typical ASBR granule (bar = 5μm)

Study on Mixing Patterns

The study on mixing patterns was conducted on four consecutive days in Reactors A and B. The MLVSS concentration in each reactor maintained a relatively constant level. Three intermittent mixing patterns (1. 2.5 min/30 min, 2. 5 min/hour, and 3. 100 sec/20 min) with the same hourly mixing duration and a continuous mixing pattern were investigated. The results are summarized in Section E of the Appendix.

Figures 5.19 and 5.20 show the soluble COD remaining curves for four mixing patterns in Reactors A and B, respectively. The SCOD curves shown in Figures 5.19 and 5.20 have the general appearance of a decay curve, flattening out near the end of the cycle. Continuous mixing appears to result in a somewhat more rapid rate of COD removal in Reactor A during the first four hours of the cycle but there is essentially no difference in overall COD remaining at the end of the six-hour cycle.

Figures 5.21 and 5.22 compare methane productions under the same mixing patterns as in Figures 5.19 and 5.20. As shown, the reactor under intermittent mixing conditions actually produced a somewhat greater total amount of methane over the six-hour sequence period than did the reactor under the continuous mixing condition. Although no ready explanation for this observation is at hand from this research, it can be stated that intermittent mixing was preferable to continuous mixing from both COD removal, methane production, and energy conservation standpoints. This confirms the observation of Dague, et al. of some years ago (1966, 1970) that intermittent mixing has a positive effect on the performance of batch-fed anaerobic reactors.

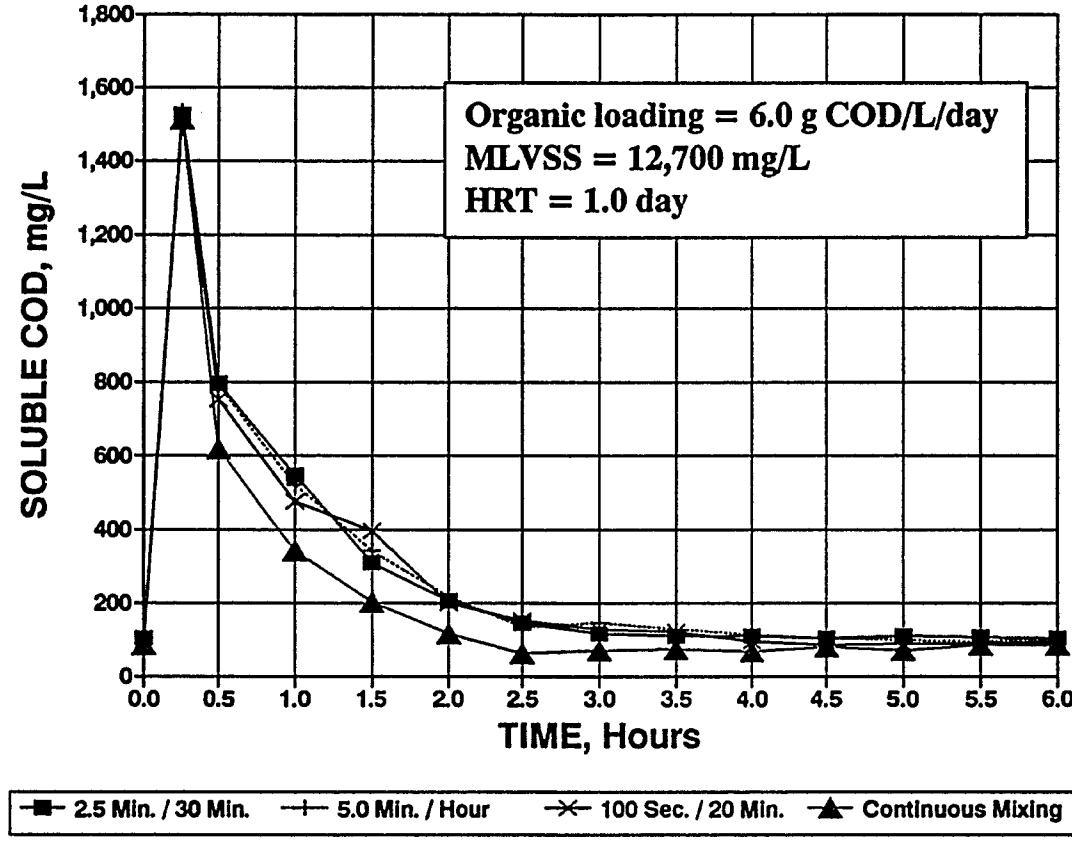

Figure 5.19. SCOD remaining curves for four mixing patterns in Reactor A

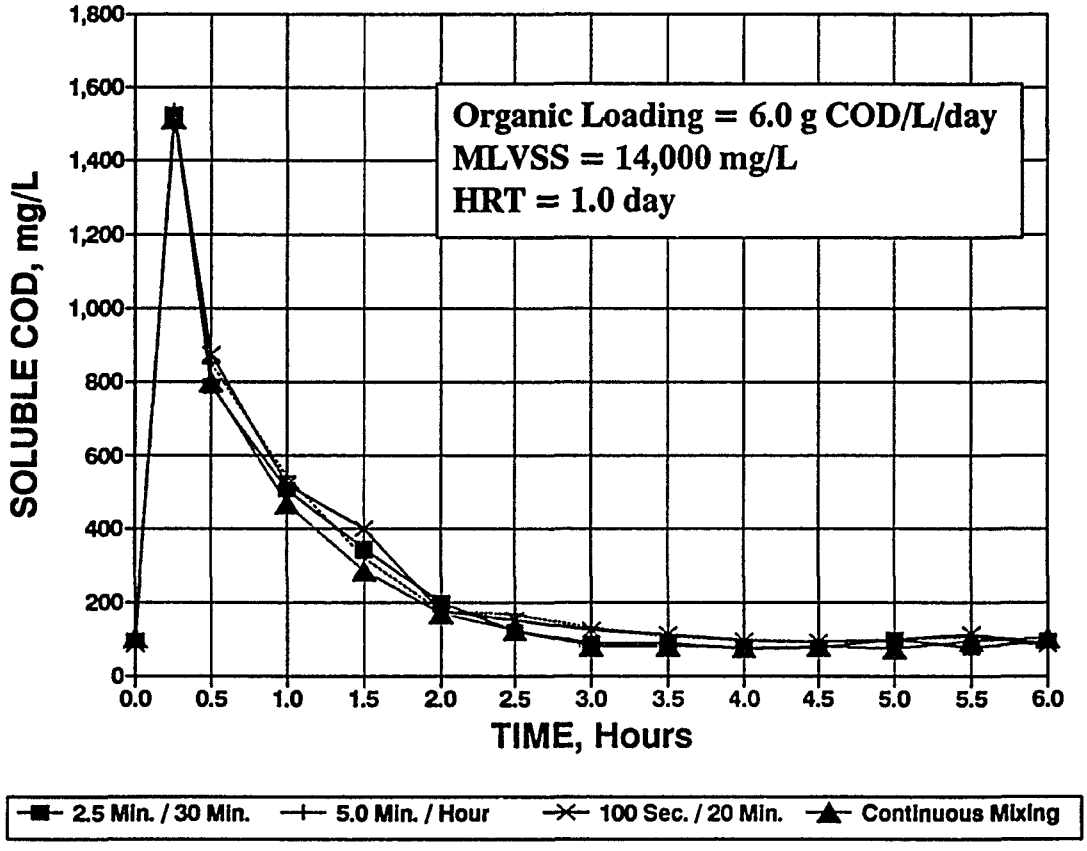

Figure 5.20. SCOD remaining curves for four mixing patterns in Reactor B

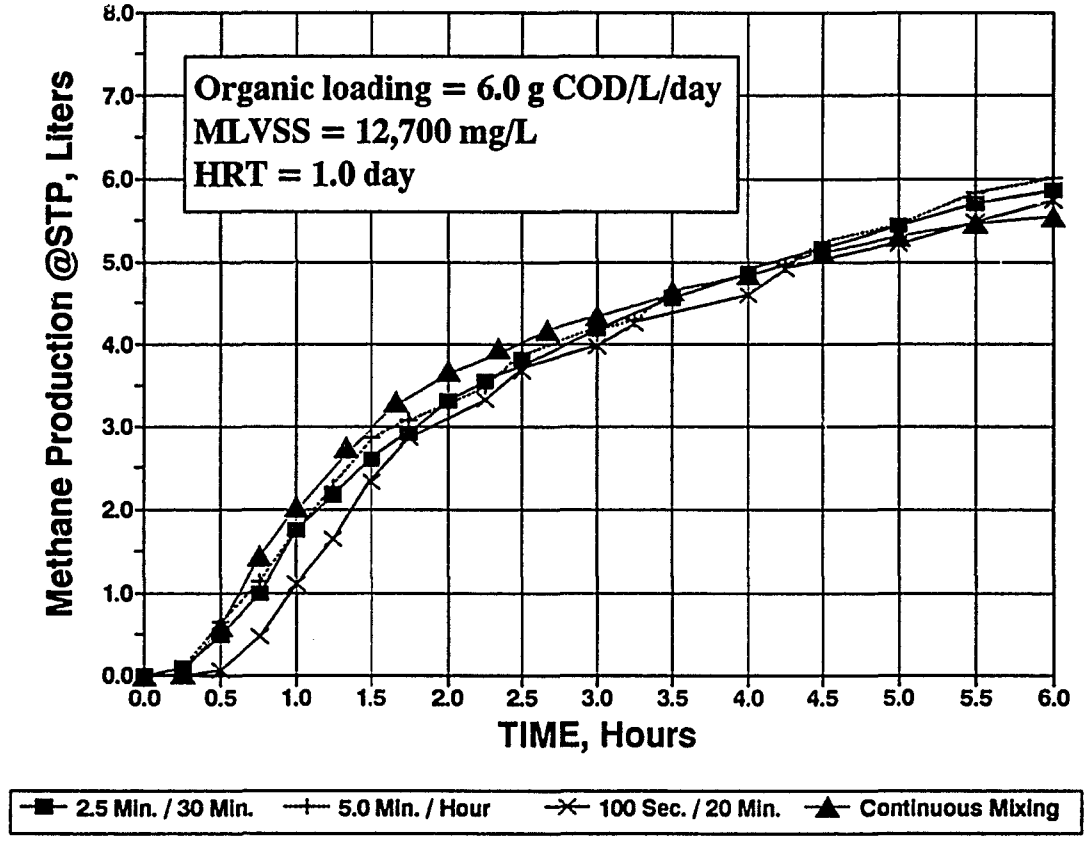

Figure 5.21. Methane production curves for four mixing patterns in Reactor A

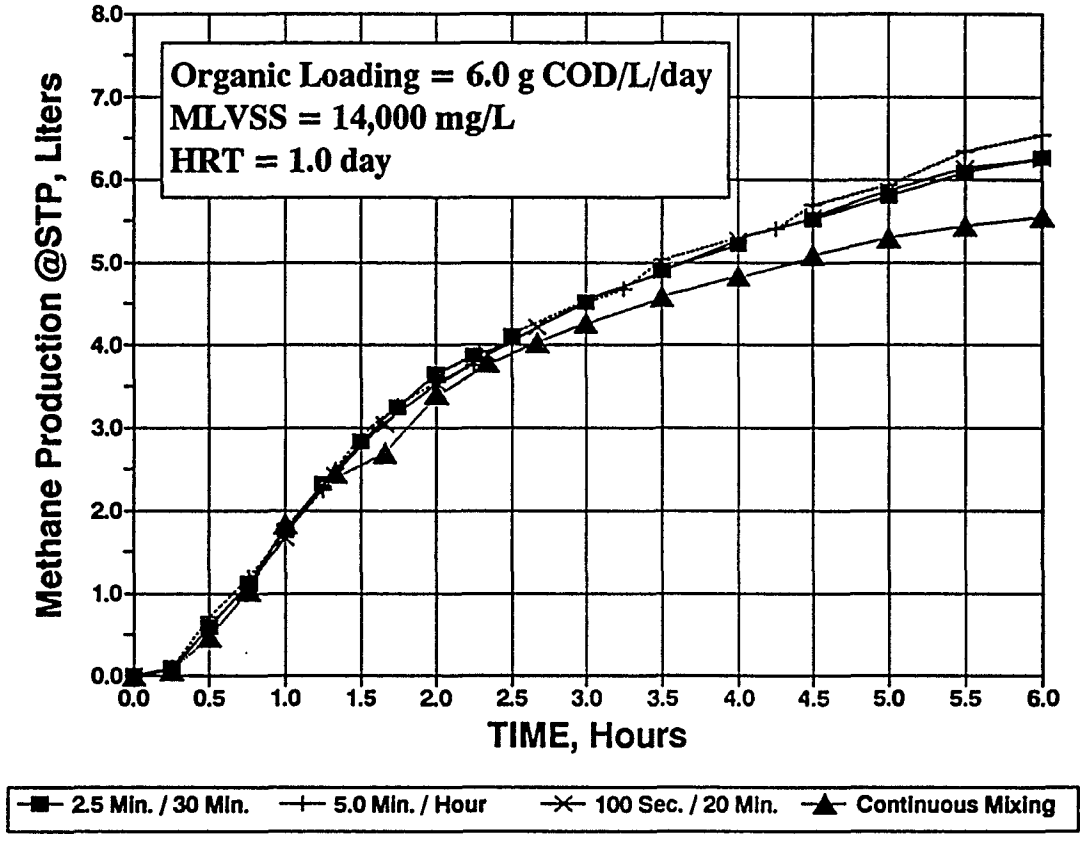

Figure 5.22. Methane production curves for four mixing patterns in Reactor B

The methane production rate is the slope of the methane production curve. Figures 5.23 and 5.24 illustrate the variation in methane production rate for intermittent mixing vs continuous mixing in Reactors A and B, respectively. The two intermittent mixing patterns illustrated are 2.5 min/30 min and 5 min/hour with a velocity gradient of 100 1/sec. With reference to Figures 5.23 and 5.24, it can be seen that continuous mixing results in a much more uniform pattern of methane production as compared with intermittent mixing. The peak production is higher with continuous mixing (with the peak occurring in about 40 min) and declines to a low level at the end of the six-hour cycle. For the reactor that is mixed only five minutes per hour, the peak methane production rate is lower and spread over a longer time period, as opposed to the continuously-mixed reactor. The "saw-tooth" pattern of methane production reflects the increase in methane release from the biomass during mixing periods. Also, the methane production rate appears to remain somewhat higher at the end of the six-hour cycle for the intermittently-mixed reactor as compared to the continuously-mixed reactor.

Biosorption

Figures 5.25, 5.26, 5.27, and 5.28 illustrate the variations in both soluble COD and methane COD (COD remaining based on methane production) in Reactor A for four mixing patterns. The methane COD values are calculated on the basis that 0.35 L of methane (STP) are produced for one gram of COD removed. The results showed that the initial uptake and biosorption of the NFDM substrate was quite rapid. The process was capable of removing about 50% of the COD within 30 min at a COD loading of 6 g/L/day.

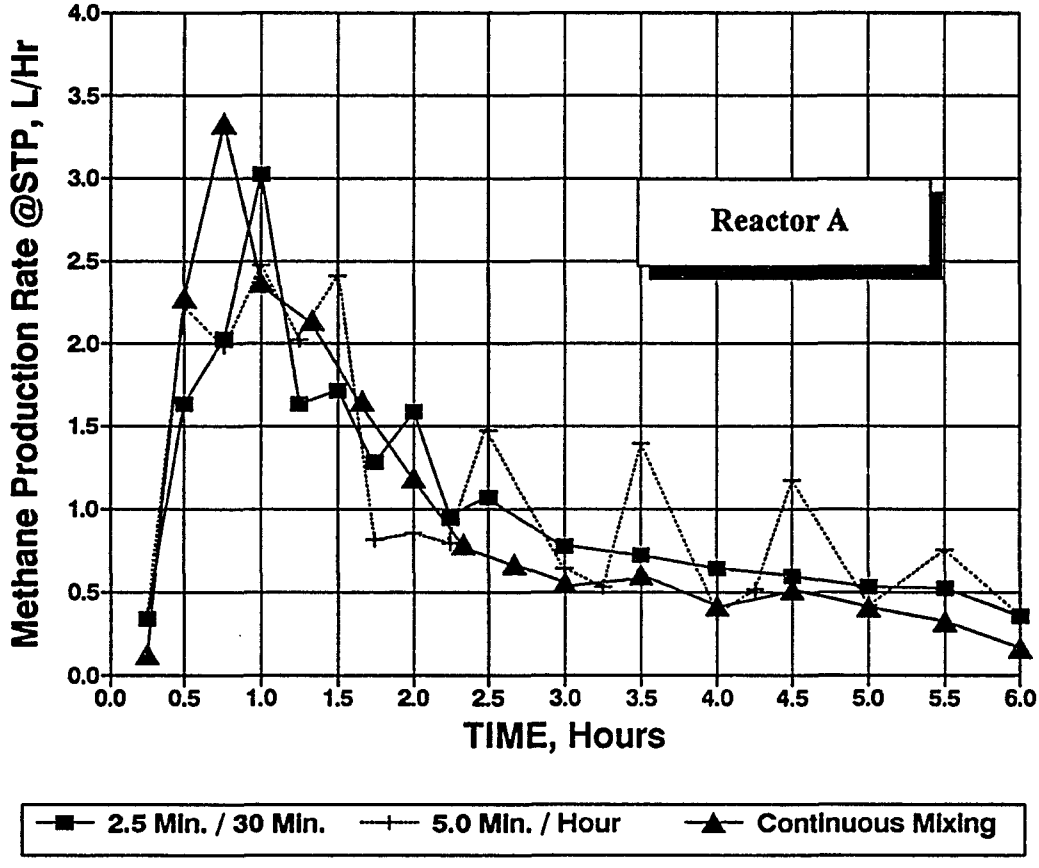

Figure 5.23. Effect of mixing pattern on methane production rate in Reactor A

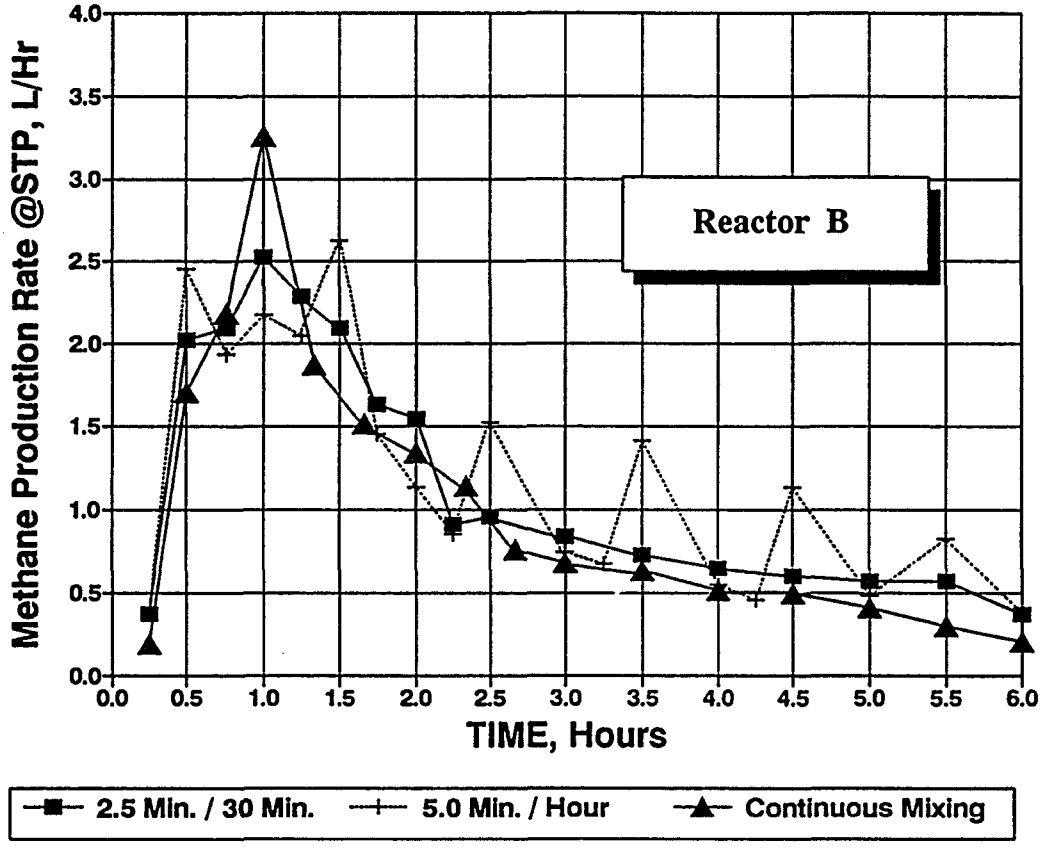

Figure 5.24. Effect of mixing patterns on methane production rate in Reactor B

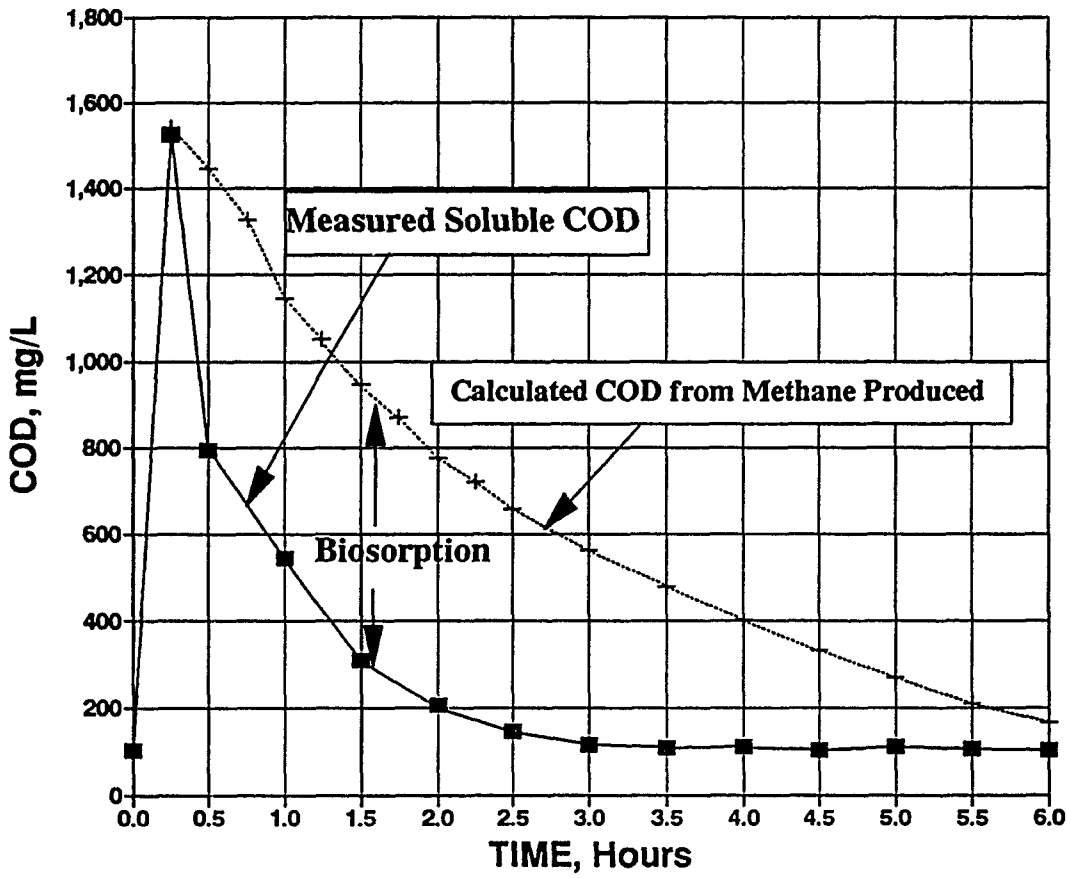

Figure 5.25. SCOD and Methane COD removal curves at mixing pattern of 5 min/hour

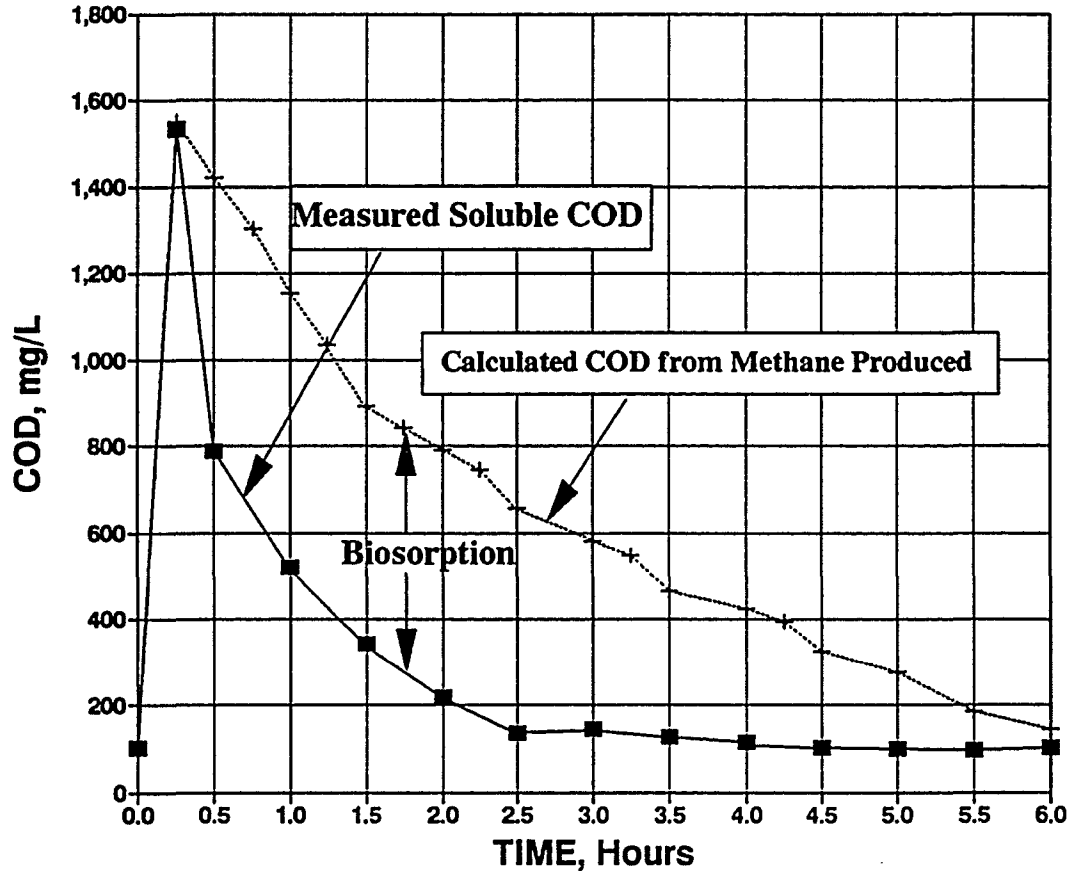

Figure 5.26.SCOD and Methane COD removal curves at mixing pattern of 2.5 min/30 min

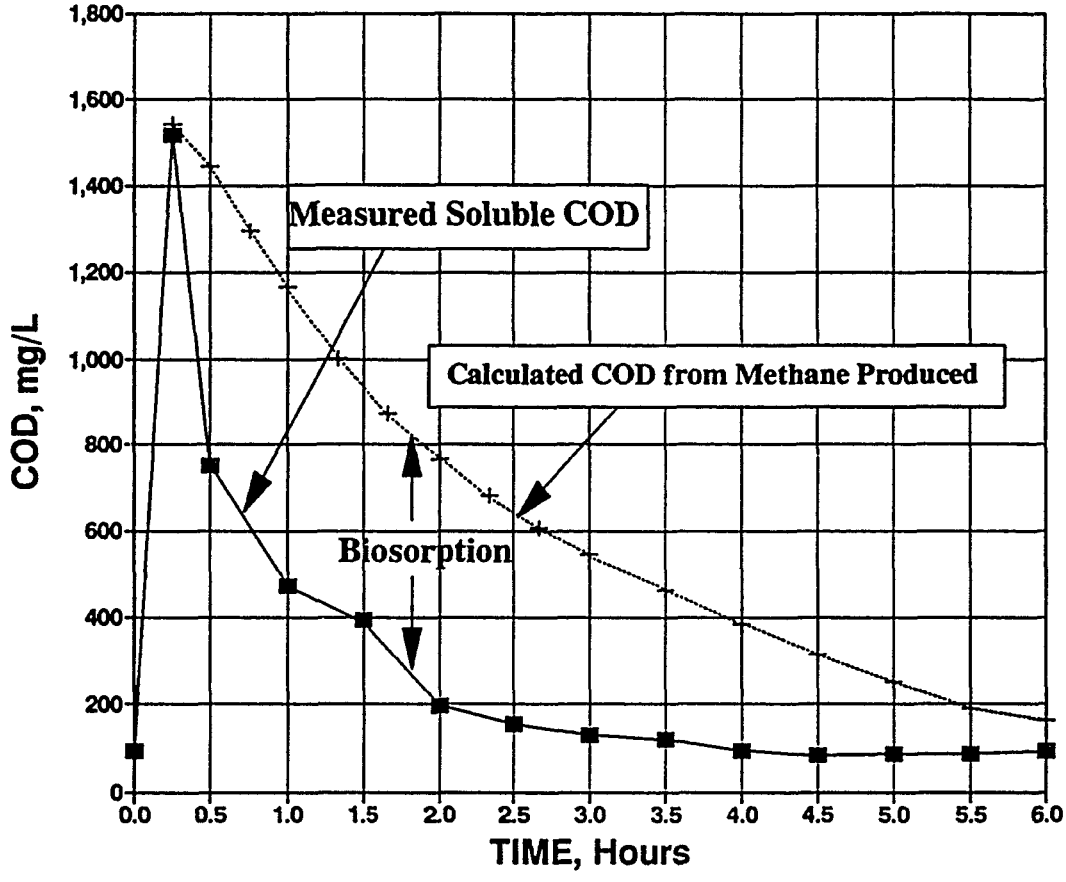

Figure 5.27. SCOD and Methane COD removal curves at mixing pattern of 100 sec/20 min

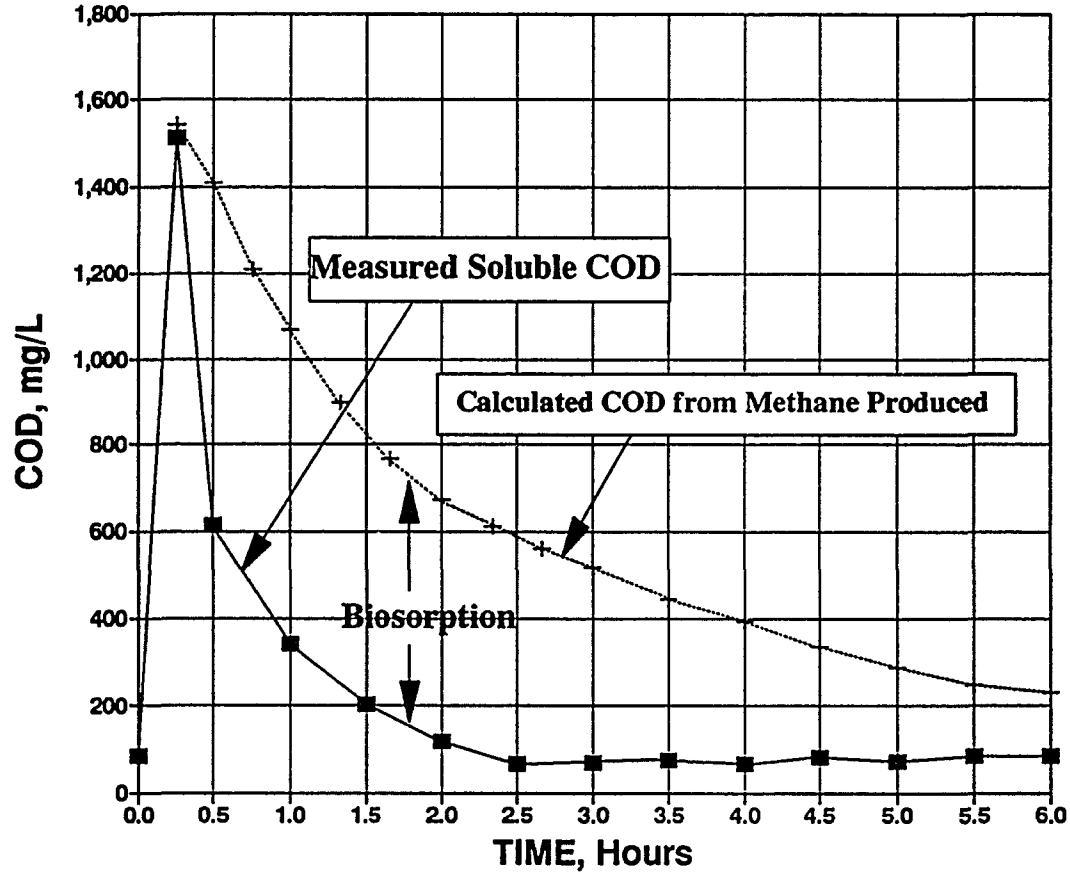

Figure 5.28. SCOD and Methane COD removal curves at continuous mixing condition

The four figures also show a similar pattern and indicate that actual removal of COD in the form of methane lags behind the COD removal as reflected by soluble COD remaining. This lag could be attributed to biosorption of COD followed by later conversion to methane.

VI. ASBR DESIGN MODEL AND DESIGN CONSIDERATIONS

Mathematical Model of the ASBR

A relatively simple mathematical model derived either from the Monod kinetic expression or first-order kinetics is used for ASBR modeling. The model is able to predict the effluent SCOD level for a given set of operating conditions, or to estimate the minimum sequencing cycle time required to meet specific effluent requirements.

The ASBR system is a time-oriented process and sequences through four steps: settle, decant, feed, and react. The duration of each step is determined on the basis of either the physical operational limits or effluent quality requirements. The minimum cycle length (T_{min}) for the ASBR is the sum of the settle time (t_s), decant time (t_d), feed time (t_f), and reactor time (t_r), as shown in Equation 6.1.

$$T_{min} = t_s + t_d + t_f + t_r \tag{6.1}$$

Minimum settle time (t_s) is a function of biosolids zone settling velocity (v), the volume of liquid to be decanted (V_d), and reactor cross sectional area (A) and can be calculated using Equation 6.2. The Equation shows that the reactor with a large cross-sectional area (stout shape reactor) requires less settling time.

$$t_s = \frac{V_d}{v \cdot A} \tag{6.2}$$

The decant (t_d) and feed (t_f) times are governed by the system capacity for liquid transfer. At decant or feeding rates of Q_d or Q_f, the time required to decant a volume (V_d) or feed a volume (V_f) can be calculated using Equation 6.3. In order to maintain a

constant liquid volume in the reactor, the feed volume is generally equal to the decant volume.

$$t_d = \frac{V_d}{Q_d} \quad \text{or} \quad t_f = \frac{V_f}{Q_f} \tag{6.3}$$

The ASBR is a non-steady-state, suspended growth, anaerobic activated sludge system. The active volume of the reactor increases during the feed step and the substrate concentration rises from a minimum just prior to feeding to a maximum at the end of the feed cycle. The substrate concentration then declines during the react cycle as substrate is converted to biogas. The minimum time necessary for the react step depends on the rate of substrate conversion to biogas and the desired effluent quality.

The ASBR can be modeled as a non-steady-state, completely-mixed reactor (feed cycle) followed by a true batch reactor (react cycle). Figure 6.1 illustrates a reactor configuration upon which the model is based.

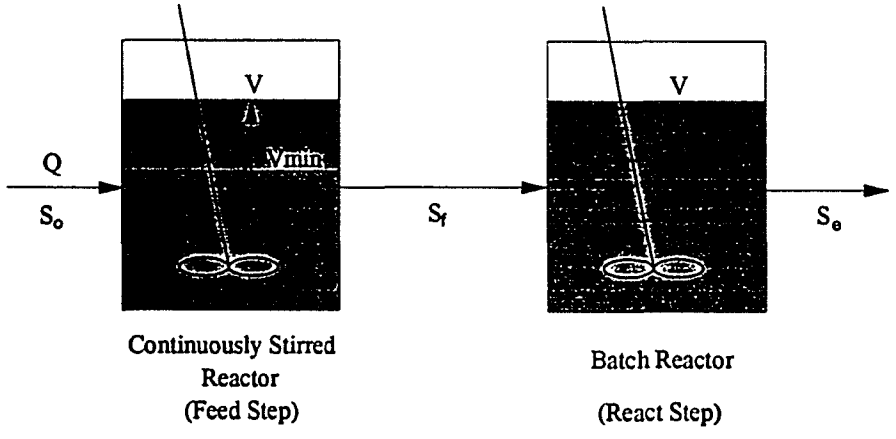

Figure 6.1. Reactor configurations for the ASBR model

The substrate degradation most likely follows either Monod or first-order kinetics, depending on individual substrate characteristics. Both the Monod and first-order kinetic functions are presented to define the rate of substrate removal in the system as follows:

$$\textbf{Monod kinetics: } \frac{dS}{dt} = - \frac{k \cdot X \cdot S}{K_s + S} \qquad (2.7)$$

where, S = concentration of substrate, mg/L ;

X = concentration of biomass, mg/L;

k = maximum specific substrate utilization rate, l/time;

K_s = half-saturation constant, mg/L.

$$\textbf{First-order kinetics: } \frac{dS}{dt} = - k_1 \cdot S \qquad (6.4)$$

Where, k_1 = first-order rate constant, 1/day.

The metabolic activity is initiated at the beginning of the feed cycle when the substrate makes contact with the microorganisms. A mass balance for substrate across the completely-mixed reactor during the feed cycle is given by Equation 6.5 under the assumption of Monod kinetics or Equation 6.6 using first-order kinetics. The reactor volume, as a function of time, is formulated as Equation 6.7.

$$\frac{dS}{dt} = \frac{Q}{V_{min} + V_f} \cdot (S_0 - S) - \frac{k \cdot X \cdot S}{K_s + S} \qquad (6.5)$$

$$\frac{dS}{dt} = \frac{Q}{V_{min} + V_f} \cdot (S_o - S) - k_1 \cdot S \qquad (6.6)$$

$$V_f = \int_0^{t_f} Q\, dt \qquad (6.7)$$

Where, V_{min} = reactor active volume prior to the feed cycle;

S_o = feed substrate concentration, mg/L.

Substrate concentration in the reactor at the end of the feed step (S_f) can be determined by integrating Equations 6.5 and 6.7 or Equations 6.6 and 6.7 jointly using numerical methods and substituting the appropriate kinetic constants and design values into the equations.

An analytical solution of Equations 6.5 and 6.7 or Equations 6.6 and 6.7 is difficult to obtain by applying variable separation methods. The substrate concentration at the end of the feed period (S_f) can be derived by using a computer program (numerical approach). This program, written in high-level programming language, BASIC, for IBM PC or a compatible computer is presented in section F of the Appendix. The illustration of the numerical method is shown below.

The substrate concentration (S_t) at time (t) of the feed period can be expressed by the following equation:

$$S_t = \frac{(\text{Mass of substrate in the reactor})_t}{(\text{Total volume of liquid in the reactor})_t} \qquad (6.8)$$

Because of the low biomass yield in the anaerobic methanogenic processes and the relatively high biomass level retained in the ASBR, one can assume that the quantity of biomass does not change significantly during the feed and react cycles. Then, the substrate

concentration at time t+Δt can be inferred from Equation 6.9 or 6.10 by substituting the known substrate concentration at time t.

$$S_{t+\Delta t} = \frac{(S_t \cdot V_t) + (Q \cdot \Delta t \cdot S_o)}{V_{min} + Q \cdot (t + \Delta t)} - \frac{k \cdot X \cdot S}{K_s + S_t} \cdot \Delta t \qquad (6.9)$$

$$S_{t+\Delta t} = \frac{(S_t \cdot V_t) + (Q \cdot \Delta t \cdot S_o)}{V_{min} + Q \cdot (t + \Delta t)} - k_1 \cdot S \cdot \Delta t \qquad (6.10)$$

where, S_t = substrate concentration at time t, mg/L;

V_t = total liquid volume in the reactor at time t;

Δt = time increment from t to t+Δt;

V_{min} = liquid volume at beginning of the feed period.

If the time interval (Δt) is short, Equation 6.9 or 6.10 can then be used to predict the substrate concentration at the end of the feed period (S_f) by integrating the substrate concentration (S_t) within the time limits between zero and t_f.

Substrate degradation kinetics for the non-steady-state batch reactor is given in Equation 6.11 or 6.12. The react time can then be integrated from Equation 6.11 or 6.12 within the limits of time equal to zero to time equal to t_r yielding the Equations 6.13 and 6.14.

$$\textbf{Monod kinetics: } \frac{dS}{dt} = - \frac{k \cdot X \cdot S}{K_s + S} \qquad (6.11)$$

$$\text{First-order kinetics: } \frac{dS}{dt} = -k_1 \cdot S \qquad (6.12)$$

$$\text{Monod kinetics: } t_r = \frac{K_s}{k \cdot X} \cdot \left(\ln \frac{S_f}{S_e} + \frac{S_f - S}{K_s} \right) \qquad (6.13)$$

$$\text{First-order kinetics: } t_r = \frac{1}{k_1} \cdot \ln \frac{S_f}{S_e} \qquad (6.14)$$

where, S_e = predetermined effluent substrate concentration, mg/L.

Model Verification

The ASBR design model presented above was tested using the experimental data. The model testing procedures included two steps: 1) determination of the kinetic constants, and 2) verification of the model predicted data with the experimental data.

Monod kinetic constants, half-saturation constant (K_s) and maximum specific substrate utilization rate (k), can be found in the literature presented by other researchers and/or determined in this experimental study. Henze and Harremoës (1983) concluded, on the basis of the theoretical relationship between substrate metabolic energy and biomass yield, and considerations of biomass yield differences between the acid producing and methane producing bacteria, that the maximum specific substrate utilization rate at 35°C was 2.0 g COD/g VSS-day. In practice, 50% of the MLVSS was recommended as active biomass. This provides the constant of approximately 1.0 g COD/g VSS-day (Henze and Harremoës, 1983). The suggested value compares well with the values found with various soluble wastes in the literature (Table 2.7). The substrate utilization rate constant of 1.0 g

COD/g VSS-day is also adopted for the NFDM substrate for testing of the ASBR model.

The half-saturation constant (K_s) is highly substrate dependent. Values ranging from 200 to 4,000 mg COD/L are found in the literature (Table 2.7). The half-saturation constant (K_s) and first-order kinetic constant (k_1) are experimentally determined. The kinetic constants are determined by graphical curve fitting with the experimental data. Figure 6.2 shows an example of a 6-hour-cycle measured SCOD curve and two other SCOD curves plotted according to the data calculated from the ASBR model. The curve on the top is based on the Monod kinetics. The curve in the middle is determined on the basis of first-order kinetics. By varying the kinetic constants (K_s and k_1) in the design model, the model-predicted curves can be adjusted to intercept the measured SCOD curve at the time equal to 5.25 hours which is the end point of the react period and the effluent sampling time. These three curves should overlap near the end of the cycle, if the representative kinetic constants of Ks and k_1 are properly defined.

The kinetic constants of k_s of 450 mg COD/mg MLVSS-day and k_1 of 13.0 1/day are retested with several other sets of measured SCOD data following the same plotting procedure described above. The results of the new curves shown in Figure 6.3 agree with the kinetic constants nomographically determined in Figure 6.2. The curve fitting exercises are always focused near the end of each cycle, because the SCOD data at this period cannot truly reflect the reactor substrate level. As the author noticed earlier, a significant amount of the soluble NFDM substrate is absorbed on the surface of the biosolids matrix and gradually converts to methane and carbon dioxide. The methane

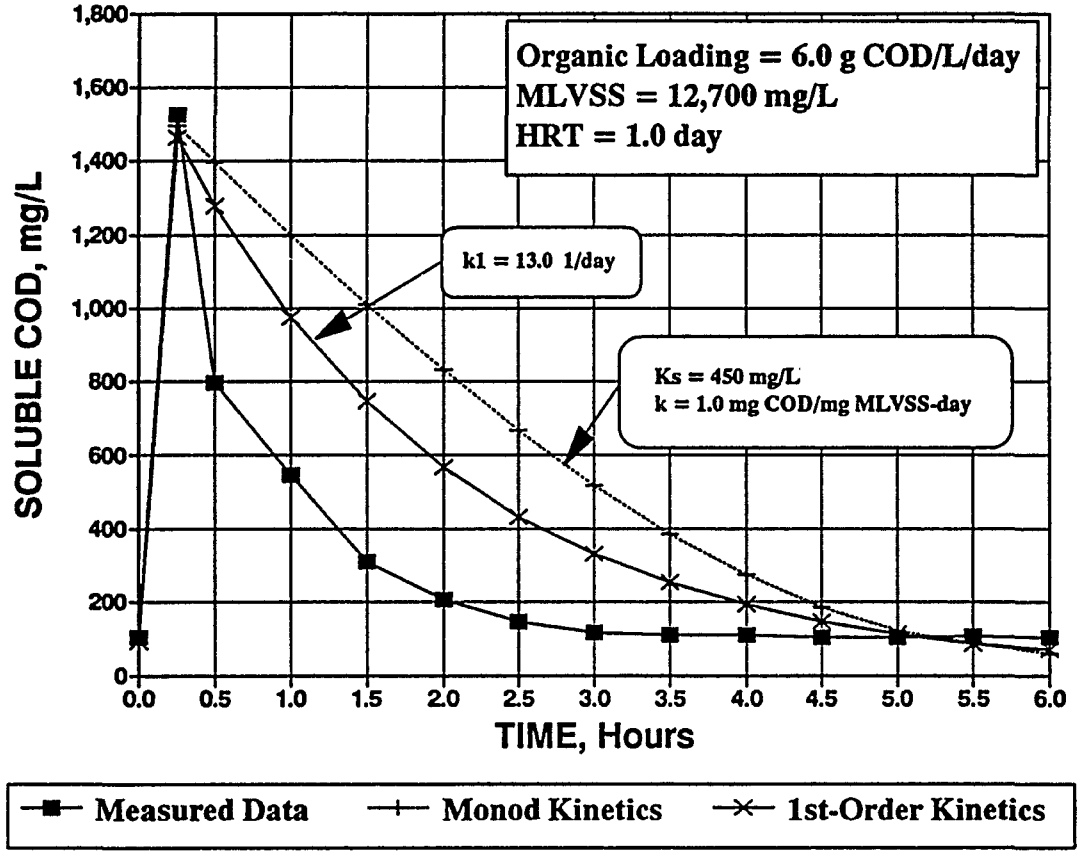

Figure 6.2. Comparison of the measured SCOD curve to SCOD curves derived from the kinetic model (CASE 1)

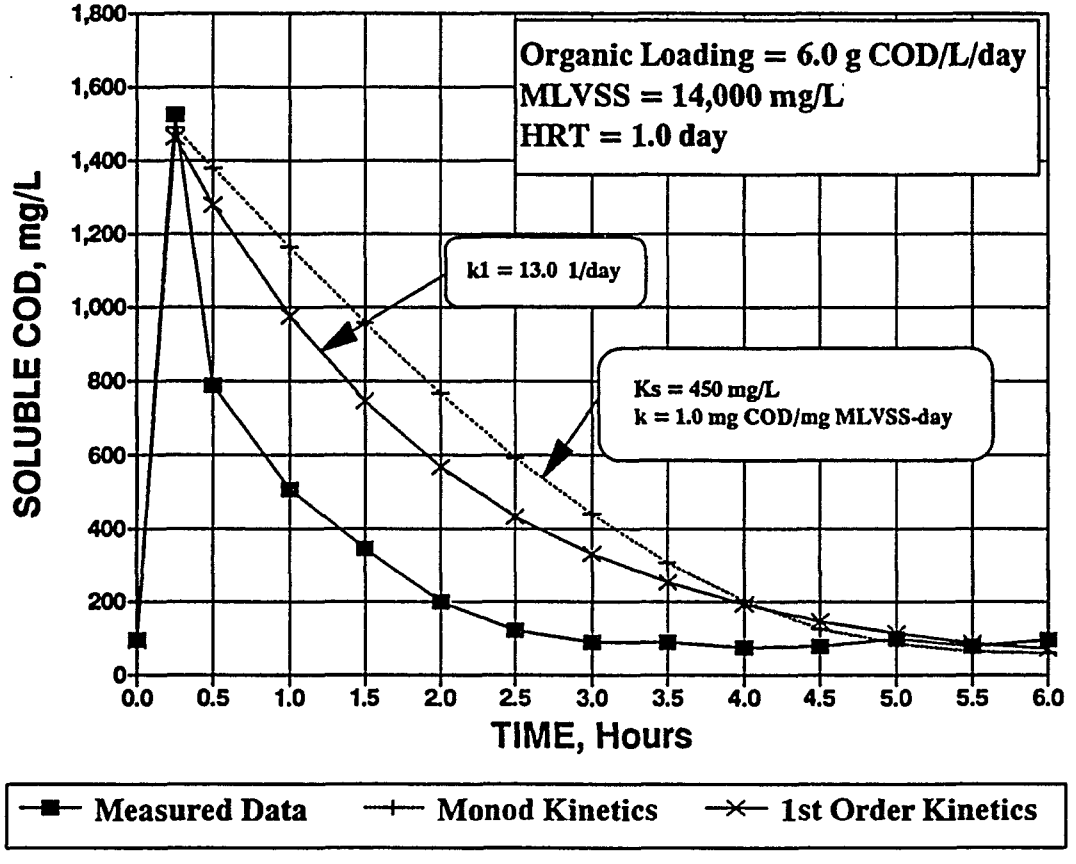

Figure 6.3. Comparison of the measured SCOD curve to SCOD curves derived from the kinetic model (CASE 2)

COD (COD remaining based on methane production) curve is merged and closely parallel to the SCOD curve as the time toward the end of the cycle. This phenomenon can be seen in Figures 5.25, 5.26, 5.27, and 5.28, and explains why the SCOD data measured from the reactor liquid content cannot truly represent the reactor substrate level, and the discrepancy between the measured SCOD curve and the model predicted SCOD curves. The above assumption can be illustrated by introducing the methane COD remaining data for the same operation cycle. The methane COD values are calculated on the basis that 0.35 L of methane (STP) are produced for one gram of COD removed. Figure 6.4 adds the methane COD remaining curve to Figure 6.2. In Figure 6.4, the first-order kinetic curve closely parallels the methane COD curve with an increasing vertical gap toward the end of the cycle. The amount of the COD removed is not 100% converted to methane COD in the anaerobic degradation process. Some portion of the substrate COD is attributed to new biomass synthesis or release as heat (minor). Using anaerobic degradation of glucose as an example of the chemically bound energy in glucose, 8% is stored in the biomass, 3% released as heat, and 89% is in the methane formed (Norrman, 1987). If the determination of the methane COD remaining data also takes biosynthesis COD and heat loss COD into account, the first-order kinetic curve could well match the methane COD remaining curve. This match provides a clue as to why the NFDM substrate degradation follows first-order kinetics.

Once the kinetic constants, K_s of 450 mg/L, k of 1.0 g COD/g MLVSS-day, and k_1 of 13.0 1/day, were determined, the pseudo-steady-state effluent SCOD data was compared

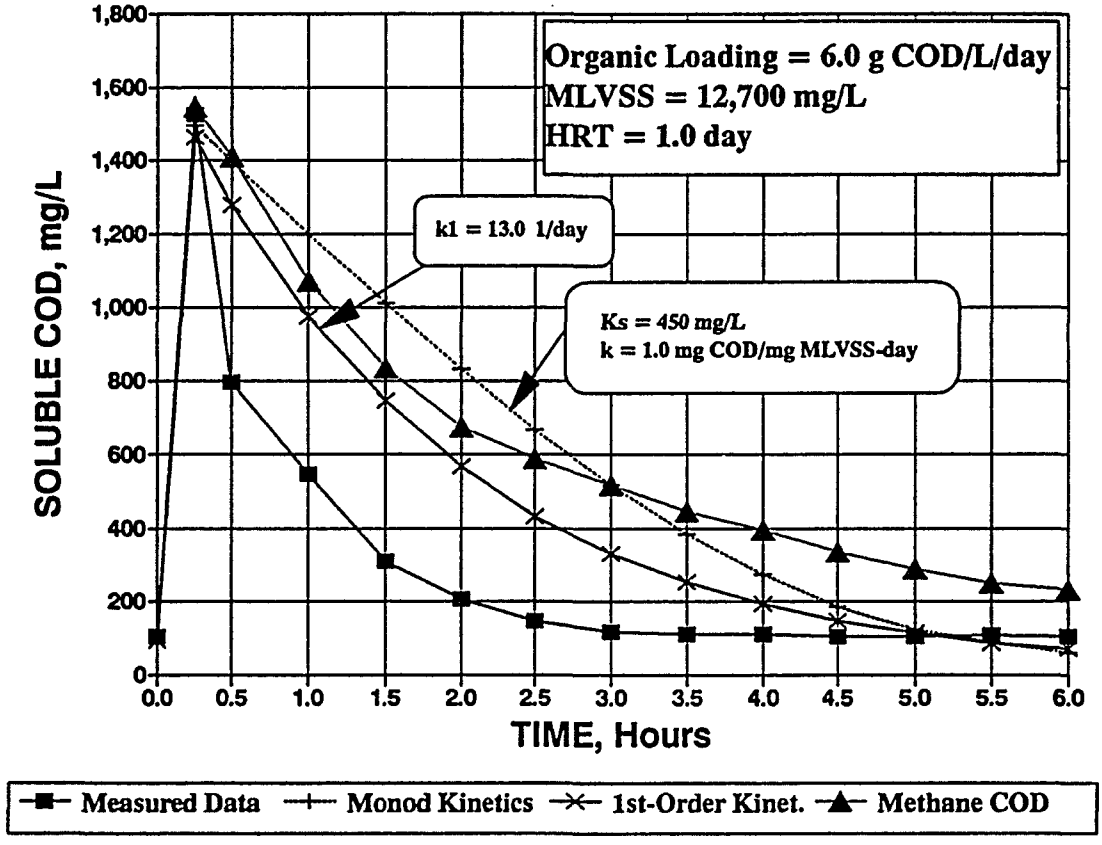

Figure 6.4. Comparison of methane COD remaining curve to SCOD curves derived form the kinetic model

to the model predicted-values at various operating conditions. Table 6.1 summarizes the effluent SCOD data calculated from the Monod kinetics ASBR model. The substrate concentrations at the end of feed period (S_f) are calculated by Equations 6.5 and 6.7. The proper kinetic constants and operating parameters, such as MLVSS concentration (X), feed substrate concentration (S_o), and feed flow rate (Q), are substituted into the equations in the above calculations. The model estimated SCOD values are then solved by Equation 6.13 with the proper react time and S_f data. The react time in Phases 1 and 2 operations (HRTs of 48 and 24 hours) is 5.0 hours, and in Phase 3 operations (HRT of 12 hours) is 3.25 hours. The result of the Monod kinetic model calculations shown in Table 6.1 indicates poor correlation with the experimental data. This poor correlation is possibly attributed to: 1) difficulty in measuring accurate MLVSS levels in the reactor with granular biosolids, 2) variable active biomass concentration or as a function of sludge age, 3) variable biomass activity between flocculent and granular biomass, and 4) complexity of the anaerobic degradation of the NFDM substrate.

Table 6.2 summarizes the effluent SCOD data calculated from the first-order kinetic ASBR model. The calculations of the ASBR model by the two kinetic approaches are quite similar, but MLVSS concentration is not a variable in first-order kinetics. The S_f concentration of each pseudo-steady-state data point is calculated by Equations 6.6 and 6.7 S_e concentration is then determined by Equation 6.14. The result of the first-order kinetic model calculations shown in Table 6.2 indicates an exceptionally good correlation with the experimental data. It is concluded that the ASBR system treating the NFDM substrate can

Table 6.1. Summary of the effluent SCOD data generated from the experimental study and the Monod kinetic ASBR model

HRT	COD Load	REACTOR A				REACTOR B				REACTOR C				REACTOR D			
		MLVSS	Sf	Eff. SCOD	Est. SCOD	MLVSS	Sf	Eff. SCOD	Est. SCOD	MLVSS	Sf	Eff. SCOD	Est. SCOD	MLVSS	Sf	Eff. SCOD	Est. SCOD
Hours	g/L/day	mg/L	mg/L	mg/L	mg/L	mg/L	mg/L	mg/L	mg/L	mg/L	mg/L	mg/L	mg/L	mg/L	mg/L	mg/L	mg/L
48	2	11,200	519	69	9	11,230	513	62	9	9,810	521	65	17	10,460	526	74	78
48	2	12,420	492	40	5	12,620	499	50	4	11,550	494	38	7	11,920	498	46	49
48	4	12,250	993	59	29	12,070	1,006	74	33	14,130	1,002	82	13	18,380	1,006	114	51
48	4	17,850	953	43	2	18,440	955	50	2	17,600	961	52	3	24,010	934	57	9
48	6	14,460	1,503	96	47	18,230	1,484	100	9	18,380	1,482	99	8	21,640	1,526	111	91
48	6	15,320	1,469	61	30	19,580	1,450	68	4	22,700	1,449	89	1	23,490	1,443	88	47
48	8	20,570	1,997	143	12	21,670	1,984	137	7	21,340	1,990	141	8	25,280	1,959	135	107
48	8	21,120	1,946	86	8	23,200	1,908	55	3	25,790	1,936	110	1	27,630	1,939	97	59
24	2	17,920	482	61	0	15,010	490	58	1	16,570	487	62	1	17,150	485	61	12
24	2	21,080	461	44	0	19,930	462	40	0	24,030	449	39	0	19,440	472	53	6
24	4	13,410	991	76	20	9,375	1,041	118	108	11,500	1,011	92	42	14,310	1,046	162	145
24	4	13,890	968	47	13	14,790	977	65	9	21,280	949	70	1	22,180	957	88	16
24	6	14,280	1,502	112	51	13,205	1,535	150	85	17,950	1,482	114	10	18,815	1,500	146	159
24	6	18,680	1,453	78	6	16,260	1,485	104	21	21,580	1,439	81	2	22,170	1,447	97	66
24	8	14,930	2,008	135	130	12,125	2,043	160	333	22,440	1,955	127	5	23,640	1,980	172	159
24	8	18,280	1,955	91	30	12,900	2,008	118	253	23,190	1,924	89	3	24,170	1,941	122	131
12	4	7,120	699	91	232	5,435	707	92	323	20,080	652	101	7	26,735	618	87	1
12	4	9,440	672	63	131	10,400	654	40	99	22,880	612	50	2	28,450	601	67	1
12	6	9,400	1,059	156	322	8,190	1,062	152	396	20,790	1,004	159	17	22,370	1,007	177	11
12	6	10,370	1,031	121	255	9,950	1,021	101	271	23,840	966	120	6	24,225	966	124	6
12	8	10,600	1,406	194	467	8,800	1,417	195	607	24,270	1,348	222	17	23,410	1,348	215	22
12	8	11,350	1,341	98	376	12,830	1,351	127	296	26,940	1,305	175	7	26,510	1,290	147	8
12	10									25,940	1,699	278	28	25,180	1,706	281	36
12	10									30,100	1,624	196	7	28,810	1,618	173	10
12	12									18,910	2,179	447	391	22,930	2,242	585	208
12	12									22,500	2,099	358	174	25,930	2,053	319	69

Sf: Model Predicted Substrate COD Concentration at the Beginning of REACT Step
Eff. SCOD: Pseudo-Staedy-State Experimental Effluent SCOD Data
Est. SCOD: Effluent SCOD Data Predicted by the ASBR Model Using Monod Kinetics
Monod Kinetics Constants: Half Saturation Constant = 450 mg COD/L
Max. Substrate Utilization Rate = 1.0 mg COD/mg MLVSS-day

Table 6.2. Summary of the effluent SCOD data generated from the experimental study and the first-order kinetic ASBR model

HRT	COD LOAD	REACTOR A			REACTOR B			REACTOR C			REACTOR D		
		Sf	Eff. SCOD	Est. SCOD	Sf	Eff. SCOD	Est. SCOD	Sf	Eff. SCOD	Est. SCOD	Sf	Eff. SCOD	Est. SCOD
Hours	g/L/day	mg/L	mg/L	mg/L	mg/L	mg/L	mg/L	mg/L	mg/L	mg/L	mg/L	mg/L	mg/L
48	2	522	69	35	517	62	34	519	65	35	526	74	35
48	2	500	40	33	507	50	34	498	38	33	504	46	34
48	4	981	59	65	995	74	66	1,001	82	67	1,025	114	68
48	4	971	43	65	977	50	65	978	52	65	982	57	65
48	6	1,481	96	99	1,484	100	99	1,483	99	99	1,492	111	99
48	6	1,454	61	97	1,460	68	97	1,476	89	98	1,475	88	98
48	8	1,986	143	132	1,982	137	132	1,985	141	132	1,980	135	132
48	8	1,943	86	129	1,919	55	128	1,961	110	131	1,951	97	130
24	2	508	61	34	506	58	34	508	62	34	508	61	34
24	2	497	44	33	494	40	33	493	39	33	502	53	33
24	4	985	76	66	1,013	118	68	996	92	66	1,042	162	69
24	4	966	47	64	978	65	65	981	70	65	993	88	66
24	6	1,476	112	98	1,501	150	100	1,478	114	99	1,499	146	100
24	6	1,454	78	97	1,471	104	98	1,456	81	97	1,467	97	98
24	8	1,959	135	131	1,976	160	132	1,954	127	130	1,983	172	132
24	8	1,939	91	129	1,948	118	130	1,929	89	129	1,951	122	130
12	4	678	91	117	679	92	117	684	101	118	676	87	116
12	4	662	63	114	648	40	111	654	50	112	664	67	114
12	6	1,028	156	177	1,026	152	176	1,030	159	177	1,040	177	179
12	6	1,008	121	173	996	101	171	1,007	120	173	1,010	124	174
12	8	1,363	194	234	1,363	195	234	1,379	222	237	1,375	215	236
12	8	1,307	98	225	1,324	127	228	1,352	175	233	1,336	147	230
12	10							1,724	278	296	1,726	281	297
12	10							1,677	196	288	1,663	173	286
12	12							2,135	447	367	2,215	585	381
12	12							2,083	358	358	2,061	319	354

Sf: Model Predicted Substrate COD Concentration at the biginning of REACT Step
Eff. SCOD: Pseudo-Steady-State Experimental Effluent SCOD Data
Est. SCOD: Effluent SCOD Data Predicted by the ASBR Model Using First Order Kinetics
First Order Kinetics Constant = 13.0 1/day

be successfully modeled by the non-steady-state first-order kinetic model.

The statistic analysis of the data presented in Tables 6.1 and 6.2 shows 1) the two kinetic models are statistically different with a significant level higher than 95%, and 2) the mean value of the difference between the model predicted data and measured data in the first-order kinetic model is 31.0 and in the Monod kinetic model is 97.0. The Monod kinetic model shows a poor correlation with a more than three times higher difference between the mean value than is the case for the first-order kinetic model.

Design Considerations

The experimental studies on the ASBR provided valuable information for the design of a full-scale reactor. Unlike the research system, the practical application of the ASBR requires broader considerations like economic feasibility, performance liability assessment, wastewater flowrates and characteristics, equipment design, etc. In this discussion of design considerations, the primary focus is on the technical issues learned from the experimental study.

Overall Design Concepts

The ASBR design model presented in the previous section is a valuable tool in determining reactor biological performance. The model can estimate minimum react time required for a necessary effluent quality and provide the system HRT information in order to size the ASBR. The success of the ASBR depends not only on proper design of the system biological removal rate but, more importantly, on the ability of the reactor to

separate and retain biosolids. The physical aspects, such as reactor geometry and mixing duration and intensity, are known from the experimental study to affect biosolids retention. The ASBR system design should also focus on the system hardware, especially on the reactor mixing device. The mixing device should provide sufficient mixing for biological activities and should be gentle enough to enhance the bioflocculation and the granulation processes.

The reactor operating F/M ratio is another important parameter affecting biosolids separation and retention in the ASBR system. A reactor operated with a flocculent type biomass can tolerate only a low degree of biomass selection pressure and must be operated within the limits of low F/M ratios (0.1 - 0.4 g/g-day) in order to prevent severe biomass washout. The experimental study indicates that the reactor with heavier biosolids or granular biosolids can be operated at higher F/M ratios (0.7 - 0.9 g/g-day).

Treatability Study

Lab-scale, or preferably pilot-scale, ASBR treatability studies are highly recommended in designing a full-scale ASBR system, especially for wastewaters from industries with unfamiliar characteristics. The study can be used to characterize the wastes in terms of determining their degradation kinetic coefficients, to learn whether pretreatment is required, and to define the system's operating parameters. The operating parameters including start-up procedure, operating strategies, biosolids production rate, biosolids settling characteristics, and additional nutrients and buffer chemical needs are the primary focus points of the treatability study. Also, general performance data such as organic

loading rate, organic removal rate, and biogas production rate, provide important information required to model and design the full-scale system.

Flow Equalization

For the single tank ASBR system, normally a front end equalization basin is needed, because the reactor receives the wastewater only during the feed phase which could occupy 10 to 50% of the total cycle time. The wastewater generated during the reactor in react, settle, and decant phases must be stored in the basin. The basin is not only equalizing wastewater flow but also leveling wastewater strength fluctuation. For the design of industrial wastewaters, or for wastewaters with great fluctuation in strength or flow rate, the flow equalization basin is recommended. Sizing the equalization basin is associated with the system hydraulic retention time and maximum flow rate. For the multiple-tank ASBR system, the equalization tank can be eliminated. During the reactor, settle, and decant sequences the wastewater flow can be directed to another ASBR tank in the system.

pH Buffer Capacity

Because the ASBR is a non-steady state, batch system, the substrate concentration is high immediately after feeding and declines until the reactor is fed again. The total volatile acids concentration is also varied in the cycle. Due to the kinetic differences between acidogenesis (organic acids forming process) and methanogenesis (acetic acid consuming process), the organic acids concentrations build up during the feed period and reach the peak after feeding. The high acids concentrations could depress the pH and adversely

affect the activity of the methane forming bacteria, if the system does not have sufficient buffering capacity. The buffering capacity against pH decreases results from the presence of bicarbonate of elements such as calcium, magnesium, sodium, potassium, or ammonium. The other general term in expressing buffer intensity is the concentration of bicarbonate alkalinity.

The ASBR system requires higher buffer capacity to neutralize the organic acids formed at the end of feed sequence, as compared with a continuous flow system with a lower constant organic acids level. Alkalinity addition is suggested for the system without sufficient natural alkalinity in the wastewater. The amount of alkalinity addition can be determined from the treatability study. An increase of operating cost associated with the chemical addition should be considered in the design. For the system requiring a large amount of alkalinity addition, a precaution of cationic toxicity should be taken by using a combination of different alkaline chemicals.

Peak volatile acids concentrations are affected by number of cycles per day. Varying number of cycles in an ASBR changes the substrate concentration at the beginning of the react step, if the reactor is operated at the same organic load and HRT. The substrate concentration at the beginning of the react step is lower when the ASBR is operated at a higher number of the cycles per day (or a shorter cycle length), and vice versa. The lower substrate concentration in the ASBR leads to a less pH buffer requirement.

High Solids Waste Applications

One of the advantages of the ASBR over the other high rate anaerobic systems, such as the upflow anaerobic sludge blanket (UASB), the fluidized bed, and the anaerobic filter, is its ability to treat high solids wastewater. Both the UASB and the fluidized bed reactors are continuous flow systems that operate at an upward velocity created by the influent flow and mixed liquor recirculation. Influent solids can be easily washed out with the effluent flow. The ASBR system does not have the media clogging problem like the anaerobic filter. Thus, the ASBR is more suitable for treating high solids wastes. A lab-scale ASBR was successfully demonstrated using the ASBR in treating non-screened, high solids swine wastes (Pidaparti, 1992 and Schmit, 1993).

When treating the high solids wastes, a thorough influent solids biodegradability study should be conducted. Inorganic or non-biodegradable solids contained in the influent waste stream will end up accumulating in the reactor and take some of the reactor space. A phenomenon called the "crowding-out" effect demonstrates the consequence of the inviable solids accumulation. The crowding-out effect will occur in the ASBR fed with a waste containing high concentration of inorganic or non-biodegradable solids. Non-biodegradable solids retained in the reactor result in a faster increase in mixed liquor suspended solids concentration and a continuously decreasing biological solids activity. In order to ensure a high level of performance and to protect effluent quality from an over-crowd mixed liquor solids condition, routine solids wasting is required. Consequently, a portion of the active biomass is wasted out with inviable solids of the system. The worst-

case scenario of the crowding-out effect could happen if the inviable solids accumulation rate was higher than the net biomass yield in the reactor. This condition could result in a gradually decreasing SRT as the operating time lapses and finally lead the reactor to failure due to inadequate SRT. The amount of the inorganic and non-biodegradable solids sets a limit on the ASBR in high solids wastes applications. For a waste stream containing a significant amount of inorganic or non-biodegradable solids, a pretreatment application designed for grit removal should be considered.

Seed Granular Biomass

The ASBR can gain stability with the system operating with granular biomass. In the experimental study, strong evidence proved that the ASBRs with granular biomass were able to achieve both higher hydraulic and higher organic loads, as compared to the system with flocculent biomass. Granular biomass is less sensitive to the effect of biogas internal gassing and much more efficient in solids separation and retention. As the result of the granulation process, the ASBR can be operated at a higher F/M ratio.

Prolonged start-up periods has been the focus of criticism of high rate anaerobic processes. Seeding the reactor with granular biomass does provide an advantage in shortening the start-up period, although the ASBR is not dependent on granular biomass. The commercial availability of granular biomass makes this approach more feasible.

Vacuum Enhancement in Solids Separation

Effective biosolids separation is of most critical concern when the ASBR is applied to treat low strength wastes or wastes with a low biomass yield, or when the ASBR is operated with poorly settling flocculent biomass. A simple technique of applying a vacuum to the reactor right before the settle step can be used to enhance solids separation and to shorten the settling time required for biosolids clarification. A shorter settle time also means a longer allowable decant time before the occurrence of solids/liquid interface disruption caused by internal gassing. A study on the effect of vacuum on ASBR performance reported positive results on biosolids separation (Herum, 1993).

A vacuum should be applied to the reactor head space with a magnitude at least equal to the scale of hydraulic pressure drop during the decant step in order to degasify the internal gassing biogas before the settle and decant steps. A vacuum can be applied right before the settle step for 5 to 10 minutes at a suggested pressure range between -1 and -5 pound per square inch (psi), which is equivalent to 2.3 to 11.5 feet of a water column.

Biogas Storage

Biogas production rate varies throughout the reactor sequence, as shown in the experimental results. If biogas produced by the process is designed to be used for recovering energy, a constant biogas supply should be handled by a proper sized storage or flow equalization space. A multi-tank ASBR system will assist in equalizing biogas production and might avoid the necessity for biogas storage space. When one reactor is at low end of the biogas production during the settle and decant steps, the other reactor is at

maximum biogas production period of feed and react steps.

A membrane or floating cover provides an ideal space for biogas storage and decant volume displacement, but it eliminates the possibility of vacuum application. A pressurized biogas storage tank may be used for a ridge cover reactor, but it increases the complexity in the gas pressurization.

System Automation

The ASBR is a time oriented process and the four sequences (feed, react, settle, and decant) are operated according to a predetermined time table. This time oriented nature serves as an ideal circumstance for an automatic process control system. System automation can be implemented by a programmable logic control (PLC) unit. The PLC receives signals from the sensing devices such as a level sensor, a float switch, a temperature or pH probe, a flow meter, etc. and sends out the signals to activate equipment according to the programmed operating logic. A personal computer can be combined with the PLC to function as an operating data acquisition station, and an on-screen monitoring and programming terminal.

Feeding and decanting can be controlled by a combination of time data from an internal clock in the PLC and liquid level from a level sensor or a float switch in the reactor. The PLC can be programmed to shut off a feed pump or valve after a predetermined time in case the level sensing device malfunctioned. The end of decanting can also be controlled by a minimum liquid level and a time schedule following the same control logic as a feed control system. The process control in the react and settle

sequences can be simply implemented by controlling a mixing device according to a programmed time schedule. When the internal clock in the PLC is at the scheduled settling time, the mixing device is deactivated and reactivated at the beginning of the next feeding step.

Design Example

As a design example, a meat packing waste having a flow of 0.4 MGD with a COD of 5,000 mg/L is used. The plant is managed in two shifts of kill followed by one shift of clean-up for a 20-hour day operation. Waste is only discharged during the 20-hour operation period. An effluent COD quality of 200 mg/L (removal rate of 96.0%) is set as the treatment goal.

Treatability studies have shown that anaerobic degradation of the waste follows first-order kinetics with a kinetic constant (k_1) of 10.0 1/day. A maximum F/M ratio of 0.5 lb COD/lb MLVSS-day is also recommended based on the findings of the treatability studies. A two-tank ASBR system is considered in this application. A front end waste holding basin is sized to equalize the flow for continuous operation of the ASBR system.

The following design parameters are suggested: 1) a maximum one hour of feed time per cycle, 2) 30 minutes of allowable settle time, and 3) 30 minutes of decant time with a maximum decant rate of 4,000 gpm. A decant volume should be equal to or less than one third of the reactor working volume in order to maintain a safety layer during the decant step between the biosolids blanket and decanted liquid surface.

System HRT is translated into volume requirement for the reactor. The HRT is determined by the kinetic time required to meet the predetermined substrate removal efficiency. A minimum HRT of 20.3 hours is calculated by the ASBR model and Equation 6.1 ($T_r = T_{cycle} - T_f - T_s - T_d$). At the HRT of 20.3 hours (design option No.1), the reactor volume of 169,167 gallons is calculated. The computer program listed in Appendix F for the first-order kinetics ASBR model is used for the calculations. A computer printout presented in Table 6.3 shows that the substrate concentration at the end of the feed period and the minimum react time (kinetic time) are 1,451 mg COD/L and 4.76 hours, respectively. The model-predicted react time of 4.76 hours is reasonable close to the maximum allowable react time of 4.77 hours determined by Equation 6.1 ($T_{cycle} - T_f - T_s - T_d = 6.77 - 1.0 - 0.5 - 0.5$). With the above minimum HRT design (minimum reactor volume), the system will operated at 6.77 hours per cycle (3.55 cycles per day) which is not a common practice. Another design using the cycle length of 6.0 hours is calculated and presented as design option No. 2. The summary of the design example is shown as follows:

1) System design parameters

Design Flow, MGD	0.4
Influent COD, mg/L	5,000
Effluent SCOD, mg/L	200
COD Removal %	96.0
F / M ratio, lb COD/lb MLVSS-day	0.40

2) ASBR design

	Option No. 1	Option No. 2
Number of ASBR, tanks	2	2
Reactor Dimensions WxLxD, ft	39x39x18	42x42x18
Maximum Liquid Depth, ft	15	15

3) System operating parameters

	Option No. 1	Option No. 2
Organic Loading Rate, g COD/L/day	5.9	5.0
MLVSS, mg/L	14,800	12,500
HRT, hour	20.3	24.0
Cycle Length, hour/cycle	6.77	6.0
Cycle per Day	3.55	4
Feed Time, hour	1.0	0.7
React Time, hour	4.76	4.30
Settle Time, min	30	30
Decant Time, min	30	30
Feed Volume/Cycle, gal	56,389	50,000
Feed Flow Rate, gpm	940	1,200
Decant Volume/Cycle, gal	56,389	50,000
Decant Flow Rate, gpm	1,880	1,667

The methane production and heating value of this design example can be determined based on an estimated value for COD reduction and the relationship that 5.61 cubic feet of methane is produced per pound of COD destroyed (at STP). A methane production of 80,850 cubic feet per day at STP is estimated. Heating value of biogas (assuming methane has a heating value of 1,000 BTU per cubic feet) is calculated to be 81 million BUT/day.

Table 6.3. The computer printout of ASBR modeling for the design example

```
*****    A S B R    D E S I G N    M O D E L    *****
*****  F i r s t - O r d e r   K i n e t i c s  *****

==================================================

  Reactor  Working  Volume      =     169,200 gal
  'FEED'  Volume  per  Cycle    =      56,389 gal
  'FEED'   Flow   Rate          =         940 gpm
  Influent   C O D              =       5,000 mg/L
  Expected  Effluent  SCOD      =         200 mg/L
  1st Order Kinetic Constant    =       10.00 1/day

==================================================

 FEED Time, hr     SCOD, mg/L      No. of Integrations

     0.25              688                250
     0.50            1,033                500
     0.75            1,278                750
     1.00            1,451              1,000

 'FEED' Time =  1.00 Hours


Cycle Time, hr     SCOD, mg/L      No. of Integrations

     1.50            1,178                500
     2.00              956              1,000
     2.50              777              1,500
     3.00              630              2,000
     3.50              512              2,500
     4.00              416              3,000
     4.50              337              3,500
     5.00              274              4,000
     5.50              222              4,500
     6.00              181              5,000
     6.50              147              5,500
     7.00              119              6,000
==================================================

 Minimum 'REACT' Time =   4.76 Hours
 At Effluent S C O D  =    200 mg/L

==================================================
```

VII. CONCLUSIONS

The ASBR system was proven in this research to be a promising high rate anaerobic process in terms of its simplest mode of operation, its effective biosolids separation and retention, and its convincing organic removal rate. The following conclusions are derived from the development work on the ASBR:

1. The ASBR has intrinsic characteristics that enable the achievement of lower substrate levels and lower biogas production rates during the biomass settling and decanting cycles. This enables a greater efficiency of solids separation and retention than is the case for continuously-fed and mixed systems such as the anaerobic contact process.

2. Biosolids selection pressure imposed through the decanting process in the ASBR system can be factored into three parameters: 1) decant volume, 2) static hydraulic pressure difference in the decant step, and 3) operating F/M. The degree of the selection pressure increases as any one of these three parameters increases.

3. Reactor geometry (depth-to-diameter ratio) appears to be significant in the performance of the ASBR, particularly with regard to biosolids retention and the development of granular biosolids. Tall, slender reactors imposed higher selection pressure on biosolids and were more effective in developing granular biosolids. However, the short, stout reactors were able to achieve higher concentrations of mixed liquor suspended solids and higher solids retention times (SRTs).

4. Strong evidence from this and previous research indicates that intermittent mixing, rather than continuous mixing, shows superior performance of solids retention in suspended growth anaerobic processes that rely on solids separation and retention to achieve high SRT values.

5. The results of the mixing study indicated that overall COD removal between intermittent mixing and continuous mixing was essentially no different, but overall methane production was higher with intermittent mixing. The intermittent mixing (5 min mixing/hour) proved to be sufficient in biological conversion of NFDM substrate in the ASBR.

6. The anaerobic granulation process was successfully cultivated in the ASBR. The developed granular biomass was considered to be one of the primary advantages of the ASBR process because it increased the system stability in terms of the effectiveness of solids separation and retention. The granular particle size was the function of the selection pressure and operating time. The particle sizes increased at an exponential rate as the hydraulic pressure on the system was increased by reducing HRTs from 48 hour to 24 hour and then to 12 hour.

7. The results of this research indicate that the ASBR is highly effective in the bioconversion of a soluble milk substrate with SCOD removals in excess of 90% across a range of COD loads from 2 g/L/day to 12 g/L/day at HRTs of 48 hour, 24 hour, and 12 hour.

8. A non-steady state mathematical model is developed for the ASBR. NFDM substrate degradation appears to agree with first-order kinetics better than Monod kinetics. The ASBR is modeled upon a completely mixed reactor (feed phase) followed by a true batch reactor (react phase). The model provides minimum cycle time, effluent quality, and reactor sizing information.

BIBLIOGRAPHY

Aeroa, H. C., and Chattopadhya, S. N. "Anaerobic contact filter process: a suitable method for the treatment of vegetable tanning effluents." Water Pollution Control, 79, 501-506 (1980).

Anderson, G. K. "Research and application of anaerobic process." Environmental Technology Letters, 484-493 (1980).

Backman, R. C., Blanc, F. C., and O'Shaughnessy, J. C. "The treatment of dairy wastewater by the anaerobic up-flow packed bed reactor." Proceeding of the 41th Industrial Waste Conference, Purdue University, West Lafayette, Indiana, 234-241 (1986).

van den Berg, L., Lentz, C. P., and Armstrong, D. W. "Anaerobic waste treatment efficiency comparisons between fixed film reactors, contact digesters, contact digesters, and fully mixed, continuously fed digesters." Proceedings of the 35th industrial waste conference, Purdue University, West Lafayette, Indiana, 788-793 (1980a).

van den Berg, L., and Lentz, C. P. "Comparison between up- and down-flow anaerobic fixed film reactors of varying surface-to-volume ratios for the treatment of bean blanching waste." Proceedings of the 34th Industrial Waste Conference, Purdue University, Waet Lafayette, Indiana, 319-325 (1980b).

Chyi, Y. T., and Dague, R. R. "Effects of particulates size in anaerobic acidogenesis using cellulose as a carbon source." Water Environment Research, 66, 670-679 (1994)

Cohen, A., Zoetemeyer, K. ., van Deursen, A., and van Andel, J. G. "Anaerobic digestion of glucose with separated acid production and methane formation." Water Research, 13, 571-580 (1979).

Colberg, P. J. "Anaerobic microbial degradation of cellulose, lignin, oligolignols, and monoaromatic lignin derivatives." Biology of Anaerobic Microorganisms, Zehnder, A. J. B. ed., John Wiley & Sons, Inc., 333-372 (1988).

Coulter, J. B., Soneda, S., and Ettinger, M. B. "Anaerobic contact process for sewage disposal." Sewage and Industrial Wastes, 29, 468-477 (1957).

Dague, R. R. "Solids retention in anaerobic waste treatment systems." Doctoral Dissertation, University of Kansas, Lawrence, Kansas (1967).

Dague, R. R., McKinney, R. E., and Pfeffer, J. T. "Anaerobic activated sludge." Journal Water Pollution Control Federation, 38, 2, 220-226 (1966).

Dague, R. R., McKinney, R. E., and Pfeffer, J. T. "Solids retention in anaerobic waste treatment systems." Journal Water Pollution Control Federation, 42, 2, Part 2, Feb, R29-R45 (1970).

Daniels, L., Fuchs, G., Thauer, R. K., and Zeikus, J. G. "Carbon monoxide oxidationby methanogenic bacteria." Journal of Bacteriology, 132, 118-126 (1977).

Daniels, L., Sparling R., and Sprott, G. D. "The bioenergetics of methanogenesis." Biochimica et Biophysica Acta, 768, 113-163 (1984).

DeWalle, F. B., and Chian, E. S. K. "Kinetics of substrate removal in a completely mixed anaerobic filter." Biotechnology and Bioengineering, 18, 1275-1296 (1976).

Dolfing, J. "Acetogenesis." Biology of Anaerobic Microorganisms, Zehnder, A. J. B. ed., John Wiley & Sons, Inc., 417-468 (1988).

Dolfing, J., Griffioen, A., van Neerven, A. R. W., and Zevenhuizen, L. P. T. M. "Chemical and bacteriological composition of granular methanogenic sludge." Canadian Journal of Microbiology, 31, 744-750 (1985).

Dubourguier, H. C., Prensier, G., and Albagnac, G. "Structure and microbial activities of granular anaerobic sludge." Lettinga, A. J. B. et al. Eds., Granular Anaerobic Sludge, Pudoc, Wageningen, The Netherlands, 18-33 (1988).

Eastman, J. A. and Ferguson, J. F. "Solubilization of particulate organic carbon during the acid phase of anaerobic digestion." Journal Water Pollution Control Fedration, 53, 352-366 (1981).

Fan, L. T., Gharpuray, M. M. and Lee, Y. H., Cellulose Hydrolysis, Berlin; New York: Springer-Verlag (1987).

Fang, H. H. P., Chui, H. K., and Li, Y. Y. "Microbial structure and activity of UASB granules treating different wastewaters." Proceedings of the Seventh International Symposium on Anaerobic Digestion, Cape Town, South Africa, 80-90 (1994).

Fox, P., Suidan, M. T., and Bandy, J. T. "A comparison of media types in acetate fed expanded-bed anaerobic reactors." Water Research, 24, 7, :827-835 (1990).

Frostel, B. "Anaerobic treatment in a sludge bed system compared with a filter dystem." Journal of Water Pollution Control Federation, 53, 216-222 (1981)

Fukuzaki, S., Nishio, N., and Nagai, S. "Kinetics of methanogenic fermentation of acetate." Applied Environmental Microbiology, 56, 3158-3162 (1990).

Fullen, W. J. "Anaerobic digestion of packing plant waste." Sewage and Industrial Wastes, 25, 576 (1953).

Gates, W. E., Smith J. H., Lin, S. D., and RisIII, C. H. "A rational model for the anaerobic contact process." Journal Water Pollution Control Fedration, 39, 12, 1951-1970 (1967).

Ghosh, S. "Comparative studies of temperature effects on single-stage and two-phase anaerobic digestion." Biotechnology and Bioengineering Symposium, 17, 365-377 (1986).

Ghosh, S., and Poland, F. G. "Development in anaerobic stabilization of organic wastes - the two phase concept." Envioronmental Letters, 4, 255-263 (1971).

Grotenhuis, J. T. C., Kissel, J. C., Plugge, C. M., Stams, A. J. M., and Zehnder, A. J. B. "Role of substrate concentration in particle size distribution of methanogenic granular sludge in UASB reactors." Water Research, 25, 1, 21-27 (1991).

Guiot, S. R. and van den Berg, L. "Performance of an upflow anaerobic reactor combining a sludge blanket and a filter treating sugar waste." Biotechnology and Bioengineering, 27, 800-806 (1985).

Habben, C. E. "Initial studies of the anaerobic sequencing batch reactor." M.S. thesis, Iowa State University, Ames, Iowa (1991).

Hakulinen, R. and Salkinoja-Salonen, M. "Treatment of pulp and paper industrial wastewaters in an anaerobic fluidized bed reactor." Process Biochemistry, March/April, 18-22 (1982).

Hanaki, K., Matsuo, T., and Kumazaki, K. "Treatment of oily cafeteria wastewater by single-phase and two-phase anaerobic filter." Water Science and Technology, 22, 3/4, 299-306 (1990).

Harremoës, P., Biofilm Kinetics, In R. Mitchell (Ed.), Water Pollution Microbiology, Vol. 2. John Wiley & Sons, Chichester, UK. Chapter 4, 71-109 (1978).

Henze, M., and Harremoës, P "Anaerobic treatment of wastewater in fixed film reactors - a literature review." Water Science Technology, 15 1-101 (1983).

Herum, B. A. "The effect of applied vacuum on the performance of the anaerobic sequencing batch reactor." M.S. Thesis, Iowa State University, Ames, Iowa (1993).

Hobson, P. N., and Shaw, B. G. "The anaerobic digestion of waste from an intensive pig unit." Water Research, 7, 437-449 (1973).

Houwen, F. P., Plokker, J., Dijkema, C., and Stams, A. J. M. "Syntrophic propionate oxidation." Bélaich, J. P., Bruschi, M., Garcia, J. L. edited, Microbiology and Biochemistry of Strict Anaerobes Involved in Interspecies Hydrogen Transfer, Plenum Pubilshing Co., New York, NY, 281-290 (1990).

Hulshoff Pol, L. W. The phenomenon of granulation of anaerobic sludge. Ph. D. dissertation, Wageningen Agricultural University, Wageningen, The Netherlands (1989).

Hulshoff Pol, L. W., Heijnekamp, K., and Lettinga, G. "The selection pressure as a driving force behind the granulation of anaerobic sludge." Proceeding GASMAT workshop, Lunteren, The Netherlands, October 25-27, 153-161 (1987).

Hulshoff Pol, L. W., and Lettinga, G. "New technologies for anaerobic wastewater treatment." Water Science Technology, 18, 12, 41-53 (1986).

Hunt, S. "Diversity of biopolymer structure and its potential for ion binding applications." Immobilization of Ions by bio-sorption, Eds. Eccles, H., and Hunt, S. Chichester: Ellis Horwood, 15-46 (1986).

Hulshoff pol Pol, L. W., Dolfing, J., Velzeboer, C. T. M., and Lettinga, G. "Anaerobic Treatment of Wastewater Using UASB Reactor." In IAWPR-specialized Seminar, Anaerobic Treatment of Wastewater in Fixed Film Reactors, Copenhogen, Demark (1982).

Hulshoff pol Pol, L., and Lettinga, G. "New technology for anaerobic wastewater treatment." Water Science and Technology, 18(12):41-53 (1986).

Jennett, J. C., and Dennis, N. D. "Anaerobic filter treatment of pharmaceutical waste." Journal of Water Pollution Control Federation, 47(1):104-121 (1975).

Jetten, M. S. M., Stams, A. J. M., and Zehnder, A. J. B. "Acetate threshold values and acetate activating enzymes in methanogenic bacteria." FEMS Microial Ecology, 73, 339-349 (1990).

Jern, N. W., Kean, C. K. "Two-stage anaerobic digestion of piggery wastewaters." Water Science and Technology, 18:149-151 (1986).

Jeris, J. S. "Industrial wastewater treatment using anaerobic fluidized bed reactors." In Proceedinf of IAWPR-specialized Seminar, Anaerobic Treatment of Wastewater in Fixed Film Reactors, Copenhogen, Demark (1982).

Jones, W. J., Nagel, D. P. Jr., and Whitman, W. B. "Methanogens and the diversity of archaebacteria." Microbiological Review, 51, 1, 135-177 (1987).

Kaiser, S. K. "Initial studies on the anaerobic sequencing batch reactor at thermophilic temperatures." M.S. Thesis, Library, Iowa State University, Ames, Iowa (1991).

Kennedy, K. J., Sanchez, W. A., Hamoda, M. F., and Droste, R. L. "Performance of anaerobic sludge blanket sequencing batch reactors." Research Journal WPCE, 63, 1, 75-83 (1991).

Komatsu, T., Hanaki, K., and Matsuo, T. "Prevention of lipid inhibition in anaerobic processes by introducing a two-phase system." Water Science and Technology, 23, 1189-1200 (1991).

Lawerce A. W. "Application of process kinetics to design of anaerobic processes." Gould, R. F., Ed., Advances in Chemistry Series No. 105, American Chemical Society, Washington, D. C., 163 (1971).

Lettinga, G., Hulshoff Pol, L. W., Koster, I. W., Wiegant, W. M., de Zeeuw, W. J., Rinzema, A., Grin, P. C., Roersma, R. E.,and Hobma, S. W. "High-rate anaerobic wastewater treatment using the UASB-reactor under a wide range of temperature conditions." Biotechnology and Engineering Reviews, 2, 253-284 (1984).

Lettinga, G., van Velsen, A. F. M., de Zeeuw, W. J., and Hobma, S. W. "Feasibility of the UASB-Process." Proceedings of the National Conference in Environmental Engineering, San Francisco, CA, 35-45. American Society of Civil Engineers (1979).

Lettinga, G., van Velsen, A. F. M., De Zeeuw, W., Hobma, S. "The application of anaerobic digestion to industrial pollution treatment." Anaerobic Digestion, Stafford et al., Ed, Applied Science Publishers, London, England, 167-186 (1979).

Lettinga, G., and Vinken, J. N. "Feasibility of the upflow anaerobic sludge blanket (UASB) process for the treatment of low-strength wastes." Proceeding of the 35th Industrial Waste Conference, Purdue University, West Lafayette, Indiana (1980).

Lettinga, G., van Velsen, A. F. M., Hobma, S., De Zeeuw, W., and Klapwijk, A. "Use of the upflow sludge blanket (UASB) reactor concept for biological wastewater treatment, especially for Anaerobic for Treatment." Biotechnology and Bioengineering, 22, 699-734 (1980).

Lettinga, G., Hobma, S. W., Hulshoff pol Pol, L. W., De Zeeuw, W., De Jong, P., Grin, P., and Roersma, R. "Design, operation, and economy of anaerobic treatment." Water Science and Technology, 15, 8/9, 177-196 (1983).

Lettinga, G., Roersma, R. E., and Grin, P. "Anaerobic treatment of domestic sewage using a granular sludge bed UASB-reactor." Biotechnology and Bioengineering, 25, 1701-1712 (1983).

Lettinga, G., Hulshoff pol Pol, L. W., Koster. I. W., Wiegant, W. M., De Zeeuw, W. J., Rinzema, A., Grin, P. C., Roersma, R. E., and Hobma, S. W. "High-rate anaerobic waste-water treatment using the UASB reactor under a wide range of temperature conditions." Biotechnology and Genetic Engineering Review, 2, 253-281 (1984).

Lettinga, G., De Zeeuw, W., Hulshoff pol Pol, L. W., Wiegant, W. M, and Rinzema, A. "Anaerobic wastewater treatment based on biomass retention with emphasis on the UASB process." In Anaerobic Digestion, Proceeding of the Fourth International Symposium on Anaerobic Digestion, China, 11-15 November, 279-301 (1985).

Lettinga, G., Hulshoff Pol, L. W. "Advanced reactor design, operation and economy." Water Science and Technology, 18, 12, 55-69 (1986).

Lettinga, G., Hulshoff Pol, L. W. "UASB-process design for various types of wastewaters." Water Science and Technology, 24, 8, 87-107 (1991).

Llabres-Luengo, P., and Mata-Alvarez, J. "The hydrolytic step in a dry digestion system.", Biology Wastes, 23, 25-37 (1988).

MacLeod, F. A., Guiot, S. R., and Costerton, J. W. "Layered structure of bacterial aggregates produced in an upflow anaerobic sludge bed and filter reactor." Applied and Environmental Microbiology, 56, 6, 1598-1607 (1990).

Mahoney, E. M., Varangu, L. K., Cairns, W. L., Kosaric, N., and Murray, R. G. E. "The effect of calcium on microbial aggregation during UASB reactor start-up." Water Science and Technology, 19, 249-260 (1987).

McCarty, P. L. "Anaerobic treatment of soluble wastes." Paper presented at the special lecture series on Advances in Water Quality Improvement, The University of Texas, Austin, TX, April 4-7 (1966).

McCarty, P. L. "Anaerobic waste treatment fundamentals, part one: chemistry and microbiology." Public Works, 107-112 (September, 1964a).

McCarty, P. L. "Anaerobic waste treatment fundamentals, part two: environmental requirements and control." Public Works, 123-126 (October, 1964b).

McCarty, P. L., and Smith, D. P. "Anaerobic wastewater treatment." Environmental Science and Technology, 20, 12, 1200-1206 (1986).

McInerney, M. J., and Bryant, M. P. "Basic principles of bioconversions in anaerobic digestion and methanogenisis." Biomass Conversion Process for Energy and Fuels, Plenum Publishing Co., New York, NY (1981).

McInemey, J. G., and Bryant, M. P. Anaerobes and Anaerobic Infections, G. Gottschalk (Ed.) Gustav Fisher Verlag Stuttgart, New York (1980).

McInerney, M. J. "Anaerobic hydrolysis and fermentation of fats and proteins." Biology of Anaerobic Microorganisms, Zehnder, A. J. B. ed., John Wiley & Sons, Inc., 373-416 (1988).

Metcalf and Eddy, Inc., "Sedimentation." Wastewater Engineering: Treatment Disposal Reuse, 3nd Edition, 220-221, McGraw-Hill, Inc. (1991).

Min, H., and Zinder, S. H. "Kinetics of acetate utilization by two thermophilic acetotrophic methanogens: *Methanosarcina* sp. strain CALS-1 and *Methanothrix* sp. strain SALS-1." Applied Environmental Microbiology, 55, 488-496 (1986).

Monod, J., "The growth of bacterial cultures." Annual Review of Microbiology, 3, 371 (1949).

Morgan, J. W., Evison, L. M., and Forster, C. F. "The internal architecture of anaerobic sludge granules." Journal of Chemical Biotechnology, 50, 211-226 (1991).

Mortenson, E. N. U. S. Patent 2,661,332. Dec. 1 (1953).

Murray, W. D., and van den Berg, L. "Effect of support material on the development of microbial fixed films converting acetic acid to methane." Journal of Applied Bacteriology, 51, 257-265 (1981).

van Niekerk, A., Kawahigashi, J., Reichlin, D., Malea, A., and Jenkins, D. "Foaming in anaerobic digesters - a survey and laboratory investigation." Journal Water Pollution Control Federation, 59, 5, 249-253 (1987).

Norrman, Jonas " Depollution of pig waste combined with energy recovery." Grobal Bioconversions, V3, 163-201, CRC Press, Inc., Boca Raton, Florida (1987).

Oremland, R. S. "Biogeochemistry of methanogenic bacteria." Biology of Anaerobic Microorganisms, Zehnder, A. J. B. ed., John Wiley & Sons, Inc., 641-706 (1988).

Parkin, G. F. and Owen W. F. "Fundamentals of anaerobic digestion of wastewater sludges." Journal of Environmental Engineering, 112, 5, 869-920 (1986).

Pavlostathis, G. S., and Giraldo-Gomez, E. "Kinetics of anaerobic treatment: a critical review." Critical Reviews in Environmental Control, 21(5,6), 411-490 (1991).

Pauss, A., Samson, R., and Guiot, S. "Thermodynamic evidence of trophic microniches in methanogenic granular sludge-bed reactors." Applied Microbiology and Biotechnology, 33, 88-92 (1990).

Pidaparti, S. R.,"Anaerobic sequencing batch reactor treatment of swine wastes at 35°C and 25°C." M.S. Thesis, Library, Iowa State University, Ames, Iowa (1992).

Plummer, A. H., Malina, J. F., and Eckenfelder, W. W. " Stabilization of low solids carbohydrate waste by anaerobic submerged filter." Proceeding of the 23rd Industrial Waste Conference, Purdue University, West Lafayette, Indiana (1969).

Portier, R. J. "Chitin immobilization systems for hazardous waste detoxification and biodegradation." In Immobilization of Ions by bio-sorption, Eds. Eccles, H., and Hunt, S. Chichester: Ellis Horwood, 229-239 (1986).

Pretorius, W. A. "Anaerobic digestion III. kinetics of anaerobic fermentation." Water Research Pergamon Press, 3, 545-558 (1969).

Rittman, B. E., Strubler, C. E., and Ruzicka, T. "Anaerobic-filter pretreatment kinetics." Journal of the Environmental Division, Proceeding of the American Society of Civil Engineers, 108(EE5), 900-912 (October, 1982).

Ross, W. R. "The phenomenon of sludge pelletisation in the anaerobic treatment of a maize processing waste." Water SA, 10, 4, 197-203 (1984).

Roy, D., and Jones, L. M. "Acidogenesis in the two-phase anaerobic process." Journal of Science and Health, A20, 1, 1-20 (1985).

Salkinoja-Salonen, M. S., Nyns, E. J., Sutton, P. M., van den Berg, L. and Wheatley, A. D. "Starting-up of an anaerobic fixed film reactor." In Proceeding of IAWPR-specialized seminar on anaerobic treatment, June, Copenhagen, Demark (1982).

Sameh, S., de Seeuw, W., and Lettinga, G. "Anaerobic treatment of slaughterhouse waste using a flocculant sludge UASB reactor." Agricultural Wastes, 11, 197-226 (1984).

Sawyer, C. N. "Activated sludge modifications." Journal Water Pollution Control Federation, 32, 3, 232 (1960).

Schink, B. "Principles and limits of anaerobic degradation: environmental and technological aspects." Biology of Anaerobic Microorganisms, Zehnder, A. J. B. ed., John Wiley & Sons, Inc., 771-846 (1988).

Schink, B. and Thauer, R. K. "Energetics of syntrophic methane formation and the influence of aggregation." Lettinga, A. J. B. et al. Eds., Granular Anaerobic Sludge, Pudoc, Wageningen, The Netherlands, 5-17 (1988).

Schmit, C. G. "Anaerobic sequencing batch reactor treatment of swine waste at 20oC." Master Thesis, Iowa State University, Ames, Iowa (1992).

Schroepher, G. J., Johnson, A. S., Ziemke, N. R., and Anderson, J. J. "The anaerobic contact process as applied to packinghouse wastes." Sewage and Industrial Wastes, 27, 460 (1955).

Schroepher, G. J., Ziemke, N. R. "Development of the anaerobic contact process: I. pilot-plant investigations and economics." Sewage and Industrial Wastes, 31, 164 (1959).

Schroepher, G. J., Ziemke, N. R. "Development of the anaerobic contact process: II. ancillary investigations and special experiments." Sewage and Industrial Wastes, 31, 697 (1959).

Schwitzguébel, J. P., and Péringer, P. "Anaerobic digestion of proteins, piptides and amino acids." Bélaich, J. P., Bruschi, M., Garcia, J. L. edited, Microbiology and Biochemistry of Strict Anaerobes Involved in Interspecies Hydrogen Transfer, Plenum Pubilshing Co., New York, NY, 471-472 (1990).

Shin, H. S., Bae, B. U., Lee, J. J., and Paik, B. C. "Anaerobic digestion of distillery wastewater in a two-phase UASB system." Water Science and Technology, 25, 7, 361-371 (1992).

Speece, R. E. "Anaerobic biotechnology for industrial wastewater treatment." Environmental Science and Technology, 17, 9, 416A-427A (1983).

Standard Practice in Separate Sludge Digestion. Committee Report, Transactions, American Society of Civil Engineers, 103, 1662, 2014 (1938).

Stams, A. J. M., and Zehnder, A. J. B. "Ecological impact of syntrophic alcohol and fatty acid oxidation." Bélaich, J. P., Bruschi, M., Garcia, J. L. edited, Microbiology and Biochemistry of Strict Anaerobes Involved in Interspecies Hydrogen Transfer, Plenum Pubilshing Co., New York, NY, 87-98 (1990).

Stebor, T. W., Macaulay, M. N., and Berndt, C. L. "Anaerobic contact pretreatment of slaughterhouse wastewater." Proceedings of Food Processing Waste Conference, Atlanta, George (September 1-2, 1987).

Steffen, A. J. "Treatment of packing house wastes by anaerobic digestion." Biological Treatment of Sewage and Industrial Wastes, Reinhold Publishing Corp., New York, N. Y., 2 (1958).

Streeter, H. W. "Standard practice in separate sludge digestion." Sewage Works Journal, 9, 317 (1937).

Thiele, J. H., and Zeikus, J. G. "Control of interspecies electron flow during anaerobic digestion: Significance of formate transfer versus hydrogen transfer during syntrophic methanogenesis in flocs." Applied and Environmental Microbiology, 54, 1, 20-29 (1988).

Tsezos, M., and Bell, J. P. "Comparison of the biosorption and desorption of hazardous organic pollutants by live and dead biomass." Water Research, 23, 5, 561 (1989).

Ullrich, A. H., and Smith M. W. "The biosorption process of sewage and waste treatment." Sewage and Industrial Wastes, 23, 10, 1248 (1951).

Ullrich, A. H., and Smith M. W. "Operation experience with activated sludge - biosorption at Austin, Texas." Sewage and Industrial Wastes, 29, 4, 400 (1957).

U. S. Environmental Protection Agency. Handbook for analytical quality control in water and wastewater laboratories. EPA-600/4-79-091 (March, 1979).

Vogels, G. D., Keltjens, J. T., and Drift, C. van der "Biochemistry of methane production." Biology of Anaerobic Microorganisms, Zehnder, A. J. B. ed., John Wiley & Sons, Inc., 707-770 (1988).

Wang, Yin-Tin, Suidan, M. T., and Rittman, B. E. "Performance of expended-bed methanogenic reactor." Journal of Environmental Engineering, 114, 4, 460-471 (1985).

Westermann, P., Ahring, B. K., and Mah, R. "Threshold acetate concentrations for acetate catabolism by aceticlastic methanogenic bacteria." Applied Environmental Microbiology, 55, 514-521 (1989).

Widdel, F. "Microbiology and ecology of sulfate- and sulfur-reducing bacteria." Biology of Anaerobic Microorganisms, Zehnder, A. J. B. ed., John Wiley & Sons, Inc., 469-586 (1988).

Winfrey, M. R. "Microbial methane production." Petroleum Microbiology, Atlas, R. M., ed., Macmillan, New York, 153-219 (1984).

Yang, G., and Anderson, G. K. "Effects of wastewater composition on stability of UASB." Journal of Environmental Engineering, 119, 5, 958-975 (1993).

Young, J. C., McCarty, P. L. "The anaerobic filter for waste treatment." Proceedings of the 22nd Industrial Waste Conference, Purdue University, Lafayette, IN (1967). Also Journal Water Pollution Control Federation, 41, 5, R160 (1969).

Young, J. C., and Dahab, M. F. "Effect of media design on the performance of fixed-bed anaerobic reactors." In Proceeding of IAWPR-specialized seminar on anaerobic treatment, June, Copenhagen, Demark (1982).

Young, J. C. "The anaerobic filter for waste treatment." Doctoral Dissertation, Stanford University, Palo Alto, CA (1968).

Zeikus, J. G. "The biology of methanogenic bacteria." Bacteriological Review, 41, 2, 514-541 (1977).

Zeikus, J. G. "Microbial population in digesters." The 4th International Symposium on Anaerobic Digestion, Kwangchow, Kwangtung, China (1985).

Zinder, S. H. "Microbiology of anaerobic conversion of organic waste to methane: recent developments." ASM News, 50, 294-298 (1984).

ACKNOWLEDGEMENTS

Sincere appreciation is extended to the author's major professor, Dr. Richard R. Dague, for his guidance, support, and patience throughout the graduate work. Appreciation also goes to my other committee members, Dr. Lacy Daniels, Dr. Charles E. Glatz, Dr. LaDon C. Jones, Dr. Tom E. Loynachan, Dr. Say-Kee Ong, Dr. Gene F. Parkin, and Dr. Ruihong Zhang for their precious comments and efforts added to the quality of this project.

The author would like to give thanks to his parents and especially to his wife, Weiwen, for her enduring support and boundless love during his four years of study at Iowa State University, to his lovely son, Eric, for providing babbling inspiration, and to his brother-in-law Yaw-Tzuu Chyi for his continuous help in the lab work, .

Finally, the author would like to thank the U.S. Department of Agriculture for providing financial support for the research through contract number 89-34188-4370 (Charles D. Hungerford, Administrative Contact, and David R. MacKenzie, Programmatic Contact), through the Iowa Biotechnology Byproducts Consortium.

APPENDIX A

VELOCITY GRADIENT CALIBRATION DATA

VELOCITY GRADIENT CALCULATIONS

Date: April 22, 1991
Reactor A

Flow Control Scale	Biogas Flow Qg, L/Min.	Gas Pressure @ Diffuser P1, cm	Flow Qg m^3/s	Pressure P1 KN/m^2	Energy Dissipated E, KW	Velocity Gradient G, 1/sec.
1	0.132	90.3	2.04E-06	107.43	1.65E-05	43
2	0.322	90.7	4.98E-06	107.47	4.01E-05	68
3	0.570	91.3	8.80E-06	107.53	7.10E-05	90
4	0.841	92.7	1.30E-05	107.66	1.05E-04	110
5	1.066	94.5	1.64E-05	107.84	1.32E-04	123
6	1.280	97.0	1.97E-05	108.08	1.59E-04	135
7	1.497	99.8	2.29E-05	108.35	1.85E-04	146
8	1.708	102.8	2.61E-05	108.65	2.11E-04	155
9	1.909	106.0	2.91E-05	108.96	2.35E-04	164
10	1.989	107.6	3.03E-05	109.11	2.44E-04	167

Date: April 22, 1991
Reactor B

Flow Control Scale	Biogas Flow Qg, L/Min.	Gas Pressure @ Diffuser P1, cm	Flow Qg m^3/s	Pressure P1 KN/m^2	Energy Dissipated E, KW	Velocity Gradient G, 1/sec.
1	0.100	50.0	1.60E-06	103.50	6.11E-06	26
2	0.252	50.1	4.04E-06	103.51	1.54E-05	42
3	0.478	50.3	7.67E-06	103.53	2.92E-05	58
4	0.738	50.9	1.18E-05	103.59	4.50E-05	72
5	0.957	51.5	1.53E-05	103.65	5.84E-05	82
6	1.211	51.9	1.94E-05	103.69	7.39E-05	92
7	1.475	52.5	2.36E-05	103.74	8.99E-05	102
8	1.719	53.5	2.75E-05	103.84	1.05E-04	110
9	1.946	53.9	3.11E-05	103.88	1.18E-04	117
10	2.002	54.5	3.20E-05	103.94	1.22E-04	118

VELOCITY GRADIENT CALCULATIONS

Date: April 23, 1991
Reactor C

Flow Control Scale	Biogas Flow Qg, L/Min.	Gas Pressure @ Diffuser P1, cm	Flow Qg m^3/s	Pressure P1 KN/m^2	Energy Dissipated E, KW	Velocity Gradient G, 1/sec.
1	0.238	36.2	3.87E-06	102.16	9.51E-06	33
2	0.505	36.4	8.21E-06	102.17	2.02E-05	48
3	0.965	36.6	1.57E-05	102.19	3.85E-05	67
4	1.446	36.8	2.35E-05	102.21	5.77E-05	81
5	1.902	37.0	3.09E-05	102.23	7.59E-05	93
6	2.358	37.2	3.83E-05	102.25	9.41E-05	104
7	2.797	37.4	4.54E-05	102.27	1.12E-04	113
8	3.172	37.8	5.15E-05	102.31	1.27E-04	121
9	3.529	38.4	5.72E-05	102.37	1.41E-04	127
10	3.711	38.8	6.02E-05	102.41	1.48E-04	130

Date: April 23, 1991
Reactor D

Flow Control Scale	Biogas Flow Qg, L/Min.	Gas Pressure @ Diffuser P1, cm	Flow Qg m^3/s	Pressure P1 KN/m^2	Energy Dissipated E, KW	Velocity Gradient G, 1/sec.
1	0.200	30.6	3.27E-06	101.61	6.56E-06	27
2	0.581	30.6	9.49E-06	101.61	1.91E-05	47
3	1.029	30.6	1.68E-05	101.61	3.38E-05	62
4	1.478	30.6	2.42E-05	101.61	4.85E-05	75
5	1.894	30.8	3.09E-05	101.63	6.22E-05	84
6	2.281	31.0	3.73E-05	101.65	7.48E-05	93
7	2.817	31.2	4.60E-05	101.67	9.24E-05	103
8	3.203	31.4	5.23E-05	101.69	1.05E-04	110
9	3.589	31.6	5.86E-05	101.71	1.18E-04	116
10	3.629	31.7	5.92E-05	101.72	1.19E-04	117

APPENDIX B

ASBR BIOSOLIDS PROFILE AND DAILY METHANE PRODUCTION

LABORATORY STUDY DAILY LOG

REACTOR A
COD LOADING: 2.0 g/L/day (Start-Up Phase)
HRT = 48 Hours (4 cycles /day)

Date	MLSS mg/l	MLVSS mg/l	Volatile %	CH4 Prod. Liters @STP	Remark
Apr 18, '91	~8,500				Reactor Seeded
19					
20					
21					
22					
23					
24	6,530				
25	5,540				
26	~11,000				Additional Seed Added
27					
28					
29					
30					
May 1	12,060	10,670	88		
2	12,235	10,550	86		
3					
4				6.7	
5					
6					
7	12,870	11,000	85	5.7	
8				6.1	
9	13,110	11,780	90	7.1	
10				8.7	
11				7.9	
12				7.5	
13				7.7	
14				8.3	
15	13,385	11,890	89	8.2	Biosorption Study
16	13,230	11,090	84	8.0	Biosorption Study
17				7.6	
18				7.8	
19				7.8	
20	13,750	11,160	81	7.9	
21				7.8	

REACTOR A
COD LOADING: 2.0 g/L/day
HRT = 48 Hours (4 cycles /day)

Date	MLSS mg/l	MLVSS mg/l	Volatile %	CH4 Prod. Liters @STP	Remark
May 22, '91	14,040	11,200	80	7.8	Performance Analyzed
23	14,040	11,460	82	7.8	Performance Analyzed
24				7.9	
25				7.8	
26				7.7	
27	14,760	12,060	82	7.9	
28				7.9	
29	15,180	12,420	82	7.8	Performance Analyzed
30				7.8	
31	15,330	12,570	82	7.9	

COD LOADING: 4.0 g/L/day
HRT = 48 Hours (4 cycles /day)

Date	MLSS mg/l	MLVSS mg/l	Volatile %	CH4 Prod. Liters @STP	Remark
Jun 1, '91					
2	14,920	12,660	85		
3	13,870	11,370	82	14.8	
4	14,670	12,210	83	14.7	
5	15,050	12,250	81	15.3	Performance Analyzed
6					
7				15.2	
8				15.5	
9				15.9	
10	16,540	13,600	82	16.0	Performance Analyzed
11				16.2	
12				15.9	
13	17,770	14,990	84	16.1	Performance Analyzed
14				15.9	
15				15.9	
16				15.7	
17	19,750	17,265	87	16.2	
18	20,420	17,850	87	16.1	Performance Analyzed
19	20,750			16.0	

REACTOR A
COD LOADING: 6.0 g/L/day
HRT = 48 Hours (4 cycles /day)

Date	MLSS mg/l	MLVSS mg/l	Volatile %	CH4 Prod. Liters @STP	Remark
Jun 20, '91	15,930			20.7	
21	14,370	12,660	88	22.5	
22	14,230	12,470	88	24.6	
23	15,890	14,280	90	24.7	
24				25.1	
25	16,880	14,460	86	24.8	Performance Analyzed
26				24.9	
27	16,920	14,670	87	25.2	Performance Analyzed
28				25.8	
29				25.7	
30				26.0	
Jul 1				25.6	
2	17,670	15,320	87	25.6	Performance Analyzed
3				25.0	

COD LOADING: 8.0 g/L/day
HRT = 48 Hours (4 cycles /day)

Date	MLSS mg/l	MLVSS mg/l	Volatile %	CH4 Prod. Liters @STP	Remark
Jul 4, '91					
5	11,845	10,180	86	27.7	
6	11,550	9,850	85	28.3	
7	9,045	7,645	85	28.6	
8	8,270	6,955	84	26.5	
9	21,540	17,980	83	27.3	Eff. Biosolids Returned
10				28.8	
11	22,620	18,965	84	30.0	
12				29.4	
13				29.8	
14	23,930	20,570	86	29.4	Performance Analyzed
15				30.1	
16	24,580	21,120	86	30.0	Performance Analyzed
17				30.2	
18	24,270	20,790	86	29.7	Performance Analyzed
19					COD= 4 g/L/day
20	25,970	21,760	84	15.4	
21	26,280	22,070	84	15.2	Settling Test
22	24,040			35.9	COD= 10 g/L/day
23	22,380	19,040	85		Biosolids Washout

REACTOR A
COD LOADING: 2.0 g/L/day
HRT = 24 Hours (4 cycles /day)

Date	MLSS mg/l	MLVSS mg/l	Volatile %	CH4 Prod. Liters @STP	Remark
Jul 24, '91					
25	23,920	20,160	84	7.4	
26	24,647	21,000	85	7.9	Performance Analyzed
27				8.0	
28	22,990	20,500	89	8.0	
29				7.7	
30	19,450	17,210	88	7.4	
31				7.5	
Aug 1	22,960	19,790	86	7.5	
2	20,030	17,770	89	7.7	
3				7.3	
4				7.5	
5	21,950	19,030	87		
6	20,490	17,900	87	7.6	
7	21,550	17,920	83	7.8	Performance Analyzed
8				7.7	
9	21,450	18,630	87	7.9	Performance Analyzed
10				7.6	
11				8.0	
12	23,020	19,630	85	7.8	Performance Analyzed

REACTOR A
COD LOADING: 4.0 g/L/day
HRT = 24 Hours (4 cycles /day)

Date	MLSS mg/l	MLVSS mg/l	Volatile %	CH4 Prod. Liters @STP	Remark
Aug 13, '91					
14					
15	16,650	13,870	83	14.8	
16				15.6	
17	17,640	15,430	87	15.5	
18				15.4	
19	14,930	13,560	91	15.5	Performance Analyzed
20				15.3	
21					Biogas Line Leak
22					Gas Meter Calibrated
23					Mixing Flow Calibrated
24	17,340	14,890	86		
25				14.5	
26				14.7	
27	17,260	15,210	88	15.1	
28				15.4	
29	19,590	17,030	87	15.5	
30	17,560	15,580	89	15.3	
31				15.3	
Sep 1	16,600	14,520	87	15.3	
2				15.7	
3	15,920	13,950	88	15.5	
4	15,325	13,410	88	15.5	Performance Analyzed
5				15.7	
6	16,090	13,890	86	15.4	Performance Analyzed
7				15.0	

COD LOADING: 6.0 g/L/day
HRT = 24 Hours (4 cycles /day)

Date	MLSS mg/l	MLVSS mg/l	Volatile %	CH4 Prod. Liters @STP	Remark
Sep 8, '91					
9					
10	10,940	9,705	89	21.9	
11				21.3	
12	13,210	11,310	86	22.1	
13				22.9	
14				22.2	
15				22.0	
16				21.9	
17	14,350	12,620	88	22.5	
18	15,050	13,170	88	24.6	
19				24.5	

REACTOR A
COD LOADING: 6.0 g/L/day
HRT = 24 Hours (4 cycles /day)

Date	MLSS mg/l	MLVSS mg/l	Volatile %	CH4 Prod. Liters @STP	Remark
Sep 20, '91				24.0	
21				21.4	
22				21.8	
23				22.1	
24				24.6	
25				24.5	
26	16,260	14,280	88	24.1	Performance Analyzed
27				24.5	
28				24.0	
29				23.0	
30				23.9	
Oct 1	20,750	18,650	90	23.9	Performance Analyzed
2				23.7	
3	17,120	15,560	91	23.6	
4	17,910	16,050	90	22.8	
5				23.6	
6	18,090	16,260	90	23.7	
7	19,410	17,470	90	23.7	Performance Analyzed
8				23.6	
9	20,690	18,680	90	24.1	Performance Analyzed

REACTOR A
COD LOADING: 8.0 g/L/day
HRT = 24 Hours (4 cycles /day)

Date	MLSS mg/l	MLVSS mg/l	Volatile %	CH4 Prod. Liters @STP	Remark
Oct 10, '91					
11				27.1	
12	18,630	16,570	89	28.3	
13	17,345	15,360	89	34.4	
14				30.2	
15				36.1	
16				34.0	
17				29.7	
18	19,810	18,280	92	29.8	Performance Analyzed
19	16,740	14,930	89	29.7	Performance Analyzed
20				29.8	
21	17,640	15,890	90	29.6	Performance Analyzed

REACTOR A
COD LOADING: 2.0 g/L/day
HRT = 12 Hours (6 cycles /day)

Date	MLSS mg/l	MLVSS mg/l	Volatile %	CH4 Prod. Liters @STP	Remark
Oct 22, '91					
23	14,650	12,340	84	7.9	Biosolids Washout
24				7.5	"
25					"
26					"
27				5.6	"
28				7.8	"
29				7.8	"
30				7.0	"
31	12,410	10,950	88	7.1	"
Nov 1				6.9	"
2				6.8	"
3	11,900	10,320	87	7.0	"
4				6.8	"
5	10,940	9,700	89	7.2	"
6	9,960	8,630	87	7.3	"

REACTOR A
COD LOADING: 4.0 g/L/day
HRT = 12 Hours (6 cycles /day)

Date	MLSS mg/l	MLVSS mg/l	Volatile %	CH4 Prod. Liters @STP	Remark
Nov 7, '91					
8				14.9	
9	7,950	6,895	87	15.4	
10					
11				15.0	
12				15.1	
13	8,360	7,120	85	15.4	Performance Analyzed
14	10,780	9,440	88	15.2	Performance Analyzed
15	10,570	9,160	87	15.4	Performance Analyzed

REACTOR A
COD LOADING: 6.0 g/L/day
HRT = 12 Hours (6 cycles /day)

Date	MLSS mg/l	MLVSS mg/l	Volatile %	CH4 Prod. Liters @STP	Remark
Nov 16, '91					
17					
18				23.1	
19				23.8	
20				23.5	
21				22.7	
22				22.2	
23	10,740	9,400	88	22.7	Performance Analyzed
24	11,210	10,050	90	22.5	Performance Analyzed
25	12,620	10,375	82	23.1	Performance Analyzed

REACTOR A
COD LOADING: 8.0 g/L/day
HRT = 12 Hours (6 cycles /day)

Date	MLSS mg/l	MLVSS mg/l	Volatile %	CH4 Prod. Liters @STP	Remark
Nov 26, '91					
27				32.9	
28				30.9	
29				29.8	
30				30.3	
Dec 1				30.6	
2	12,890	11,040	86	29.9	Performance Analyzed
3	13,290	11,350	85	30.0	Performance Analyzed
4	12,980	10,600	82	30.3	Performance Analyzed
5				30.0	
6				31.6	COD = 10.0 g/L/day
7					"
8					"
9					"
10				22.4	COD = 6.0 g/L/day
11				28.6	
12				28.9	
13				29.7	
14				30.4	
15				30.3	
16				29.6	
17				29.8	
18				30.2	
19					
20					
21					
22					
23					

LABORATORY STUDY DAILY LOG

REACTOR B
COD LOADING: 2.0 g/L/day (Start-Up Phase)
HRT = 48 Hours (4 cycles /day)

Date	MLSS mg/l	MLVSS mg/l	Volatile %	CH4 Prod. Liters @STP	Remark
Apr 18, '91	~8,500				Reactor Seeded
19					
20					
21					
22					
23					
24	7,720				
25	7,790				
26	~11,000				Additional Seed Added
27					
28					
29					
30					
May 1	12,140	10,630	88		
2	12,330	10,640	86		
3					
4				5.5	
5					
6					
7	13,160	11,370	86	5.7	
8				5.8	
9	12,980	11,290	87	7.1	
10				7.9	
11					
12					
13				7.8	
14				7.9	
15	13,420	11,800	88	7.4	Biosorption Study
16	13,800	12,010	87	7.7	Biosorption Study
17				7.5	
18				7.9	
19				7.5	
20	13,660	11,740	86	7.7	
21				7.6	

REACTOR B
COD LOADING: 2.0 g/L/day
HRT = 48 Hours (4 cycles /day)

Date	MLSS mg/l	MLVSS mg/l	Volatile %	CH4 Prod. Liters @STP	Remark
May 22, '91	13,590	11,230	83	7.7	Performance Analyzed
23	13,760	11,300	82	7.7	Performance Analyzed
24				7.4	
25				7.8	
26				7.6	
27	13,560	11,360	84	7.8	
28				7.7	
29	14,580	12,620	87	7.5	Performance Analyzed
30				7.5	
31	14,600	11,940	82	7.4	

COD LOADING: 4.0 g/L/day
HRT = 48 Hours (4 cycles /day)

Date	MLSS mg/l	MLVSS mg/l	Volatile %	CH4 Prod. Liters @STP	Remark
Jun 1, '91					
2	14,500	12,030	83		
3	14,590	11,990	82	14.7	
4	15,040	12,370	82	14.7	
5	15,140	12,070	80	14.9	Performance Analyzed
6				15.6	
7				16.1	
8				14.8	
9				15.8	
10	16,540	13,600	82	16.1	Performance Analyzed
11				16.4	
12				15.8	
13	18,210	15,250	84	16.3	Performance Analyzed
14				16.0	
15				16.4	
16				16.4	
17	21,130	18,460	87	16.5	
18	21,410	18,440	86	16.6	Performance Analyzed
19	22,080			16.7	

REACTOR B
COD LOADING: 6.0 g/L/day
HRT = 48 Hours (4 cycles /day)

Date	MLSS mg/l	MLVSS mg/l	Volatile %	CH4 Prod. Liters @STP	Remark
Jun 20, '91	20,430			20.8	
21	19,820	17,640	89	23.2	
22	20,750	18,720	90	21.3	
23	20,420	17,720	87	23.7	
24				24.0	
25	21,240	18,230	86	24.1	Performance Analyzed
26				24.4	
27	21,410	18,630	87	24.3	Performance Analyzed
28				24.4	
29				24.0	
30				23.8	
Jul 1				23.8	
2	22,540	19,580	87	24.3	Performance Analyzed
3				24.5	

COD LOADING: 8.0 g/L/day
HRT = 48 Hours (4 cycles /day)

Date	MLSS mg/l	MLVSS mg/l	Volatile %	CH4 Prod. Liters @STP	Remark
Jul 4, '91					
5	20,050	17,230	86	28.1	
6				29.3	
7				27.7	
8	22,870	19,390	85	30.3	
9	24,260	21,280	88	31.3	
10				30.8	
11	24,960	22,000	88	30.5	
12				29.9	
13				29.7	
14	25,420	21,670	85	31.0	Performance Analyzed
15				30.1	
16	25,820	22,080	86	30.6	Performance Analyzed
17				31.0	
18	26,510	23,200	88	30.3	Performance Analyzed
19					COD= 4 g/L/day
20	27,340	23,150	85	14.9	
21	27,970	23,760	85	14.8	
22	23,760			37.1	COD= 10 g/L/day
23	21,810	19,280	88		Biosolids Washout

REACTOR B
COD LOADING: 2.0 g/L/day
HRT = 24 Hours (4 cycles /day)

Date	MLSS mg/l	MLVSS mg/l	Volatile %	CH4 Prod. Liters @STP	Remark
Jul 24, 91					
25	22,590	20,020	89	7.7	
26	22,640	19,930	88	7.9	Performance Analyzed
27				8.0	
28	23,020	19,860	86	8.1	
29				7.7	
30	23,840	20,870	88	7.3	
31				7.3	
Aug 1	24,980	21,640	87	7.0	
2	25,590	22,550	88	7.5	
3	~17,000				Biosolids Wasted
4				8.0	
5	17,260	15,210	88	8.1	
6	17,260	15,010	87	8.3	
7	17,130	15,010	88	7.9	Performance Analyzed
8				7.9	
9	17,890	15,730	88	8.4	Performance Analyzed
10				8.0	
11				8.2	
12	19,660	17,620	90	8.2	Performance Analyzed

REACTOR B
COD LOADING: 4.0 g/L/day
HRT = 24 Hours (4 cycles /day)

Date	MLSS mg/l	MLVSS mg/l	Volatile %	CH4 Prod. Liters @STP	Remark
Aug 13, '91					
14					
15	18,800	16,020	85	14.0	
16				15.0	
17	18,430	16,250	88	14.6	
18				15.4	
19	17,500	14,790	85	15.1	Performance Analyzed
20				14.9	
21				14.9	
22					Gas Meter Calibrated
23					Mixing Flow Calibrated
24	21,440	19,080	89		
25				13.9	
26				15.8	
27	19,610	17,240	88	15.5	
28				15.8	Timer Malfunction
29	10,450	9,080	87		
30	10,800	9,485	88		
31				16.0	
Sep 1	9,730	8,340	86	15.6	
2				15.4	
3	11,070	9,670	87	15.4	
4	10,530	9,375	89	15.4	Performance Analyzed
5				15.9	
6	11,900	10,080	85	16.0	Performance Analyzed
7				15.2	

COD LOADING: 6.0 g/L/day
HRT = 24 Hours (4 cycles /day)

Date	MLSS mg/l	MLVSS mg/l	Volatile %	CH4 Prod. Liters @STP	Remark
Sep 8, '91					
9					
10	11,940	10,350	87	14.0	
11				18.6	
12	11,210	9,510	85	17.6	
13				15.5	
14					
15					
16				21.5	
17	13,310	11,590	87	21.0	
18	13,910	12,270	88	23.4	
19				22.6	

REACTOR B
COD LOADING: 6.0 g/L/day
HRT = 24 Hours (4 cycles /day)

Date	MLSS mg/l	MLVSS mg/l	Volatile %	CH4 Prod. Liters @STP	Remark
Sep 20, '91				24.0	
21				20.9	
22				23.0	
23				24.2	
24	14,685	12,855	88	23.1	
25				24.0	
26	14,610	13,205	90	23.9	Performance Analyzed
27				22.7	
28				21.6	
29				23.1	
30				22.5	
Oct 1	16,740	14,930	89	23.2	Performance Analyzed
2				23.0	
3	16,940	14,940	88	23.6	
4	17,560	15,580	89	23.8	
5				24.0	
6	17,810	15,920	89	23.5	
7	16,510	14,290	87	23.6	Performance Analyzed
8				23.8	
9	18,090	16,260	90	23.0	Performance Analyzed

REACTOR B
COD LOADING: 8.0 g/L/day
HRT = 24 Hours (4 cycles /day)

Date	MLSS mg/l	MLVSS mg/l	Volatile %	CH4 Prod. Liters @STP	Remark
Oct 10, '91					
11				25.9	
12	15,550	13,830	89	27.2	
13	16,110	14,650	91	30.0	
14				30.5	
15				27.2	
16				26.9	
17				26.8	
18	13,970	12,125	87	27.5	Performance Analyzed
19	14,460	12,580	87	27.3	Performance Analyzed
20				28.0	
21	14,790	12,900	87	27.2	Performance Analyzed
22				32.0	COD = 10 g/L/day
23	11,970	10,490	88	36.4	Biosolids Washout
24					

REACTOR B
COD LOADING: 2.0 g/L/day
HRT = 12 Hours (6 cycles /day)

Date	MLSS mg/l	MLVSS mg/l	Volatile %	CH4 Prod. Liters @STP	Remark
Oct 25, '91					
26	9,820	8,690	88	7.0	Biosolids Washout
27				7.2	"
28					"
29				7.4	"
30				7.6	"
31				7.6	"
Nov 1	8,010	6,890	86	7.2	"
2				7.0	"
3	7,450	6,540	88	6.6	"
4				6.6	"
5	6,840	6,105	89	7.0	
6	6,870	6,160	90	7.1	

REACTOR B
COD LOADING: 4.0 g/L/day
HRT = 12 Hours (6 cycles /day)

Date	MLSS mg/l	MLVSS mg/l	Volatile %	CH4 Prod. Liters @STP	Remark
Nov 7, '91					
8					
9	6,075	5,435	89	15.8	Performance Analyzed
10				15.9	
11				16.0	
12				15.8	
13	9,875	8,365	85	16.0	
14	11,710	10,400	89	15.8	Performance Analyzed
15	9,750	8,450	87	15.5	Performance Analyzed

REACTOR B
COD LOADING: 6.0 g/L/day
HRT = 12 Hours (6 cycles /day)

Date	MLSS mg/l	MLVSS mg/l	Volatile %	CH4 Prod. Liters @STP	Remark
Nov 16, '91					
17				22.8	
18				22.5	
19				23.0	
20				23.5	
21				23.0	
22				22.7	
23	9,190	8,190	89	23.1	Performance Analyzed
24	11,480	9,950	87	23.0	Performance Analyzed
25	9,860	8,820	89	22.9	Performance Analyzed

REACTOR B
COD LOADING: 8.0 g/L/day
HRT = 12 Hours (6 cycles /day)

Date	MLSS mg/l	MLVSS mg/l	Volatile %	CH4 Prod. Liters @STP	Remark
Nov 26, '91					
27				33.0	
28					
29				30.8	
30				30.5	
Dec 1				29.4	
2	11,450	9,920	87	29.8	Performance Analyzed
3	14,730	12,830	87	30.0	Performance Analyzed
4	10,010	8,800	88	30.0	Performance Analyzed
5				29.8	
6					
7					
8					
9					Decrease COD Loadin
10					to COD = 6.0 g/L/day
11					
12					
13					
14					
15					
16					
17					
18					
19					
20					
21					
22					
23					

LABORATORY STUDY DAILY LOG

REACTOR C
COD LOADING: 2.0 g/L/day (Start-Up Phase)
HRT = 48 Hours (4 cycles /day)

Date	MLSS mg/l	MLVSS mg/l	Volatile %	CH4 Prod. Liters @STP	Remark
Apr 18, '91	~8,500				Reactor Seeded
19					
20					
21					
22					
23					
24	10,860				
25	9,715				
26	9,940				
27					
28					
29					
30					
May 1	10,570	9,220	87		
2	10,630	9,180	86		
3					
4					
5					
6					
7	10,970			7.6	
8				7.4	
9	11,310	9,870	87	7.8	
10				7.8	
11					
12					
13				7.4	
14				7.2	
15	11,440	9,680	85	7.0	
16	11,460	9,610	84	7.5	
17				7.3	
18				7.2	
19				7.2	
20	11,540	9,580	83	7.5	
21				7.5	

REACTOR C
COD LOADING: 2.0 g/L/day
HRT = 48 Hours (4 cycles /day)

Date	MLSS mg/l	MLVSS mg/l	Volatile %	CH4 Prod. Liters @STP	Remark
May 22, '91	11,860	9,810	83	7.5	Performance Analyzed
23	11,980	9,700	81	7.5	Performance Analyzed
24				7.4	
25				7.6	
26				7.4	
27	13,430	11,310	84	7.3	
28				7.3	
29	13,680	11,550	84	7.0	Performance Analyzed
30				7.1	
31	14,370	12,230	85	7.3	

COD LOADING: 4.0 g/L/day
HRT = 48 Hours (4 cycles /day)

Date	MLSS mg/l	MLVSS mg/l	Volatile %	CH4 Prod. Liters @STP	Remark
Jun 1, '91					
2	15,180	12,770	84		
3	14,860	12,300	83	15.3	
4	15,880	13,730	86	15.6	
5	16,780	14,130	84	14.5	Performance Analyzed
6				15.2	
7				14.8	
8				15.1	
9				15.2	
10	18,210	15,250	84	15.6	Performance Analyzed
11					
12				14.9	
13	19,820	16,430	83	15.0	Performance Analyzed
14				15.5	
15				15.4	
16				16.0	
17	19,940	17,140	86	16.0	
18	20,470	17,600	86	15.3	Performance Analyzed
19				15.8	

REACTOR C
COD LOADING: 6.0 g/L/day
HRT = 48 Hours (4 cycles /day)

Date	MLSS mg/l	MLVSS mg/l	Volatile %	CH4 Prod. Liters @STP	Remark
Jun 20, '91					
21					
22	23,020	19,860	86	23.5	
23	22,640	19,880	88	23.8	
24				23.7	
25	21,140	18,380	87	23.4	Performance Analyzed
26				24.1	
27	24,880	21,950	88	24.3	Performance Analyzed
28				23.7	
29				24.0	
30				24.0	
Jul 1	26,480			24.2	
2	26,040	22,700	87	23.8	Performance Analyzed
3				23.8	

COD LOADING: 8.0 g/L/day
HRT = 48 Hours (4 cycles /day)

Date	MLSS mg/l	MLVSS mg/l	Volatile %	CH4 Prod. Liters @STP	Remark
Jul 4, '91					
5	25,950	22,280	86	27.6	
6				27.9	
7				27.2	
8	25,350	22,070	87	27.0	
9	26,860	22,920	85	29.4	
10				30.0	
11	24,980	21,640	87	29.3	
12				29.1	
13				29.0	
14	24,425	21,340	87	29.4	Performance Analyzed
15				30.0	
16	29,210	25,790	88	29.9	Performance Analyzed
17				29.2	
18	25,570	22,320	87	29.7	Performance Analyzed
19				38.6	COD= 10 g/L/day
20					

REACTOR C
COD LOADING: 2.0 g/L/day
HRT = 24 Hours (4 cycles /day)

Date	MLSS mg/l	MLVSS mg/l	Volatile %	CH4 Prod. Liters @STP	Remark
Jul 21, '91					
22	26,900	23,490	87	7.8	
23	25,990	22,970	88	7.5	
24				7.8	
25	27,460	24,270	88	7.4	
26	27,140	24,030	89	7.9	Performance Analyzed
27				7.9	
28	28,520	24,840	87	7.9	
29				7.3	
30	28,230	24,750	88	7.2	
31				7.2	
Aug 1	29,020	25,650	88	7.6	
2	28,190	24,940	88	7.7	
3	~20,000				Biosolids Wasted
4					
5	19,190	16,980	88	8.0	
6	20,107	17,750	88	7.6	
7	18,940	16,550	87	7.6	Performance Analyzed
8				7.8	
9	21,770	19,010	87	7.2	Performance Analyzed
10				7.5	
11				7.0	
12	18,630	16,570	89	7.2	Performance Analyzed

REACTOR C
COD LOADING: 4.0 g/L/day
HRT = 24 Hours (4 cycles /day)

Date	MLSS mg/l	MLVSS mg/l	Volatile %	CH4 Prod. Liters @STP	Remark
Aug 13, '91					
14					
15	19,080	16,490	86	14.9	
16				15.3	
17	20,590	18,140	88	15.0	
18				14.8	
19	24,260	21,280	88	14.8	Performance Analyzed
20				15.0	
21				15.5	
22					Gas Meter Calibrated
23					Mixing Flow Calibrated
24	21,755	18,945	87		
25				14.9	
26				14.6	
27	21,910	18,950	86	14.5	
28				14.1	Timer Malfunction
29	12,490	10,950	88		
30	13,580	11,780	87		
31				14.0	
Sep 1	11,060	9,390	85	14.7	
2				14.6	
3	12,120	10,290	85	15.0	
4	12,880	11,500	89	15.3	Performance Analyzed
5				14.9	
6	14,350	12,410	86	15.0	Performance Analyzed
7				14.5	

COD LOADING: 6.0 g/L/day
HRT = 24 Hours (4 cycles /day)

Date	MLSS mg/l	MLVSS mg/l	Volatile %	CH4 Prod. Liters @STP	Remark
Sep 8, '91					
9					
10	14,530	13,050	90	20.5	
11				21.9	
12	14,910	13,580	91	22.9	
13				20.4	
14				21.9	
15				23.8	
16				23.2	
17	16,930	15,120	89	23.1	
18	17,710	15,930	90	23.0	
19				22.5	

REACTOR C
COD LOADING: 6.0 g/L/day
HRT = 24 Hours (4 cycles /day)

Date	MLSS mg/l	MLVSS mg/l	Volatile %	CH4 Prod. Liters @STP	Remark
Sep 20, '91				23.0	
21				23.2	
22				22.6	
23				24.0	
24	21,690	18,680	86	23.5	
25				24.0	
26	19,960	17,950	90	23.9	Performance Analyzed
27					
28				22.1	
29				22.5	
30				23.0	
Oct 1	21,250	18,860	89	22.5	Performance Analyzed
2				21.7	
3				22.6	
4	23,330	20,630	88	23.7	
5				23.2	
6	25,540	22,760	89	22.5	
7	23,500	20,370	87	22.9	Performance Analyzed
8				22.6	
9	24,970	21,580	86	23.0	Performance Analyzed

REACTOR C
COD LOADING: 8.0 g/L/day
HRT = 24 Hours (4 cycles /day)

Date	MLSS mg/l	MLVSS mg/l	Volatile %	CH4 Prod. Liters @STP	Remark
Oct 10, '91					
11				28.8	
12	24,400	21,560	88	29.0	
13	23,920	20,950	88	28.5	
14				28.5	
15				29.2	
16				28.4	
17				29.0	
18	25,000	23,190	93	28.5	Performance Analyzed
19	26,070	23,020	88	28.7	Performance Analyzed
20				29.1	
21	25,690	22,440	87	28.4	Performance Analyzed
22				33.6	COD = 10 g/L/day
23	26,110	22,560	86	36.4	
24					

REACTOR C
COD LOADING: 2.0 g/L/day
HRT = 12 Hours (6 cycles /day)

Date	MLSS mg/l	MLVSS mg/l	Volatile %	CH4 Prod. Liters @STP	Remark
Oct 25, '91					
26	25,310	22,110	87	7.7	
27				7.5	
28				7.3	
29				6.9	
30				7.0	
31				7.6	
Nov 1	24,930	21,640	87	7.3	
2				7.5	
3	25,960	22,790	88	7.5	
4				7.4	
5	22,760	19,630	86	7.2	
6	24,540	21,670	88	7.7	

REACTOR C
COD LOADING: 4.0 g/L/day
HRT = 12 Hours (6 cycles /day)

Date	MLSS mg/l	MLVSS mg/l	Volatile %	CH4 Prod. Liters @STP	Remark
Nov 7, '91					
8					
9	24,400	21,840	90	15.7	
10				15.0	
11				15.5	
12				15.0	
13	25,970	22,580	87	15.3	Performance Analyzed
14	23,160	20,080	87	15.6	Performance Analyzed
15	26,020	22,880	88	15.6	Performance Analyzed

REACTOR C
COD LOADING: 6.0 g/L/day
HRT = 12 Hours (6 cycles /day)

Date	MLSS mg/l	MLVSS mg/l	Volatile %	CH4 Prod. Liters @STP	Remark
Nov 16, '91					
17				22.7	
18					
19					
20				23.0	
21				22.5	
22				23.2	
23	27,010	23,840	88	23.0	Performance Analyzed
24	24,270	20,790	86	22.6	Performance Analyzed
25	27,510	23,660	86	22.9	Performance Analyzed

REACTOR C
COD LOADING: 8.0 g/L/day
HRT = 12 Hours (6 cycles /day)

Date	MLSS mg/l	MLVSS mg/l	Volatile %	CH4 Prod. Liters @STP	Remark
Nov 26, '91					
27				27.0	
28					
29				29.3	
30				28.4	
Dec 1				29.8	
2	29,230	25,440	87	29.1	Performance Analyzed
3	27,460	24,270	88	30.0	Performance Analyzed
4	31,190	26,940	86	29.7	Performance Analyzed
5				28.7	

REACTOR C
COD LOADING: 10.0 g/L/day
HRT = 12 Hours (6 cycles /day)

Date	MLSS mg/l	MLVSS mg/l	Volatile %	CH4 Prod. Liters @STP	Remark
Dec 6, '91					
7				39.0	
8	31,380	26,670	85	35.5	
9	30,190	25,940	86	34.9	Performance Analyzed
10				36.0	
11				34.4	
12				35.6	
13	33,665	30,100	89	35.9	Performance Analyzed
14	31,030	27,220	88	35.0	Performance Analyzed

REACTOR C
COD LOADING: 12.0 g/L/day
HRT = 12 Hours (6 cycles /day)

Date	MLSS mg/l	MLVSS mg/l	Volatile %	CH4 Prod. Liters @STP	Remark
Dec 15, '91					
16				44.2	
17	28,520	24,780	87	42.8	
18					
19				38.2	
20				41.7	
21	24,250	21,410	88	39.9	
22	25,450	22,500	88	41.9	Performance Analyzed
23	22,040	18,910	86	37.8	Performance Analyzed

LABORATORY STUDY DAILY LOG

REACTOR D
COD LOADING: 2.0 g/L/day (Start-Up Phase)
HRT = 48 Hours (4 cycles /day)

Date	MLSS mg/l	MLVSS mg/l	Volatile %	CH4 Prod. Liters @STP	Remark
Apr 18, '91	~8,500				Reactor Seeded
19					
20					
21					
22					
23					
24	9,930				
25	10,120				
26	10,470				
27					
28					
29					
30					
May 1	10,800	9,070	84		
2	10,650	9,170	86		
3					
4					
5					
6					
7	11,120	9,470	85	7.7	
8				7.1	
9	11,170	9,420	84	7.0	
10				7.0	
11					
12					
13				8.2	
14				8.0	
15	12,580	10,820	86	7.1	
16	13,530	11,550	85	7.8	
17				7.0	
18				7.0	
19				7.5	
20	13,940	11,550	83	7.6	
21				7.2	

REACTOR D
COD LOADING: 2.0 g/L/day
HRT = 48 Hours (4 cycles /day)

Date	MLSS mg/l	MLVSS mg/l	Volatile %	CH4 Prod. Liters @STP	Remark
May 22, '91	13,270			7.0	Performance Analyzed
23	12,340	10,460	85	7.5	Performance Analyzed
24				7.7	
25				7.3	
26				7.5	
27	15,220	12,820	84		
28				7.5	
29	14,710	11,920	81	7.5	Performance Analyzed
30				7.0	
31	14,930	12,250	82	7.9	

COD LOADING: 4.0 g/L/day
HRT = 48 Hours (4 cycles /day)

Date	MLSS mg/l	MLVSS mg/l	Volatile %	CH4 Prod. Liters @STP	Remark
Jun 1, '91					
2	15,340	12,880	84		
3	17,345	14,470	83	14.2	
4	19,190	16,000	83	14.5	
5	20,810	18,380	88	14.5	Performance Analyzed
6				14.3	
7				14.3	
8				15.0	
9				14.9	
10	22,740	19,430	85	15.3	Performance Analyzed
11				15.0	
12				14.4	
13	24,250	22,410	92	14.9	Performance Analyzed
14				15.0	
15				14.6	
16				15.1	
17	24,170	20,690	86	15.0	
18	27,890	24,010	86	15.2	Performance Analyzed
19				15.4	

REACTOR D
COD LOADING: 6.0 g/L/day
HRT = 48 Hours (4 cycles /day)

Date	MLSS mg/l	MLVSS mg/l	Volatile %	CH4 Prod. Liters @STP	Remark
Jun 20, '91					
21					
22	26,510	23,200	88	22.0	
23	25,350	22,170	87	24.0	
24				23.8	
25	24,980	21,640	87	23.6	Performance Analyzed
26				24.4	
27	26,900	23,490	87	23.5	Performance Analyzed
28				22.9	
29				23.2	
30				22.8	
Jul 1	27,530	24,010	87	23.4	
2	25,690	22,440	87	23.5	Performance Analyzed
3				23.3	

COD LOADING: 8.0 g/L/day
HRT = 48 Hours (4 cycles /day)

Date	MLSS mg/l	MLVSS mg/l	Volatile %	CH4 Prod. Liters @STP	Remark
Jul 4, '91					
5	29,460	25,540	87	28.8	
6					
7					
8	28,920	24,770	86	28.3	
9	27,310	23,610	86	28.4	
10				28.0	
11	29,230	25,440	87	28.4	
12				28.5	
13				28.6	
14	29,290	25,280	86	28.9	Performance Analyzed
15				29.1	
16	31,480	27,630	88	29.8	Performance Analyzed
17				29.0	
18	29,350	25,590	87	29.2	Performance Analyzed
19				33.3	COD= 10 g/L/day
20					

REACTOR D
COD LOADING: 2.0 g/L/day
HRT = 24 Hours (4 cycles /day)

Date	MLSS mg/l	MLVSS mg/l	Volatile %	CH4 Prod. Liters @STP	Remark
Jul 21, '91					
22	30,170	26,850	89	7.4	
23	29,520	25,840	88	7.7	
24				8.6	
25	31,470	28,050	89	7.9	
26	31,940	28,710	90	8.1	Performance Analyzed
27				8.0	
28	33,890	29,730	88	7.7	
29				5.9	
30	30,190	25,940	86	6.1	
31				6.0	
Aug 1	30,060	26,880	89	7.5	
2	32,540	27,720	85		
3	~20,000				Biosolids Wasted
4					
5	21,310	18,410	86	7.7	
6	19,350	16,590	86	7.0	
7	19,555	17,150	88	7.8	Performance Analyzed
8				7.5	
9	22,210	19,440	88	7.5	Performance Analyzed
10				7.1	
11				7.5	
12	21,250	18,470	87	7.9	Performance Analyzed

REACTOR D
COD LOADING: 4.0 g/L/day
HRT = 24 Hours (4 cycles /day)

Date	MLSS mg/l	MLVSS mg/l	Volatile %	CH4 Prod. Liters @STP	Remark
Aug 13, '91					
14					
15	23,640	20,770	88	14.4	
16				13.8	
17	24,530	22,420	91	13.5	
18				14.0	
19	24,670	22,180	90	14.2	Performance Analyzed
20				13.9	
21				13.5	
22					Gas Meter Calibrated
23					Mixing Flow Calibrated
24	26,910	22,860	85		
25				15.0	
26				14.9	
27	27,860	24,300	87	15.3	
28				14.1	
29	~17,000				Biosolids Wasted
30	17,210	14,830	86		
31				15.1	
Sep 1	15,350	13,320	87	14.4	
2				15.4	
3	16,780	14,900	89	14.5	
4	16,140	14,310	89	15.2	Performance Analyzed
5				15.0	
6	17,050	14,830	87	14.6	Performance Analyzed
7				14.9	

COD LOADING: 6.0 g/L/day
HRT = 24 Hours (4 cycles /day)

Date	MLSS mg/l	MLVSS mg/l	Volatile %	CH4 Prod. Liters @STP	Remark
Sep 8, '91					
9					
10	18,240	16,300	89	20.5	
11				21.9	
12	18,270	15,750	86	22.9	
13				20.4	
14				21.9	
15				23.8	
16				23.2	
17	19,850	17,250	87	23.1	
18	19,730	17,170	87	23.0	
19				22.5	

REACTOR D
COD LOADING: 6.0 g/L/day
HRT = 24 Hours (4 cycles /day)

Date	MLSS mg/l	MLVSS mg/l	Volatile %	CH4 Prod. Liters @STP	Remark
Sep 20, '91				22.5	
21				22.9	
22				24.1	
23				23.4	
24	20,540	17,930	87	23.0	
25				22.6	
26	20,765	18,815	91	23.0	Performance Analyzed
27				23.0	
28				22.5	
29				22.0	
30				23.8	
Oct 1	23,290	20,550	88	22.2	Performance Analyzed
2				22.4	
3				23.1	
4	24,850	22,220	89	23.5	
5				22.1	
6	24,560	21,910	89	22.1	
7	25,380	22,170	87	22.2	Performance Analyzed
8				23.2	
9	24,900	21,710	87	22.8	Performance Analyzed

REACTOR D
COD LOADING: 8.0 g/L/day
HRT = 24 Hours (4 cycles /day)

Date	MLSS mg/l	MLVSS mg/l	Volatile %	CH4 Prod. Liters @STP	Remark
Oct 10, '91					
11					
12	25,340	22,850	90	30.0	
13	26,540	22,750	86	25.6	
14				30.2	
15				29.8	
16				29.7	
17				30.0	
18	26,190	24,090	92	29.7	Performance Analyzed
19	27,610	23,640	86	29.0	Performance Analyzed
20				29.6	
21	28,440	24,170	85	29.6	Performance Analyzed
22				33.8	COD = 10 g/L/day
23	29,050	24,940	86	34.8	
24					

REACTOR D
COD LOADING: 2.0 g/L/day
HRT = 12 Hours (6 cycles /day)

Date	MLSS mg/l	MLVSS mg/l	Volatile %	CH4 Prod. Liters @STP	Remark
Oct 25, '91					
26	29,160	25,810	89	6.5	
27				6.0	
28				7.4	
29				5.8	
30				6.7	
31				7.5	
Nov 1	28,790	24,910	87	6.4	
2				6.5	
3	28,350	24,500	86	7.0	Performance Analyzed
4				6.5	
5	30,660	27,810	91	6.7	Performance Analyzed
6	29,930	27,070	90	6.7	Performance Analyzed

REACTOR D
COD LOADING: 4.0 g/L/day
HRT = 12 Hours (6 cycles /day)

Date	MLSS mg/l	MLVSS mg/l	Volatile %	CH4 Prod. Liters @STP	Remark
Nov 7, '91					
8					
9	32,360	29,540	91	14.6	
10				14.7	
11				15.0	
12				14.9	
13	29,440	26,735	91	15.2	Performance Analyzed
14	31,720	28,450	90	15.5	Performance Analyzed
15	30,180	26,460	88	15.8	Performance Analyzed

REACTOR D
COD LOADING: 6.0 g/L/day
HRT = 12 Hours (6 cycles /day)

Date	MLSS mg/l	MLVSS mg/l	Volatile %	CH4 Prod. Liters @STP	Remark
Nov 16, '91	~24,000				Biosolids Wasted
17	24,380			20.5	
18				21.3	
19				22.7	
20				23.0	
21				22.2	
22				22.8	
23	26,430	23,280	88	22.5	Performance Analyzed
24	25,500	22,370	88	22.4	Performance Analyzed
25	26,655	24,225	91	22.9	Performance Analyzed

REACTOR D
COD LOADING: 8.0 g/L/day
HRT = 12 Hours (6 cycles /day)

Date	MLSS mg/l	MLVSS mg/l	Volatile %	CH4 Prod. Liters @STP	Remark
Nov 26, '91					
27				29.6	
28					
29				27.1	
30				28.6	
Dec 1				28.2	
2	26,230	23,410	89	28.5	Performance Analyzed
3	29,050	26,510	91	29.0	Performance Analyzed
4	27,410	24,245	88	28.5	Performance Analyzed
5				28.7	

REACTOR D
COD LOADING: 10.0 g/L/day
HRT = 12 Hours (6 cycles /day)

Date	MLSS mg/l	MLVSS mg/l	Volatile %	CH4 Prod. Liters @STP	Remark
Dec 6, '91					
7				37.5	
8	28,660	25,200	88	36.9	
9	28,670	25,180	88	37.2	Performance Analyzed
10				37.0	
11				37.5	
12				37.0	
13	29,110	26,120	90	36.8	Performance Analyzed
14	32,460	28,810	89	36.5	Performance Analyzed

REACTOR D
COD LOADING: 12.0 g/L/day
HRT = 12 Hours (6 cycles /day)

Date	MLSS mg/l	MLVSS mg/l	Volatile %	CH4 Prod. Liters @STP	Remark
Dec 15, '91					
16				45.5	
17	30,590	27,870	91	45.2	
18					
19				40.8	
20				41.5	
21	29,130	25,930	89	40.1	
22	25,410	22,930	90	39.7	Performance Analyzed
23	28,250	25,660	91	38.0	Performance Analyzed

APPENDIX C

SIX-HOUR SETTLING TEST RESULTS

Time	1st Hour		2nd Hour		3rd Hour		4th Hour		5th Hour		6th Hour	
	Interface	Velocity	Interface	Velocity	Interface	Velocity	Interface	Velocity	Interface	Velocity	Interface	Velocity
Minutes	cm	cm/min	cm	cm/min	cm	cm/min	cm	cm/min	cm	cm/min	cm	cm/min
0.0	78.5		78.5		78.5		78.5		78.5		78.5	
2.0	76.7	0.9	77.1	0.7	74.5	2.0	75.3	1.6	74.9	1.8	74.5	2.0
4.0	75.1	0.8	75.3	0.9	71.1	1.7	71.3	2.0	71.2	1.9	71.6	1.5
6.0	72.3	1.4	73.5	0.9	68.1	1.5	68.1	1.6	67.4	1.9	67.6	2.0
8.0	69.1	1.6	71.7	0.9	64.9	1.6	64.9	1.6	63.4	2.0	63.4	2.1
10.0	66.3	1.4	70.1	0.8	61.5	1.7	61.1	1.9	59.2	2.1	59.0	2.2
12.0	63.5	1.4	68.3	0.9	57.9	1.8	57.3	1.9	55.2	2.0	54.8	2.1
14.0	60.9	1.3	66.3	1.0	54.3	1.8	53.5	1.9	51.8	1.7	51.4	1.7
16.0	58.3	1.3	64.9	0.7	51.3	1.5	50.3	1.6	49.2	1.3	48.5	1.4
18.0	55.9	1.2	62.5	1.2	49.1	1.1	47.9	1.2	47.2	1.0	46.2	1.1
20.0					47.4	0.9	46.0	0.9	45.8	0.7	45.0	0.6
22.0					46.2	0.6	44.8	0.6	44.6	0.6	44.0	0.5
24.0					45.5	0.4	43.7	0.5	43.8	0.4	43.2	0.4
26.0					44.8	0.4	43.0	0.4	43.1	0.3	42.4	0.4
29.0					43.9	0.3	42.2	0.3	42.1	0.3	41.6	0.3
32.0					43.1	0.3	42.0	0.1	41.0	0.4	40.8	0.3
35.0					42.6	0.2	41.6	0.1	40.5	0.2	40.1	0.2
40.0							41.4	0.0	39.9	0.1	39.7	0.1
45.0											39.3	0.1

Zone Settling Velocity, cm/min					
1st Hour	2nd Hour	3rd Hour	4th Hour	5th Hour	6th Hour
1.45	0.91	1.73	1.82	1.95	2.10

Operating Conditions:
Date: July 21, 1991
Reactor A
Organic Loading = 4.0 g COD/L/day
MLSS/MLVSS = 26,280/22,070 mg/L
Mixing Pattern = 5.0 min/hr
HRT = 48 hrs; Cycle Length = 6 hrs

Time	1st Hour		2nd Hour		3rd Hour		4th Hour		5th Hour		6th Hour	
	Interface	Velocity	Interface	Velocity	Interface	Velocity	Interface	Velocity	Interface	Velocity	Interface	Velocity
Minutes	cm	cm/min	cm	cm/min	cm	cm/min	cm	cm/min	cm	cm/min	cm	cm/min
0.0	78.5		78.5		78.5		78.5		78.5		78.5	
1.0	77.5	1.0	77.6	0.9	77.8	0.7	78.0	0.5	78.1	0.4	78.0	0.5
2.0	76.8	0.7	77.0	0.6	77.1	0.7	77.4	0.6	77.5	0.6	77.6	0.4
3.0	75.7	1.1	76.0	1.1	76.3	0.9	76.4	1.1	76.1	1.4	76.2	1.4
4.0	74.4	1.3	75.2	0.8	75.0	1.3	74.9	1.4	74.6	1.5	74.6	1.5
5.0	73.2	1.1	74.3	0.9	73.8	1.2	73.5	1.4	73.1	1.5	73.1	1.6
6.0	72.0	1.3	73.5	0.8	72.5	1.2	72.1	1.3	71.6	1.5	71.5	1.6
7.0	70.7	1.3	72.5	0.9	71.4	1.1	70.8	1.3	70.1	1.5	70.0	1.5
8.0	69.6	1.0	71.7	0.8	70.2	1.2	69.5	1.3	68.6	1.4	68.4	1.6
9.0	68.5	1.2			69.0	1.2	68.2	1.3	67.4	1.3	66.8	1.5
10.0	67.5	1.0			67.9	1.1	66.9	1.3	66.2	1.2	65.2	1.6
11.0	66.3	1.2			66.8	1.1			65.0	1.2	63.7	1.5
12.0					65.7	1.1	64.4	1.2	63.5	1.4	62.2	1.5
13.0					64.6	1.1			62.3	1.2	60.7	1.5
14.0							62.2	1.1	60.9	1.4	59.4	1.4
15.0									59.6	1.4	57.9	1.5
16.0							59.9	1.1	58.3	1.3	56.5	1.4
17.0									57.1	1.2	55.4	1.1
18.0							58.0	0.9	56.0	1.1	54.6	0.8
19.0									55.2	0.8	53.8	0.7
20.0									54.7	0.6	53.3	0.6
21.0												
22.0											52.6	0.4
23.0									53.5	0.4		
24.0											51.9	0.4
25.0												
26.0											51.2	0.3

Zone Settling Velocity, cm/min

1st Hour	2nd Hour	3rd Hour	4th Hour	5th Hour	6th Hour
1.17	0.88	1.20	1.33	1.45	1.54

Operating Conditions:
Date: June 17, 1991
Reactor A
Organic Loading = 4.0 g COD/L/day
MLSS/MLVSS = 19,750/17,265 mg/L
Mixing Pattern = 5.0 min/hr
HRT = 48 hrs; Cycle Length = 6 hrs

APPENDIX D

AIA DATA SUMMARY

AIA DATA SUMMARY

DATE: April 18, 1991

SAMPLE FROM: SEED BIOSOLIDS

Class Limit Particle Area (sq um)	Particle Count	Class Limit Equiv. Circular Dia. (mm)	Class Geom. Meam Diam. (mm)	Total Particle Area (sq mm)	Total Particle Volume (mm^3)	Class Partical Weight Percentage (%)	Partical Accum. Wt. Percentage (%)
4.6E+01	0	0.008					
1.0E+02	590	0.011	0.009	4.15E−02	2.62E−04	0.42	0.42
2.2E+02	982	0.017	0.014	1.51E−01	1.41E−03	2.28	2.70
4.6E+02	816	0.024	0.020	2.69E−01	3.66E−03	5.91	8.61
1.0E+03	403	0.036	0.030	2.84E−01	5.66E−03	9.13	17.74
2.2E+03	114	0.053	0.044	1.76E−01	5.19E−03	8.37	26.10
4.6E+03	40	0.077	0.065	1.32E−01	5.68E−03	9.15	35.26
1.0E+04	5	0.113	0.095	3.52E−02	2.22E−03	3.58	38.84
2.2E+04	1	0.167	0.140	1.54E−02	1.44E−03	2.32	41.16
4.6E+04	5	0.242	0.205	1.65E−01	2.25E−02	36.19	77.35
1.0E+05	1	0.357	0.299	7.04E−02	1.41E−02	22.65	100.00
		0.000	0.000	0.00E+00	0.00E+00	0.00	100.00
Total				1.34E+00	6.20E−02		

AIA DATA SUMMARY

DATE: October 22, 1991

SAMPLE FROM: REACTOR A

Class Limit Particle Area (sq um)	Particle Count	Class Limit Equiv. Circular Dia. (mm)	Class Geom. Meam Diam. (mm)	Total Particle Area (sq mm)	Total Particle Volume (mm^3)	Class Partical Weight Percentage (%)	Partical Accum. Wt. Percentage (%)
4.6E+02	0	0.024					
1.0E+03	87	0.036	0.030	6.13E−02	1.22E−03	0.02	0.02
2.2E+03	352	0.053	0.044	5.43E−01	1.60E−02	0.31	0.33
4.6E+03	298	0.077	0.065	9.81E−01	4.23E−02	0.81	1.14
1.0E+04	187	0.113	0.095	1.32E+00	8.31E−02	1.59	2.73
2.2E+04	139	0.167	0.140	2.14E+00	2.00E−01	3.82	6.55
4.6E+04	99	0.242	0.205	3.26E+00	4.45E−01	8.49	15.04
1.0E+05	54	0.357	0.299	3.80E+00	7.59E−01	14.50	29.55
2.2E+05	24	0.529	0.443	3.70E+00	1.09E+00	20.88	50.43
4.6E+05	5	0.765	0.647	1.65E+00	7.10E−01	13.57	63.99
1.0E+06	1	1.128	0.947	7.04E−01	4.44E−01	8.49	72.49
2.2E+06	1	1.674	1.401	1.54E+00	1.44E+00	27.51	100.00
Total				1.97E+01	5.23E+00		

SAMPLE FROM: REACTOR B

1.0E+02	0	0.011					
2.2E+02	6	0.017	0.014	9.25E−04	8.64E−06	0.00	0.00
4.6E+02	11	0.024	0.020	3.62E−03	4.94E−05	0.00	0.00
1.0E+03	31	0.036	0.030	2.18E−02	4.36E−04	0.02	0.02
2.2E+03	74	0.053	0.044	1.14E−01	3.37E−03	0.16	0.19
4.6E+03	85	0.077	0.065	2.80E−01	1.21E−02	0.58	0.77
1.0E+04	146	0.113	0.095	1.03E+00	6.49E−02	3.12	3.89
2.2E+04	88	0.167	0.140	1.36E+00	1.27E−01	6.10	9.99
4.6E+04	41	0.242	0.205	1.35E+00	1.84E−01	8.86	18.86
1.0E+05	41	0.357	0.299	2.89E+00	5.76E−01	27.75	46.60
2.2E+05	15	0.529	0.443	2.31E+00	6.83E−01	32.89	79.49
4.6E+05	3	0.765	0.647	9.87E−01	4.26E−01	20.51	100.00
Total				1.03E+01	2.08E+00		

DATE: October 22, 1991

SAMPLE FROM: REACTOR C

Class Limit Particle Area (sq um)	Particle Count	Class Limit Equiv. Circular Dia. (mm)	Class Geom. Meam Diam. (mm)	Total Particle Area (sq mm)	Total Particle Volume (mm^3)	Class Partical Weight Percentage (%)	Partical Accum. Wt. Percentage (%)
4.6E+01	0	0.008					
1.0E+02	1	0.011	0.009	7.04E−05	4.44E−07	0.00	0.00
2.2E+02	0	0.017	0.014	0.00E+00	0.00E+00	0.00	0.00
4.6E+02	0	0.024	0.020	0.00E+00	0.00E+00	0.00	0.00
1.0E+03	15	0.036	0.030	1.06E−02	2.11E−04	0.01	0.01
2.2E+03	71	0.053	0.044	1.09E−01	3.23E−03	0.12	0.12
4.6E+03	72	0.077	0.065	2.37E−01	1.02E−02	0.37	0.49
1.0E+04	60	0.113	0.095	4.22E−01	2.67E−02	0.96	1.46
2.2E+04	133	0.167	0.140	2.05E+00	1.92E−01	6.91	8.37
4.6E+04	184	0.242	0.205	6.05E+00	8.26E−01	29.82	38.19
1.0E+05	66	0.357	0.299	4.65E+00	9.28E−01	33.48	71.67
2.2E+05	11	0.529	0.443	1.70E+00	5.01E−01	18.08	89.75
4.6E+05	2	0.765	0.647	6.58E−01	2.84E−01	10.25	100.00
Total				1.59E+01	2.77E+00		

SAMPLE FROM: REACTOR D

4.6E+01	0	0.008					
1.0E+02	4	0.011	0.009	2.82E−04	1.78E−06	0.00	0.00
2.2E+02	18	0.017	0.014	2.77E−03	2.59E−05	0.00	0.00
4.6E+02	23	0.024	0.020	7.57E−03	1.03E−04	0.00	0.00
1.0E+03	60	0.036	0.030	4.22E−02	8.43E−04	0.03	0.03
2.2E+03	159	0.053	0.044	2.45E−01	7.24E−03	0.25	0.29
4.6E+03	209	0.077	0.065	6.88E−01	2.97E−02	1.04	1.33
1.0E+04	182	0.113	0.095	1.28E+00	8.09E−02	2.84	4.18
2.2E+04	116	0.167	0.140	1.79E+00	1.67E−01	5.87	10.05
4.6E+04	94	0.242	0.205	3.09E+00	4.22E−01	14.84	24.89
1.0E+05	67	0.357	0.299	4.72E+00	9.42E−01	33.11	58.00
2.2E+05	20	0.529	0.443	3.08E+00	9.11E−01	32.02	90.02
4.6E+05	2	0.765	0.647	6.58E−01	2.84E−01	9.98	100.00
Total				1.56E+01	2.84E+00		

AIA DATA SUMMARY

DATE: November 27, 1991

SAMPLE FROM: REACTOR A

Class Limit Particle Area (sq um)	Particle Count	Class Limit Equiv. Circular Dia. (mm)	Class Geom. Meam Diam. (mm)	Total Particle Area (sq mm)	Total Particle Volume (mm ^ 3)	Class Partical Weight Percentage (%)	Partical Accum. Wt. Percentage (%)
2.2E+02	0	0.017					
4.6E+02	2	0.024	0.020	6.58E−04	8.98E−06	0.00	0.00
1.0E+03	214	0.036	0.030	1.51E−01	3.01E−03	0.02	0.02
2.2E+03	318	0.053	0.044	4.90E−01	1.45E−02	0.11	0.14
4.6E+03	290	0.077	0.065	9.54E−01	4.12E−02	0.32	0.46
1.0E+04	118	0.113	0.095	8.31E−01	5.24E−02	0.41	0.87
2.2E+04	40	0.167	0.140	6.17E−01	5.76E−02	0.45	1.31
4.6E+04	19	0.242	0.205	6.25E−01	8.53E−02	0.66	1.98
1.0E+05	21	0.357	0.299	1.48E+00	2.95E−01	2.30	4.28
2.2E+05	32	0.529	0.443	4.93E+00	1.46E+00	11.34	15.62
4.6E+05	31	0.765	0.647	1.02E+01	4.40E+00	34.27	49.89
1.0E+06	8	1.128	0.947	5.63E+00	3.56E+00	27.68	77.58
2.2E+06	2	1.674	1.401	3.08E+00	2.88E+00	22.42	100.00
Total				2.90E+01	1.28E+01		

SAMPLE FROM: REACTOR B

2.2E+02	0	0.017					
4.6E+02	1	0.024	0.020	3.29E−04	4.49E−06	0.00	0.00
1.0E+03	113	0.036	0.030	7.96E−02	1.59E−03	0.02	0.02
2.2E+03	149	0.053	0.044	2.30E−01	6.78E−03	0.08	0.09
4.6E+03	97	0.077	0.065	3.19E−01	1.38E−02	0.15	0.25
1.0E+04	58	0.113	0.095	4.08E−01	2.58E−02	0.29	0.53
2.2E+04	35	0.167	0.140	5.40E−01	5.04E−02	0.56	1.09
4.6E+04	27	0.242	0.205	8.88E−01	1.21E−01	1.34	2.43
1.0E+05	96	0.357	0.299	6.76E+00	1.35E+00	14.95	17.39
2.2E+05	49	0.529	0.443	7.55E+00	2.23E+00	24.72	42.11
4.6E+05	11	0.765	0.647	3.62E+00	1.56E+00	17.31	59.42
1.0E+06	5	1.128	0.947	3.52E+00	2.22E+00	24.63	84.04
2.2E+06	1	1.674	1.401	1.54E+00	1.44E+00	15.96	100.00
Total				2.55E+01	9.02E+00		

DATE: November 27, 1991

SAMPLE FROM: REACTOR C

Class Limit Particle Area (sq um)	Particle Count	Class Limit Equiv. Circular Dia. (mm)	Class Geom. Meam Diam. (mm)	Total Particle Area (sq mm)	Total Particle Volume (mm^3)	Class Partical Weight Percentage (%)	Partical Accum. Wt. Percentage (%)
4.6E+02	0	0.024					
1.0E+03	87	0.036	0.030	6.13E−02	1.22E−03	0.02	0.02
2.2E+03	117	0.053	0.044	1.80E−01	5.33E−03	0.07	0.08
4.6E+03	85	0.077	0.065	2.80E−01	1.21E−02	0.15	0.24
1.0E+04	62	0.113	0.095	4.37E−01	2.76E−02	0.35	0.58
2.2E+04	62	0.167	0.140	9.56E−01	8.93E−02	1.13	1.71
4.6E+04	72	0.242	0.205	2.37E+00	3.23E−01	4.09	5.80
1.0E+05	166	0.357	0.299	1.17E+01	2.33E+00	29.49	35.29
2.2E+05	25	0.529	0.443	3.85E+00	1.14E+00	14.39	49.67
4.6E+05	3	0.765	0.647	9.87E−01	4.26E−01	5.38	55.06
1.0E+06	8	1.128	0.947	5.63E+00	3.56E+00	44.94	100.00
Total				2.64E+01	7.91E+00		

SAMPLE FROM: REACTOR D

4.6E+02	0	0.024					
1.0E+03	35	0.036	0.030	2.46E−02	4.92E−04	0.01	0.01
2.2E+03	58	0.053	0.044	8.94E−02	2.64E−03	0.05	0.05
4.6E+03	60	0.077	0.065	1.97E−01	8.52E−03	0.15	0.20
1.0E+04	68	0.113	0.095	4.79E−01	3.02E−02	0.53	0.73
2.2E+04	111	0.167	0.140	1.71E+00	1.60E−01	2.79	3.52
4.6E+04	138	0.242	0.205	4.54E+00	6.20E−01	10.83	14.35
1.0E+05	117	0.357	0.299	8.24E+00	1.64E+00	28.74	43.09
2.2E+05	20	0.529	0.443	3.08E+00	9.11E−01	15.91	59.01
4.6E+05	4	0.765	0.647	1.32E+00	5.68E−01	9.93	68.93
1.0E+06	4	1.128	0.947	2.82E+00	1.78E+00	31.07	100.00
Total				2.25E+01	5.72E+00		

AIA DATA SUMMARY

DATE: November 30, 1991

SAMPLE FROM: REACTOR A

Class Limit Particle Area (sq um)	Particle Count	Class Limit Equiv. Circular Dia. (mm)	Class Geom. Meam Diam. (mm)	Total Particle Area (sq mm)	Total Particle Volume (mm^3)	Class Partical Weight Percentage (%)	Partical Accum. Wt. Percentage (%)
2.2E+02	3	0.017	0.008	1.65E−04	9.21E−07	0.00	0.00
4.6E+02	8	0.024	0.020	2.63E−03	3.59E−05	0.00	0.00
1.0E+03	16	0.036	0.030	1.13E−02	2.25E−04	0.00	0.00
2.2E+03	31	0.053	0.044	4.78E−02	1.41E−03	0.02	0.03
4.6E+03	17	0.077	0.065	5.59E−02	2.41E−03	0.04	0.06
1.0E+04	25	0.113	0.095	1.76E−01	1.11E−02	0.18	0.24
2.2E+04	18	0.167	0.140	2.77E−01	2.59E−02	0.41	0.65
4.6E+04	21	0.242	0.205	6.91E−01	9.43E−02	1.50	2.15
1.0E+05	23	0.357	0.299	1.62E+00	3.23E−01	5.13	7.28
2.2E+05	14	0.529	0.443	2.16E+00	6.37E−01	10.12	17.39
4.6E+05	14	0.765	0.647	4.61E+00	1.99E+00	31.55	48.94
1.0E+06	4	1.128	0.947	2.82E+00	1.78E+00	28.21	77.15
2.2E+06	1	1.674	1.401	1.54E+00	1.44E+00	22.85	100.00
Total				1.40E+01	6.30E+00		

SAMPLE FROM: REACTOR B

1.0E+02	0	0.011					
2.2E+02	1	0.017	0.014	1.54E−04	1.44E−06	0.00	0.00
4.6E+02	18	0.024	0.020	5.92E−03	8.08E−05	0.00	0.00
1.0E+03	24	0.036	0.030	1.69E−02	3.37E−04	0.01	0.01
2.2E+03	41	0.053	0.044	6.32E−02	1.87E−03	0.03	0.04
4.6E+03	42	0.077	0.065	1.38E−01	5.96E−03	0.09	0.13
1.0E+04	127	0.113	0.095	8.94E−01	5.64E−02	0.88	1.00
2.2E+04	328	0.167	0.140	5.06E+00	4.72E−01	7.33	8.33
4.6E+04	183	0.242	0.205	6.02E+00	8.22E−01	12.75	21.09
1.0E+05	68	0.357	0.299	4.79E+00	9.56E−01	14.83	35.92
2.2E+05	13	0.529	0.443	2.00E+00	5.92E−01	9.19	45.11
4.6E+05	3	0.765	0.647	9.87E−01	4.26E−01	6.61	51.72
1.0E+06	7	1.128	0.947	4.93E+00	3.11E+00	48.28	100.00
Total				2.49E+01	6.44E+00		

DATE: November 30, 1991

SAMPLE FROM: REACTOR C

Class Limit Particle Area (sq um)	Particle Count	Class Limit Equiv. Circular Dia. (mm)	Class Geom. Meam Diam. (mm)	Total Particle Area (sq mm)	Total Particle Volume (mm^3)	Class Partical Weight Percentage (%)	Partical Accum. Wt. Percentage (%)
1.0E+02	0	0.011					
2.2E+02	1	0.017	0.014	1.54E−04	1.44E−06	0.00	0.00
4.6E+02	43	0.024	0.020	1.41E−02	1.93E−04	0.00	0.00
1.0E+03	80	0.036	0.030	5.63E−02	1.12E−03	0.02	0.03
2.2E+03	109	0.053	0.044	1.68E−01	4.96E−03	0.11	0.13
4.6E+03	58	0.077	0.065	1.91E−01	8.24E−03	0.17	0.31
1.0E+04	38	0.113	0.095	2.68E−01	1.69E−02	0.36	0.67
2.2E+04	42	0.167	0.140	6.47E−01	6.05E−02	1.28	1.95
4.6E+04	71	0.242	0.205	2.34E+00	3.19E−01	6.77	8.71
1.0E+05	74	0.357	0.299	5.21E+00	1.04E+00	22.07	30.78
2.2E+05	17	0.529	0.443	2.62E+00	7.74E−01	16.43	47.21
4.6E+05	5	0.765	0.647	1.65E+00	7.10E−01	15.07	62.28
1.0E+06	4	1.128	0.947	2.82E+00	1.78E+00	37.72	100.00
Total				1.60E+01	4.71E+00		

SAMPLE FROM: REACTOR D

2.2E+02	0	0.017					
4.6E+02	40	0.024	0.020	1.32E−02	1.80E−04	0.00	0.00
1.0E+03	72	0.036	0.030	5.07E−02	1.01E−03	0.01	0.02
2.2E+03	165	0.053	0.044	2.54E−01	7.51E−03	0.11	0.12
4.6E+03	143	0.077	0.065	4.71E−01	2.03E−02	0.29	0.41
1.0E+04	227	0.113	0.095	1.60E+00	1.01E−01	1.44	1.86
2.2E+04	207	0.167	0.140	3.19E+00	2.98E−01	4.26	6.11
4.6E+04	170	0.242	0.205	5.59E+00	7.63E−01	10.90	17.02
1.0E+05	103	0.357	0.299	7.25E+00	1.45E+00	20.68	37.69
2.2E+05	15	0.529	0.443	2.31E+00	6.83E−01	9.76	47.45
4.6E+05	4	0.765	0.647	1.32E+00	5.68E−01	8.11	55.56
1.0E+06	7	1.128	0.947	4.93E+00	3.11E+00	44.44	100.00
Total				2.70E+01	7.00E+00		

AIA DATA SUMMARY

DATE: January 03, 1992

SAMPLE FROM: REACTOR A

Class Limit Particle Area (sq um)	Particle Count	Class Limit Equiv. Circular Dia. (mm)	Class Geom. Meam Diam. (mm)	Total Particle Area (sq mm)	Total Particle Volume (mm^3)	Class Partical Weight Percentage (%)	Partical Accum. Wt. Percentage (%)
4.6E+02	0	0.024					
1.0E+03	21	0.036	0.030	1.48E−02	2.95E−04	0.00	0.00
2.2E+03	50	0.053	0.044	7.71E−02	2.28E−03	0.01	0.01
4.6E+03	35	0.077	0.065	1.15E−01	4.97E−03	0.02	0.02
1.0E+04	28	0.113	0.095	1.97E−01	1.24E−02	0.04	0.07
2.2E+04	15	0.167	0.140	2.31E−01	2.16E−02	0.07	0.14
4.6E+04	13	0.242	0.205	4.28E−01	5.84E−02	0.19	0.33
1.0E+05	13	0.357	0.299	9.15E−01	1.83E−01	0.60	0.93
2.2E+05	30	0.529	0.443	4.62E+00	1.37E+00	4.50	5.43
4.6E+05	28	0.765	0.647	9.21E+00	3.98E+00	13.09	18.52
1.0E+06	33	1.128	0.947	2.32E+01	1.47E+01	48.29	66.81
2.2E+06	7	1.674	1.401	1.08E+01	1.01E+01	33.19	100.00
Total				4.98E+01	3.04E+01		

SAMPLE FROM: REACTOR B

4.6E+02	0	0.024					
1.0E+03	12	0.036	0.030	8.45E−03	1.69E−04	0.00	0.00
2.2E+03	38	0.053	0.044	5.86E−02	1.73E−03	0.01	0.01
4.6E+03	41	0.077	0.065	1.35E−01	5.82E−03	0.03	0.04
1.0E+04	33	0.113	0.095	2.32E−01	1.47E−02	0.08	0.13
2.2E+04	26	0.167	0.140	4.01E−01	3.74E−02	0.22	0.35
4.6E+04	37	0.242	0.205	1.22E+00	1.66E−01	0.96	1.31
1.0E+05	56	0.357	0.299	3.94E+00	7.87E−01	4.55	5.85
2.2E+05	87	0.529	0.443	1.34E+01	3.96E+00	22.89	28.74
4.6E+05	29	0.765	0.647	9.54E+00	4.12E+00	23.80	52.54
1.0E+06	12	1.128	0.947	8.45E+00	5.33E+00	30.82	83.36
2.2E+06	2	1.674	1.401	3.08E+00	2.88E+00	16.64	100.00
Total				4.05E+01	1.73E+01		

DATE: January 03, 1992

SAMPLE FROM: REACTOR C

Class Limit Particle Area (sq um)	Particle Count	Class Limit Equiv. Circular Dia. (mm)	Class Geom. Meam Diam. (mm)	Total Particle Area (sq mm)	Total Particle Volume (mm^3)	Class Partical Weight Percentage (%)	Partical Accum. Wt. Percentage (%)
4.6E+02	0	0.024					
1.0E+03	11	0.036	0.030	7.75E-03	1.55E-04	0.00	0.00
2.2E+03	13	0.053	0.044	2.00E-02	5.92E-04	0.00	0.01
4.6E+03	22	0.077	0.065	7.24E-02	3.12E-03	0.02	0.03
1.0E+04	28	0.113	0.095	1.97E-01	1.24E-02	0.09	0.12
2.2E+04	32	0.167	0.140	4.93E-01	4.61E-02	0.35	0.48
4.6E+04	38	0.242	0.205	1.25E+00	1.71E-01	1.30	1.78
1.0E+05	42	0.357	0.299	2.96E+00	5.90E-01	4.50	6.27
2.2E+05	77	0.529	0.443	1.19E+01	3.51E+00	26.72	32.99
4.6E+05	26	0.765	0.647	8.56E+00	3.69E+00	28.13	61.12
1.0E+06	5	1.128	0.947	3.52E+00	2.22E+00	16.93	78.06
2.2E+06	2	1.674	1.401	3.08E+00	2.88E+00	21.94	100.00
Total				3.20E+01	1.31E+01		

SAMPLE FROM: REACTOR D

4.6E+02	0	0.024					
1.0E+03	15	0.036	0.030	1.06E-02	2.11E-04	0.00	0.00
2.2E+03	23	0.053	0.044	3.55E-02	1.05E-03	0.01	0.01
4.6E+03	18	0.077	0.065	5.92E-02	2.56E-03	0.02	0.03
1.0E+04	14	0.113	0.095	9.86E-02	6.22E-03	0.05	0.08
2.2E+04	13	0.167	0.140	2.00E-01	1.87E-02	0.15	0.23
4.6E+04	15	0.242	0.205	4.94E-01	6.74E-02	0.53	0.76
1.0E+05	32	0.357	0.299	2.25E+00	4.50E-01	3.54	4.30
2.2E+05	95	0.529	0.443	1.46E+01	4.33E+00	34.09	38.39
4.6E+05	23	0.765	0.647	7.57E+00	3.27E+00	25.74	64.13
1.0E+06	7	1.128	0.947	4.93E+00	3.11E+00	24.52	88.65
2.2E+06	1	1.674	1.401	1.54E+00	1.44E+00	11.35	100.00
Total				3.18E+01	1.27E+01		

AIA DATA SUMMARY

DATE: February 22, 1992

SAMPLE FROM: REACTOR A

Class Limit Particle Area (sq um)	Particle Count	Class Limit Equiv. Circular Dia. (mm)	Class Geom. Meam Diam. (mm)	Total Particle Area (sq mm)	Total Particle Volume (mm^3)	Class Partical Weight Percentage (%)	Partical Accum. Wt. Percentage (%)
2.2E+02	0	0.017					
4.6E+02	1	0.024	0.020	3.29E−04	4.49E−06	0.00	0.00
1.0E+03	21	0.036	0.030	1.48E−02	2.95E−04	0.00	0.00
2.2E+03	22	0.053	0.044	3.39E−02	1.00E−03	0.00	0.00
4.6E+03	25	0.077	0.065	8.23E−02	3.55E−03	0.00	0.00
1.0E+04	28	0.113	0.095	1.97E−01	1.24E−02	0.01	0.02
2.2E+04	6	0.167	0.140	9.25E−02	8.64E−03	0.01	0.03
4.6E+04	3	0.242	0.205	9.87E−02	1.35E−02	0.01	0.04
1.0E+05	6	0.357	0.299	4.22E−01	8.43E−02	0.08	0.12
2.2E+05	7	0.529	0.443	1.08E+00	3.19E−01	0.32	0.44
4.6E+05	15	0.765	0.647	4.94E+00	2.13E+00	2.12	2.56
1.0E+06	55	1.128	0.947	3.87E+01	2.44E+01	24.34	26.90
2.2E+06	19	1.674	1.401	2.93E+01	2.74E+01	27.24	54.13
4.6E+06	4	2.420	2.047	1.32E+01	1.80E+01	17.88	72.02
1.0E+07	2	3.568	2.994	1.41E+01	2.81E+01	27.98	100.00
Total				1.02E+02	1.00E+02		

SAMPLE FROM: REACTOR B

4.6E+02	0	0.024					
1.0E+03	18	0.036	0.030	1.27E−02	2.53E−04	0.00	0.00
2.2E+03	24	0.053	0.044	3.70E−02	1.09E−03	0.00	0.00
4.6E+03	20	0.077	0.065	6.58E−02	2.84E−03	0.01	0.01
1.0E+04	17	0.113	0.095	1.20E−01	7.56E−03	0.02	0.03
2.2E+04	21	0.167	0.140	3.24E−01	3.02E−02	0.07	0.10
4.6E+04	14	0.242	0.205	4.61E−01	6.29E−02	0.14	0.24
1.0E+05	21	0.357	0.299	1.48E+00	2.95E−01	0.68	0.92
2.2E+05	70	0.529	0.443	1.08E+01	3.19E+00	7.30	8.22
4.6E+05	97	0.765	0.647	3.19E+01	1.38E+01	31.55	39.77
1.0E+06	26	1.128	0.947	1.83E+01	1.16E+01	26.47	66.24
2.2E+06	4	1.674	1.401	6.17E+00	5.76E+00	13.19	79.43
4.6E+06	2	2.420	2.047	6.58E+00	8.98E+00	20.57	100.00
Total				7.63E+01	4.37E+01		

DATE: February 22, 1992

SAMPLE FROM: REACTOR C

Class Limit Particle Area (sq um)	Particle Count	Class Limit Equiv. Circular Dia. (mm)	Class Geom. Meam Diam. (mm)	Total Particle Area (sq mm)	Total Particle Volume (mm^3)	Class Partical Weight Percentage (%)	Partical Accum. Wt. Percentage (%)
2.2E+02	0	0.017					
4.6E+02	1	0.024	0.020	3.29E−04	4.49E−06	0.00	0.00
1.0E+03	60	0.036	0.030	4.22E−02	8.43E−04	0.00	0.00
2.2E+03	113	0.053	0.044	1.74E−01	5.15E−03	0.02	0.02
4.6E+03	78	0.077	0.065	2.57E−01	1.11E−02	0.05	0.07
1.0E+04	59	0.113	0.095	4.15E−01	2.62E−02	0.11	0.18
2.2E+04	52	0.167	0.140	8.02E−01	7.49E−02	0.30	0.48
4.6E+04	40	0.242	0.205	1.32E+00	1.80E−01	0.73	1.21
1.0E+05	41	0.357	0.299	2.89E+00	5.76E−01	2.35	3.56
2.2E+05	74	0.529	0.443	1.14E+01	3.37E+00	13.72	17.28
4.6E+05	79	0.765	0.647	2.60E+01	1.12E+01	45.67	62.94
1.0E+06	14	1.128	0.947	9.86E+00	6.22E+00	25.33	88.28
2.2E+06	2	1.674	1.401	3.08E+00	2.88E+00	11.72	100.00
Total				5.62E+01	2.46E+01		

SAMPLE FROM: REACTOR D

4.6E+02	0	0.024					
1.0E+03	44	0.036	0.030	3.10E−02	6.18E−04	0.00	0.00
2.2E+03	84	0.053	0.044	1.29E−01	3.82E−03	0.02	0.02
4.6E+03	83	0.077	0.065	2.73E−01	1.18E−02	0.05	0.07
1.0E+04	75	0.113	0.095	5.28E−01	3.33E−02	0.14	0.21
2.2E+04	63	0.167	0.140	9.71E−01	9.07E−02	0.39	0.61
4.6E+04	69	0.242	0.205	2.27E+00	3.10E−01	1.34	1.94
1.0E+05	71	0.357	0.299	5.00E+00	9.98E−01	4.31	6.25
2.2E+05	68	0.529	0.443	1.05E+01	3.10E+00	13.37	19.62
4.6E+05	60	0.765	0.647	1.97E+01	8.52E+00	36.78	56.40
1.0E+06	13	1.128	0.947	9.15E+00	5.78E+00	24.95	81.35
2.2E+06	3	1.674	1.401	4.62E+00	4.32E+00	18.65	100.00
Total				5.32E+01	2.32E+01		

APPENDIX E

MIXING STUDY DATA SUMMARY

ASBR Performance at Various Mixing Patterns

DATE: Dec 17, 1991
Mixing Pattern: 2.5 Min. Mixing / 30 Min. Cycle
Methane Content: Reactor A = 61.4 %; Reactor B = 62.4 %
Barometer Reading: 747.0 mm Hg Temp. = 35 Deg. C

Time	Biogas Meter Reading		Methane Production		Methane Prod. Rate		Equiv. Methane COD		Measured SCOD	
	Reactor A Liter	Reactor B Liter	Reactor A Liter	Reactor B Liter	Reactor A L/hr	Reactor B L/hr	Reactor A mg/L	Reactor B mg/L	Reactor A mg/L	Reactor B mg/L
0.00	73.97	6.58							101	95
0.25	74.13	6.75	0.09	0.09	0.34	0.37	20	22	1,525	1,525
0.50	74.89	7.68	0.49	0.60	1.63	2.02	117	142	796	789
0.75	75.84	8.64	1.00	1.12	2.03	2.09	238	267		
1.00	77.25	9.80	1.75	1.75	3.02	2.52	418	417	546	506
1.25	78.01	10.85	2.16	2.32	1.63	2.28	515	553		
1.50	78.81	11.81	2.59	2.84	1.71	2.09	616	677	309	345
1.75	79.41	12.56	2.91	3.25	1.28	1.63	693	774		
2.00	80.15	13.27	3.31	3.64	1.58	1.54	787	866	204	198
2.25	80.59	13.69	3.54	3.87	0.94	0.91	843	920		
2.50	81.09	14.13	3.81	4.10	1.07	0.96	907	977	144	121
3.00	81.81	14.90	4.19	4.52	0.77	0.84	999	1077	115	87
3.50	82.48	15.57	4.55	4.89	0.72	0.73	1084	1164	108	88
4.00	83.08	16.17	4.87	5.21	0.64	0.65	1160	1241	110	72
4.50	83.63	16.72	5.17	5.51	0.59	0.60	1230	1312	103	76
5.00	84.13	17.24	5.43	5.80	0.53	0.57	1294	1380	110	99
5.50	84.62	17.76	5.70	6.08	0.52	0.57	1356	1447	106	77
6.00	84.95	18.10	5.87	6.26	0.35	0.37	1398	1491	101	95

DATE: Dec 18, 1991
Mixing Pattern: 5.0 Min. Mixing / Hour Cycle
Methane Content: Reactor A = 61.0 %; Reactor B = 62.1 %
Barometer Reading: 748.8 mm Hg Temp. = 35 Deg. C

Time	Biogas Meter Reading		Methane Production		Methane Prod. Rate		Equiv. Methane COD		Measured SCOD	
	Reactor A Liter	Reactor B Liter	Reactor A Liter	Reactor B Liter	Reactor A L/hr	Reactor B L/hr	Reactor A mg/L	Reactor B mg/L	Reactor A mg/L	Reactor B mg/L
0.00	17.62	51.58							103	82
0.25	17.79	51.75	0.09	0.09	0.36	0.37	22	22	1,535	1,535
0.50	18.83	52.88	0.64	0.71	2.22	2.45	153	168	790	847
0.75	19.76	53.77	1.14	1.19	1.98	1.93	271	283		
1.00	20.92	54.77	1.76	1.73	2.47	2.17	419	412	521	540
1.25	21.87	55.71	2.26	2.24	2.02	2.04	539	533		
1.50	23.00	56.92	2.87	2.90	2.41	2.62	682	690	342	319
1.75	23.38	57.59	3.07	3.26	0.81	1.45	731	776		
2.00	23.78	58.11	3.28	3.54	0.85	1.13	781	843	216	175
2.25	24.15	58.50	3.48	3.75	0.79	0.85	828	894		
2.50	24.84	59.20	3.85	4.13	1.47	1.52	916	984	134	167
3.00	25.44	59.88	4.17	4.50	0.64	0.74	992	1072	143	131
3.25	25.69	60.19	4.30	4.67	0.53	0.67	1024	1112		
3.50	26.34	60.84	4.65	5.02	1.39	1.41	1106	1196	127	105
4.00	26.69	61.34	4.83	5.29	0.37	0.54	1150	1260	113	97
4.25	26.93	61.55	4.96	5.41	0.51	0.46	1181	1287		
4.50	27.48	62.07	5.25	5.69	1.17	1.13	1251	1355	103	91
5.00	27.87	62.51	5.46	5.93	0.42	0.48	1300	1411	100	97
5.50	28.57	63.27	5.83	6.34	0.75	0.82	1389	1509	95	106
6.00	28.90	63.62	6.01	6.53	0.35	0.38	1431	1555	103	82

ASBR Performance at Various Mixing Patterns

DATE: Dec 19, 1991
Mixing Pattern: 100 Sec. Mixing / 20 Min. Cycle
Methane Content: Reactor A = 61.0 %; Reactor B = 61.4 %
Barometer Reading: 737.0 mm Hg Temp. = 35 Deg. C

Time	Biogas Meter Reading		Methane Production		Methane Prod. Rate		Equiv. Methane COD		Measured SCOD	
	Reactor A Liter	Reactor B Liter	Reactor A Liter	Reactor B Liter	Reactor A L/hr	Reactor B L/hr	Reactor A mg/L	Reactor B mg/L	Reactor A mg/L	Reactor B mg/L
0.00	61.59	96.58							93	84
0.25	61.70	96.70	0.06	0.06	0.23	0.25	14	15	1,518	1,518
0.50	62.49	97.71	0.47	0.60	1.66	2.13	112	142	752	873
0.75	63.68	98.66	1.10	1.10	2.50	2.01	261	261		
1.00	64.72	99.73	1.64	1.66	2.18	2.26	391	396	474	520
1.33	66.03	101.17	2.33	2.42	2.06	2.28	554	577		
1.67	67.07	102.34	2.87	3.04	1.64	1.85	684	724	394@1.5hr	400@1.5hr
2.00	67.92	103.26	3.32	3.53	1.34	1.46	790	839	197	175
2.33	68.60	103.93	3.68	3.88	1.07	1.06	875	924		
2.67	69.19	104.58	3.98	4.22	0.93	1.03	949	1005	153@2.5hr	151@2.5hr
3.00	69.70	105.12	4.25	4.51	0.80	0.85	1012	1073	128	122
3.50	70.34	105.84	4.59	4.89	0.67	0.76	1092	1164	121	112
4.00	70.98	106.54	4.92	5.26	0.67	0.74	1172	1252	93	93
4.50	71.55	107.10	5.22	5.55	0.60	0.59	1243	1322	84	90
5.00	72.06	107.70	5.49	5.87	0.53	0.63	1307	1397	86	99
5.50	72.54	108.20	5.74	6.13	0.50	0.53	1367	1460	87	112
6.00	72.76	108.43	5.86	6.25	0.23	0.24	1394	1489	93	84

DATE: Dec 20, 1991
Mixing Pattern: Continuous Mixing
Methane Content: Reactor A = 60.5 %; Reactor B = 60.3 %
Barometer Reading: 737.2 mm Hg Temp. = 35 Deg. C

Time	Biogas Meter Reading		Methane Production		Methane Prod. Rate		Equiv. Methane COD		Measured SCOD	
	Reactor A Liter	Reactor B Liter	Reactor A Liter	Reactor B Liter	Reactor A L/hr	Reactor B L/hr	Reactor A mg/L	Reactor B mg/L	Reactor A mg/L	Reactor B mg/L
0.00	7.07	41.36							84	101
0.25	7.13	41.45	0.03	0.05	0.12	0.19	7	11	1,512	1,512
0.50	8.22	42.27	0.60	0.47	2.27	1.70	142	112	615	800
0.75	9.82	43.32	1.43	1.02	3.33	2.18	341	242		
1.00	10.96	44.89	2.02	1.83	2.37	3.26	482	436	341	467
1.33	12.33	46.09	2.74	2.45	2.14	1.87	651	584		
1.67	13.39	47.06	3.29	2.96	1.65	1.51	783	704	201@1.5hr	283@1.5hr
2.00	14.15	47.92	3.68	3.40	1.19	1.34	877	810	116	171
2.33	14.65	48.65	3.94	3.78	0.78	1.14	939	900		
2.67	15.07	49.14	4.16	4.03	0.66	0.76	991	960	64@2.5hr	125@2.5hr
3.00	15.42	49.58	4.34	4.26	0.55	0.68	1034	1015	68	82
3.50	16.00	50.19	4.65	4.58	0.60	0.63	1106	1090	75	79
4.00	16.40	50.68	4.85	4.83	0.42	0.51	1156	1150	66	76
4.50	16.89	51.16	5.11	5.08	0.51	0.50	1216	1210	80	82
5.00	17.28	51.56	5.31	5.29	0.41	0.41	1264	1259	71	72
5.50	17.59	51.85	5.47	5.44	0.32	0.30	1303	1295	83	93
6.00	17.74	52.04	5.55	5.54	0.16	0.20	1321	1318	84	101

APPENDIX F

ASBR MODELING PROGRAMS

```
10 CLS
20 '
30 '       *****  ASBR MODELING PROGRAM  *****
40 '       *****  The  Monod  Kinetics   *****
50 DEFDBL A-H, O-Z
60 DEFINT I-N
70 LOCATE 5,6:PRINT "*******    INPUT  FOLLOWING  PARAMETERS    *******"
80 LOCATE 7,6: INPUT "  Reactor  Working  Volume  in  gal       ";V
90 LOCATE 8,6: INPUT "  'FEED'  Volume  per  Cycle  in  gal     ";VF
100 LOCATE 9,6: INPUT "  'FEED'  Flow  Rate  in  gpm             ";Q
110 LOCATE 10,6: INPUT "  Influent  COD  in  mg/L                ";SO
120 LOCATE 11,6: INPUT "  Expected  Effluent  SCOD  in  mg/L     ";SE
130 LOCATE 12,6: INPUT "  Active  Biomass  ( MLVSS ) in mg/L     ";X
140 LOCATE 13,6: INPUT "  Half Saturation Constant in mg/L       ";CKS
150 LOCATE 14,6: INPUT "  Max. Substrate Utilization Rate in 1/day";CK
160 '    ****   END OF PARAMETERS INPUT   ****
170 LPRINT:LPRINT "*****    A S B R    D E S I G N    M O D E L    *****"
180 LPRINT "*****    T h e   M o n o d   K i n e t i c s    *****"
190 LPRINT: LPRINT "=============================================================="
200 LPRINT
210 LPRINT USING "  Reactor  Working  Volume        = #,###,### gal";V
220 LPRINT USING "  'FEED'  Volume  per  Cycle      = #,###,### gal";VF
230 LPRINT USING "  'FEED'   Flow   Rate            =    ##,### gpm";Q
240 LPRINT USING "  Influent   C O D                =    ##,### mg/L";SO
250 LPRINT USING "  Expected  Effluent  SCOD        =     #,### mg/L";SE
260 LPRINT USING "  Active  Biomass  ( MLVSS )      =    ##,### mg/L";X
270 LPRINT USING "  Half  Saturation  Constant      =     #,### mg/L";CKS
280 LPRINT USING "  Max. Substrate Utilization Rate =      ##.# 1/day";CK
290 LPRINT: LPRINT "=============================================================="
300 LPRINT
310 T = 0: IND = 0: DELTAT = .001
320 NO = 1: Q = Q * 60
330 V1 = V-VF: S1 = SE: CK = CK/24
340 CLS: LPRINT " FEED Time, hr    SCOD, mg/L    No. of Integrations"
350 LPRINT
360 IF V1 <= V THEN 370 ELSE 430
370 T = T+DELTAT: IND = IND+1
380 TEMP = (Q*DELTAT *SO+S1*V1)/(V1+Q*DELTAT)
390 S2 = TEMP-(CK*S1*X)/(CKS+S1)*DELTAT
400 IF NO = (IND/250) THEN LPRINT USING "    ##.##          ##,###
##,###";T,S2,IND:NO = NO+1
410 V1 = V1+Q*DELTAT: S1=S2
420 GOTO 360
430 LPRINT: LPRINT USING " 'FEED' Time = ##.## Hours     ";T
440 LPRINT
450 SF = S2: NO = 1: IND = 0
460 LPRINT: LPRINT "Cycle Time, hr    SCOD, mg/L    No. of Integrations":LPRINT
470 IF SF > 100 THEN 480 ELSE 530
480 T = T + DELTAT: IND = IND + 1
490 DELTAS = -(CK*X*SF)/(CKS+SF)*DELTAT
500 SF = SF + DELTAS
510 IF NO = (IND/500) THEN LPRINT USING "    ##.##          ##,###
##,###";T,SF,IND:NO = NO+1
520 GOTO 470
530 TR = CKS/(CK*X)*(LOG(S2/SE)+(S2-SE)/CKS)
540 LPRINT "=============================================================="
550 LPRINT: LPRINT USING " Minimum 'REACT' Time = ###.## Hours";TR
560 LPRINT USING " At Effluent S C O D  =  #,### mg/L";SE
570 LPRINT: LPRINT "=============================================================="
580 END
```

```
10 CLS
20 '
30 '       *****  ASBR MODELING PROGRAM  *****
40 '       *****  First-Order Kinetics   *****
50 DEFDBL A-H, O-Z
60 DEFINT I-N
70 LOCATE 5,6:PRINT "*******    INPUT  FOLLOWING  PARAMETERS    *******"
80 LOCATE 7,6: INPUT "  Reactor  Working  Volume  in  gal       ";V
90 LOCATE 8,6: INPUT "  'FEED'  Volume  per  Cycle  in  gal     ";VF
100 LOCATE 9,6: INPUT "  'FEED'  Flow  Rate  in  gpm             ";Q
110 LOCATE 10,6: INPUT "  Influent  COD  in  mg/L                ";SO
120 LOCATE 11,6: INPUT "  Expected  Effluent  SCOD  in  mg/L     ";SE
130 LOCATE 12,6: INPUT "  1st Order Kinetic Constant in mg/L     ";CKP
140 '    ****   END OF PARAMETERS INPUT   ****
150 LPRINT:LPRINT "*****    A S B R    D E S I G N    M O D E L    *****"
160 LPRINT "*****  F i r s t - O r d e r   K i n e t i c s  *****"
170 LPRINT: LPRINT "=============================================================="
180 LPRINT
190 LPRINT USING "  Reactor  Working  Volume     =  #,###,### gal";V
200 LPRINT USING "  'FEED'  Volume  per  Cycle   =  #,###,### gal";VF
210 LPRINT USING "  'FEED'   Flow   Rate         =     ##,### gpm";Q
220 LPRINT USING "  Influent   C O D             =     ##,### mg/L";SO
230 LPRINT USING "  Expected  Effluent  SCOD     =      #,### mg/L";SE
240 LPRINT USING "  1st Order Kinetic Constant   =      ##.## 1/day";CKP
250 LPRINT: LPRINT "=============================================================="
260 LPRINT
270 T = 0: IND = 0: DELTAT = .001
280 NO = 1: Q = Q * 60
290 V1 = V-VF: S1 = SE
300 CKP = CKP/24
310 CLS: LPRINT " FEED Time, hr    SCOD, mg/L     No. of Integrations"
320 LPRINT
330 IF V1 <= V THEN 340 ELSE 410
340 T = T+DELTAT: IND = IND+1
350 TEMP = (Q*DELTAT *SO+S1*V1)/(V1+Q*DELTAT)
360 S2 = TEMP-(CKP*S1)*DELTAT
370 IF NO = (IND/250) THEN LPRINT USING "    ##.##          ##,###
##,###";T,S2,IND:NO = NO+1
380 V1 = V1+Q*DELTAT
390 S1 = S2
400 GOTO 330
410 LPRINT: LPRINT USING " 'FEED' Time = ##.## Hours     ";T
420 LPRINT
430 SF = S2
440 NO = 1: IND = 0
450 LPRINT: LPRINT "Cycle Time, hr    SCOD, mg/L     No. of Integrations"
460 LPRINT
470 IF SF > 100 THEN 480 ELSE 530
480 T = T + DELTAT: IND = IND + 1
490 DELTAS = -(CKP*SF)*DELTAT
500 SF = SF + DELTAS
510 IF NO = (IND/500) THEN LPRINT USING "    ##.##          ##,###
##,###";T,SF,IND:NO = NO+1
520 GOTO 470
530 TR = 1/CKP*LOG(S2/SE)
540 LPRINT "=============================================================="
550 LPRINT: LPRINT USING " Minimum 'REACT' Time = ###.## Hours";TR
560 LPRINT USING " At Effluent S C O D  =  #,### mg/L";SE
570 LPRINT: LPRINT "=============================================================="
580 END
```